PSP/IS⊙IS Energetic Particle Data - User Guide

Prepared by: Bala Poduval, Jonathan Niehof & Wouter de Wet
Bala.Poduval@unh.edu; Jonathan.Niehof@unh.edu; Wouter.deWet@unh.edu

Release Version – Release 20
September 16, 2024

Contents

List of Tables

List of Figures

PSP/IS⊙IS Energetic Particle Data - User Guide

September 16, 2024

1 INTRODUCTION

This user guide contains detailed information on the various quantities measured by the Integrated Science Investigation of the Sun (IS⊙IS) instrument suite on board the Parker Solar Probe (PSP) and how to access them from the data repository. These are the Level 2 data from the EPI-Lo (Energetic Particle Instrument - Low Energy) and EPI-Hi (Energetic Particle Instrument - High Energy) instruments. This document is divided into seven sections, including this introduction and references. Also included in the Introduction is an account of photon contamination (§ 1.3). The terms of using the PSP/IS⊙IS data is presented in § 1.1. The various properties of the solar energetic particles detected in a wide range of energies and the associated attributes such as cadence, energy bins, look directions and sectors in each CDF file that are useful for science analysis are tabulated and presented in § 2. All the variables currently available in the data repository for the scientific community are listed in § 5 and § 6 consists of a compilation of all the information of the variables from the metadata in each CDF file. The variables listed in § 5 are dynamically linked to their detailed descriptions in § 6. The EPI-Lo Decoder Ring is presented in § 4 and a list acronyms in § 7, followed by References.

1.1 TERMS OF USE: IS⊙IS DATA

Production of Integrated Science Investigation of the Sun (IS⊙IS) data is funded as part of NASA's Parker Solar Probe mission under contract NNN06AA01C. Use of any IS⊙IS data should include the following acknowledgement and also refer to the publication provided below.

Acknowledgement:

"Thanks to the Integrated Science Investigation of the Sun (IS⊙IS) Science Team (PI: David McComas, Princeton University)."

Reference Publication:

McComas, D. J. et al. (2016), Integrated Science Investigation of the Sun (IS⊙IS): Design of the Energetic Particle Investigation, Space Science Reviews, 204, 187–256, doi:10.1007/s11214-014-0059-1.

1.2 RELEASE NOTES

1.2.1 RELEASE 1

Released 2019-11-15.

Proper analysis of this first release of the data requires knowledge of several caveats and possible instrumental effects.

- Pitch angles are using preliminary calibrations from the FIELDS magnetic field instrument. This may result in errors in pitch angle determination up to about 1.5 degrees.
- EPI-Hi and EPI-Lo data use different units for energies and thus for fluxes. EPI-Hi data are reported MeV for protons and electrons, and MeV/nuc for heavy ions. EPI-Lo uses keV for all species except for time-of-flight only data, which uses keV/nuc. These differences are important when combiningdata across the two sensors.
- Ions heavier than helium and electrons are likely to have substantial background, including from other species, and are thus provided as count rates only until commissioning of these species can be completed for inclusion in a future release.
- EPI-Hi data below approximately 2MeV may be subject to instrumental effects that are currently being quantified. At these energies, the incident energy may be under reported by as much as 10% and the flux may be underreported by as much as 30%.
- EPI-Hi hourly (3600) data is compiled on the hour according to the spacecraft clock. The first integration after turn-on may be substantially shorter than an hour depending on when turn-on occurred. This may result in poor counting statistics from a short integration and unrealistic spectra for this first integration. The same effect is present, but less apparent, for the first integration of shorter periods.
- Spacecraft position is provided for every timebase in a file. Position is in HCI (variable names starting with HCI_R, HCI_Lat, HCI_Lon for each timebase) and HGC (names starting with HGC_R, HGC_Lat, HGC_Lon). Particle flow direction for each look direction is provided as unit vectors in HCI and RTN, as well as pitch angle, also on every timebase; variable names start with HCI, RTN, and PA.

1.2.2 RELEASE 2

Released 2020-01-27.

This release extends the dataset through 2019-10-10 (after third encounter). Files included cover the entire mission; thus it supersedes release 1. Contact the SOC for access to release 1 data if needed for comparison.

- Pitch angles for 2019 use updated FIELDS calibrations. The 2018 pitch angles have not changed from release 1, as FIELDS calibrations from 2018 required no updating.
- The summary product (psp_isois_l2-summary) includes a new variable, A_Heavy_Rate_TS. This is a total heavy-ion count rate from the EPI-Hi LET1A telescope.

1.2.3 RELEASE 3

Released 2020-04-14.

This release extends the dataset through 2020-01-06. This includes the end of Orbit 3 and beginning of Orbit 4, including Venus Flyby 2, but with no new encounter data. Files included cover the entire mission; thus it supersedes previous releases. Contact the SOC for access to release 1 and 2 data if needed for comparison.

- Much of the CDF metadata has been updated to provide better descriptions and make data easier to find. In particular, pitch angle and related pointing data are tagged as `data` rather than `support_data` to make them more visible in many tools. Variable names have not been changed.
- Updated calibration tables for EPI-Lo have been applied. This results in small (a few percent) changes in energy channels and fluxes throughout the mission.

1.2.4 RELEASE 4

Released 2020-08-04.

This release extends the dataset through 2020-04-29. This includes Encounter 4 and the rest of orbit 4. Files included cover the entire mission; thus this release supersedes all previous releases. Contact the SOC for access to release 1-3 data if needed for comparison.

- The EPI-Hi instrument was off for operational reasons from 2019-10-07 through 2020-02-12.
- Due to a dust impact on 2019-04-03 around 16:45Z, look direction 31 of the EPI-Lo TOF-only products (channel T) is highly susceptible to UV photon contamination after this time (see http://dx.doi.org/10.3847/1538-4365/ab643d). Release 3 removed calibrated fluxes for this look direction after this time. In release 4, L31 is also excluded from count rate products that are summed over look direction. This includes `H_CountRate_ChanT_SP` in `psp_isois_l2-summary` and related quicklook plots. This exclusion is for all time, so that rates before and after the dust impact can be compared. Look directions 34 and 35, although they retain intact foils, can also be heavily contaminated by UV and are excluded from summed count rate products as well.
- During the EPI-Lo high voltage ramp-up immediately after turn-on (approximately 15 minutes), count rates and fluxes are not accurate measurements of the incident population. These periods have been filtered out from the flux and count rate variables.
- All pitch angle variables now have a corresponding "spiral angle" variable, containing the angle the particle flow direction makes with the outward nominal Parker Spiral. "Nominal" is defined as 400km/s v_{sw} with corotation breakdown at $10R_S$. For EPI-Lo, these variables are named like `SA_ChanX`; for EPI-Hi, names are similar to `LET1_A_SA` and `LET1_A_R1_SECT_SA` (for non-sectored and sectored rates, respectively.)
- Many small metadata updates have been made for greater clarity; variable names remain the same.

– EPI-Hi energy unit labeling is consistent (MeV/nuc for ions heavier than protons; MeV for all else) and all energy labels have consistent formatting.

1.2.5 RELEASE 5

Released 2020-09-24.

This release includes data through 2020-04-29, with no additional dates since release 4. This includes Encounter 4 and the rest of orbit 4. Files included cover the entire mission; thus this release supersedes all previous releases. Contact the SOC for access to release 1-4 data if needed for comparison.

- Release 4 was made using the EPI-Lo calibration data from release 2; release 5 uses the latest calibration data. This results in small (a few percent) changes in energy channels and fluxes throughout the mission, similar to release 3.
- Release 4 also included fluxes for look direction 31 of the time-of-flight products after the dust impact on 2019-04-03; these fluxes are largely from UV photon contamination and should not be used. They are properly filtered from release 5.
- EPI-Hi data are the same as release 4, but the files are reproduced in release 5 to avoid confusion.
- IS⊙IS summary data are largely the same as release 4, but may have small changes in energy channels in the variables related to EPI-Lo.

1.2.6 RELEASE 6

Released 2020-11-16.

This release extends the dataset through 2020-08-13. This includes Encounter 5 and the rest of orbit 5. Files included cover the entire mission; thus this release supersedes all previous releases. Contact the SOC for access to release 1-5 data if needed for comparison.

- Data may include brief periods of counts generated internally to the instrument for calibration purposes. These will be filtered in a future release and are noted in the Data Anomalies & Quality list (https://spp-isois.sr.unh.edu/Released-Data-Anomalies-and-Quality-Notes.html).
- Pitch angles for the periods 2019 Jan through Aug and 2020 Jan through Feb were added for this release.

1.2.7 RELEASE 7

Released 2021-04-05.

This release extends the dataset through 2021-01-04. This includes Encounter 6 and the rest of orbit 6. Files included cover the entire mission; thus this release supersedes all previous releases. Contact the SOC for access to release 1-6 data if needed for comparison.

- EPI-Hi LET electron count rate variables are now included. These match the naming scheme for the HET electron variables, e.g. `A_Electrons_Rate` is the count rate for electrons in LET1-A.
- Most quantities that are included as a count rate are now also reported as counts per integration, for those interested in performing their own statistical analysis. These variables have descriptions with simply "counts", units of "counts", and variable names with "Counts" or no specific notation. Examples are `A_H` for EPI-Hi A-side protons or `H_Counts_ChanP` for EPI-Lo triple-coincidence protons. Count rate variables have "Rate" or "CountRate" in the name, "count rate" in the description, and units of "counts/s". Examples `A_H_Rate`; `H_CountRate_ChanP`. Count rates are properly corrected for instrument livetime; counts are not.
- EPI-Lo calibrations were updated based on observations from the large event of 29 November 2020. This is not the final calibration that will result from that event, but it is significant enough of an improvement that we are releasing it now.
  - Updated efficiencies were calculated for H, He, O, and Fe. These incorporate contributions from grid transmission fraction, scattering, and MCP detection efficiency. Updates primarily affect the ion composition triple coincidence channels P and C. The ion composition TOF-only channel T was corrected based on the updated channel P values.
  - Updated instrument geometric factors were calculated, including large-scale instrument geometry, not finer corrections such as grid transmission. Flat fielding corrections were calculated from a period of high isotropy (November 30, 2020 19:00 to December 1, 2020 02:00)
- Due to a dust impact on 2020-12-30 between 02:00 and 07:00Z (while EPI-Lo was off), look direction 35 of the EPI-Lo TOF-only products (channel T) is highly susceptible to UV photon contamination after this time. Release 7 removed calibrated fluxes for this look direction after this time. This look direction was excluded from look-averaged TOF-only products starting in release 3.
- The large event of 2020-11-30 through 2020-12-02 was the first event of the mission where EPI-Hi switched into operational modes for handling high rates. These modes have not been fully calibrated: count rate and flux data for this period should not be used without consulting the EPI-Hi team.

1.2.8 RELEASE 8

Released 2021-06-28.

This release extends the dataset through 2021-03-27. This includes Encounter 7 and the rest of orbit 7. Files included cover the entire mission; thus this release supersedes all previous releases. Contact the SOC for access to release 1-7 data if needed for comparison.

- The large event of 2020-11-30 through 2020-12-02 was the first event of the mission where EPI-Hi switched into operational modes for handling high rates. These modes have not been

fully calibrated: count rate and flux data for this period should not be used without consulting the EPI-Hi team.

1.2.9 RELEASE 9

Released 2021-09-20.

This release contains data quality enhancements only and ends on 2021-03-27. Files included cover the entire mission; thus this release supersedes all previous releases. Contact the SOC for access to release 1-8 data if needed for comparison.

- EPI-Hi processing and calibrations have been improved for high rate periods, the most notable of which to date is the large event of 2020-11-30 through 2020-12-02.
  - Count rates and fluxes are corrected to account for the fraction of particle detections which are not fully processed by the flight software. This is described in more detail in the data user guide.
  - Calibrations for high rate operational modes have been updated. HET calibrations for dynamic threshold mode 1 are those used by Cohen et al. (2021, https://doi.org/10.1051/0004-6361/202140967). HET modes 2 and 3, and all high rate modes of LET1 and LET2, do not have mature calibrations at this time, so fluxes are not reported for the high rate modes.
- Minor adjustments to EPI-Lo telemetry processing may result in slightly higher (of order one percent) count rates and fluxes during active times.
- EPI-Lo ion composition (IC) files have new count rate variables for N and Ne, in anticipation of refined tracks for these species. These variables contain no records until the refined tracks are implemented on-orbit.
- Due to ongoing dust effects, several more look directions are excluded from the look-averaged TOF-only products in the summary file. The complete list is now 21, 24-29, 31, 34, 35, and 39.

1.2.10 RELEASE 10

Released 2021-10-26.

This release extends the dataset through 2021-07-24. This includes all of orbit 8, including Encounter 8, and part of the inbound leg of orbit 9. Files included cover the entire mission; thus this release supersedes all previous releases. Contact the SOC for access to release 1-9 data if needed for comparison.

No changes have been made to the processing of the data; caveats remain the same.

- EPI-Lo species identification tables were updated on 2021-06-14. Ion composition (IC) files after this day will have records populated in the N and Ne count rate variables added in release 9.

1.2.11 RELEASE 11

Released 2022-02-07.

This release extends the dataset through 2021-11-04. This includes the rest of orbit 9, including Encounter 9, and part of the inbound leg of orbit 10, including Venus Flyby 5. Files included cover the entire mission; thus this release supersedes all previous releases. Contact the SOC for access to release 1-10 data if needed for comparison.

No changes have been made to the processing of the EPI-Hi data; caveats remain the same. The following updates have been made to EPI-Lo data.

- Updated EPI-Lo energy channel assignments and efficiencies for all species and energies before 14 June 2021, reflecting the imprecise on-board energy normalization that was in use at that time. The resulting energies are much more strongly dependent on look direction.
- Minor updates to the calculation of EPI-Lo livetimes, resulting in flux increases of order 1% in some circumstances.
- Corrected EPI-Lo energy assignments for electron channels after 14 June 2021 (release 10 erroneously used development tables which were not uploaded).

1.2.12 RELEASE 12

Released 2022-04-25.

This release extends the dataset through 2022-01-23. This includes the rest of orbit 10, including Encounter 10, and part of the inbound leg of orbit 11. Files included cover the entire mission; thus this release supersedes all previous releases. Contact the SOC for access to release 1-11 data if needed for comparison.

The following changes and caveats apply to both EPI-Hi and EPI-Lo data, or to IS⊙IS suite products:

- `H_CountRate_ChanT`-related variables have been removed from the `psp_isois_l2-summary` files, as these time-of-flight only rates contain substantial background. They have been replaced with `H_CountRate_ChanP`-derived varaibles, containing protrons with a triple coincidence (TOFxE) requirement. These contain all look directions and a similar energy range to the previous `ChanT` variables. As a reminder, these `summary` files are intended to support high-level surveys for periods of interest and should not be used for science analysis.
- Pitch angles are not available after 2021-12-31.

The following changes apply to EPI-Hi:

- Calibrations for high rate operational modes have been updated. HET calibrations H and He for dynamic threshold mode 1 have been updated; initial LET calibrations are included for H and He in dynamic threshold mode 1.

- HET calibrations for H and He in dynamic threshold mode 0 (the normal mode for the lowest count rates) have been updated to account for the non-flat response of the instrument.
- Processing of the data at EPI-Hi dynamic threshold changes has been updated to ensure proper timing of the transition.

No changes have been made to processing of the EPI-Lo data.

1.2.13 RELEASE 13

Release 2022-08-01.

This release extends the dataset through 2022-04-29. This includes the rest of orbit 11, including Encounter 11, and part of the inbound leg of orbit 12. Files included cover the entire mission; thus this release supersedes all previous releases. Contact the SOC for access to release 1-12 data if needed for comparison.

- Pitch angles are included for all times where FIELDS data are available, including times omitted in release 12.
- EPI-Lo calibrations have been updated for apertures with thick entrance foils (L23, L30–L33, L40). The energy binning for these look directions is substantially different from others, particularly at lower energies, and care should be used when combining data from multiple look directions.

1.2.14 RELEASE 14

Release 2022-11-14.

This release extends the dataset through 2022-08-15. This includes the rest of orbit 12, including Encounter 12, and part of the inbound leg of orbit 13. Files included cover the entire mission; thus this release supersedes all previous releases. Contact the SOC for access to release 1-13 data if needed for comparison.

- EPI-Lo livetime calculations have been updated to better account for quadrant-specific dead-time effects. This will have little effect on fluxes averaged over all apertures; however, quadrant 1 (look directions 20–39) fluxes and count rates may be increased with a smaller decrease in all other quadrants. This effect is most pronounced for high-rate periods and may reach a 50% effect in quadrant 1.
- EPI-Lo underwent two tests characterizing instrument performance leading up to and during the first portion of encounter 12. During these tests, the data is quadrant 1 are not entirely of science quality. The fluxes have been replaced with fill values and count rates should not be used. Tests were run 2022-05-24T16:13:09 through 2022-05-29T16:13:09 and 2022-05-30T11:50:08 through 2022-06-04T11:50:08. Future work may recover some quadrant 1 science data from this period.

No changes have been made to the processing of the EPI-Hi data.

1.2.15 RELEASE 15

Release 2023-02-20.

This release extends the dataset through 2022-11-14. This includes the rest of orbit 13, including Encounter 13, and part of the inbound leg of orbit 14. Files included cover the entire mission; thus this release supersedes all previous releases. Contact the SOC for access to release 1-14 data if needed for comparison.

No changes have been made to the processing of the IS⊙IS data.

1.2.16 RELEASE 16

Release 2023-05-12.

This release extends the dataset through 2023-02-09. This includes the rest of orbit 14, including Encounter 14, and part of the inbound leg of orbit 15. Files included cover the entire mission; thus this release supersedes all previous releases. Contact the SOC for access to release 1-15 data if needed for comparison.

- Relative to release 15, pitch angle tags for the period 2022-09-22 through 2022-11-14 were added; they are included for the entire release (through 2023-02-09).
- To avoid an instrument overcurrent condition, EPI-Lo raised thresholds during periods of high rates. This happened on 2022-12-11 from 8:20:40 through 8:45:40. Data in look directions 40 – 59 are not science quality during this period and fluxes have been replaced with fill.

No other changes have been made to the processing of the IS⊙IS data. There are no updates to the IS⊙IS event list.

1.2.17 RELEASE 17

Release 2023-08-28.

This release extends the dataset through 2023-06-04. This includes the rest of orbit 15, including Encounter 15, and part of the inbound leg of orbit 16. Files included cover the entire mission; thus this release supersedes all previous releases. Contact the SOC for access to release 1-16 data if needed for comparison.

- EPI-Lo and EPI-Hi data have new variables with quality flags; these variables and their interpretation are described in section 3.
- EPI-Lo data have been updated with improved geometric factors for the “particle” SSD; this affects the calibration of the TOF-only (T) flux.

1.2.18 RELEASE 18

Release 2023-10-30.

This release extends the dataset through 2023-08-03. This includes Encounter 16 and most of the outbound leg of orbit 16. Files included cover the entire mission; thus this release supersedes all previous releases. Contact the SOC for access to release 1-17 data if needed for comparison.

- The IS⊙IS event list has been updated through the beginning of orbit 16.
- No changes have been made to the processing of IS⊙IS data.

1.2.19 RELEASE 19

Release 2024-03-08.

This release extends the dataset through 2023-12-14. This includes Encounter 17, the outbound leg of orbit 17, and some of the inbound leg of orbit 18. Files included cover the entire mission; thus this release supersedes all previous releases. Contact the SOC for access to release 1-18 data if needed for comparison.

- No changes have been made to the IS⊙IS event list.
- No changes have been made to the processing of IS⊙IS data.

1.2.20 RELEASE 20

Release 2024-09-16.

This release extends the dataset through 2024-06-16. This includes Encounter 18 and outbound orbit 18, all of orbit 19, and some of the inbound leg of orbit 20. Pitch angle tags are provided through 2024-04-29. Files included cover the entire mission; thus this release supersedes all previous releases. Contact the SOC for access to release 1-19 data if needed for comparison.

- No changes have been made to the processing of IS⊙IS data.
- The IS⊙IS event list has been updated through 2024-04-09 (outbound orbit 19).

1.3 PHOTON CONTAMINATION

EPI-Lo was designed to investigate the physics of energetic particles, however in the special lowest-energy "time-of-flight only" product used in this study, it also responds to solar photons in a subset of approximately sunward–looking apertures lacking special light–attenuating foils. This topic is discussed in detail by Hill et al. (2019) but we provide some details here.

1.3.1 PHOTONS AND DUST

The EPI-Lo design is robust against the detrimental effects of ambient dust or light entering any of EPI-Lo's eighty apertures. The mitigation for light contamination includes employing thicker start foils in the six look directions dominated by photospheric light that is Thomson scattering off electrons near the Sun, and thus visible away from the solar disk where there is no shielding from PSP's thermal protection system (TPS). In addition to thicker foils, we employ baffles and

multiple coincidence logic to cut down photon contamination. Also, to protect against dust and resulting dust–hole–admitted light, an extra "collimator foil" was added to all collimator turrets so that pinholes from dust impacts either penetrate only the collimator foil (for the smallest dust grains $\leq$ 100 nm) or only admit light from very tiny solid angles where these holes line up, resulting in a greatly reduced geometry factor for post-impact light contamination than would occur with only one foil. The first dust impact directly detectable by EPI-Lo (i.e., an impact resulting in noticeable light–admitting damage) took place after the second perihelion on 2019–04–03 (DOY 093) 16:45 in the L31 direction (see Figure 2 for description of EPI-Lo look directions). This L31 hole resulted in elevated photon background in one look direction but at a level that has not diminish EPI-Lo's scientific capabilities. This dust impact is discussed in more detail by Szalay et al. (2019).

A second dust impact occurred in the L35 direction on 2020-12-30 (DOY 365) sometime between 02:00 and 07:00 when the instrument was off. This hole is larger than the L31 hole and is under current investigation.

During Orbit 8, two more dust impacts were detected. L55 on 2021-04-19 12:00 and L21 on 2021-04-27 18:29. TOF-only products have increased in noise, but triple-coincidence products are not impacted by photon contamination.

1.3.2 LOOK DIRECTIONS

We divided the field of view (FOV) into three independent sets of look directions: the generally sunward-looking Bright Look directions with very clear photon viewing (composed of the look directions L22, L25, L34–L37, L44, and L46); the Dim Look directions surrounding the bright area, where there are reduced indications of photons (composed of look directions L24, L26, L27, L41, L45, L47); and the Dark Look direction region, where there is no strong sign of photons (composed of the apertures that are neither the bright look direction or the dim look direction lists and which are mostly composed of wedges W0, W1, and W5–W7, which look away from the Sun). Explicitly, the list of dark look directions is L00–L21, L23, L28–L33, L38–L40, L42, L43, and L48–L79, with the sum of the Bright, Dim, and Dark look directions incorporating all 80 apertures. Although the bright look directions are roughly those most directed at the Sun, an important distinction is that the six apertures closest to the Sun with thicker light-blocking start foils (L23, L30–L33, and L40) are not included in the bright FOV or dim FOV because the thick foils effectively block the scattered light.

1.3.3 ENERGY RANGES

In addition to the division of the FOV, the energy channels are also split into three independent ranges: Low Energy (channels T030 and T031, 1-4 keV/nuc detected energy, based on the TOF measurement, corresponding to incident energies below 34 keV when H is assumed), where accidentals dominate during quiet times; Medium Energy (channels T016–T029, 4-350 keV/nuc detected and 34–370 keV for incident H), where foreground ion measurements are the strongest; and High Energy (channels T001–T015, 350 keV/nuc – 37 MeV/nuc detected and 370 keV – 39 MeV for incident H), where crosstalk events dominate during quiet times. Although the upper energy limit is high, no ions were detected above a few hundred keV/nuc (confirmed by EPI-Hi observations). The reason that accidental coincidences are associated with lower energy intensifications is because randomly distributed start and stop events that accidentally satisfy the TOF logic result in a flat distribution in TOF-space, but because of the inverse square relationship between energy and

TOF, a large fraction of the longer end of the TOF range corresponds to a small, low-energy range of energies.

1.3.4 PROXIES

With these definitions we found that a good proxy for the clean ion signal is found by combining Low Energy/Dark Look Directions, Medium-Energy/Dim Look Directions, and Medium-Energy/Dark Look Directions and a good proxy for photon contamination is the Low-Energy/Bright Look Direction measurements. That is, Ion Proxy = Low Dark + Medium Dim + Medium Dark and Photon Proxy = Low Bright.

1.3.5 SUMMARY

EPI-Lo measures ion intensity, energy, composition, and anisotropy, by design, and also responds to photons that are most likely scattered by zodiacal dust. Utilizing thicker start foils to suppress photon contamination unfortunately degrades low–energy ion response, so this mitigation was used sparingly; consequently, there are several generally sunward apertures with thin start foils where photons produce backgrounds, mostly through accidental coincidence of uncorrelated transmitted photon start and stop triggers. The result is that EPI-Lo responds to SEPs and solar photons, and through directional and energy filtering as well as accidental coincidence calculations, the ion signal can be largely separated from the photon backgrounds, as we have detailed.

2 SUMMARY: SCIENCE DATA

In this section, the energetic particle measurements of *PSP*/IS⊙IS that are useful for science investigations are presented. The various quantities measured by the EPI-Lo (Energetic Particle Instrument - Low Energy) and EPI-Hi (Energetic Particle Instrument - High Energy) instruments are tabulated in Tables 2.2.1 – 2.3.57.

2.1 EPHEMERIS AND POINTING

A high-level view of the spacecraft position and attitude can be found in the `psp_isois_l2-ephem` file. The central attitude question is usually "is the spacecraft in a nominal orientation?". For this the first variable of concern is `Sun_Angle` (6.16.2.14), the angle between the spacecraft TPS (thermal protection system, heat shield) and the Sun-spacecraft line. Normally this is 0 unless some distance from the Sun; a simple flag to determine this is the variable `Umbra_Pointing` (6.16.2.15). If the spacecraft is in umbra orientation, the `Roll_Angle` (6.16.2.9) variable is a simple rotation around the Sun-spacecraft axis. Nominally IS⊙IS is on the ram-facing side, roll angle is 0, and this is indicated by `Ram_Pointing` (6.16.2.8).

If the spacecraft is not in umbra orientation, the roll angle is still defined but is much less intuitively useful; the ephemeris defines a `Clock_Angle` (6.16.2.1) which describes in which direction the TPS is off-pointing from the Sun. The TPS tilted up out of the ecliptic in the 12 o'clock position is zero clock angle. Down out of the ecliptic, 180/-180 degrees. "Left" when sun-facing (i.e. anti-ram) is 90 degrees; and "right" (TPS into ram), -90.

The ephemeris also includes basic spacecraft location in HGC and HCI and the direction of the main EPI-Lo instrument, LET1A, LET2C, HETA relative to the nominal Parker Spiral. These values are also included in each science data file.

Each science data file, for each cadence included in a file, includes ephemeris and attitude information on the same cadence, i.e. at the point-in-time of the `Epoch` variable. For any quantitative treatment of particle direction, using these variables is *highly recommended* rather than trying to infer direction from the ephemeris files.

Spacecraft position is provided in HGC and HCI spherical polar coordinates after Fränz and Harper, 2002 (`https://www2.mps.mpg.de/homes/fraenz/systems/`). For EPI-Hi, there is only one cadence per file and these are simply named like `HCI_R`, `HCI_Lat`, `HCI_Lon` and similarly for `HGC`. For EPI-Lo, each channel has its own cadence and set of variables, e.g. `HCI_Lat_ChanP`.

Pointing information is provided in several forms. Each is provided for each aperture of EPI-Lo (all 80 apertures for channels with a valid start pulse and 8 wedges for those without), the main telescope boresight for each EPI-Hi telescope, and a geometrically nominal "center direction" for the EPI-Hi sectored rates. Note that the angular response of the EPI-Hi sectored rates is complex and simply assuming all incident particles are coming from the center direction is likely to be highly inaccurate.

For each of these directions, unit vectors are provided representing the direction of travel of an incident particle that is coming straight into the instrument, as represented in the RTN coordinate system. For instrument look direction, multiply each component of the unit vector by -1. No corrections are made for aberration due to spacecraft motion. The variables for these unit vectors include

RTN. For EPI-Lo, there is one variable (containing an array) for each channel, e.g. RTN_ChanP. For EPI-Hi, there is one for each telescope end, e.g. HET_A_RTN as well as an array for sectored rates, e.g. HET_A_R17_SECT_RTN. There are similar variables representing the particle motion direction in HCI coordinates (with HCI instead of RTN); again, no aberration corrections are made.

Particle directions are also expressed as a pitch angle, i.e the angle between particle motion and the ambient magnetic field. The field is taken from the FIELDS instrument and averaged over the IS⊙IS integration period by the FIELDS team. 0 represents particles directed parallel to the field; 180, antiparallel. Only 0-180 is used; there is no gyrophase information. EPI-Lo variables are named like PA_ChanP; EPI-Hi, like HET_A_PA, HET_A_R17_SECT_PA. In addition to the ambient field, a similar angle is calculated from the nominal Parker Spiral. This is assumed to always point outwards (i.e. no hemispheric or solar cycle polarity is applied) and is derived from a 400km/s constant solar wind with corotation breakdown at $10R_{\odot}$. These are named with SA (for "spiral angle") instead of PA.

2.2 EPI-LO SCIENCE DATA

Figure 1 shows the EPI-Lo instrument layout and Figure 2 depicts the view of the sky of the 80 apertures. The files containing the EPI-Lo data are named as: <mission>_<suite-instrument>_<data level>_<file-descriptor> (e.g., psp_isois-epilo_l2_ic). There are four primary science data files corresponding to the four modes (depicted by <file-descriptor>) of observation: ion composition (ic), ion energy (ie), particle composition (pc) and particle energy (pe). The tables in this section summarize the science data available for the following EPI-Lo data files:

psp_isois-epilo_l2-ic (ion composition)
psp_isois-epilo_l2-pe (particle energy)

Species without energy ranges specified are measured in this mode but are not yet commissioned. They will be included in future releases.

EPI-Lo constantly (eight times per second) cycles between "modes" with slightly different techniques for measuring the ambient plasma; the effective result is an apparent simultaneous measurement with all four modes. Modes with "composition" in the name trigger off a valid measurement from the TOF system; in these modes, a simultaneous valid measurement in a SSD may also be present (and is used if so), but is not required. Modes named "energy" trigger off a valid energy signal in a solid state detector; in these modes, a valid TOF measurement (or at least the corresponding start signals) may be used if present, but is not required. There are two sets of SSDs: the "particle" detectors have an aluminum flashing that rejects low-energy ions (improving the fraction of counts which are electrons); the "ion" detectors lack this flashing. Which SSD is checked for a signal depends on the current instrument mode. Thus the four modes: ion composition, particle energy, particle composition, ion energy. Only ion composition and particle composition have calibrated data at this time.

EPI-Lo products are integrated over different periods by "channel" (described below). These integration periods usually change a few times per orbit: upon encounter entrance and exit, and when updates are made to manage data allocation. For this reason, each channel has its own Epoch variable (and associated DELTA) which should always be used rather than assuming a cadence.

Similarly, EPI-Lo energies may vary by look direction, and vary occasionally in time when new tables are uploaded. The actual energy value recorded in the file should be examined rather than making assumptions about the energy channels. The energy labels thus also vary in look direction and time. Because these variables *may* change in time and look, they are included as fully-populated arrays for every time and look direction. The most notable change with look direction is the higher minimum energy (and resulting changes to the lowest bins) for the look directions with thick foils: L23, L30–L33, and L40.

The size of the energy variables reflects the maximum possible number of energy bins for that species and channel; the actual number of bins used may be smaller. Bins which are not used are given fill values for energy, and should be ignored. Similarly, bins which are not fully calibrated may be included. Fluxes corresponding to these bins are populated with fill but there may be count rates and best current evaluation of incident energy. This may include bins of zero width. Most science users should ignore any energy bins where the flux is entirely fill.

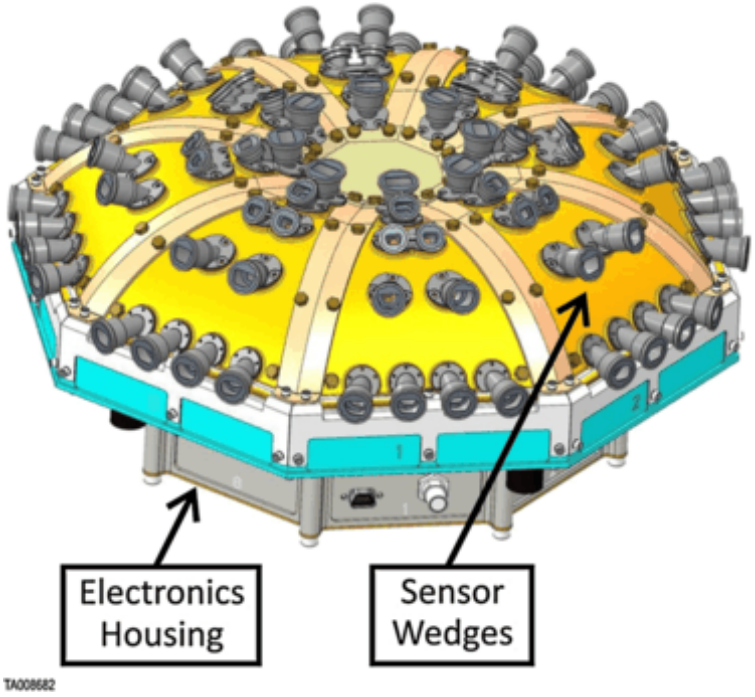

Figure 1: The EPI-Lo Instrument (see McComas et al., 2016, for details).

2.2.1 FILE: PSP_ISOIS-EPILO_L2-IC

This file contains the EPI-Lo ion composition (ic) data for various particle species such as C, Fe, H, ^{3}He, ^{4}He, Mg, O and Si. The variable name is structured as <species>_<quantity>_<channel>, where, <species> is one of the particle species; <quantity> takes 'Counts', 'CountRate' (counts/s) or 'Flux' (cm^{-2} sr^{-1} sec^{-1} keV^{-1}); and <channel> takes one of the values in Column 2. The Columns 'Look Direction' and 'Energy' imply the available look directions (0 – 79) and energy ranges, respectively, in the data file. For details on look directions, see McComas et al. (2016). Examples: C_CountRate_ChanD; H_Flux_ChanT.

Channels C, D, and P are triple-coincidence, or TOFxE, measurements, all measuring ions with a valid time of flight and a signal in the ion SSD. The difference is in their cadence. P is the highest cadence and used exclusively for protons. Other ions are split between C (moderate cadence) and D (slowest cadence of the three).

Channel R is a derived product from channel P. It is telemetered more frequently and constructed by joining adjacent bins from channel P. It is only of use when very high time resolution is required.

Channel T is a TOF-only channel, measuring all ions with a valid time of flight but no signal in the ion SSD. Incident energies are thus calculated in keV/nucleon and fluxes are calculated using the efficiencies and geometric factors for protons. This may be very wrong in the presence of a substantial population with Z>1. Because of the double coincidence requirement (rather than triple), counting statistics may be quite good at the price of poorer background rejection. By contrast the P channels are quite "clean", but with lower count rates.

Species	Channel	Size	Count Rate		Counts		Flux	
			Look Direction 80	Energy (keV) (bins)	Look Direction 80	Energy (keV) (bins)	Look Direction 80	Energy (keV) (bins)
C	D	80x48	0 – 79	178 – 22872 (21)	0 – 79	178 – 22872 (21)	0 – 79	178 – 22872 (21)
Fe	C	80x48	0 – 79	431 – 24868 (41)	0 – 79	431 – 24868 (41)	0 – 79	431 – 24868 (41)
H	R	80x48	0 – 79	67 – 8736 (14)	0 – 79	67 – 8736 (14)	0 – 79	67 – 8736 (14)
	P	80x48	0 – 79	67 – 10252 (39)	0 – 79	67 – 10252 (38)	0 – 79	67 – 10252 (38)
	T	80x48	0 – 79	21 – 46367 (32)	0 – 79	21 – 46367 (32)	0 – 79	21 – 46367 (32)
He3	D	80x48	0 – 79	95 – 22536 (44)	0 – 79	95 – 22536 (44)	0 – 79	95 – 22536 (44)
He4	C	80x48	0 – 79	83 – 22540 (44)	0 – 79	83 – 22540 (44)	0 – 79	83 – 22540 (44)
Mg	D	80x48	0 – 79	218 – 23672 (22)	0 – 79	218 – 23672 (22)	0 – 79	218 – 23672 (22)
Ne	D	80x48	0 – 79	830 – 23392 (6)	0 – 79	830 – 23392 (6)	0 – 79	830 – 23392 (6)
O	C	80x48	0 – 79	205 – 23114 (43)	0 – 79	205 – 23114 (43)	0 – 79	205 – 23114 (43)
Si	D	80x48	0 – 79	327 – 23946 (20)	0 – 79	327 – 23946 (20)	0 – 79	327 – 23946 (20)

Table 2.2.1: PSP_ISOIS-EPILO_L2-IC: The EPI-Lo ion composition (ic) data for C, Fe, H, He3, He4, Mg, Ne, O and Si in channels D, C, R, P and T.

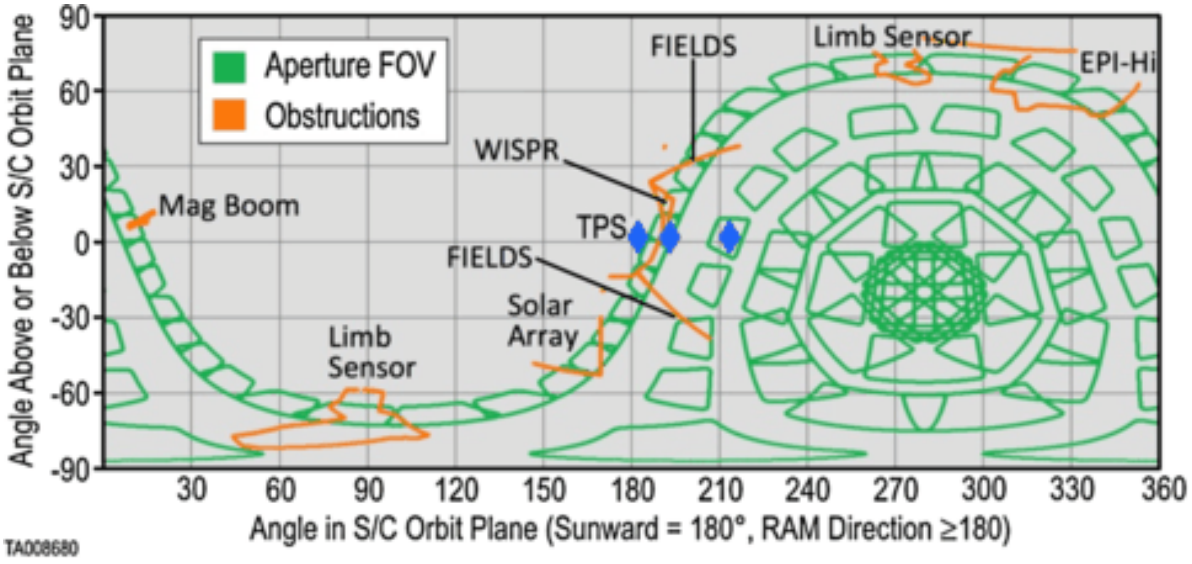

Figure 2: EPI-Lo Skymap (see McComas et al., 2016, for details).

2.2.2 FILE: PSP_ISOIS-EPILO_L2-PE

EPI-Lo particle energy (pe) data for different particle species, C, electron, H, ^{3}He, He, and O. The general form of the variable name is: <species>_<quantity>_<channel>. Here, <species> refers to one of the particle species; <quantity> takes 'Counts', 'CountRate' (counts/s) or 'Flux' (cm^{-2} sr^{-1} sec^{-1} keV^{-1}); and <channel> takes to one of the values in Column 2.
Examples: C_Flux_ChanN; O_Counts_ChanX; Electron_CountRate_ChanE.

Channel E is the primary electron measurement, although there is substantial ion background. It does not require a valid start pulse, and thus there is limited direction information, only the knowledge that the particle was incident from one of the eight wedges. Channel F is a high-time-resolution variant of channel E; it consistents of several channel E bins combined but telemetered more frequently.

Channel G contains particles with a valid SSD measurement and start pulse; as such, it has full directional information. However, incident electrons trigger a start pulse with very low efficiency, so count rates are quite low. As with channels E and F, the non-electron component is also quite high.

Species	Channel	Size	Count Rate		Counts		Flux	
			Look Direction (bins)	Energy (keV) (bins)	Look Direction (bins)	Energy (keV) (bins)	Look Direction (bins)	Energy (keV) (bins)
C	X	8 x 48	0 – 7 (8)	–	0 – 7 (8)	–	0 – 7 (8)	–
electron	E	8 x 48	0 – 7 (8)	27 – 375 (16)	0 – 7 (8)	27 – 375 (16)	0 – 7 (8)	27 – 375 (16)
	G	80 x 48	0 – 79 (80)	27 – 375 (16)	0 – 79 (80)	27 – 375 (16)	0 – 79 (80)	27 – 375 (16)
	F	8 x 48	0 – 7 (8)	33 – 375 (9)	0 – 7 (8)	33 – 375 (9)	0 – 7 (8)	33 – 375 (9)
H	E	8 x 48	0 – 7 (8)	–	0 – 7 (8)	–	0 – 7 (8)	–
	G	80 x 48	0 – 79 (80)	–	0 – 79 (80)	–	0 – 79 (80)	–
	F	8 x 48	0 – 7 (8)	–	0 – 7 (8)	–	0 – 7 (8)	–
	X	8 x 64	0 – 7 (8)	–	0 – 7 (8)	–	0 – 7 (8)	–
3He	X	8 x 48	0 – 7 (8)	–	0 – 7	–	0 – 7	–
He	X	8 x 48	0 – 7 (8)	–	0 – 7	–	0 – 7	–
O	X	8 x 48	0 – 7 (8)	–	0 – 7 (8)	–	0 – 7 (8)	–

Table 2.2.2: PSP_ISOIS-EPILO_L2-PE. The EPI-Lo particle energy (pe) data for electron, H, 3He, He and O in channels E, G, F and X.

2.3 EPI-HI SCIENCE DATA

The following tables summarize the science data for the EPI-Hi Instrument. The files are named as: <mission>_<suite-instrument>_<data level>_<file-descriptor> The EPI-Hi instrument consists of three telescopes HET, LET1 and LET2. The HET and LET1 telescopes have two sides (A, B) and let2 has one side (C). Sides A on LET1 and HET look sunward along the Parker Spiral and sides B on LET1 and HET look antisunward. Side C LET2 looks in the spacecraft ram direction. Full pointing information (RTN/HCI) is available in the L2 files (see McComas et al., 2016, and Figure 3). The numerical values following rates in the <file-descriptor> represent the cadence in seconds (e.g., rates10; rates300). If no value is present, the cadence is assumed to be 1 second. Listed below are the EPI-Hi data files. The 60 s cadence products containing only the engineering singles are excluded from public release.

EPI-Hi science rates are accumulated at several cadences. The 10 s and 1 s rates are an encounter–only product. The 60 s rates are also, at a baseline, encounter–only. The 3600 s rates are the main cruise phase product. EPI-Hi produces several engineering rates that overflow their counters when accumulated for 3600 s. For those, a 1/60 sample of the 60 s rates are included in cruise data. The 60 s products are thus produced for the whole mission but those containing no science data are excluded from the public release.

HET	LET1	LET2
psp_isois-epihi_l2-het-rates10	psp_isois-epihi_l2-let1-rates10	psp_isois-epihi_l2-let2-rates10
psp_isois-epihi_l2-het-rates300	psp_isois-epihi_l2-let1-rates300	psp_isois-epihi_l2-let2-rates300
psp_isois-epihi_l2-het-rates3600	psp_isois-epihi_l2-let1-rates3600	psp_isois-epihi_l2-let2-rates3600
psp_isois-epihi_l2-het-rates60	psp_isois-epihi_l2-let1-rates60	psp_isois-epihi_l2-let2-rates60
HET, LET1 & LET2		psp_isois-epihi_l2-second-rates

The front-end logic for each telescope is capable of accepting candidate particle detection events at a higher rate than the telescope's flight software can process. During periods of high count rates, then, some of these events are not processed and the measured count rate is depressed relative to the incident. EPI-Hi fluxes and science count rates are corrected for this effect, starting in release 9. Counts (per sample) are uncorrected.

2.3.1 FILE: PSP_ISOIS-EPIHI_L2-HET-RATES10

This file contains the 10 s data of energetic particle Counts, Flux (cm^{-2} sr^{-1} sec^{-1} MeV^{-1}) and Count Rate (counts/s) for electrons, H, He and NEUT_DET for sides A and B, for different ranges (R1 – R7) of the High Energy Telescope (HET). The naming convention of the variables in the data files is: <side>_<species>_<quantity> for those quantities independent of range. Here, <side> stands for A or B; <species> stands for the particle species (electrons, H, He, etc.); and <quantity> represents Counts (not used in variable names, in general), Flux or Rate. For those parameters measured as a function of range, the naming convention is: <range><side>_<species>_<quantity>, where, <range> goes from R1 to R7 and <side> takes either A or B. Variable names without ranges (e.g., A_Electrons_Flux) or with double digit range (e.g., R17) have the values integrated over all

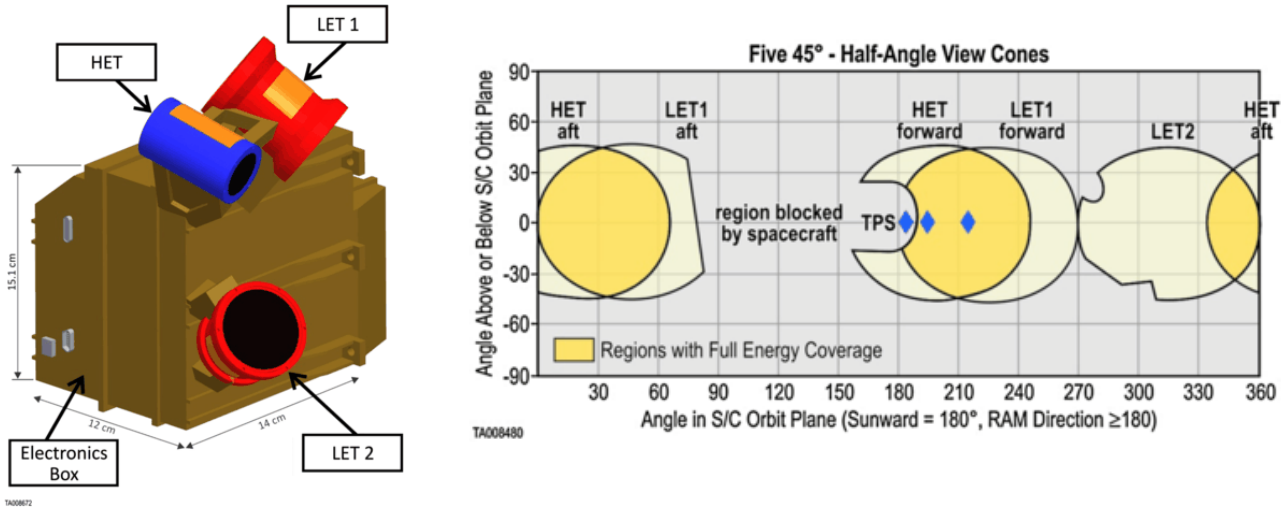

(a) EPI-Hi Instrument.

(b) EPI-Hi field of view.

Figure 3: The EPI-Hi instrument and field of view. Sides A on LET1 and HET look sunward along the Parker Spiral while sides B on LET1 and HET look antisunward. Side C on LET2 looks in the spacecraft ram direction. Full pointing information (RTN/HCI) is available in the L2 files (see McComas et al., 2016, for details on the sides A, B and C given in the tables.)

the available ranges (R1 to R7, in general).
Examples: A_H (measured quantity is “counts”); A_Electrons_Flux; R1A_Electrons_Rate.

Side	Range	Quantity	Electrons		H		He		NEUT_DET	
			E-bins	E-range (MeV/nuc) (bins)	E-bins	E-range (MeV/nuc) (bins)	E-bins	E-range (MeV/nuc) (bins)	E-bins	E-range (MeV/nuc) (bins)
A/B		Count	16	1 - 9 (16)	11	10 - 59 (11)	12	10 - 70 (12)	35	0 - 495 (35)
		Flux	16	1 - 9 (16)	11	10 - 59 (11)	12	10 - 70 (12)		
		Count Rate	16	1 - 9 (16)	11	10 - 59 (11)	12	10 - 70 (12)	35	0 - 495 (35)
	R1	Count	12	1 - 4 (12)	7	9 - 25 (7)	8	9 - 29 (8)		
		Flux	12	1 - 4 (12)	7	9 - 25 (7)	8	9 - 29 (8)		
		Count Rate	12	1 - 4 (12)	7	9 - 25 (7)	8	9 - 29 (8)		
	R2	Count	12	1 - 4 (12)	7	15 - 42 (7)	8	15 - 50 (8)		
		Flux	12	1 - 4 (12)	7	15 - 42 (7)	8	15 - 50 (8)		
		Count Rate	12	1 - 4 (12)	7	15 - 42 (7)	8	15 - 50 (8)		
	R3	Count	10	1 - 5 (10)	6	21 - 50 (6)	7	21 - 59 (7)		
		Flux	10	1 - 5 (10)	6	21 - 50 (6)	7	21 - 59 (7)		
		Count Rate	10	1 - 5 (10)	6	21 - 50 (6)	7	21 - 59 (7)		
	R4	Count	10	1 - 6 (10)	4	29 - 50 (4)	5	29 - 59 (5)		
		Flux	10	1 - 6 (10)	4	29 - 50 (4)	5	29 - 59 (5)		
		Count Rate	10	1 - 6 (10)	4	29 - 50 (4)	5	29 - 59 (5)		
	R5	Count	9	2 - 7 (9)	4	35 - 59 (4)	5	35 - 70 (5)		
		Flux	9	2 - 7 (9)	4	35 - 59 (4)	5	35 - 70 (5)		
		Count Rate	9	2 - 7 (9)	4	35 - 59 (4)	5	35 - 70 (5)		
	R6	Count	9	2 - 9 (9)	4	35 - 59 (4)	5	35 - 70 (5)		
		Flux	9	2 - 9 (9)	4	35 - 59 (4)	5	35 - 70 (5)		
		Count Rate	9	2 - 9 (9)	4	35 - 59 (4)	5	35 - 70 (5)		
	R7	Count	9	3 - 10 (9)	4	42 - 70 (4)	5	42 - 83 (5)		
		Flux	9	3 - 10 (9)	4	42 - 70 (4)	5	42 - 83 (5)		
		Count Rate	9	3 - 10 (9)	4	42 - 70 (4)	5	42 - 83 (5)		

Table 2.3.1: PSP_ISOIS-EPIHI_L2-HET-RATES10. The 10 s HET data of particle Counts, Flux and Count Rate for electrons, H, He and NEUT_DET for sides A and B, and for ranges R1 – R7.

2.3.2 FILE: PSP_ISOIS-EPIHI_L2-HET-RATES300

This file provides the 300 s rates of energetic particle Counts, Flux (cm^{-2} sr^{-1} sec^{-1} MeV^{-1}) and Count Rate (counts/s) for CNO, FeGroup and NetoSi ions for ranges R1 – R7 of the High Energy Telescope (HET) for sides A and B. The variables (summarized in Table 2.3.2) are named as: <side>_<species>_<quantity> for those quantities independent of range. Here, <side> stands for A or B; <species> stands for the particle species (CNO_SECT, FeGroup_SECT and NetoSi_SECT), and <quantity> represents Counts (not used in the variable names, in general), Flux or Rate.
Examples: A_CNO_SECT (measured quantity is "counts"); A_FeGroup_SECT_Flux; A_NetoSi_SECT_Rate.

Side	Quantity	CNO_SECT			FeGroup_SECT			NetoSi_SECT		
		E-bins	E-range (MeV/nuc)	Sectors (bins)	E-bins	E-range (MeV/nuc)	Sectors (bins)	E-bins	E-range (MeV/nuc)	Sectors (bins)
A/B	Count	2	36 – 68	0 – 8 (9)	1	81 – 81	0 – 8 (9)	1	57 – 57	0 – 8 (9)
	Flux	2	36 – 68	0 – 8 (9)	1 1	81 – 81	0 – 8 (9)	1 1	57 – 57	0 – 8 (9)
	Count Rate	2	36 – 68	0 – 8 (9)	1 1	81 – 81	0 – 8 (9)	1 1	57 – 57	0 – 8 (9)
	ENB_SECT - measured quantity is Count; Size 1 X 25; E-bins: 1; E-range: 12 - 12; Sectors: 0 -8 (9).									

Table 2.3.2: PSP_ISOIS-EPIHI_L2-HET-RATES300. The 300 s cadence HET data of particle Counts, Flux and Count Rate for CNO, FeGroup and NetoSi ions for sides A and B, and integrated over ranges R1 – R7.

2.3.3 FILE: PSP_ISOIS-EPIHI_L2-HET-RATES3600

In this file, the 3600 s cadence data of particle Counts, Flux (cm^{-2} sr^{-1} sec^{-1} MeV^{-1}) and Count Rate (counts/s) measured by High Energy Telescope (HET) are available. The names of variables (summarized in Tables 2.3.3 – 2.3.11) follow the general pattern: <side>_<species>_<quantity>, where, <side> stands for A or B; <species> stands for the particle species (Al, Ar, C, etc., in column 2); and <quantity> represents Counts, Flux or Count Rate. Note that "Count" is not used in the variable names, in general. Variable names without ranges (e.g., A_C) or with double digit range (e.g., R17) have the values integrated over all the available ranges (R1 to R7, in general: e.g., B_H_SECT_Flux has values averaged over R1 – R7 in Table 2.3.3).
Examples: A_C, NEUT1, NEUT2_DET, (measured quantity is "counts"); B_FeGroup_SECT_Flux; PENA_C_Rate; R1A_32to50_Flux.

Side	Species	Count			Flux			Count Rate		
		Size (bins)	Range SECT (bins)	Energy (MeV/nuc)	Size (bins)	Range SECT (bins)	Energy (MeV/nuc)	Size (bins)	Range SECT (bins)	Energy (MeV/nuc)
A/B	Al	15	–	21 – 236	15	–	21 – 236	15	–	21 – 236
	Ar	15	–	25 – 280	15	–	25 – 280	15	–	25 – 280
	C	15	–	12 – 140	15	–	12 – 140	15	–	12 – 140
	CNO_SECT	2x25 (2 bins)	R17 0 – 8 (9)	36 – 68	2x25	R17 0 – 8 (9)	36 – 68	2x25	R17 0 – 8 (9)	36 – 68
	Ca	15	–	25 – 280	15	–	25 – 280	15	–	25 – 280
	Cr	16	–	25 – 333	16	–	25 – 333	16		25 – 333
	Electrons	19	–	0 – 10	19	–	0 – 10	19	–	0 – 10
	Electron_SECT	2x25 (2 bins)	R17 0 – 8 (9)	2 – 3	2x25	R17 0 – 8 (9)	3 – 3	2x25	R17 0 – 8 (9)	2 – 3
	Fe	15	–	29 - 333	15	–	29 – 333	15	–	29 – 333
	FeGroup_SECT	1x25 (1 bin)	R17 0 – 8 (9)	81 – 81	1x25 (1 bin)	R17 0 – 8 (9)	81 – 81	1x25 (1 bin)	R17 0 – 8 (9)	81 – 81
	H	15	–	7 – 83	15	–	7 – 83	15	–	7 – 83
	H_SECT	2x25 (2 bins)	R17 0 – 8 (9)	18 – 34	2x25 (2 bins)	R17 0 – 8 (9)	18 – 34	2x25 (2 bins)	R17 0 – 8 (9)	18 – 34
	He	16	–	7 – 99	16	–	7 – 99	16	–	7 - 99
	He_SECT	2x25 (2 bins)	R17 0 – 8 (9)	18 – 34	2x25 (2 bins)	R17 0 – 8 (9)	18 – 34	2x25 (2 bins)	R17 0 – 8 (9)	18 – 34
	Mg	15	–	21 – 236	15	–	21 – 236	15	–	21 – 236
	N	15	–	12 – 140	15	–	12 – 140	15	–	12 – 140
	Na	15	–	18 – 198	15	–	18 – 198	15	–	18 – 198
	Ne	15	–	18 – 198	15	–	18 – 198	15	–	18 – 198
	NetoSi_SECT	1x25 (1 bin)	R17 0 – 8 (9)	57 – 57	1x25 (1 bin)	R17 0 – 8 (9)	57 – 57	1x25 (1 bin)	R17 0 – 8 (9)	57 – 57
	Ni	15	–	29 - 333	15	–	29 – 333	15	–	29 – 333
	O	15	–	15 - 167	15	–	15 – 167	15	–	15 – 167
	S	16	–	21 – 280	16	–	21 – 280	16	–	21 – 280
	Si	15	–	21 – 236	15	–	21 – 236	15	–	21 – 236
	NEUT1	35x21	–	0 – 495	–	–	–	35x21	–	0 – 495
	NEUT2_DET	35x6	–	0 – 495	–	–	–	35x6	–	0 – 495

Table 2.3.3: PSP_ISOIS-EPIHI_L2-HET-RATES3600. The 3600 s cadence HET data of the particle Counts, Flux and Count Rates for different particle species for sides A and B and ranges R1 – R7. R17 implies integration of the measured values over ranges R1 – R7.

Side	Species	Count		Count Rate	
		Size (bins)	Energy (MeV/nuc)	Size (bins)	Energy (MeV/nuc)
A/B	PENx_C	9	45 – 583	9	45 – 583
	PENx_Fe	9	108 – 793	9	108 – 793
	PENx_H	9	27 – 521	9	27 – 521
	PENx_He	9	27 – 521	9	27 – 521
	PENx_Mg	9	64 – 646	9	64 – 646
	PENx_N	9	45 – 583	9	45 – 583
	PENx_Ne	8	64 – 612	8	64 – 612
	PENx_O	9	54 – 612	9	54 – 612
	PENx_Si	9	76 – 687	9	76 – 687

Table 2.3.4: PSP_ISOIS-EPIHI_L2-HET-RATES3600 (contd.). Here, 'x' stands for sides A & B.

Side	Species	Count		Flux		Count Rate	
		Size (bins)	Energy (MeV/nuc)	Size (bins)	Energy (MeV/nuc)	Size (bins)	Energy (MeV/nuc)
A/B	xxx_29to32	6	14 – 538	6	14 – 538	6	14 – 538
	xxx_32to50	6	14 – 538	6	14 – 538	6	14 – 538
	xxx_Al	11	10 – 476	11	10 – 476	11	10 – 476
	xxx_Ar	11	11 – 484	11	11 – 484	11	11 – 484
	xxx_C	12	6 – 463	12	6 – 463	12	6 – 463
	xxx_Ca	11	11 – 484	11	11 – 484	11	11 – 484
	xxx_Cr	12	11 – 495	12	11 – 495	12	11 – 495
	xxx_Electrons	15	0 – 433	15	0 – 433	15	0 – 433
	xxx_Fe	11	14 – 495	11	14 – 495	11	14 – 495
	xxx_H	11	4 – 447	11	4 – 447	11	4 – 447
	xxx_He	12	4 – 450	12	4 – 450	12	4 – 450
	xxx_He_BIN xxx_He_BIN (MASS)	5x16 (5) 16 bins 0 – 15 seg	9 – 32 – –	– – –	– – –	– – –	– – –
	xxx_Mg	11	10 – 476	11	10 – 476	11	10 – 476
	xxx_N	12	6 – 463	12	6 – 463	12	6 – 463
	xxx_Na	11	8 – 469	11	8 – 469	11	8 – 469
	xxx_Ne	11	8 – 469	11	8 – 469	11	8 – 469
	xxx_Ne_BIN xxx_Ne_BIN (MASS)	4x8 (4) 8 bins 0 – 7 seg	23 – 65 – –	– – –	– – –	– – –	– – –
	xxx_Ni	12	14 – 507	12	14 – 507	12	14 – 507
	xxx_O	11	7 – 463	11	7 – 463	11	7 – 463
	xxx_S	12	10 – 484	12	10 – 484	12	10 – 484
	xxx_Si	11	10 – 476	11	10 – 476	11	10 – 476
	xxx_gt50	6	14 – 538	6	14 – 538	6	14 – 538

Table 2.3.5: PSP_ISOIS-EPIHI_L2-HET-RATES3600 (contd.). Here 'xxx' stands for R1A & R1B.

Side	Species	Count		Flux		Count Rate	
		Size (bins)	Energy (MeV/nuc)	Size (bins)	Energy (MeV/nuc)	Size (bins)	Energy (MeV/nuc)
A/B	xxx_29to32	5	23 – 538	5	23 – 538	5	23 – 538
	xxx_32to50	5	23 – 538	5	23 – 538	5	23 – 538
	xxx_Al	11	14 – 495	11	14 – 495	11	14 – 495
	xxx_Ar	11	19 – 521	11	19 – 521	11	19 – 521
	xxx_C	11	10 – 476	11	10 – 476	11	10 – 476
	xxx_Ca	11	19 – 521	11	19 – 521	11	19 – 521
	xxx_Cr	12	19 – 538	12	19 – 538	12	19 – 538
	xxx_Electrons	15	0 – 433	15	0 – 433	15	0 – 433
	xxx_Fe	11	23 – 538	11	23 – 538	11	23 – 538
	xxx_H	11	6 – 457	11	6 – 457	11	6 – 457
	xxx_He	12	6 – 463	12	6 – 463	12	6 – 463
	xxx_He_BIN xxx_He_BIN (MASS)	4x16 (4) 16 bins 0 – 15 seg	16 – 46 – –	– – –	– – –	– – –	– – –
	xxx_Mg	11	14 – 495	11	14 – 495	11	14 – 495
	xxx_N	11	10 – 476	11	10 – 476	11	10 – 476
	xxx_Na	11	14 – 495	11	14 – 495	11	14 – 495
	xxx_Ne	11	14 – 495	11	14 – 495	11	14 – 495
	xxx_Ne_BIN xxx_Ne_BIN (MASS)	4x8 (4) 8 bins 0 – 7 seg	32 – 92 – –	– – –	– – –	– – –	– – –
	xxx_Ni	11	23 – 538	11	23 – 538	11	23 – 538
	xxx_O	11	11 – 484	11	11 – 484	11	11 – 484
	xxx_S	12	16 – 521	12	16 – 521	12	16 – 521
	xxx_Si	11	16 – 507	11	16 – 507	11	16 – 507
	xxx_gt50	5	23 – 538	5	23 – 538	5	23 – 538

Table 2.3.6: PSP_ISOIS-EPIHI_L2-HET-RATES3600 (contd.). Here, 'xxx' stands for R2A and R2B.

Side	Species	Count		Flux		Count Rate	
		Size (bins)	Energy (MeV/nuc)	Size (bins)	Energy (MeV/nuc)	Size (bins)	Energy (MeV/nuc)
A/B	xxx_29to32	5	38 – 612	5	38 – 612	5	38 – 612
	xxx_32to50	5	38 – 612	5	38 – 612	5	38 – 612
	xxx_Al	9	23 – 507	9	23 – 507	9	23 – 507
	xxx_Ar	9	32 – 538	9	32 – 538	9	32 – 538
	xxx_C	9	16 – 484	9	16 – 484	9	16 – 484
	xxx_Ca	9	32 – 538	9	32 – 538	9	32 – 538
	xxx_Cr	10	32 – 559	10	32 – 559	10	32 – 559
	xxx_Electrons	13	1 – 433	13	1 – 433	13	1 – 433
	xxx_Fe	10	32 – 559	10	32 – 559	10	32 – 559
	xxx_H	10	8 – 463	10	8 – 463	10	8 – 463
	xxx_He	11	8 – 469	11	8 – 469	11	8 – 469
	xxx_He_BIN xxx_He_BIN (MASS)	4x16 (4) 16 bins 0 - 15 seg	23 – 65 – –	– – –	– – –	– – –	– – –
	xxx_Mg	9	23 – 507	9	23 – 507	9	23 – 507
	xxx_N	9	16 – 484	9	16 – 484	9	16 – 484
	xxx_Na	10	19 – 507	10	19 – 507	10	19 – 507
	xxx_Ne	10	19 – 507	10	19 – 507	10	19 – 507
	xxx_Ne_BIN xxx_Ne_BIN (MASS)	4x8 (4) 8 bins 0 - 7 seg	46 – 130 – –	– – –	– – –	– – –	– – –
	xxx_Ni	10	32 – 559	10	32 – 559	10	32 – 559
	xxx_O	9	19 – 495	9	19 – 495	9	19 – 495
	xxx_S	10	27 – 538	10	27 – 538	10	27 – 538
	xxx_Si	9	27 – 521	9	27 – 521	9	27 – 521
	xxx_gt50	5	38 – 612	5	38 – 612	5	38 – 612

Table 2.3.7: PSP_ISOIS-EPIHI_L2-HET-RATES3600 (contd.). Here, ‘xxx’ stands for R3A and R3B.

Side	Species	Count		Flux		Count Rate	
		Size (bins)	Energy (MeV/nuc)	Size (bins)	Energy (MeV/nuc)	Size (bins)	Energy (MeV/nuc)
A/B	xxx_29to32	5	38 – 612	5	38 – 612	5	38 – 612
	xxx_32to50	5	38 – 612	5	38 – 612	5	38 – 612
	xxx_Al	9	27 – 521	9	27 – 521	9	27 – 521
	xxx_Ar	8	38 – 538	8	38 – 538	8	38 – 538
	xxx_C	9	19 – 495	9	19 – 495	9	19 – 495
	xxx_Ca	8	38 – 538	8	38 – 538	8	38 – 538
	xxx_Cr	9	38 – 559	9	38 – 559	9	38 – 559
	xxx_Electrons	12	1 – 434	12	1 – 434	12	1 – 434
	xxx_Fe	8	45 – 559	8	45 – 559	8	45 – 559
	xxx_H	8	11 – 463	8	11 – 463	8	11 – 463
	xxx_He	9	11 – 469	9	11 – 469	9	11 – 469
	xxx_He_BIN xxx_He_BIN (MASS)	3x16 (3) 16 bins 0 - 15 seg	32 – 65 – –	– – –	– – –	– – –	– – –
	xxx_Mg	9	27 – 521	9	27 – 521	9	27 – 521
	xxx_N	9	19 – 495	9	19 – 495	9	19 – 495
	xxx_Na	8	27 – 507	8	27 – 507	8	27 – 507
	xxx_Ne	8	27 – 507	8	27 – 507	8	27 – 507
	xxx_Ne_BIN xxx_Ne_BIN (MASS)	3x8 (3) 8 bins 0 - 7 seg	65 – 130 – –	– – –	– – –	– – –	– – –
	xxx_Ni	9	45 – 583	9	45 – 583	9	45 – 583
	xxx_O	8	23 – 495	8	23 – 495	8	23 – 495
	xxx_S	9	32 – 538	9	32 – 538	9	32 – 538
	xxx_Si	9	32 – 538	9	32 – 538	9	32 – 538
	xxx_gt50	5	38 – 612	5	38 – 612	5	38 – 612

Table 2.3.8: PSP_ISOIS-EPIHI_L2-HET-RATES3600 (contd.). Here, ‘xxx’ stands for R4A and R4B.

Side	Species	Count		Flux		Count Rate	
		Size (bins)	Energy (MeV/nuc)	Size (bins)	Energy (MeV/nuc)	Size (bins)	Energy (MeV/nuc)
A/B	xxx_29to32	4	64 – 612	4	64 – 612	4	64 – 612
	xxx_32to50	4	64 – 612	4	64 – 612	4	64 – 612
	xxx_Al	9	32 – 538	9	32 – 538	9	32 – 538
	xxx_Ar	8	45 – 559	8	45 – 559	8	45 – 559
	xxx_C	8	23 – 495	8	23 – 495	8	23 – 495
	xxx_Ca	8	45 – 559	8	45 – 559	8	45 – 559
	xxx_Cr	9	45 – 583	9	45 – 583	9	45 – 583
	xxx_Electrons	11	1 – 435	11	1 – 435	11	1 – 435
	xxx_Fe	8	54 – 583	8	54 – 583	8	54 – 583
	xxx_H	8	14 – 469	8	14 – 469	8	14 – 469
	xxx_He	9	14 – 476	9	14 – 476	9	14 – 476
	xxx_He_BIN xxx_He_BIN (MASS)	3x16 (3) 16 bins 0 - 15 seg	32 – 65 – –	– – –	– – –	– – –	– – –
	xxx_Mg	9	32 – 538	9	32 – 538	9	32 – 538
	xxx_N	8	23 – 495	8	23 – 495	8	23 – 495
	xxx_Na	8	32 – 521	8	32 – 521	8	32 – 521
	xxx_Ne	8	32 – 521	8	32 – 521	8	32 – 521
	xxx_Ne_BIN xxx_Ne_BIN (MASS)	2x8 (2) 8 bins 0 - 7 seg	92 – 130 – –	– – –	– – –	– – –	– – –
	xxx_Ni	9	54 – 612	9	54 – 612	9	54 – 612
	xxx_O	8	27 – 507	8	27 – 507	8	27 – 507
	xxx_S	9	38 – 559	9	38 – 559	9	38 – 559
	xxx_Si	8	38 – 538	8	38 – 538	8	38 – 538
	xxx_gt50	4	64 – 612	4	64 – 612	4	64 – 612

Table 2.3.9: PSP_ISOIS-EPIHI_L2-HET-RATES3600 (contd.). Here, 'xxx' stands for R5A and R5B.

Side	Species	Count		Flux		Count Rate	
		Size (bins)	Energy (MeV/nuc)	Size (bins)	Energy (MeV/nuc)	Size (bins)	Energy (MeV/nuc)
A/B	xxx_29to32	4	64 – 612	4	64 – 612	4	64 – 612
	xxx_32to50	4	64 – 612	4	64 – 612	4	64 – 612
	xxx_Al	8	38 – 538	8	38 – 538	8	38 – 538
	xxx_Ar	9	45 – 583	9	45 – 583	9	45 – 583
	xxx_C	8	27 – 507	8	27 – 507	8	27 – 507
	xxx_Ca	9	45 – 583	9	45 – 583	9	45 – 583
	xxx_Cr	10	45 – 612	10	45 – 612	10	45 – 612
	xxx_Electrons	11	1 – 435	11	1 – 435	11	1 – 435
	xxx_Fe	9	54 – 612	9	54 – 612	9	54 – 612
	xxx_H	8	14 – 469	8	14 – 469	8	14 – 469
	xxx_He	9	14 – 476	9	14 – 476	9	14 – 476
	xxx_He_BIN xxx_He_BIN (MASS)	3x16 (3) 16 bins 0 - 15 seg	32 – 65 – –	– – –	– – –	– – –	– – –
	xxx_Mg	8	38 – 538	8	38 – 538	8	38 – 538
	xxx_N	8	27 – 507	8	27 – 507	8	27 – 507
	xxx_Na	8	38 – 538	8	38 – 538	8	38 – 538
	xxx_Ne	8	38 – 538	8	38 – 538	8	38 – 538
	xxx_Ne_BIN xxx_Ne_BIN (MASS)	3x8 (3) 8 bins 0 - 7 seg	92 – 184 – –	– – –	– – –	– – –	– – –
	xxx_Ni	9	54 – 612	9	54 – 612	9	54 – 612
	xxx_O	8	32 – 521	8	32 – 521	8	32 – 521
	xxx_S	9	45 – 583	9	45 – 583	9	45 – 583
	xxx_Si	8	45 – 559	8	45 – 559	8	45 – 559
	xxx_gt50	4	64 – 612	4	64 – 612	4	64 – 612

Table 2.3.10: PSP_ISOIS-EPIHI_L2-HET-RATES3600 (contd.). Here, ‘xxx’ stands for R6A and R6B.

Side	Species	Count		Flux		Count Rate	
		Size (bins)	Energy (MeV/nuc)	Size (bins)	Energy (MeV/nuc)	Size (bins)	Energy (MeV/nuc)
A/B	xxx_29to32	4	64 – 612	4	64 – 612	4	64 – 612
	xxx_32to50	4	64 – 612	4	64 – 612	4	64 – 612
	xxx_Al	8	45 – 559	8	45 – 559	8	45 – 559
	xxx_Ar	7	64 – 583	7	64 – 583	7	64 – 583
	xxx_C	7	32 – 507	7	32 – 507	7	32 – 507
	xxx_Ca	7	64 – 583	7	64 – 583	7	64 – 583
	xxx_Cr	8	64 – 612	8	64 – 612	8	64 – 612
	xxx_Electrons	11	1 – 436	11	1 – 436	11	1 – 436
	xxx_Fe	8	64 – 612	8	64 – 612	8	64 – 612
	xxx_H	8	16 – 476	8	16 – 476	8	16 – 476
	xxx_He	9	16 – 484	9	16 – 484	9	16 – 484
	xxx_He_BIN xxx_He_BIN (MASS)	2x16 (2) 16 bins 0 - 15 seg	46 – 65 – –	– – –	– – –	– – –	– – –
	xxx_Mg	8	45 – 559	8	45 – 559	8	45 – 559
	xxx_N	7	32 – 507	7	32 – 507	7	32 – 507
	xxx_Na	8	38 – 538	8	38 – 538	8	38 – 538
	xxx_Ne	8	38 – 538	8	38 – 538	8	38 – 538
	xxx_Ne_BIN xxx_Ne_BIN (MASS)	3x8 (3) 8 bins 0 - 7 seg	92 – 184 – –	– – –	– – –	– – –	– – –
	xxx_Ni	8	64 – 612	8	64 – 612	8	64 – 612
	xxx_O	7	38 – 521	7	38 – 521	7	38 – 521
	xxx_S	8	54 – 583	8	54 – 583	8	54 – 583
	xxx_Si	7	54 – 559	7	54 – 559	7	54 – 559
	xxx_gt50	4	64 – 612	4	64 – 612	4	64 – 612

Table 2.3.11: PSP_ISOIS-EPIHI_L2-HET-RATES3600 (contd.). Here, ‘xxx’ stands for R7A and R7B.

2.3.4 FILE: PSP_ISOIS-EPIHI_L2-HET-RATES60

This file contains the 60-second cadence data of particle Counts, Flux (cm^{-2} sr^{-1} sec^{-1} MeV^{-1}) and Count Rate (counts/s) for Al, Ar, C, Ca, Cr, Electrons, Fe, H, He, Mg, N, Na, Ne, Ni, O, S and Si ions for ranges R1 – R7) of the High Energy Telescope (HET) for sides A and B. The measured values are summarized in Tables 2.3.12 – 2.3.20. The variable names follow the structure: <side>_<species>_<quantity>, where, <side> stands for A or B; <species> stands for the particle species; and <quantity> represents Counts (not used in the variable names, in general), Flux or Count Rate. Variable names without ranges (e.g., A_C) or with double digit range (e.g., R17) have their values integrated over all the available ranges (R1 to R7, in general).
Examples: A_Fe (measured quantity is "counts"); B_Electron_SECT_Flux; PENB_Mg_Flux; R7A_Ni_Rate.

Side	Species	Count			Flux			Count Rate		
		Size (bins)	Range SECT (bins)	Energy (MeV/nuc)	Size (bins)	Range SECT (bins)	Energy (MeV/nuc)	Size (bins)	Range SECT (bins)	Energy (MeV/nuc)
A/B	Al	15	–	21 – 236	15	–	21 – 236	15	–	21 – 236
	Ar	15	–	25 – 280	15	–	25 – 280	15	–	25 – 280
	C	15	–	12 – 140	15	–	12 – 140	15	–	12 – 140
	Ca	15	–	25 – 280	15	–	25 – 280	15	–	25 – 280
	Cr	16	–	25 – 333	16	–	25 – 333	16		25 – 333
	Electrons	19	–	0 – 10	19	–	0 – 10	19	–	0 – 10
	Electron_SECT	2x25 (2 bins)	R17 0 – 8 (9)	2 – 3	2x25	R17 0 – 8 (9)	3 – 3	2x25	R17 0 – 8 (9)	2 – 3
	Fe	15	–	29 – 333	15	–	29 – 333	15	–	29 – 333
	H	15	–	7 – 83	15	–	7 – 83	15	–	7 – 83
	H_SECT	2x25 (2 bins)	R17 0 – 8 (9)	18 – 34	2x25 (2 bins)	R17 0 – 8 (9)	18 – 34	2x25 (2 bins)	R17 0 – 8 (9)	18 – 34
	He	16	–	7 – 99	16	–	7 – 99	16	–	7 – 99
	He_SECT	2x25 (2 bins)	R17 0 – 8 (9)	18 – 34	2x25 (2 bins)	R17 0 – 8 (9)	18 – 34	2x25 (2 bins)	R17 0 – 8 (9)	18 – 34
	Mg	15	–	21 – 236	15	–	21 – 236	15	–	21 – 236
	N	15	–	12 – 140	15	–	12 – 140	15	–	12 – 140
	Na	15	–	18 – 198	15	–	18 – 198	15	–	18 – 198
	Ne	15	–	18 – 198	15	–	18 – 198	15	–	18 – 198
	Ni	15	–	29 – 333	15	–	29 – 333	15	–	29 – 333
	O	15	–	15 – 167	15	–	15 – 167	15	–	15 – 167
	S	16	–	21 – 280	16	–	21 – 280	16	–	21 – 280
	Si	15	–	21 – 236	15	–	21 – 236	15	–	21 – 236

Table 2.3.12: PSP_ISOIS-EPIHI_HET-RATES60. The HET 60 s cadence data for various particle species. R17 implies integration of the measured values over ranges R1 – R7.

Side	Species	Count		Count Rate	
		Size (bins)	Energy (MeV/nuc)	Size (bins)	Energy (MeV/nuc)
A/B	PENx_C	9	45 – 583	9	45 – 583
	PENx_Fe	9	108 – 793	9	108 – 793
	PENx_H	9	27 – 521	9	27 – 521
	PENx_He	9	27 – 521	9	27 – 521
	PENx_Mg	9	64 – 646	9	64 – 646
	PENx_N	9	45 – 583	9	45 – 583
	PENx_Ne	8	64 – 612	8	64 – 612
	PENx_O	9	54 – 612	9	54 – 612
	PENx_Si	9	76 – 687	9	76 – 687

Table 2.3.13: PSP_ISOIS-EPIHI_L2-HET-RATES60 (contd.). Here, 'x' stands for sides A & B.

Side	Species	Count		Flux		Count Rate	
		Size (bins)	Energy (MeV/nuc)	Size (bins)	Energy (MeV/nuc)	Size (bins)	Energy (MeV/nuc)
A/B	xxx_29to32	6	14 – 538	6	14 – 538	6	14 – 538
	xxx_32to50	6	14 – 538	6	14 – 538	6	14 – 538
	xxx_Al	11	10 – 476	11	10 – 476	11	10 – 476
	xxx_Ar	11	11 – 484	11	11 – 484	11	11 – 484
	xxx_C	12	6 – 463	12	6 – 463	12	6 – 463
	xxx_Ca	11	11 – 484	11	11 – 484	11	11 – 484
	xxx_Cr	12	11 – 495	12	11 – 495	12	11 – 495
	xxx_Electrons	15	0 – 433	15	0 – 433	15	0 – 433
	xxx_Fe	11	14 – 495	11	14 – 495	11	14 – 495
	xxx_H	11	4 – 447	11	4 – 447	11	4 – 447
	xxx_He	12	4 – 450	12	4 – 450	12	4 – 450
	xxx_Mg	11	10 – 476	11	10 – 476	11	10 – 476
	xxx_N	12	6 – 463	12	6 – 463	12	6 – 463
	xxx_Na	11	8 – 469	11	8 – 469	11	8 – 469
	xxx_Ne	11	8 – 469	11	8 – 469	11	8 – 469
	xxx_Ni	12	14 – 507	12	14 – 507	12	14 – 507
	xxx_O	11	7 – 463	11	7 – 463	11	7 – 463
	xxx_S	12	10 – 484	12	10 – 484	12	10 – 484
	xxx_Si	11	10 – 476	11	10 – 476	11	10 – 476
	xxx_gt50	6	14 – 538	6	14 – 538	6	14 – 538

Table 2.3.14: PSP_ISOIS-EPIHI_HET-RATES60 (contd.). Here, 'xxx' stands for R1A and R1B.

Side	Species	Count		Flux		Count Rate	
		Size (bins)	Energy (MeV/nuc)	Size (bins)	Energy (MeV/nuc)	Size (bins)	Energy (MeV/nuc)
A/B	xxx_29to32	5	23 – 538	5	23 – 538	5	23 – 538
	xxx_32to50	5	23 – 538	5	23 – 538	5	23 – 538
	xxx_Al	11	14 – 495	11	14 – 495	11	14 – 495
	xxx_Ar	11	19 – 521	11	19 – 521	11	19 – 521
	xxx_C	11	10 – 476	11	10 – 476	11	10 – 476
	xxx_Ca	11	19 – 521	11	19 – 521	11	19 – 521
	xxx_Cr	12	19 – 538	12	19 – 538	12	19 – 538
	xxx_Electrons	15	0 – 433	15	0 – 433	15	0 – 433
	xxx_Fe	11	23 – 538	11	23 – 538	11	23 – 538
	xxx_H	11	6 – 457	11	6 – 457	11	6 – 457
	xxx_He	12	6 – 463	12	6 – 463	12	6 – 463
	xxx_He_BIN xxx_He_BIN (MASS)	4x16 (4) 16 bins 0 – 15 seg	16 – 46 – –	– – –	– – –	– – –	– – –
	xxx_Mg	11	14 – 495	11	14 – 495	11	14 – 495
	xxx_N	11	10 – 476	11	10 – 476	11	10 – 476
	xxx_Na	11	14 – 495	11	14 – 495	11	14 – 495
	xxx_Ne	11	14 – 495	11	14 – 495	11	14 – 495
	xxx_Ne_BIN xxx_Ne_BIN (MASS)	4x8 (4) 8 bins 0 – 7 seg	32 – 92 – –	– – –	– – –	– – –	– – –
	xxx_Ni	11	23 – 538	11	23 – 538	11	23 – 538
	xxx_O	11	11 – 484	11	11 – 484	11	11 – 484
	xxx_S	12	16 – 521	12	16 – 521	12	16 – 521
	xxx_Si	11	16 – 507	11	16 – 507	11	16 – 507
	xxx_gt50	5	23 – 538	5	23 – 538	5	23 – 538

Table 2.3.15: PSP_ISOIS-EPIHI_L2-HET-RATES60 (contd.). Here, 'xxx' stands for R2A and R2B.

Side	Species	Count		Flux		Count Rate	
		Size (bins)	Energy (MeV/nuc)	Size (bins)	Energy (MeV/nuc)	Size (bins)	Energy (MeV/nuc)
A/B	xxx_29to32	5	38 – 612	5	38 – 612	5	38 – 612
	xxx_32to50	5	38 – 612	5	38 – 612	5	38 – 612
	xxx_Al	9	23 – 507	9	23 – 507	9	23 – 507
	xxx_Ar	9	32 – 538	9	32 – 538	9	32 – 538
	xxx_C	9	16 – 484	9	16 – 484	9	16 – 484
	xxx_Ca	9	32 – 538	9	32 – 538	9	32 – 538
	xxx_Cr	10	32 – 559	10	32 – 559	10	32 – 559
	xxx_Electrons	13	1 – 433	13	1 – 433	13	1 – 433
	xxx_Fe	10	32 – 559	10	32 – 559	10	32 – 559
	xxx_H	10	8 – 463	10	8 – 463	10	8 – 463
	xxx_He	11	8 – 469	11	8 – 469	11	8 – 469
	xxx_He_BIN xxx_He_BIN (MASS)	4x16 (4) 16 bins 0 – 15 seg	23 – 65 – –	– – –	– – –	– – –	– – –
	xxx_Mg	9	23 – 507	9	23 – 507	9	23 – 507
	xxx_N	9	16 – 484	9	16 – 484	9	16 – 484
	xxx_Na	10	19 – 507	10	19 – 507	10	19 – 507
	xxx_Ne	10	19 – 507	10	19 – 507	10	19 – 507
	xxx_Ne_BIN xxx_Ne_BIN (MASS)	4x8 (4) 8 bins 0 – 7 seg	46 – 130 – –	– – –	– – –	– – –	– – –
	xxx_Ni	10	32 – 559	10	32 – 559	10	32 – 559
	xxx_O	9	19 – 495	9	19 – 495	9	19 – 495
	xxx_S	10	27 – 538	10	27 – 538	10	27 – 538
	xxx_Si	9	27 – 521	9	27 – 521	9	27 – 521
	xxx_gt50	5	38 – 612	5	38 – 612	5	38 – 612

Table 2.3.16: PSP_ISOIS-EPIHI_L2-HET-RATES60 (contd.). Here, 'xxx' stands for R3A and R3B.

Side	Species	Count		Flux		Count Rate	
		Size (bins)	Energy (MeV/nuc)	Size (bins)	Energy (MeV/nuc)	Size (bins)	Energy (MeV/nuc)
A/B	xxx_29to32	5	38 – 612	5	38 – 612	5	38 – 612
	xxx_32to50	5	38 – 612	5	38 – 612	5	38 – 612
	xxx_Al	9	27 – 521	9	27 – 521	9	27 – 521
	xxx_Ar	8	38 – 538	8	38 – 538	8	38 – 538
	xxx_C	9	19 – 495	9	19 – 495	9	19 – 495
	xxx_Ca	8	38 – 538	8	38 – 538	8	38 – 538
	xxx_Cr	9	38 – 559	9	38 – 559	9	38 – 559
	xxx_Electrons	12	1 – 434	12	1 – 434	12	1 – 434
	xxx_Fe	8	45 – 559	8	45 – 559	8	45 – 559
	xxx_H	8	11 – 463	8	11 – 463	8	11 – 463
	xxx_He	9	11 – 469	9	11 – 469	9	11 – 469
	xxx_He_BIN xxx_He_BIN (MASS)	3x16 (3) 16 bins 0 – 15 seg	32 – 65 – –	– – –	– – –	– – –	– – –
	xxx_Mg	9	27 – 521	9	27 – 521	9	27 – 521
	xxx_N	9	19 – 495	9	19 – 495	9	19 – 495
	xxx_Na	8	27 – 507	8	27 – 507	8	27 – 507
	xxx_Ne	8	27 – 507	8	27 – 507	8	27 – 507
	xxx_Ne_BIN xxx_Ne_BIN (MASS)	3x8 (3) 8 bins 0 – 7 seg	65 – 130 – –	– – –	– – –	– – –	– – –
	xxx_Ni	9	45 – 583	9	45 – 583	9	45 – 583
	xxx_O	8	23 – 495	8	23 – 495	8	23 – 495
	xxx_S	9	32 – 538	9	32 – 538	9	32 – 538
	xxx_Si	9	32 – 538	9	32 – 538	9	32 – 538
	xxx_gt50	5	38 – 612	5	38 – 612	5	38 – 612

Table 2.3.17: PSP_ISOIS-EPIHI_L2-HET-RATES60 (contd.). Here, 'xxx' stands for R4A and R4B.

Side	Species	Count		Flux		Count Rate	
		Size (bins)	Energy (MeV/nuc)	Size (bins)	Energy (MeV/nuc)	Size (bins)	Energy (MeV/nuc)
A/B	xxx_29to32	4	64 – 612	4	64 – 612	4	64 – 612
	xxx_32to50	4	64 – 612	4	64 – 612	4	64 – 612
	xxx_Al	9	32 – 538	9	32 – 538	9	32 – 538
	xxx_Ar	8	45 – 559	8	45 – 559	8	45 – 559
	xxx_C	8	23 – 495	8	23 – 495	8	23 – 495
	xxx_Ca	8	45 – 559	8	45 – 559	8	45 – 559
	xxx_Cr	9	45 – 583	9	45 – 583	9	45 – 583
	xxx_Electrons	11	1 – 435	11	1 – 435	11	1 – 435
	xxx_Fe	8	54 – 583	8	54 – 583	8	54 – 583
	xxx_H	8	14 – 469	8	14 – 469	8	14 – 469
	xxx_He	9	14 – 476	9	14 – 476	9	14 – 476
	xxx_He_BIN xxx_He_BIN (MASS)	3x16 (3) 16 bins 0 - 15 seg	32 – 65 – –	– – –	– – –	– – –	– – –
	xxx_Mg	9	32 – 538	9	32 – 538	9	32 – 538
	xxx_N	8	23 – 495	8	23 – 495	8	23 – 495
	xxx_Na	8	32 – 521	8	32 – 521	8	32 – 521
	xxx_Ne	8	32 – 521	8	32 – 521	8	32 – 521
	xxx_Ne_BIN xxx_Ne_BIN (MASS)	2x8 (2) 8 bins 0 - 7 seg	92 – 130 – –	– – –	– – –	– – –	– – –
	xxx_Ni	9	54 – 612	9	54 – 612	9	54 – 612
	xxx_O	8	27 – 507	8	27 – 507	8	27 – 507
	xxx_S	9	38 – 559	9	38 – 559	9	38 – 559
	xxx_Si	8	38 – 538	8	38 – 538	8	38 – 538
	xxx_gt50	4	64 – 612	4	64 – 612	4	64 – 612

Table 2.3.18: PSP_ISOIS-EPIHI_L2-HET-RATES60 (contd.). Here, 'xxx' stands for R5A and R5B.

Side	Species	Count		Flux		Count Rate	
		Size (bins)	Energy (MeV/nuc)	Size (bins)	Energy (MeV/nuc)	Size (bins)	Energy (MeV/nuc)
A/B	xxx_29to32	4	64 – 612	4	64 – 612	4	64 – 612
	xxx_32to50	4	64 – 612	4	64 – 612	4	64 – 612
	xxx_Al	8	38 – 538	8	38 – 538	8	38 – 538
	xxx_Ar	9	45 – 583	9	45 – 583	9	45 – 583
	xxx_C	8	27 – 507	8	27 – 507	8	27 – 507
	xxx_Ca	9	45 – 583	9	45 – 583	9	45 – 583
	xxx_Cr	10	45 – 612	10	45 – 612	10	45 – 612
	xxx_Electrons	11	1 – 435	11	1 – 435	11	1 – 435
	xxx_Fe	9	54 – 612	9	54 – 612	9	54 – 612
	xxx_H	8	14 – 469	8	14 – 469	8	14 – 469
	xxx_He	9	14 – 476	9	14 – 476	9	14 – 476
	xxx_He_BIN xxx_He_BIN (MASS)	3x16 (3) 16 bins 0 – 15 seg	32 – 65 – –	– – –	– – –	– – –	– – –
	xxx_Mg	8	38 – 538	8	38 – 538	8	38 – 538
	xxx_N	8	27 – 507	8	27 – 507	8	27 – 507
	xxx_Na	8	38 – 538	8	38 – 538	8	38 – 538
	xxx_Ne	8	38 – 538	8	38 – 538	8	38 – 538
	xxx_Ne_BIN xxx_Ne_BIN (MASS)	3x8 (3) 8 bins 0 – 7 seg	92 – 184 – –	– – –	– – –	– – –	– – –
	xxx_Ni	9	54 – 612	9	54 – 612	9	54 – 612
	xxx_O	8	32 – 521	8	32 – 521	8	32 – 521
	xxx_S	9	45 – 583	9	45 – 583	9	45 – 583
	xxx_Si	8	45 – 559	8	45 – 559	8	45 – 559
	xxx_gt50	4	64 – 612	4	64 – 612	4	64 – 612

Table 2.3.19: PSP_ISOIS-EPIHI_L2-HET-RATES60 (contd.). Here, 'xxx' stands for R6A and R6B.

Side	Species	Count		Flux		Count Rate	
		Size (bins)	Energy (MeV/nuc)	Size (bins)	Energy (MeV/nuc)	Size (bins)	Energy (MeV/nuc)
A/B	xxx_29to32	4	64 – 612	4	64 – 612	4	64 – 612
	xxx_32to50	4	64 – 612	4	64 – 612	4	64 – 612
	xxx_Al	8	45 – 559	8	45 – 559	8	45 – 559
	xxx_Ar	7	64 – 583	7	64 – 583	7	64 – 583
	xxx_C	7	32 – 507	7	32 – 507	7	32 – 507
	xxx_Ca	7	64 – 583	7	64 – 583	7	64 – 583
	xxx_Cr	8	64 – 612	8	64 – 612	8	64 – 612
	xxx_Electrons	11	1 – 436	11	1 – 436	11	1 – 436
	xxx_Fe	8	64 – 612	8	64 – 612	8	64 – 612
	xxx_H	8	16 – 476	8	16 – 476	8	16 – 476
	xxx_He	9	16 – 484	9	16 – 484	9	16 – 484
	xxx_He_BIN xxx_He_BIN (MASS)	2x16 (2) 16 bins 0 - 15 seg	46 – 65 – –	– – –	– – –	– – –	– – –
	xxx_Mg	8	45 – 559	8	45 – 559	8	45 – 559
	xxx_N	7	32 – 507	7	32 – 507	7	32 – 507
	xxx_Na	8	38 – 538	8	38 – 538	8	38 – 538
	xxx_Ne	8	38 – 538	8	38 – 538	8	38 – 538
	xxx_Ne_BIN xxx_Ne_BIN (MASS)	3x8 (3) 8 bins 0 - 7 seg	92 – 184 – –	– – –	– – –	– – –	– – –
	xxx_Ni	8	64 – 612	8	64 – 612	8	64 – 612
	xxx_O	7	38 – 521	7	38 – 521	7	38 – 521
	xxx_S	8	54 – 583	8	54 – 583	8	54 – 583
	xxx_Si	7	54 – 559	7	54 – 559	7	54 – 559
	xxx_gt50	4	64 – 612	4	64 – 612	4	64 – 612

Table 2.3.20: PSP_ISOIS-EPIHI_L2-HET-RATES60 (contd.). Here, ‘xxx’ stands for R7A and R7B.

2.3.5 FILE: PSP_ISOIS-EPIHI_L2-LET1-RATES10

This file contains the 10-second cadence data of particle Counts, Flux (cm^{-2} sr^{-1} sec^{-1} MeV^{-1}) and Count Rate (counts/s) for Electrons, H and He ions for various ranges (R1 – R7) of the Low Energy Telescope (LET1), for sides A and B. The measured values are summarized in Table 2.3.21. The variable names follow the pattern: <side>_<species>_<quantity>, where, <side> stands for A or B; <species> stands for the particle species; and <quantity> represents Counts (not used in the variable names, in general), Flux or Count Rate, for variables independent of range (R1, R2, etc.). The variables for different ranges has the structure: <range><side>_<species>_<quantity>. For electrons, the structure is: <Electrons>_<range><side>. Variable names without ranges (e.g., A_C) or with double digit range (e.g., R17) have the values integrated over all the available ranges (e.g., R1 to R7, in general).
Examples: A_Fe (measured quantity is "count"); Electrons_R6B_Rate; and R1A_He_Rate.

Side	Range	Quantity	Electrons		H		He	
			E-bins	E-range (MeV/nuc) (bins)	E-bins	E-range (MeV/nuc) (bins)	E-bins	E-range (MeV/nuc) (bins)
A/B		Count			16	1 - 12 (16)	20	1 - 25 (20)
		Flux			16	1 - 12 (16)	20	1 - 25 (20)
		Count Rate			16	1 - 12 (16)	20	1 - 25 (20)
	R1	Count			8	1 - 3 (8)	8	1 - 3 (8)
		Flux			8	1 - 3 (8)	8	1 - 3 (8)
		Count Rate			8	1 - 3 (8)	8	1 - 3 (8)
	R2	Count			13	2 - 12 (13)	13	2 - 15 (13)
		Flux			13	2 - 12 (13)	13	2 - 15 (13)
		Count Rate			13	2 - 12 (13)	13	2 - 15 (13)
	R3	Count	10	1 - 3 (10)				
		Flux						
		Count Rate	10	1 - 3 (10)				
	R4	Count	10	1 - 4 (10)				
		Flux						
		Count Rate	10	1 - 4 (10)				
	R5	Count	9	1 - 4 (9)				
		Flux						
		Count Rate	9	1 - 4 (9)				
	R6	Count	8	2 - 5 (8)			3	21 - 29 (3)
		Flux					3	21 - 29 (3)
		Count Rate	8	2 - 5 (8)			3	21 - 29 (3)
	R7	Count						
		Flux						
		Count Rate						

Table 2.3.21: PSP_ISOIS-EPIHI_L2-LET1-RATES10. The LET1 10 s data of various energetic particle species.

2.3.6 FILE: PSP_ISOIS-EPIHI_L2-LET1-RATES300

This file contains the 300 s cadence data of particle Counts, Flux (cm^{-2} sr^{-1} sec^{-1} MeV^{-1}) and Count Rate (counts/s) for various particle species for ranges R1 & R26 (integrated over ranges R2 to R6) measured by the Low Energy Telescope (LET1), for sides A and B. The measured values are summarized in Table 2.3.22. The variable nomenclature is: <range><side>_<species>_<quantity>, where, <range> denotes the range (R1 to R7), <side> stands for A or B; <species> takes one of the particle species; and <quantity> represents Counts (not used in variable names, in general), Flux or Count Rate. Variable names without ranges (e.g., A_C) or with double digit range (e.g., R26) have the values integrated over all the available ranges (e.g., R2 to R6).
Examples: R1B_NetoSi_SECT_Rate; R26A_CNO_SECT_Flux.

Side	Range	Quantity	CNO_SECT			FeGroup_SECT			NetoSi_SECT		
			E-bins	E-range (MeV/nuc)	Sectors (bins)	E-bins	E-range (MeV/nuc)	Sectors (bins)	E-bins	E-range (MeV/nuc)	Sectors (bins)
A/B	R1	Count	1	3 - 3	0 - 8 (9)	1	3 - 3	0 - 8 (9)	1	3 - 3	0 - 8 (9)
		Flux	1	3 - 3	0 - 8 (9)	1	3 - 3	0 - 8 (9)	1	3 - 3	0 - 8 (9)
		Count Rate	1	3 - 3	0 - 8 (9)	1	3 - 3	0 - 8 (9)	1	3 - 3	0 - 8 (9)
A/B	R26	Count	3	6 - 24	0 - 24 (25)	3	6 - 24	0 - 24 (25)	3	6 - 24	0 - 24 (25)
		Flux	3	6 - 24	0 - 24 (25)	3	6 - 24	0 - 24 (25)	3	6 - 24	0 - 24 (25)
		Count Rate	3	6 - 24	0 - 24 (25)	3	6 - 24	0 - 24 (25)	3	6 - 24	0 - 24 (25)
	R1 ENB_SECT - measured quantity is Counts; Size 3 x 9; E-bins: 3; E-range: 1 - 2 (MeV/nuc); Sectors: 0 - 8 (9).										
	R26 ENB_SECT - measured quantity is Counts; Size 4 x 25; E-bins: 4; E-range: 2 - 12 (MeV/nuc); Sectors: 0 - 24 (25).										

Table 2.3.22: PSP_ISOIS-EPIHI_L2-LET1-RATES300. The LET1 300 s cadence measurements of various energetic particle species for ranges R1 and integrated over ranges R2 – R6 (R26).

2.3.7 FILE: PSP_ISOIS-EPIHI_L2-LET1-RATES3600

This file contains the 3600 s cadence measurements of particle Counts, Count Rate (counts/sec) and Flux (cm^{-2} sr^{-1} sec^{-1} MeV^{-1}) for Al, Ar, C, Ca, Cr, Fe, H, He, Mg, N, Na, Ne, Ni, O, S and Si by the Low Energy Telescope (LET1), for sides A and B for different ranges (R1 – R6). The measured values are summarized in Tables 2.3.23 – 2.3.32 and the variables are named as: <side>_<species>_<quantity>. Here, <side> stands for A or B; <species> stands for the particle species; and <quantity> represents Counts (not used in variable names, in general), Flux or Rate. Variable names without ranges (e.g., A_C) or with double digit range (e.g., R35) have their values integrated over all the available ranges (e.g., R3 to R5).
Examples: A_C_Flux; PENB_C_Rate; R1A_32to50_Flux; Electrons_R5B.

Side	Species	Count		Flux		Count Rate	
		Size (bins)	Energy (MeV/nuc)	Size (bins)	Energy (MeV/nuc)	Size (bins)	Energy (MeV/nuc)
A/B	Al	28	1 – 118	28	1 – 118	28	1 – 118
	Ar	29	1 – 140	29	1 – 140	29	1 – 140
	C	27	1 – 99	27	1 – 99	27	1 – 99
	Ca	30	1 – 140	30	1 – 140	30	1 – 140
	Cr	31	1 – 140	31	1 – 140	31	1 – 140
	Fe	32	1 – 167	32	1 – 167	32	1 – 167
	H	25	1 – 42	25	1 – 42	25	1 – 42
	He	26	1 – 50	26	1 – 50	26	1 – 50
	Mg	28	1 – 118	28	1 – 118	28	1 – 118
	N	27	1 – 99	27	1 – 99	27	1 – 118
	Na	28	1 – 118	28	1 – 118	28	1 – 118
	Ne	28	1 – 118	28	1 – 118	28	1 – 118
	Ni	33	1 – 198	33	1 – 198	33	1 – 198
	O	28	1 – 118	28	1 – 118	33	1 – 118
	S	29	1 – 140	29	1 – 140	29	1 – 140
	Si	29	1 – 140	29	1 – 140	29	1 – 140

Table 2.3.23: PSP_ISOIS-EPIHI_L2-LET1-RATES3600. The 3600 s cadence LET1 data for various particle species for sides A and B.

Side	Species	Count		Count Rate	
		Size (bins)	Energy (MeV/nuc)	Size (bins)	Energy (MeV/nuc)
A/B	PENx_C	11	23 – 364	11	23 – 364
	PENx_Fe	11	45 – 471	11	45 – 471
	PENx_He	11	11 – 310	11	11 – 310
	PENx_Mg	10	38 – 408	10	38 – 408
	PENx_N	11	23 – 364	11	23 – 364
	PENx_Ne	11	27 – 384	11	27 – 384
	PENx_O	11	27 – 384	11	27 – 384
	PENx_Si	10	38 – 408	11	38 – 408

Table 2.3.24: PSP_ISOIS-EPIHI_L2-LET1-RATES3600 (contd.). Here ‘x’ denotes sides A & B.

Side	Species	Count			Flux			Count Rate		
		Size (bins)	Range SECT (bins)	Energy (MeV/nuc)	Size (bins)	Range SECT (bins)	Energy (MeV/nuc)	Size (bins)	Range SECT (bins)	Energy (MeV/nuc)
A/B	xxx_29to32	7	29 – 32	0 – 264	7	29 – 32	0 – 264	7	29 – 32	0 – 264
	xxx_32to50	7	32 – 50	0 – 264	7	32 – 50	0 – 264	7	32 – 50	0 – 264
	xxx_Al	14	–	1 – 260	14	–	1 – 260	14	–	1 – 260
	xxx_Ar	15	–	1 – 261	15	–	1 – 261	15	–	1 – 261
	xxx_C	12	–	1 – 259	12	–	1 – 259	12	–	1 – 259
	xxx_Ca	16	–	1 – 261	16	–	1 – 262	16	–	1 – 261
	xxx_CNO_SECT	1x9 (1 bin)	R1 0 – 8 (9)	3 – 3	1x9 (1 bin)	R1 0 – 8 (9)	3 – 3	1x9 (1 bin)	R1 0 – 8 (9)	3 – 3
	xxx_Cr	17	–	1 – 261	17	–	1 – 261	17	–	1 – 261
	xxx_Fe	17	–	1 – 261	17	–	1 – 261	17	–	1 – 261
	xxx_FeGroup_SECT	1x9 (1 bin)	R1 0 – 8 (9)	3 – 3	1x9 (1 bin)	R1 0 – 8 (9)	3 – 3	1x9 (1 bin)	R1 0 – 8 (9)	3 – 3
	xxx_H	12	–	0 – 258	12	–	0 – 258	12	–	0 – 258
	xxx_H_SECT	1x9 (1 bin)	R1 0 – 8 (9)	2 – 2	1x9 (1 bin)	R1 0 – 8 (9)	2 – 2	1x9 (1 bin)	R1 0 – 8 (9)	2 – 2
	xxx_He	12	–	0 – 258	12	–	0 – 258	12	–	0 – 258
	xxx_He_SECT	1x9 (1 bin)	R1 0 – 8 (9)	2 – 2	1x9 (1 bin)	R1 0 – 8 (9)	2 – 2	1x9 (1 bin)	R1 0–8 (9)	2 – 2
	xxx_He_BIN xxx_He_BIN (MASS)	5x16 (5) 16 bins 0 – 15 seg	– – –	1 – 3 – –	– – –	– – –	– – –	– – –	– – –	– – –
	xxx_Mg	14	–	1 – 260	14	–	1 – 260	14	–	1 – 260
	xxx_N	12	–	1 – 259	12	–	1 – 259	12	–	1 – 259
	xxx_Na	13	–	1 – 259	13	–	1 – 259	12	–	1 – 259
	xxx_Ne	13	–	1 – 259	13	–	1 – 259	13	–	1 – 259
	xxx_Ne_BIN xxx_Ne_BIN (MASS)	5x8 (5) 8 bins 0 - 7 seg	– – –	1 – 6 – –	– – –	– – –	– – –	– – –	– – –	– – –
	xxx_Ni	17	–	1 – 261	17	–	1 – 261	17	–	1 – 261
	xxx_O	13	–	1 – 259	13	–	1 – 259	13	–	1 – 259
	xxx_S	15	–	1 – 261	15	–	1 – 261	15	–	1 – 261
	xxx_Si	14	–	1 – 260	14	–	1 – 260	14	–	1 – 260
	xxx_NetoSi_SECT	1x9 (1 bin)	R1 0 – 8 (9)	3 – 3	1x9 (1 bin)	R1 0 – 8 (9)	3 – 3	1x9 (1 bin)	R1 0–8 (9)	3 – 3
	xxx_gt50	7	–	0 – 264	7	–	0 – 264	7	–	0 – 264

Table 2.3.25: PSP_ISOIS-EPIHI_L2-LET1-RATES3600 (contd.). Here, 'xxx' denotes R1A and R1B.

Side	Species	Count		Flux		Count Rate	
		Size (bins)	Energy (MeV/nuc)	Size (bins)	Energy (MeV/nuc)	Size (bins)	Energy (MeV/nuc)
A/B	xxx_29to32	8	1 – 320	8	1 – 320	8	1 – 320
	xxx_32to50	8	1 – 320	8	1 – 320	8	1 – 320
	xxx_Al	18	2 – 279	18	2 – 279	18	2 – 279
	xxx_Ar	20	2 – 288	20	2 – 288	20	2 – 288
	xxx_C	18	1 – 272	18	1 – 272	18	1 – 272
	xxx_Ca	20	2 – 288	20	2 – 288	20	2 – 288
	xxx_Cr	20	2 – 288	20	2 – 288	20	2 – 288
	xxx_Fe	20	2 – 288	20	2 – 288	20	2 – 288
	xxx_H	17	1 – 264	17	1 – 264	17	1 – 264
	xxx_He	17	1 – 266	17	1 – 266	17	1 – 266
	xxx_He_BIN xxx_He_BIN (MASS)	7x16 (7) 16 bins 0 – 15 seg	2 – 16 – –	– – –	– – –	– – –	– – –
	xxx_Mg	18	2 – 279	18	2 – 279	18	2 – 279
	xxx_N	18	1 – 272	18	1 – 272	18	1 – 272
	xxx_Na	18	1 – 275	18	1 – 275	18	1 – 275
	xxx_Ne	18	1 – 275	18	1 – 275	18	1 – 275
	xxx_Ne_BIN xxx_Ne_BIN (MASS)	8x8 (8) 8 bins 0 – 7 seg	3 – 32 – –	– – –	– – –	– – –	– – –
	xxx_Ni	21	2 – 294	21	2 – 294	21	2 – 294
	xxx_O	17	1 – 272	17	1 – 272	17	1 – 272
	xxx_S	20	2 – 288	20	2 – 288	20	2 – 288
	xxx_Si	18	2 – 279	18	2 – 279	18	2 – 279
	xxx_gt50	8	1 – 320	8	1 – 320	8	1 – 320

Table 2.3.26: PSP_ISOIS-EPIHI_L2-LET1-RATES3600 (contd.). Here, ‘xxx’ denotes R2A and R2B.

Side	Species	Count		Count Rate	
		Size (bins)	Energy (MeV/nuc)	Size (bins)	Energy (MeV/nuc)
A/B	Electrons_xxx	15	0 – 6	15	0 – 6
	xxx_He_BIN xxx_He_BIN (MASS)	5x16 (5) 16 bins 0 - 15 seg	8 – 32 – –	– – –	– – –
	xxx_Ne_BIN xxx_Ne_BIN (MASS)	6x8 (4) 8 bins 0 - 7 seg	16 – 92 – –	– – –	– – –

Table 2.3.27: PSP_ISOIS-EPIHI_L2-LET1-RATES3600 (contd.). Here, 'xxx' stands for R3A and R3B.

Side	Species	Count		Flux		Count Rate	
		Size (bins)	Energy (MeV/nuc)	Size (bins)	Energy (MeV/nuc)	Size (bins)	Energy (MeV/nuc)
A/B	xxxx_29to32	6	8 – 384	6	8 – 384	6	8 – 384
	xxxx_32to50	6	8 – 384	6	8 – 384	6	8 – 384
	xxxx_Al	13	8 – 310	13	8 – 310	13	8 – 310
	xxxx_Ar	13	10 – 320	13	10 – 320	13	10 – 320
	xxxx_C	14	5 – 294	14	5 – 294	14	5 – 294
	xxxx_Ca	14	10 – 332	14	10 – 332	14	10 – 332
	xxxx_Cr	14	10 – 332	14	10 – 332	14	10 – 332
	xxxx_Fe	14	10 – 332	14	10 – 332	14	10 – 332
	xxxx_H	13	3 – 275	13	3 – 275	13	3 – 275
	xxxx_He	14	3 – 279	14	3 – 279	14	3 – 279
	xxxx_Mg	13	8 – 310	13	8 – 310	13	8 – 310
	xxxx_N	14	5 – 294	14	5 – 294	14	5 – 294
	xxxx_Na	14	7 – 310	14	7 – 310	14	7 – 310
	xxxx_Ne	14	7 – 310	14	7 – 310	14	7 – 310
	xxxx_Ni	15	10 – 347	15	10 – 347	15	10 – 347
	xxxx_O	14	6 – 301	14	6 – 301	14	6 – 301
	xxxx_S	13	10 – 320	13	10 – 320	13	10 – 320
	xxxx_Si	14	8 – 320	14	8 – 320	14	8 – 320
	xxxx_gt50	6	8 – 384	6	8 – 384	6	8 – 384

Table 2.3.28: PSP_ISOIS-EPIHI_L2-LET1-RATES3600 (contd.). Here, 'xxxx' stands for R35A and R35B which implies the values are integratd over ranges R3 – R5 for sides A and B.

Side	Species	Count		Count Rate	
		Size (bins)	Energy (MeV/nuc)	Size (bins)	Energy (MeV/nuc)
A/B	Electrons_xxx	16	0 – 7	16	0 – 7

Table 2.3.29: PSP_ISOIS-EPIHI_L2-LET1-RATES3600 (contd.). Here, 'xxx' stands for R4A and R4B.

Side	Species	Count		Count Rate	
		Size (bins)	Energy (MeV/nuc)	Size (bins)	Energy (MeV/nuc)
A/B	Electrons_xxx	15	1 – 7	15	1 – 7

Table 2.3.30: PSP_ISOIS-EPIHI_L2-LET1-RATES3600 (contd.). Here, 'xxx' stands for R5A and R5B.

Side	Species	Count	
		Size (bins)	Energy (MeV/nuc)
A/B	xxxx_He_BIN xxxx_He_BIN (MASS)	5x16 (5) 16 bins 0 - 15 seg	16 – 92
	xxxx_Ne_BIN xxxx_Ne_BIN (MASS)	6x8 (6) 8 bins 0 - 7 seg	16 – 92

Table 2.3.31: PSP_ISOIS-EPIHI_L2-LET1-RATES3600 (contd.). Here, 'xxxx' stands for R45A and R45B and the values are integrated over ranges R4 – R5.

Side	Species	Count		Flux		Count Rate	
		Size (bins)	Energy (MeV/nuc)	Size (bins)	Energy (MeV/nuc)	Size (bins)	Energy (MeV/nuc)
A/B	xxx_29to32	4	32 – 384	4	32 – 384	4	32 – 384
	xxx_32to50	4	32 – 384	4	32 – 384	4	32 – 384
	xxx_Al	8	23 – 320	8	23 – 320	8	23 – 320
	xxx_Ar	7	32 – 332	7	32 – 322	7	32 – 332
	xxx_C	9	16 – 310	9	16 – 310	9	16 – 310
	xxx_Ca	7	32 – 332	7	32 – 332	7	32 – 332
	xxx_Cr	7	32 – 332	7	32 – 332	7	32 – 332
	Electrons_xxx	13	1 – 7	–	–	13	1 – 7
	xxx_Fe	7	38 – 347	7	38 – 347	7	38 – 347
	xxx_H	8	8 – 279	8	8 – 279	8	8 – 279
	xxx_He	9	8 – 283	9	8 – 283	9	8 – 283
	xxx_He_BIN xxx_He_BIN (MASS)	3x16 (3) 16 bins 0 - 15 seg	23 – 46 – –	– – –	– – –	– – –	– – –
	xxx_Mg	8	23 – 320	8	23 – 320	8	23 – 320
	xxx_N	9	16 – 310	9	16 – 310	9	16 – 310
	xxx_Na	9	19 – 320	9	19 – 320	9	19 – 320
	xxx_Ne	9	19 – 320	9	19 – 320	9	19 – 320
	xxx_Ne_BIN xxx_Ne_BIN (MASS)	3x8 (3) 8 bins 0 - 7 seg	46 – 92 – –	– – –	– – –	– – –	– – –
	xxx_Ni	8	38 – 364	8	38 – 364	8	38 – 364
	xxx_O	9	19 – 320	9	19 – 320	9	19 – 320
	xxx_S	7	32 – 332	7	32 – 332	7	32 – 332
	xxx_Si	8	27 – 332	8	27 – 332	8	27 – 332
	xxx_gt50	4	32 – 384	4	32 – 384	4	32 – 384

Table 2.3.32: PSP_ISOIS-EPIHI_L2-LET1-RATES3600 (contd.). Here, ‘xxx’ stands for R6A and R6B.

2.3.8 FILE: PSP_ISOIS-EPIHI_L2-LET1-RATES60

This file contains the LET1 (Low Energy Telescope) 60 s cadence measurements of particle Counts, Flux (cm^{-2} sr^{-1} sec^{-1} MeV^{-1}) and Count Rate (counts/s) of Al, Ar, C, Ca, Cr, Fe, H, He, Mg, N, Na, Ne, Ni, O, S and Si for sides A and B. The values of these variables are summarized in Tables 2.3.33 – 2.3.29. The variables are named as: <side>_<species>_<quantity>, where, <side> stands for A or B; <species> stands for the particle species; and <quantity> represents Count, Flux or Rate ("Count" is not used in the variable names, in general). Variable names without ranges (e.g. A_C) or with double digit range (e.g. R35) have the values integrated over all the available ranges (e.g. R3 to R5).
Examples: A_C_Flux, PENB_C_Rate, R1A_32to50_Flux.

Side	Species	Counts		Flux		Count Rate	
		Size (bins)	Energy (MeV/nuc)	Size (bins)	Energy (MeV/nuc)	Size (bins)	Energy (MeV/nuc)
A/B	Al	28	1 – 118	28	1 – 118	28	1 – 118
	Ar	29	1 – 140	29	1 – 140	29	1 – 140
	C	27	1 – 99	27	1 – 99	27	1 – 99
	Ca	30	1 – 140	30	1 – 140	30	1 – 140
	Cr	31	1 – 140	31	1 – 140	31	1 – 140
	Fe	32	1 – 167	32	1 – 167	32	1 – 167
	H	25	1 – 42	25	1 – 42	25	1 – 42
	He	26	1 – 50	26	1 – 50	26	1 – 50
	Mg	28	1 – 118	28	1 – 118	28	1 – 118
	N	27	1 – 99	27	1 – 99	27	1 – 99
	Na	28	1 – 118	28	1 – 118	28	1 – 118
	Ne	28	1 – 118	28	1 – 118	28	1 – 118
	Ni	33	1 – 198	33	1 – 198	33	1 – 198
	O	28	1 – 118	28	2 – 118	28	1 – 118
	S	29	1 – 140	29	1 – 140	29	1 – 140
	Si	29	1 – 140	29	1 – 140	29	1 – 140

Table 2.3.33: PSP_ISOIS-EPIHI_L2-LET1-RATES60. The LET1 measurements of different particle species at a cadence of 60 s for sides A and B.

Side	Species	Count		Count Rate	
		Size (bins)	Energy (MeV/nuc)	Size (bins)	Energy (MeV/nuc)
A/B	PENx_C	9	45 – 583	9	45 – 583
	PENx_Fe	9	108 – 793	9	108 – 793
	PENx_H	9	27 – 521	9	27 – 521
	PENx_He	9	27 – 521	9	27 – 521
	PENx_Mg	9	64 – 646	9	64 – 646
	PENx_N	9	45 – 583	9	45 – 583
	PENx_Ne	8	64 – 612	8	64 – 612
	PENx_O	9	54 – 612	9	54 – 612
	PENx_Si	9	76 – 687	9	76 – 687

Table 2.3.34: PSP_ISOIS-EPIHI_L2-LET1-RATES60 (contd.). Here, 'x' stands for sides A & B.

Side	Species	Count			Flux			Count Rate		
		Size (bins)	Range SECT (bins)	Energy (MeV/nuc)	Size (bins)	Range SECT (bins)	Energy (MeV/nuc)	Size (bins)	Range SECT (bins)	Energy (MeV/nuc)
A/B	xxx_29to32	7	–	0 – 264	7	–	0 – 264	7	–	0 – 264
	xxx_32to50	7	–	0 – 264	7	–	0 – 264	7	–	0 – 264
	xxx_Al	14	–	1 – 260	14	–	1 – 260	14	–	1 – 260
	xxx_Ar	15	–	1 – 261	15	–	1 – 261	15	–	1 – 261
	xxx_C	12	–	1 – 259	12	–	1 – 259	12	–	1 – 259
	xxx_Ca	16	–	1 – 261	16	–	1 – 261	16	–	1 – 261
	xxx_Cr	17	–	1 – 261	17	–	1 – 261	17	–	1 – 261
	xxx_Fe	17	–	1 – 261	17	–	1 – 261	17	–	1 – 261
	xxx_H	12	–	0 – 258	12	–	0 – 258	12	–	0 – 258
	xxx_H_SECT	1x9 (1 bin)	R1 0 – 8 (9)	2 – 2	1x9 (1 bin)	R1 0 – 8 (9)	2 – 2	1x9 (1 bin)	R1 0 – 8 (9)	2 – 2
	xxx_He	12	–	0 – 258	12	–	0 – 258	12	–	0 – 258
	xxx_He_SECT	1x9 (1 bin)	R1 0 – 8 (9)	2 – 2	1x9 (1 bin)	R1 0 – 8 (9)	2 – 2	1x9 (1 bin)	R1 0–8 (9)	2 – 2
	xxx_Mg	14	–	1 – 260	14	–	1 – 260	14	–	1 – 260
	xxx_N	12	–	1 – 259	12	–	1 – 259	12	–	1 – 259
	xxx_Na	13	–	1 – 259	13	–	1 – 259	13	–	1 – 259
	xxx_Ne	13	–	1 – 259	13	–	1 – 259	13	–	1 – 259
	xxx_Ni	17	–	1 – 261	17	–	1 – 261	17	–	1 – 261
	xxx_O	13	–	1 – 259	13	–	1 – 259	13	–	1 – 259
	xxx_S	15	–	1 – 259	15	–	1 – 259	15	–	1 – 259
	xxx_Si	14	–	1 – 260	14	–	1 – 260	14	–	1 – 260
	xxx_gt50	7	–	0 – 264	7	–	0 – 264	7	–	0 – 264

Table 2.3.35: PSP_ISOIS-EPIHI_L2-LET1-RATES60 (contd.). Here, 'xxx' stands for R1A and R1B.

Side	Species	Count			Flux ($1/cm^2$ sr sec MeV)			Count Rate		
		Size (bins)	Range SECT (bins)	Energy (MeV/nuc)	Size (bins)	Range SECT (bins)	Energy (MeV/nuc)	Size (bins)	Range SECT (bins)	Energy (MeV/nuc)
	xxxx_H_SECT	3x25 (3 bins)	R26 0 – 24 (25)	3 – 12	3x25 (3 bins)	R26 0 – 24	3 – 12	3x25 (3 bins)	R26 0 – 24 (25)	3 – 12
A/B	xxxx_He_SECT	3x25 (3 bins)	R26 0 – 24 (25)	3 – 12	3x25 (3 bins)	R26 0 – 24 (25)	3 – 12	3x25 (3 bins)	R26 0 – 24 (25)	3 – 12
	xxxx_ENA_SECT	8 x 25 (8 bins)	R26 0 – 24 (25)	3 – 12 – –	– – –	– – –	– – –	– – –	– – –	– – –

Table 2.3.36: PSP_ISOIS-EPIHI_L2-LET1-RATES60 (contd.). Here, 'xxxx' stands for R26A and R26B. The variables have values integrated over ranges R2 – R6.

Side	Species	Count		Flux		Count Rate	
		Size (bins)	Energy (MeV/nuc)	Size (bins)	Energy (MeV/nuc)	Size (bins)	Energy (MeV/nuc)
A/B	xxx_29to32	8	1 – 320	8	1 – 320	8	1 – 320
	xxx_32to50	8	1 – 320	8	1 – 320	8	1 – 320
	xxx_Al	18	2 – 279	18	2 – 279	18	2 – 279
	xxx_Ar	20	2 – 288	20	2 – 288	20	2 – 288
	xxx_C	18	1 – 272	18	1 – 272	18	1 – 272
	xxx_Ca	20	2 – 288	20	2 – 288	20	2 – 288
	xxx_Cr	20	2 – 288	20	2 – 288	20	2 – 288
	xxx_Fe	20	2 – 288	20	2 – 288	20	2 – 288
	xxx_H	17	1 – 264	17	1 – 264	17	1 – 264
	xxx_He	17	1 – 266	17	1 – 266	17	1 – 266
	xxx_Mg	18	2 – 279	18	2 – 279	18	2 – 279
	xxx_N	18	1 – 272	18	2 – 272	18	2 – 272
	xxx_Na	18	1 – 275	18	1 – 275	18	1 – 275
	xxx_Ne	18	1 – 275	18	1 – 275	18	1 – 275
	xxx_Ni	21	2 – 294	21	2 – 294	21	2 – 294
	xxx_O	17	1 – 272	17	1 – 272	17	1 – 272
	xxx_S	20	2 – 288	20	2 – 288	20	2 – 288
	xxx_Si	18	2 – 279	18	2 – 279	18	2 – 279
	xxx_gt50	8	1 – 320	8	1 – 320	8	1 – 320

Table 2.3.37: PSP_ISOIS-EPIHI_L2-LET1-RATES60 (contd.). Here, 'xxx' stands for R2A and R2B.

Side	Species	Count		Flux		Count Rate	
		Size (bins)	Energy (MeV/nuc)	Size (bins)	Energy (MeV/nuc)	Size (bins)	Energy (MeV/nuc)
A/B	xxxx_29to32	6	8 – 384	6	8 – 384	6	8 – 384
	xxxx_32to50	6	8 – 384	6	8 – 384	6	8 – 384
	xxxx_Al	13	8 – 310	13	8 – 310	13	8 – 310
	xxxx_Ar	13	10 – 320	13	10 – 320	13	10 – 320
	xxxx_C	14	5 – 294	14	5 – 294	14	5 – 294
	xxxx_Ca	14	10 – 332	14	10 – 332	14	10 – 332
	xxxx_Cr	14	10 – 332	14	10 – 332	14	10 – 332
	xxxx_Fe	14	10 – 332	14	10 – 332	14	10 – 332
	xxxx_H	13	3 – 275	13	3 – 275	13	3 – 275
	xxxx_He	14	3 – 279	14	3 – 279	14	3 – 279
	xxxx_Mg	13	8 – 310	13	8 – 310	13	8 – 310
	xxxx_N	14	5 – 294	14	5 – 294	14	5 – 294
	xxxx_Na	14	7 – 310	14	7 – 310	14	7 – 310
	xxxx_Ne	14	7 – 310	14	7 – 310	14	7 – 310
	xxxx_Ni	15	10 – 347	15	10 – 347	15	10 – 347
	xxxx_O	14	6 – 301	14	6 – 301	14	6 – 301
	xxxx_S	13	10 – 320	13	10 – 320	13	10 – 320
	xxxx_Si	14	8 – 320	14	8 – 320	14	8 – 320
	xxxx_gt50	6	8 – 384	6	8 – 384	6	8 – 384

Table 2.3.38: PSP_ISOIS-EPIHI_L2-LET1-RATES60 (contd.). Here, 'xxxx' stands for R35A and R35B. The values are integrated over ranges R3 – R5.

Side	Species	Count		Flux		Count Rate	
		Size (bins)	Energy (MeV/nuc)	Size (bins)	Energy (MeV/nuc)	Size (bins)	Energy (MeV/nuc)
A/B	xxx_29to32	4	32 – 384	4	32 – 384	4	32 – 384
	xxx_32to50	4	32 – 384	4	32 – 384	4	32 – 384
	xxx_Al	8	23 – 320	8	23 – 320	8	23 – 320
	xxx_Ar	7	32 – 332	7	32 – 322	7	32 – 332
	xxx_C	9	16 – 310	9	16 – 310	9	16 – 310
	xxx_Ca	7	32 – 332	7	32 – 332	7	32 – 332
	xxx_Cr	7	32 – 332	7	32 – 332	7	32 – 332
	Electrons_xxx	13	1 – 7	–	–	13	1 – 7
	xxx_Fe	7	38 – 347	7	38 – 347	7	38 – 347
	xxx_H	8	8 – 279	8	8 – 279	8	8 – 279
	xxx_He	9	8 – 283	9	8 – 283	9	8 – 283
	xxx_He_BIN xxx_He_BIN (MASS)	3x16 (3) 16 bins 0 – 15 seg	23 – 46 – –	– – –	– – –	– – –	– – –
	xxx_Mg	8	23 – 320	8	23 – 320	8	23 – 320
	xxx_N	9	16 – 310	9	16 – 310	9	16 – 310
	xxx_Na	9	19 – 320	9	19 – 320	9	19 – 320
	xxx_Ne	9	19 – 320	9	19 – 320	9	19 – 320
	xxx_Ne_BIN xxx_Ne_BIN (MASS)	3x8 (3) 8 bins 0 – 7 seg	46 – 92 – –	– – –	– – –	– – –	– – –
	xxx_Ni	8	38 – 364	8	38 – 364	8	38 – 364
	xxx_O	9	19 – 320	9	19 – 320	9	19 – 320
	xxx_S	7	32 – 332	7	32 – 332	7	32 – 332
	xxx_Si	8	27 – 332	8	27 – 332	8	27 – 332
	xxx_gt50	4	32 – 384	4	32 – 384	4	32 – 384

Table 2.3.39: PSP_ISOIS-EPIHI_L2-LET1-RATES60 (contd.). Here, 'xxx' stands for R6A and R6B.

2.3.9 FILE: PSP_ISOIS-EPIHI_L2-LET2-RATES10

This file contains the 10-second cadence data of particle Counts, Flux (cm^{-2} sr^{-1} sec^{-1} MeV^{-1}) and Count Rate (counts/s) for Electrons, H and He ions for various ranges (R1 – R7) of the single–sided (depicted as C) Low Energy Telescope (LET2). Table 2.3.40 summarizes the measured values. The variable names follow the structure: <side>_<species>_<quantity>, where, <side> stands for C; <species> stands for the particle species, and <quantity> represents Counts (not used in the variable names, in general), Flux or Rate for those variables independent of range. The variable names for different ranges (R1 – R5) are of the form: <range><side>_<species>_<quantity>. For electrons, the structure is: <Electrons>_<range><side>. Variable names without ranges (e.g., A_C) or with double digit range (e.g., R17) have the values integrated over all the available ranges (e.g., R1 to R7).
Examples: C_He (measured quantity is "count"); Electrons_R3C_Rate; R1C_He_Rate.

Side	Range	Quantity	Electrons		H		He	
			E-bins	E-range (MeV/nuc) (bins)	E-bins	E-range (MeV/nuc) (bins)	E-bins	E-range (MeV/nuc) (bins)
C		Count			16	1 - 12 (16)	20	1 - 25 (20)
		Flux			16	1 - 12 (16)	20	1 - 25 (20)
		Count Rate			16	1 - 12 (16)	20	1 - 25 (20)
	R1	Count			8	1 - 3 (8)	8	1 - 3 (8)
		Flux			8	1 - 3 (8)	8	1 - 3 (8)
		Count Rate			8	1 - 3 (8)	8	1 - 3 (8)
	R2	Count			13	2 - 12 (13)	13	2 - 15 (13)
		Flux			13	2 - 12 (13)	13	2 - 15 (13)
		Count Rate			13	2 - 12 (13)	13	2 - 15 (13)
	R35	Count			5	7 - 15 (5)	9	7 - 29 (9)
		Flux			5	7 - 15 (5)	9	7 - 29 (9)
		Count Rate			5	7 - 15 (5)	9	7 - 29 (9)
	R3	Count	10	1 - 3 (10)				
		Flux						
		Count Rate	10	1 - 3 (10)				
	R4	Count	10	1 - 4 (10)				
		Flux						
		Count Rate	10	1 - 4 (10)				
	R5	Count	9	1 - 4 (9)				
		Flux						
		Count Rate	9	1 - 4 (9)				

Table 2.3.40: PSP_ISOIS-EPIHI_L2-LET2-RATES10. The 10 s cadence data of LET2 for various energetic particle species.

2.3.10 FILE: PSP_ISOIS-EPIHI_L2-LET2-RATES300

This file contains the 300 s cadence data of particle Counts, Flux (cm^{-2} sr^{-1} sec^{-1} MeV^{-1}) and Count Rate (counts/s) for various particle species for ranges R1 & R26 (integrated over Ranges 2 – 6) measured by the single–sided (named C) Low Energy Telescope (LET2). The measured values are summarized in Table 2.3.41. The variable naming is: <range><side>_<species>_<quantity>, where, <range> denotes the range (R1 and R26), <side> stands for C; <species> takes one of the particle species; and <quantity> represents Counts (not used in variable names, in general), Flux or Rate. Variable names without ranges (e.g., A_C) or with double digit range (e.g., R25) have the values integrated over all the available ranges (e.g., R2 to R5).
Examples: R1C_NetoSi_SECT_Rate; R25C_CNO_SECT_Flux.

Side	Range	Quantity	CNO_SECT			FeGroup_SECT			NetoSi_SECT		
			E-bins	E-range (MeV/nuc)	Sectors (bins)	E-bins	E-range (MeV/nuc)	Sectors (bins)	E-bins	E-range (MeV/nuc)	Sectors (bins)
C	R1	Count	1	3 - 3	0 - 8 (9)	1	3 - 3	0 - 8 (9)	1	3 - 3	0 - 8 (9)
		Flux	1	3 - 3	0 - 8 (9)	1	3 - 3	0 - 8 (9)	1	3 - 3	0 - 8 (9)
		Count Rate	1	3 - 3	0 - 8 (9)	1	3 - 3	0 - 8 (9)	1	3 - 3	0 - 8 (9)
C	R26	Count	3	6 - 24	0 - 24 (25)	3	6 - 24	0 - 24 (25)	3	6 - 24	0 - 24 (25)
		Flux	3	6 - 24	0 - 24 (25)	3	6 - 24	0 - 24 (25)	3	6 - 24	0 - 24 (25)
		Count Rate	3	6 - 24	0 - 24 (25)	3	6 - 24	0 - 24 (25)	3	6 - 24	0 - 24 (25)
R1 ENB_SECT – measured quantity is Counts; Size 3 x 9; E-bins: 3; E-range: 1 - 2 (MeV/nuc); Sectors: 0 - 8 (9).											
R26 ENB_SECT – measured quantity is Counts; Size 4 x 25; E-bins: 4; E-range: 2 - 12 (MeV/nuc); Sectors: 0 - 24 (25).											

Table 2.3.41: PSP_ISOIS-EPIHI_L2-LET2-RATES300. The LET2 300 s cadence measurements of various energetic particle species for ranges R1 and integrated over ranges R2 – R6 (R26).

2.3.11 FILE: PSP_ISOIS-EPIHI_L2-LET2-RATES3600

This file contains the 3600 s cadence data of particle Counts, Flux (cm^{-2} sr^{-1} sec^{-1} MeV^{-1}) and Count Rate (counts/s) for Al, Ar, C, Ca, Cr, Fe, H, He, Mg, N, Na, Ne, Ni, O, S and Si by the single sided (depicted as C) Low Energy Telescope (LET2). The measured values of these variables are summarized in Tables 2.3.42 – 2.3.49. The variables are named as: <side>_<species>_<quantity>, where, <side> stands for C; <species> represents the particle species; and <quantity> denotes Counts (not used in the variable names, in general), Flux or Rate. Variable names without ranges (e.g. C_Al) or with double digit range (e.g. R25) have the values integrated over all the available ranges (e.g. R2 to R5).
Examples: C_Si_Flux; PENB_C_Rate; R1C_32to50_Flux; Electrons_R5C.

Side	Species	Count		Flux		Count Rate	
		Size (bins)	Energy (MeV/nuc)	Size (bins)	Energy (MeV/nuc)	Size (bins)	Energy (MeV/nuc)
C	Al	27	1 – 99	27	1 – 99	27	1 – 99
	Ar	29	1 – 118	28	1 – 118	28	1 – 118
	C	25	1 – 70	25	1 – 70	25	1 – 70
	Ca	30	1 – 140	30	1 – 140	30	1 – 140
	Cr	31	1 – 140	31	1 – 140	31	1 – 140
	Fe	31	1 – 140	31	1 – 140	31	1 – 140
	H	24	1 – 35	24	1 – 35	24	1 – 35
	He	25	1 – 42	25	1 – 42	25	1 – 42
	Mg	27	1 – 99	27	1 – 99	27	1 – 99
	N	25	1 – 70	25	1 – 70	25	1 – 70
	Na	27	1 – 99	27	1 – 99	27	1 – 99
	Ne	27	1 – 99	27	1 – 99	27	1 – 99
	Ni	32	1 – 167	32	1 – 167	32	1 – 167
	O	26	1 – 83	26	1 – 83	26	1 – 83
	S	28	1 – 118	28	1 – 118	28	1 – 118
	Si	28	1 – 117	28	1 – 118	28	1 – 118

Table 2.3.42: PSP_ISOIS-EPIHI_L2-LET2-RATES3600. The 3600 s cadence data for various particle species for the single–sided (side C) telescope LET2.

Side	Species	Count		Count Rate	
		Size (bins)	Energy (MeV/nuc)	Size (bins)	Energy (MeV/nuc)
C	PENx_C	11	23 – 364	11	23 – 364
	PENx_Fe	11	45 – 471	11	45 – 471
	PENx_He	11	11 – 310	11	11 – 310
	PENx_Mg	10	38 – 408	10	38 – 408
	PENx_N	11	23 – 364	11	23 – 364
	PENx_Ne	11	27 – 384	11	27 – 384
	PENx_O	11	27 – 384	11	27 – 384
	PENx_Si	10	38 – 408	11	38 – 408

Table 2.3.43: PSP_ISOIS-EPIHI_L2-LET2-RATES3600 (contd.). Here, ‘x’ stands for side C.

Side	Species	Count			Flux			Count Rate		
		Size (bins)	Range SECT (bins)	Energy (MeV/nuc)	Size (bins)	Range SECT (bins)	Energy (MeV/nuc)	Size (bins)	Range SECT (bins)	Energy (MeV/nuc)
C	xxx_29to32	7	29 – 32	0 – 264	7	29 – 32	0 – 264	7	29 – 32	0 – 264
	xxx_32to50	7	32 – 50	0 – 264	7	32 – 50	0 – 264	7	32 – 50	0 – 264
	xxx_Al	14	–	1 – 260	14	–	1 – 260	14	–	1 – 260
	xxx_Ar	15	–	1 – 261	15	–	1 – 261	15	–	1 – 261
	xxx_C	12	–	1 – 259	12	–	1 – 259	12	–	1 – 259
	xxx_Ca	16	–	1 – 261	16	–	1 – 262	16	–	1 – 261
	xxx_CNO_SECT	1x9 (1 bin)	R1 0 – 8 (9)	3 – 3	1x9 (1 bin)	R1 0 – 8 (9)	3 – 3	1x9 (1 bin)	R1 0 – 8 (9)	3 – 3
	xxx_Cr	17	–	1 – 261	17	–	1 – 261	17	–	1 – 261
	xxx_Fe	17	–	1 – 261	17	–	1 – 261	17	–	1 – 261
	xxx_FeGroup_SECT	1x9 (1 bin)	R1 0 – 8 (9)	3 – 3	1x9 (1 bin)	R1 0 – 8 (9)	3 – 3	1x9 (1 bin)	R1 0 – 8 (9)	3 – 3
	xxx_H	12	–	0 – 258	12	–	0 – 258	12	–	0 – 258
	xxx_H_SECT	1x9 (1 bin)	R1 0 – 8 (9)	2 – 2	1x9 (1 bin)	R1 0 – 8 (9)	2 – 2	1x9 (1 bin)	R1 0 – 8 (9)	2 – 2
	xxx_He	12	–	0 – 258	12	–	0 – 258	12	–	0 – 258
	xxx_He_SECT	1x9 (1 bin)	R1 0 – 8 (9)	2 – 2	1x9 (1 bin)	R1 0 – 8 (9)	2 – 2	1x9 (1 bin)	R1 0–8 (9)	2 – 2
	xxx_He_BIN xxx_He_BIN (MASS)	5x16 (5) 16 bins 0 – 15 seg	– – –	1 – 3 – –	– – –	– – –	– – –	– – –	– – –	– – –
	xxx_Mg	14	–	1 – 260	14	–	1 – 260	14	–	1 – 260
	xxx_N	12	–	1 – 259	12	–	1 – 259	12	–	1 – 259
	xxx_Na	13	–	1 – 259	13	–	1 – 259	12	–	1 – 259
	xxx_Ne	13	–	1 – 259	13	–	1 – 259	13	–	1 – 259
	xxx_Ne_BIN xxx_Ne_BIN (MASS)	5x8 (5) 8 bins 0 - 7 seg	– – –	1 – 6 – –	– – –	– – –	– – –	– – –	– – –	– – –
	xxx_Ni	17	–	1 – 261	17	–	1 – 261	17	–	1 – 261
	xxx_O	13	–	1 – 259	13	–	1 – 259	13	–	1 – 259
	xxx_S	15	–	1 – 261	15	–	1 – 261	15	–	1 – 261
	xxx_Si	14	–	1 – 260	14	–	1 – 260	14	–	1 – 260
	xxx_NetoSi_SECT	1x9 (1 bin)	R1 0 – 8 (9)	3 – 3	1x9 (1 bin)	R1 0 – 8 (9)	3 – 3	1x9 (1 bin)	R1 0–8 (9)	3 – 3
	xxx_gt50	7	–	0 – 264	7	–	0 – 264	7	–	0 – 264

Table 2.3.44: PSP_ISOIS-EPIHI_L2-LET2-RATES3600 (contd.). Here, ‘xxx’ stands for R1C.

Side	Species	Count			Flux			Count Rate		
		Size (bins)	Range SECT (bins)	Energy (MeV/nuc)	Size (bins)	Range SECT (bins)	Energy (MeV/nuc)	Size (bins)	Range SECT (bins)	Energy (MeV/nuc)
C	xxxx_CNO_SECT	3x25 (3 bins)	R25 0 – 24 (25)	6 – 24	3x25 (3 bins)	R25 0 – 24 (25)	6 – 24	3x25 (3 bins)	R25 0 – 24 (25)	6 – 24
	xxxx_FeGroup_SECT	3x25 (3 bins)	R25 0 – 24 (25)	6 – 24	3x25 (3 bins)	R25 0 – 24 (25)	6 – 24	3x25 (3 bins)	R25 0 – 24 (25)	6 – 24
	xxxx_H_SECT	3x25 (3 bins)	R25 0 – 24 (25)	3 – 12	3x25 (3 bins)	R25 0 – 24 (25)	3 – 12	3x25 (3 bins)	R25 0 – 24 (25)	3 – 12
	xxxx_He_SECT	3x25 (3 bins)	R25 0 – 24 (25)	3 – 12	3x25 (3 bins)	R25 0 – 24 (25)	3 – 12	3x25 (3 bins)	R25 0–24 (25)	3 – 12
	xxxx_NetoSi_SECT	3x25 (3 bins)	R25 0 – 24 (25)	6 – 24	3x25 (3 bins)	R25 0 – 24 (25)	6 – 24	3x25 (3 bins)	R25 0–24 (25)	6 – 24

Table 2.3.45: PSP_ISOIS-EPIHI_L2-LET2-RATES3600 (contd.). Here, 'xxxx' stands for R25C and the values are integrated over ranges R2 – R5.

Side	Species	Count		Flux		Count Rate	
		Size (bins)	Energy (MeV/nuc)	Size (bins)	Energy (MeV/nuc)	Size (bins)	Energy (MeV/nuc)
C	xxx_29to32	8	1 – 320	8	1 – 320	8	1 – 320
	xxx_32to50	8	1 – 320	8	1 – 320	8	1 – 320
	xxx_Al	18	2 – 279	18	2 – 279	18	2 – 279
	xxx_Ar	20	2 – 288	20	2 – 288	20	2 – 288
	xxx_C	18	1 – 272	18	1 – 272	18	1 – 272
	xxx_Ca	20	2 – 288	20	2 – 288	20	2 – 288
	xxx_Cr	20	2 – 288	20	2 – 288	20	2 – 288
	xxx_Fe	20	2 – 288	20	2 – 288	20	2 – 288
	xxx_H	17	1 – 264	17	1 – 264	17	1 – 264
	xxx_He	17	1 – 266	17	1 – 266	17	1 – 266
	xxx_He_BIN xxx_He_BIN (MASS)	7x16 (7) 16 bins 0 – 15 seg	2 – 16 – –	– – –	– – –	– – –	– – –
	xxx_Mg	18	2 – 279	18	2 – 279	18	2 – 279
	xxx_N	18	1 – 272	18	1 – 272	18	1 – 272
	xxx_Na	18	1 – 275	18	1 – 275	18	1 – 275
	xxx_Ne	18	1 – 275	18	1 – 275	18	1 – 275
	xxx_Ne_BIN xxx_Ne_BIN (MASS)	8x8 (8) 8 bins 0 – 7 seg	3 – 32 – –	– – –	– – –	– – –	– – –
	xxx_Ni	21	2 – 294	21	2 – 294	21	2 – 294
	xxx_O	17	1 – 272	17	1 – 272	17	1 – 272
	xxx_S	20	2 – 288	20	2 – 288	20	2 – 288
	xxx_Si	18	2 – 279	18	2 – 279	18	2 – 279
	xxx_gt50	8	1 – 320	8	1 – 320	8	1 – 320

Table 2.3.46: PSP_ISOIS-EPIHI_L2-LET2-RATES3600 (contd.). Here, 'xxx' stands for R2C.

Side	Species	Count		Count Rate	
		Size (bins)	Energy (MeV/nuc)	Size (bins)	Energy (MeV/nuc)
C	Electrons_R3C	15	0 – 6	15	0 – 6
	R3C_He_BIN	5x16 (5)	8 – 32	–	–
	R3C_He_BIN (MASS)	16 bins	–	–	–
		0 – 15 seg	–	–	–
	R3C_Ne_BIN	6x8 (6)	16 – 92	–	–
	R3C_Ne_BIN (MASS)	8 bins	–	–	–
		0 – 7 seg	–	–	–
	Electrons_R4C	16	0 – 7	16	0 – 7
	Electrons_R5C	15	1 – 7	15	1 – 7

Table 2.3.47: PSP_ISOIS-EPIHI_L2-LET2-RATES3600 (contd.). LET2 electron measurements for ranges R3, R4 and R5.

Side	Species	Count		Flux		Count Rate	
		Size (bins)	Energy (MeV/nuc)	Size (bins)	Energy (MeV/nuc)	Size (bins)	Energy (MeV/nuc)
C	xxxx_29to32	6	8 – 384	6	8 – 384	6	8 – 384
	xxxx_32to50	6	8 – 384	6	8 – 384	6	8 – 384
	xxxx_Al	13	8 – 310	13	8 – 310	13	8 – 310
	xxxx_Ar	13	10 – 320	13	10 – 320	13	10 – 320
	xxxx_C	14	5 – 294	14	5 – 294	14	5 – 294
	xxxx_Ca	14	10 – 332	14	10 – 332	14	10 – 332
	xxxx_Cr	14	10 – 332	14	10 – 332	14	10 – 332
	xxxx_Fe	14	10 – 332	14	10 – 332	14	10 – 332
	xxxx_H	13	3 – 275	13	3 – 275	13	3 – 275
	xxxx_He	14	3 – 279	14	3 – 279	14	3 – 279
	xxxx_Mg	13	8 – 310	13	8 – 310	13	8 – 310
	xxxx_N	14	5 – 294	14	5 – 294	14	5 – 294
	xxxx_Na	14	7 – 310	14	7 – 310	14	7 – 310
	xxxx_Ne	14	7 – 310	14	7 – 310	14	7 – 310
	xxxx_Ni	15	10 – 347	15	10 – 347	15	10 – 347
	xxxx_O	14	6 – 301	14	6 – 301	14	6 – 301
	xxxx_S	13	10 – 320	13	10 – 320	13	10 – 320
	xxxx_Si	14	8 – 320	14	8 – 320	14	8 – 320
	xxxx_gt50	6	8 – 384	6	8 – 384	6	8 – 384

Table 2.3.48: PSP_ISOIS-EPIHI_L2-LET2-RATES3600 (contd.). Here, ‘xxxx’ stands for R35C which implies that the values are integrated over ranges R3 – R5.

Side	Species	Count	
		Size (bins)	Energy (MeV/nuc)
C	xxxx_He_BIN xxxx_He_BIN (MASS)	5x16 (5) 16 bins 0 - 15 seg	8 – 32
	xxxx_Ne_BIN xxxx_Ne_BIN (MASS)	6x8 (6) 6 bins 0 - 7 seg	16 – 92

Table 2.3.49: PSP_ISOIS-EPIHI_L2-LET2-RATES3600 (contd.). Here, 'xxxx' stands for R45C and the values presented here are integrated over ranges R4 – R5.

2.3.12 FILE: PSP_ISOIS-EPIHI_L2-LET2-RATES60

This file contains the 60 s cadence measurements of particle Counts, Flux (cm^{-2} sr^{-1} sec^{-1} MeV^{-1}) and Count Rate (counts/s) of Al, Ar, C, Ca, Cr, Fe, H, He, Mg, N, Na, Ne, Ni, O, S and Si coming from sides A and B made by the Low Energy Telescope (LET1). The values of these variables are summarized in Tables 2.3.33 – 2.3.29. The variables are named as: <side>_<species>_<quantity>, where, <side> stands for A or B; <species> stands for the particle species; and <quantity> represents Counts (not used in the variable names, in general), Flux or Rate. Variable names without ranges (e.g. A_C) or with double digit range (e.g. R25) have the values integrated over all the available ranges (e.g. R2 to R5).
Examples: A_C_Flux; PENB_C_Rate; R1A_32to50_Flux.

Side	Species	Counts		Flux		Count Rate	
		Size (bins)	Energy (MeV/nuc)	Size (bins)	Energy (MeV/nuc)	Size (bins)	Energy (MeV/nuc)
C	Al	27	1 – 99	27	1 – 99	27	1 – 99
	Ar	28	1 – 118	28	1 – 118	28	1 – 118
	C	25	1 – 70	25	1 – 70	25	1 – 70
	Ca	30	1 – 140	30	1 – 140	30	1 – 140
	Cr	31	1 – 140	31	1 – 140	31	1 – 140
	Fe	31	1 – 140	31	1 – 140	31	1 – 140
	H	24	1 – 35	24	1 – 35	24	1 – 35
	He	25	1 – 42	25	1 – 42	25	1 – 42
	Mg	27	1 – 99	27	1 – 99	27	1 – 99
	N	25	1 – 70	25	1 – 70	25	1 – 70
	Na	27	1 – 99	27	1 – 99	27	1 – 99
	Ne	27	1 – 99	27	1 – 99	27	1 – 99
	Ni	32	1 – 167	32	1 – 167	32	1 – 167
	O	26	1 – 83	26	2 – 83	26	1 – 83
	S	28	1 – 118	28	1 – 118	28	1 – 118
	Si	28	1 – 118	28	1 – 118	28	1 – 118

Table 2.3.50: PSP_ISOIS-EPIHI_L2-LET2-RATES60. The 60 s cadence measurements of the single–sided (side C) telescope LET2 for different particle species.

Side	Species	Counts		Count Rate	
		Size (bins)	Energy (MeV/nuc)	Size (bins)	Energy (MeV/nuc)
C	PENx_C	11	23 – 364	11	23 – 364
	PENx_Fe	11	45 – 471	11	45 – 471
	PENx_He	11	11 – 310	11	11 – 310
	PENx_Mg	10	38 – 408	10	38 – 408
	PENx_N	11	23 – 364	11	23 – 364
	PENx_Ne	11	27 – 384	11	27 – 384
	PENx_O	11	27 – 384	11	27 – 384
	PENx_Si	10	38 – 408	11	38 – 408

Table 2.3.51: PSP_ISOIS-EPIHI_L2-LET2-RATES60 (contd.). Here ‘x’ stands for side C.

Side	Species	Count			Flux			Count Rate		
		Size (bins)	Range SECT (bins)	Energy (MeV/nuc)	Size (bins)	Range SECT (bins)	Energy (MeV/nuc)	Size (bins)	Range SECT (bins)	Energy (MeV/nuc)
C	xxx_29to32	7	29 – 32	0 – 264	7	29 – 32	0 – 264	7	29 – 32	0 – 264
	xxx_32to50	7	32 – 50	0 – 264	7	32 – 50	0 – 264	7	32 – 50	0 – 264
	xxx_Al	14	–	1 – 260	14	–	1 – 260	14	–	1 – 260
	xxx_Ar	15	–	1 – 261	15	–	1 – 261	15	–	1 – 261
	xxx_C	12	–	1 – 259	12	–	1 – 259	12	–	1 – 259
	xxx_Ca	16	–	1 – 261	16	–	1 – 262	16	–	1 – 261
	xxx_Cr	17	–	1 – 261	17	–	1 – 261	17	–	1 – 261
	xxx_Fe	17	–	1 – 261	17	–	1 – 261	17	–	1 – 261
	xxx_H	12	–	0 – 258	12	–	0 – 258	12	–	0 – 258
	xxx_H_SECT	1x9 (1 bin)	R1 0 – 8 (9)	2 – 2	1x9 (1 bin)	R1 0 – 8 (9)	2 – 2	1x9 (1 bin)	R1 0 – 8 (9)	2 – 2
	xxx_He	12	–	0 – 258	12	–	0 – 258	12	–	0 – 258
	xxx_He_SECT	1x9 (1 bin)	R1 0 – 8 (9)	2 – 2	1x9 (1 bin)	R1 0 – 8 (9)	2 – 2	1x9 (1 bin)	R1 0–8 (9)	2 – 2
	xxx_Mg	14	–	1 – 260	14	–	1 – 260	14	–	1 – 260
	xxx_N	12	–	1 – 259	12	–	1 – 259	12	–	1 – 259
	xxx_Na	13	–	1 – 259	13	–	1 – 259	12	–	1 – 259
	xxx_Ne	13	–	1 – 259	13	–	1 – 259	13	–	1 – 259
	xxx_Ni	17	–	1 – 261	17	–	1 – 261	17	–	1 – 261
	xxx_O	13	–	1 – 259	13	–	1 – 259	13	–	1 – 259
	xxx_S	15	–	1 – 261	15	–	1 – 261	15	–	1 – 261
	xxx_Si	14	–	1 – 260	14	–	1 – 260	14	–	1 – 260
	xxx_gt50	7	–	0 – 264	7	–	0 – 264	7	–	0 – 264
	R1 ENA_SECT - measured quantity is Counts; Size 8 x 9; E-bins: 8; E-range: 1 - 3 (MeV/nuc); Sectors: 0 - 8 (9).									

Table 2.3.52: PSP_ISOIS-EPIHI_L2-LET2-RATES60 (contd.). Here, ‘xxx’ stands for R1C.

Side	Species	Count			Flux			Count Rate		
		Size (bins)	Range SECT (bins)	Energy (MeV/nuc)	Size (bins)	Range SECT (bins)	Energy (MeV/nuc)	Size (bins)	Range SECT (bins)	Energy (MeV/nuc)
C	xxxx_H_SECT	3x25 (3 bins)	R26 0 – 24 (25)	3 – 12	3x25 (3 bins)	R26 0 – 24 (25)	3 – 12	3x25 (3 bins)	R26 0 – 24 (25)	3 – 12
	xxxx_He_SECT	3x25 (3 bins)	R26 0 – 24 (25)	3 – 12	3x25 (3 bins)	R26 0 – 24 (25)	3 – 12	3x25 (3 bins)	R26 0 – 24 (25)	3 – 12
	xxxx_ENA_SECT	8x25 (8 bins)	R26 0 – 24 (25)	2 – 12	–	–	–	–	–	–

Table 2.3.53: PSP_ISOIS-EPIHI_L2-LET2-RATES60 (contd.). Here, 'xxxx' stands for R25C which implies that the values are integrated over ranges R2 – R5.

Side	Species	Count		Flux		Count Rate	
		Size (bins)	Energy (MeV/nuc)	Size (bins)	Energy (MeV/nuc)	Size (bins)	Energy (MeV/nuc)
A/B	xxx_29to32	8	1 – 320	8	1 – 320	8	1 – 320
	xxx_32to50	8	1 – 320	8	1 – 320	8	1 – 320
	xxx_Al	18	2 – 279	18	2 – 279	18	2 – 279
	xxx_Ar	20	2 – 288	20	2 – 288	20	2 – 288
	xxx_C	18	1 – 272	18	1 – 272	18	1 – 272
	xxx_Ca	20	2 – 288	20	2 – 288	20	2 – 288
	xxx_Cr	20	2 – 288	20	2 – 288	20	2 – 288
	xxx_Fe	20	2 – 288	20	2 – 288	20	2 – 288
	xxx_H	17	1 – 264	17	1 – 264	17	1 – 264
	xxx_He	17	1 – 266	17	1 – 266	17	1 – 266
	xxx_Mg	18	2 – 279	18	2 – 279	18	2 – 279
	xxx_N	18	1 – 272	18	1 – 272	18	1 – 272
	xxx_Na	18	1 – 275	18	1 – 275	18	1 – 275
	xxx_Ne	18	1 – 275	18	1 – 275	18	1 – 275
	xxx_Ni	21	2 – 294	21	2 – 294	21	2 – 294
	xxx_O	17	1 – 272	17	1 – 272	17	1 – 272
	xxx_S	20	2 – 288	20	2 – 288	20	2 – 288
	xxx_Si	18	2 – 279	18	2 – 279	18	2 – 279
	xxx_gt50	8	1 – 320	8	1 – 320	8	1 – 320

Table 2.3.54: PSP_ISOIS-EPIHI_L2-LET2-RATES60 (contd.). Here, 'xxx' stands for R2C.

Side	Species	Count		Count Rate	
		Size (bins)	Energy (MeV/nuc)	Size (bins)	Energy (MeV/nuc)
C	Electrons_R3C	15	0 – 6	15	0 – 6
	R3C_He_BIN	5x16 (5)	8 – 32	–	–
	R3C_He_BIN (MASS)	16 bins	–	–	–
		0 – 15 seg	–	–	–
	R3C_Ne_BIN	6x8 (6)	16 – 92	–	–
	R3C_Ne_BIN (MASS)	8 bins	–	–	–
		0 – 7 seg	–	–	–
	Electrons_R4C	16	0 – 7	16	0 – 7
	Electrons_R5C	15	1 – 7	15	1 – 7

Table 2.3.55: PSP_ISOIS-EPIHI_L2-LET2-RATES60 (contd.). LET2 electron measurements for ranges R3, R4 and R5.

Side	Species	Count		Flux		Count Rate	
		Size (bins)	Energy (MeV/nuc)	Size (bins)	Energy (MeV/nuc)	Size (bins)	Energy (MeV/nuc)
C	xxxx_29to32	6	8 – 384	6	8 – 384	6	8 – 384
	xxxx_32to50	6	8 – 384	6	8 – 384	6	8 – 384
	xxxx_Al	13	8 – 310	13	8 – 310	13	8 – 310
	xxxx_Ar	13	10 – 320	13	10 – 320	13	10 – 320
	xxxx_C	14	5 – 294	14	5 – 294	14	5 – 294
	xxxx_Ca	14	10 – 332	14	10 – 332	14	10 – 332
	xxxx_Cr	14	10 – 332	14	10 – 332	14	10 – 332
	xxxx_Fe	14	10 – 332	14	10 – 332	14	10 – 332
	xxxx_H	13	3 – 275	13	3 – 275	13	3 – 275
	xxxx_He	14	3 – 279	14	3 – 279	14	3 – 279
	xxxx_Mg	13	8 – 310	13	8 – 310	13	8 – 310
	xxxx_N	14	5 – 294	14	5 – 294	14	5 – 294
	xxxx_Na	14	7 – 310	14	7 – 310	14	7 – 310
	xxxx_Ne	14	7 – 310	14	7 – 310	14	7 – 310
	xxxx_Ni	15	10 – 347	15	10 – 347	15	10 – 347
	xxxx_O	14	6 – 301	14	6 – 301	14	6 – 301
	xxxx_S	13	10 – 320	13	10 – 320	13	10 – 320
	xxxx_Si	14	8 – 320	14	8 – 320	14	8 – 320
	xxxx_gt50	6	8 – 384	6	8 – 384	6	8 – 384

Table 2.3.56: PSP_ISOIS-EPIHI_L2-LET2-RATES60 (contd.). Here, 'xxxx' stands for R35C which implies that the values are integrated over ranges R3 – R5.

2.3.13 FILE: PSP_ISOIS-EPIHI_L2-SECOND-RATES

This file contains the 1 s cadence measurements of particle Counts, Flux (cm^{-2} sr^{-1} sec^{-1} MeV^{-1}) and Count Rate (counts/s) of Electrons and H for sides A and B for the double–sided High Energy Telescope (HET) and the Low Energy Telescopes (LET1), and the single–sided Low Energy Telescope (LET2). The values of these variables are summarized in Table 2.3.57. The variables are named as: <tel>_<side>_<species>_<quantity>, where, <tel> stands for HET, LET1 or LET2; <side> stands for A, B or C; <species> stands for the particle species; and <quantity> represents Counts (not used in variable names, in general), Flux or Rate.
Examples: HET_A_Electrons_Flux; LET1_B_H_Rate; LET2_C_H.

Side	Range	Quantity	Electrons		H	
			E-bins	E-range (MeV/nuc) (bins)	E-bins	E-range (MeV/nuc) (bins)
C	HET_A	Count	3	1 – 3	2	13 – 24
		Flux	3	1 – 3	2	13 – 24
		Count Rate	3	1 – 3	2	13 – 24
	HET_B	Count	3	1 – 3	2	13 – 24
		Flux	3	1 – 3	2	13 – 24
		Count Rate	3	1 – 3	2	13 – 24
	LET1_A	Count	2	1 – 2	3	2 – 11
		Flux	2	1 – 2	3	2 – 11
		Count Rate	2	1 – 2	3	2 – 11
	LET1_B	Count	2	1 – 2	3	2 – 11
		Flux	2	1 – 2	3	2 – 11
		Count Rate	2	1 – 2	3	2 – 11
	LET2_C	Count	2	1 – 2	3	2 – 11
		Flux	2	1 – 2	3	2 – 11
		Count Rate	2	1 – 2	3	2 – 11

Table 2.3.57: PSP_ISOIS-EPIHI_L2-SECOND-RATES. The EPI-Hi 1 s data of Electrons and H for HET, LET1 and LET2.

2.4 IS⊙IS SCIENCE DATA

2.4.1 FILE: PSP_ISOIS-EPIHI_L2-SECOND-RATES

This file contains a selection of EPI-Lo and EPI-Hi level 2 data, with some averaging over direction for EPI-Lo. It is intended as a small file “quicklook” to help identify periods of interest and should not be used for quantitative analysis.

3 DATA QUALITY FLAGS AND FILL

3.1 MOTIVATION

Any data product may be affected by one or more factors that reduce the quality, and thereby compromise the interpretation, of the data. These factors fall into four broad types, listed here in order of increasing severity:

- factors that warrant an advisory or further information.
- factors that warrant using caution when deriving results.
- factors that make certain data not scientifically useful but may still be useful for analyzing instrument response. These data, including count rates, are replaced with fill values in the public release.
- factors that make certain processed data meaningless, e.g. fluxes. In these cases the relevant data will not be produced at all.

Any of these factors that impact the data product will be noted with a data-quality variable, or "quality flag". EPI-Hi level-2 data have a single quality flag variable while EPI-Lo level-2 data have one quality flag per channel (i.e., one per timebase/Epoch variable).

Flags in EPI-Hi files are named `Quality_Flag`; in EPI-Lo files, like `Quality_Flag_ChanT` (for channel T timebase).

3.2 QUALITY FLAG STRUCTURE

The quality-flag variable is an array, indexed by category. Each timestamp and category has a value from 0-127. A quality flag of 0 indicates no known factors of that category that reduce quality in the associated data at the corresponding timestamp. Nonzero quality flags indicate a known factor in the data with higher values representing increased severity. Each index in the quality flag array represents a different category which may affect different variables and products within the data, so a full understanding of a factor affecting the data requires knowledge of both the category and severity.

Unused categories are populated with zero ("perfect" data) and should be ignored.

If the severity is high enough some parts of the data may be omitted as noted below:

Low (1 – 31) there are informational warnings and caveats that are unlikely to affect the scientific validity of the data

Medium (32 – 63) users should take caution when deriving results and contact the instrument team for details, as the data may not be scientifically useful in some cases.

High (64 – 95) affected data are not scientifically useful and are removed from public release

Severe (96 – 127) data are completely invalid, affected fluxes are not calculated

The SOC aims to ensure that the interpretation of a quality-flag value within a category that applies to multiple data products does not vary drastically among those data products.

3.3 EXISTING CATEGORIES

3.3.1 WARM UP

Used for potential issues with data just after instrument turn-on. Index 0 in the quality flags variable.

EPI-Lo high-voltage ramp-up 110 (Severe): during periods flagged with this value, the EPI-Lo high voltage and/or bias voltage are still ramping up, so the instrument may not be sensitive to incident particles. Affects counts and counts rates, making fluxes meaningless. Affects all EPI-Lo level 2 science files (`psp_isois-epilo_l2-xx`), all counts, count rate, and flux variables.

3.3.2 LIVETIME

Used for potential issues in calculating instrument livetime. Index 1 in the quality flags variable.

Partial processing 45 (Medium): EPI-Hi count rates (and fluxes) are ordinarily corrected for the fraction of valid events which are not processed by the flight software. This value indicates this fraction is only available for a portion of the integration period and fluxes may be inaccurate, particularly during periods of high and rapidly-varying count rates. Affects all EPI-Hi level 2 rates (`psp_isois-hi_let1-rates3600`, etc.), count rate and flux variables.

Not calculated 55 (Medium): The fraction of events processed is completely unknown and all events are assumed to be processed. Count rates and fluxes may be inaccurate during periods of high count rates. Affects all EPI-Hi level 2 rates (`psp_isois-hi_let1-rates3600`, etc.), count rate and flux variables.

3.3.3 PITCH ANGLE CALCULATIONS

Used for potential issues with the pitch angle calculation based on magnetic field data from FIELDS. Index 2 in the quality flags variable.

Preliminary pitch angles 80 (High): Magnetic field data from FIELDS is preliminary and not suitable for pitch angle calculations. As such, pitch angles are not included in public release. Affects all level 2 files, EPI-Hi and EPI-Lo, pitch angle variables.

3.3.4 TESTING

Used for testing periods where data cannot be calibrated. Index 3 in quality flags variable.

ADC Stim test 119 (Severe): Periods during which EPI-Hi is generating internal test pulses. Not calibratable to fluxes; count rates masked from public release. Affects all EPI-Hi level 2 rates files, count rate and flux variables.

Threshold test 105 (Severe): Periods during which EPI-Lo is testing thresholds for time-of-flight subsystem. Composition mode data not calibratable to fluxes; count rates masked from public release. Affects EPI-Lo level 2 IC and PC, count rate and flux variables.

3.4 FILL VALUES

IS⊙IS data files use fill values to indicate invalid or missing data. The valid range and the fill value used are provided for each variable in the CDF files according to ISTP/SPDF metadata standards. Values outside the valid range, in particular fill values, should not be interpreted as meaningful data.

Fill usually indicates data are not recoverable and not scientifically meaningful. Do not use count rates as a substitute for filled flux values. If the instrument team and SOC are able to recover meaningful data, those will be added to a future release.

Certain well-defined quality issues, described above, will result in fill values. Other sources of fill include:

- Uncalibrated data products
- Data products with known routinely high levels of background where the background subtraction has not been completed
- Time periods known to be related to instrument testing or other nonphysical sources of apparent counts
- Times where a portion of the data has been lost or corrupted but the rest is recoverable; the known lost data are replaced with fill

Fill values are not generated during periods when the instrument is off or in a mode that does not produce a particular product (for example, encounter-only data products during the cruise phase of the orbit). Do not assume a regular cadence of timestamps; the cadence may change, samples may be cut short, and samples may be missing. Use the time variables specified according to the ISTP/SPDF metadata standard to interpret time of data collection.

4 EPI-LO DECODER RING

We have produced a summary of the EPI-Lo data called the EPI-Lo Channel Definition "crib sheet". The intent is to guide the user from a description of physical measurements to specific data products. Note that this relationship is time dependent and Figure 4 only applies during the first eight orbits (launch until 14 June 2021, LUT Regime Index = 6). The time dependence is due to instrument configuration changes (e.g., changing definitions of species and energy bins due to adjustment to lookup tables or LUTs) and unplanned changes (e.g., sensitivity variations or background increase due to dust impacts admitting more light).

The lookup tables were adjusted on 14 June 2021 and were updated to adjust box locations for species and Figure 5 reflects the updates.

The upper table in Figure 4 references only data products that include time-of-flight TOF measurements and the lower table references only measurements that employ the energy/solid state detector (SSD) system. Both have the same columns. The Mode identifies one of four instrument modes: Ion Composition (IC), Particle Composition (PC), Ion Energy (IE) or Particle Energy (PE), (PC and IE are not included in Release 1) which relate to the types of measurements made. The instrument can cycle through up to eight different mode intervals (slots) per second. Typically the slot pattern covers all four modes in an alternating pattern (e.g., IC,PE,IC,IE,IC,PE,IC,PC). The next column is the channel/rate name and the associated mnemonic. Different channels can measure multiple types of particles, so it is useful to provide a non-descriptive, but memorable, name for the different data products to help avoid confusion like "During this period the Electron data are mostly protons" in favor of 'During this period the [E] rates are mostly protons. The mnemonic and associated system is based largely on what we expect to see in each the given channel (e.g., [E] for electrons). The next column provides the official, descriptive label for each data type. The Channel ID provides the useful range and naming of individual channels associated with each data type or sub group thereof. Species mass provides the species or type (or alternate information). The energy range associated with the channel ID list is given in keV and MeV/nuc (where applicable). The CDF data file needed to study the particles described on a given row are in the Logical Source. Within each file the variable name is given for physical units and counting rate. Finally, there are miscellaneous notes on each row in the last column. See Release Notes on details for variables and calibrated data products.

PSP / ISOIS / EPI-Lo Rate Channel Definitions			LUT Regime Index 0 to 5			Orbits 1 - 8		TRIPLES (except T = DOUBLES)				
Mode	Channel / rate	Label	ChanID		species	mass	E (keV)		E (MeV/nuc)		Logical	Variable	comments
	mnemonic		low	high		amu	low	high	low	high	Source	Name	
IC	[P] Protons	High Res. Protons	P000	P040	H	1	60	8,990	0.060	8.990	psp_isois-epilo_l2-ic	H_Flux_ChanP	
IC	[P]	High Res. Protons	P041	P047									box not defined
IC	[C] Composition	Ions Group 1	C048	C093	He-3	3	84	20,000	0.028	6.667	psp_isois-epilo_l2-ic	He3_CountRate_ChanC	
IC	[C]	Ions Group 1	C094	C140	He-4	4	72	20,000	0.018	5.000	psp_isois-epilo_l2-ic	He4_Flux_ChanC	
IC	[C]	Ions Group 1	C141	C145									box not defined
IC	[C]	Ions Group 1	C146	C186	O	16	227	20,600	0.014	1.288	psp_isois-epilo_l2-ic	O_CountRate_ChanC	
IC	[C]	Ions Group 1	C187	C192									box not defined
IC	[C]	Ions Group 1	C193	C197	Fe		Null						non-standard boxes
IC	[C]	Ions Group 1	C198	C238	Fe	56	453	22,300	0.008	0.398	psp_isois-epilo_l2-ic	Fe_CountRate_ChanC	
IC	[C]	Ions Group 1	C239	C239									box not defined
IC	[D] D = Comp. + 1	Ions Group 2	D240	D260	C	12	197	20,400	0.016	1.700	psp_isois-epilo_l2-ic	C_CountRate_ChanD	
IC	[D]	Ions Group 2	D261	D351									box not defined
IC	[D]	Ions Group 2	D352	D366	Si	28	529	21,400	0.019	0.764	psp_isois-epilo_l2-ic	Si_CountRate_ChanD	
IC	[D]	Ions Group 2	D367	D431									box not defined
IC	[T] TOF Only	Ion TOF	T000	T031	Ions	1	44,900	30	44.900	0.030	psp_isois-epilo_l2-ic	H_Flux_ChanT	no composition
IC	[R] R = Proton + 1	Hi Time Res Protons	R000	R014	H	1	60	8,320	0.060	8.320	psp_isois-epilo_l2-ic	H_Flux_ChanR	
IC	[R] *skip Q = Quadrant*	Hi Time Res Protons	R015	R015	H	1	Null						non-standard boxes

PSP / ISOIS / EPI-Lo Rate Channel Definitions			LUT Regime Index 0 to 5			Orbits 1 - 8		SINGLES				
Mode	Channel / rate	Label	ChanID		species	mass	E (keV)		E (MeV/nuc)		Logical	Variable	comments
	mnemonic		low	high		amu	low	high	low	high	Source	Name	
PE	[E] Electron	High Res Electrons	E000	E000	deposited		null						hi/lo gain, no comp.
PE	[E]	High Res Electrons	E001	E047	deposited		15	250,000	0.015	250			hi/lo gain, no comp.
PE	[E]	High Res Electrons	E000	E016	e- cal		26	388	0.026	0.388	psp_isois-epilo_l2-pe	Electron_CountRate_ChanE	hi/lo gain, no comp.
PE	[E]	High Res Electrons	E002	E031	H cal	1	399	10,200	0.399	10.2	psp_isois-epilo_l2-pe	H_CountRate_ChanE	hi/lo gain, no comp.
PE	[F] F = Elect. + 1	High Time Res. Electrons	F000	F000	deposited		null						hi/lo gain, no comp.
PE	[F]	High Time Res. Electrons	F001	F015	deposited		35	250,000	0.035	250	psp_isois-epilo_l2-pe	Electron_CountRate_ChanF	hi/lo gain, no comp.
PE	[F]	High Time Res. Electrons	F000	F011	H cal	1	399	10,200	0.399	10.2	psp_isois-epilo_l2-pe	H_CountRate_ChanF	hi/lo gain, no comp.
PE	[G] G = Elect + 2	High Look Res Electrons	E000	G000	deposited		null						hi/lo gain, no comp.
PE	[G]	High Look Res Electrons	E001	G047	deposited		15	250,000	0.015	250	psp_isois-epilo_l2-pe	Electron_CountRate_ChanG	hi/lo gain, no comp.

PSP / ISOIS / EPI-Lo Rate Channel Definitions			LUT Regime Index 6 to TBD				Orbits 8 - TBD				TRIPLES (except T = DOUBLES)			
Mode	Channel / rate	Label	ChanID		species	mass	E (keV)		E (MeV/nuc)		Logical	Variable	comments	
	mnemonic		low	high		amu	low	high	low	high	Source	Name		
IC	[P] Protons	High Res. Protons	P000	P038	H	1	67.0	10,252	0.067	10.25	psp_isois-epilo_l2-ic	H_Flux_ChanP		
IC	[P]	High Res. Protons	P039	P039	H	1			0.000	0.00			box not defined	
IC	[P]	High Res. Protons	P040	P041									background box	
IC	[P]	High Res. Protons	P042	P047									background box	
IC	[C] Composition	Ions Group 1	C050	C093	He-3	3	94.8	22,536	0.032	7.51	psp_isois-epilo_l2-ic	He3_CountRate_ChanC		
IC	[C]	Ions Group 1	C094	C095	He-3 Bkg								background boxes	
IC	[C]	Ions Group 1	C100	C143	He-4	4	82.8	22,540	0.021	5.64	psp_isois-epilo_l2-ic	He4_Flux_ChanC		
IC	[C]	Ions Group 1	C144	C144	He-4 Bkg								background boxes	
IC	[C]	Ions Group 1	C150	C150	O	16							box not defined	
IC	[C]	Ions Group 1	C151	C193	O	16	204.8	23,114	0.013	1.44	psp_isois-epilo_l2-ic	O_CountRate_ChanC		
IC	[C]	Ions Group 1	C194	C194	O Bkg								background boxes	
IC	[C]	Ions Group 1	C195	C196	Fe	56							box not defined	
IC	[C]	Ions Group 1	C197	C238	Fe	56	431.2	24,868	0.008	0.44	psp_isois-epilo_l2-ic	Fe_CountRate_ChanC		
IC	[C]	Ions Group 1	C239	C239	Fe Bkg								background boxes	
IC	[D] D = Comp. + "1"	Ions Group 2	D250	D271	C	12	177.8	22,872	0.015	1.91	psp_isois-epilo_l2-ic	C_CountRate_ChanD		
IC	[D]	Ions Group 2	D272	D272	C Bkg								background box	
IC	[D]	Ions Group 2	D300	D321	Mg	24	218.3	23,672	0.009	0.99	psp_isois-epilo_l2-ic	Mg_CountRate_ChanD		
IC	[D]	Ions Group 2	D322	D322	Mg Bkg								background box	
IC	[D]	Ions Group 2	D330	D334	Ne								box not defined	
IC	[D]	Ions Group 2	D335	D340	Ne	20	830.0	23,392	0.042	1.17	psp_isois-epilo_l2-ic	Ne_CountRate_ChanD		
IC	[D]	Ions Group 2	D341	D341	Ne Bkg								background box	
IC	[D]	Ions Group 2	D352	D371	Si	28	326.8	23,946	0.012	0.86	psp_isois-epilo_l2-ic	Si_CountRate_ChanD		
IC	[D]	Ions Group 2	D372	D372	Si Bkg								background box	
IC	[T] TOF Only	Ion TOF	T000	T031	Ions	1	46,367.0	21	46.367	0.02	psp_isois-epilo_l2-ic	H_Flux_ChanT	no composition	
IC	[R] R = Proton + "1"	Hi Time Res Protons	R000	R013	H	1	67	8,736	0.067	8.74	psp_isois-epilo_l2-ic	H_Flux_ChanR		
IC	[R]	Hi Time Res Protons	R014	R014	H	1	Null						non-standard boxes	
IC	[R] *skip Q = Quadrant*	Hi Time Res Protons	R015	R015	H	1	Null						non-standard boxes	

PSP / ISOIS / EPI-Lo Rate Channel Definitions			LUT Regime Index 6 to TBD				Orbits 8 - TBD				SINGLES			
Mode	Channel / rate	Label	ChanID		species	mass	E (keV)		E (MeV/nuc)		Logical	Variable	comments	
	mnemonic		low	high		amu	low	high	low	high	Source	Name		
PE	[E] Electron	High Res Electrons	E000	E000	deposited		null						hi/lo gain, no comp.	
PE	[E]	High Res Electrons	E001	E047	deposited		15	250,000	0.015	250			hi/lo gain, no comp.	
PE	[E]	High Res Electrons	E000	E016	e- cal		26	388	0.026	0.388	psp_isois-epilo_l2-pe	Electron_CountRate_ChanE	hi/lo gain, no comp.	
PE	[E]	High Res Electrons	E002	E031	H cal	1	399	10,200	0.399	10.2	psp_isois-epilo_l2-pe	H_CountRate_ChanE	hi/lo gain, no comp.	
PE	[F] F = Elect. + 1	High Time Res. Electrons	F000	F000	deposited		null						hi/lo gain, no comp.	
PE	[F]	High Time Res. Electrons	F001	F015	deposited		35	250,000	0.035	250	psp_isois-epilo_l2-pe	Electron_CountRate_ChanF	hi/lo gain, no comp.	
PE	[F]	High Time Res. Electrons	F000	F011	H cal	1	399	10,200	0.399	10.2	psp_isois-epilo_l2-pe	H_CountRate_ChanF	hi/lo gain, no comp.	
PE	[G] G = Elect + 2	High Look Res Electrons	E000	G000	deposited		null						hi/lo gain, no comp.	
PE	[G]	High Look Res Electrons	E001	G047	deposited		15	250,000	0.015	250	psp_isois-epilo_l2-pe	Electron_CountRate_ChanG	hi/lo gain, no comp.	

5 GENERAL LIST OF VARIABLES

5.1 PSP_ISOIS-EPIHI_L2-HET-RATES10

A_Electrons
A_Electrons_Rate
A_H
A_H_Flux
A_H_Rate
A_He
A_He_Flux
A_He_Rate
B_Electrons
B_Electrons_Rate
B_H
B_H_Flux
B_H_Rate
B_He
B_He_Flux
B_He_Rate
HCI_Lat
HCI_Lon
HCI_R
HET_A_HCI
HET_A_PA
HET_A_RTN
HET_A_SA
HET_B_HCI
HET_B_PA
HET_B_RTN
HET_B_SA
HGC_Lat
HGC_Lon
HGC_R
Quality_Flag

5.2 PSP_ISOIS-EPIHI_L2-HET-RATES300

A_CNO_SECT_Rate
A_FeGroup_SECT_Rate
A_NetoSi_SECT_Rate
B_CNO_SECT_Rate
B_FeGroup_SECT_Rate
B_NetoSi_SECT_Rate

HCI_Lat
HCI_Lon
HCI_R
HET_A_HCI
HET_A_PA
HET_A_R17_SECT_HCI
HET_A_R17_SECT_PA
HET_A_R17_SECT_RTN
HET_A_R17_SECT_SA
HET_A_RTN
HET_A_SA
HET_B_HCI
HET_B_PA
HET_B_R17_SECT_HCI
HET_B_R17_SECT_PA
HET_B_R17_SECT_RTN
HET_B_R17_SECT_SA
HET_B_RTN
HET_B_SA
HGC_Lat
HGC_Lon
HGC_R
Quality_Flag

5.3 PSP_ISOIS-EPIHI_L2-HET-RATES3600

A_Al
A_Al_Rate
A_Ar
A_Ar_Rate
A_C
A_CNO_SECT_Rate
A_C_Rate
A_Ca
A_Ca_Rate
A_Cr
A_Cr_Rate
A_Electrons
A_Electrons_Rate
A_Electrons_SECT_Rate
A_Fe
A_FeGroup_SECT_Rate
A_Fe_Rate
A_H

B_H_Rate
B_H_SECT_Flux
B_H_SECT_Rate
B_He
B_He_Flux
B_He_Rate
B_He_SECT_Flux
B_He_SECT_Rate
B_Mg
B_Mg_Rate
B_N
B_N_Rate
B_Na
B_Na_Rate
B_Ne
B_Ne_Rate
B_NetoSi_SECT_Rate
B_Ni
B_Ni_Rate
B_O
B_O_Rate
B_S
B_S_Rate
B_Si
B_Si_Rate
HCI_Lat
HCI_Lon
HCI_R
HET_A_HCI
HET_A_PA
HET_A_R17_SECT_HCI
HET_A_R17_SECT_PA
HET_A_R17_SECT_RTN
HET_A_R17_SECT_SA
HET_A_RTN
HET_A_SA
HET_B_HCI
HET_B_PA
HET_B_R17_SECT_HCI
HET_B_R17_SECT_PA
HET_B_R17_SECT_RTN
HET_B_R17_SECT_SA
HET_B_RTN
HET_B_SA
HGC_Lat

HGC_Lon
HGC_R
Quality_Flag
R1A_He_BIN
R1A_Ne_BIN
R1B_He_BIN
R1B_Ne_BIN
R2A_He_BIN
R2A_Ne_BIN
R2B_He_BIN
R2B_Ne_BIN
R3A_He_BIN
R3A_Ne_BIN
R3B_He_BIN
R3B_Ne_BIN
R4A_He_BIN
R4A_Ne_BIN
R4B_He_BIN
R4B_Ne_BIN
R5A_He_BIN
R5A_Ne_BIN
R5B_He_BIN
R5B_Ne_BIN
R6A_He_BIN
R6A_Ne_BIN
R6B_He_BIN
R6B_Ne_BIN
R7A_He_BIN
R7A_Ne_BIN
R7B_He_BIN
R7B_Ne_BIN

5.4 PSP_ISOIS-EPIHI_L2-HET-RATES60

A_Al
A_Al_Rate
A_Ar
A_Ar_Rate
A_C
A_C_Rate
A_Ca
A_Ca_Rate
A_Cr
A_Cr_Rate

A_Electrons
A_Electrons_Rate
A_Electrons_SECT_Rate
A_Fe
A_Fe_Rate
A_H
A_H_Flux
A_H_Rate
A_H_SECT_Flux
A_H_SECT_Rate
A_He
A_He_Flux
A_He_Rate
A_He_SECT_Flux
A_He_SECT_Rate
A_Mg
A_Mg_Rate
A_N
A_N_Rate
A_Na
A_Na_Rate
A_Ne
A_Ne_Rate
A_Ni
A_Ni_Rate
A_O
A_O_Rate
A_S
A_S_Rate
A_Si
A_Si_Rate
B_Al
B_Al_Rate
B_Ar
B_Ar_Rate
B_C
B_C_Rate
B_Ca
B_Ca_Rate
B_Cr
B_Cr_Rate
B_Electrons
B_Electrons_Rate
B_Electrons_SECT_Rate
B_Fe

B_Fe_Rate
B_H
B_H_Flux
B_H_Rate
B_H_SECT_Flux
B_H_SECT_Rate
B_He
B_He_Flux
B_He_Rate
B_He_SECT_Flux
B_He_SECT_Rate
B_Mg
B_Mg_Rate
B_N
B_N_Rate
B_Na
B_Na_Rate
B_Ne
B_Ne_Rate
B_Ni
B_Ni_Rate
B_O
B_O_Rate
B_S
B_S_Rate
B_Si
B_Si_Rate
HCI_Lat
HCI_Lon
HCI_R
HET_A_HCI
HET_A_PA
HET_A_R17_SECT_HCI
HET_A_R17_SECT_PA
HET_A_R17_SECT_RTN
HET_A_R17_SECT_SA
HET_A_RTN
HET_A_SA
HET_B_HCI
HET_B_PA
HET_B_R17_SECT_HCI
HET_B_R17_SECT_PA
HET_B_R17_SECT_RTN
HET_B_R17_SECT_SA
HET_B_RTN

HET_B_SA
HGC_Lat
HGC_Lon
HGC_R
Quality_Flag

5.5 PSP_ISOIS-EPIHI_L2-LET1-RATES10

A_Electrons
A_Electrons_Rate
A_H
A_H_Flux
A_H_Rate
A_He
A_He_Flux
A_He_Rate
B_Electrons
B_Electrons_Rate
B_H
B_H_Flux
B_H_Rate
B_He
B_He_Flux
B_He_Rate
HCI_Lat
HCI_Lon
HCI_R
HGC_Lat
HGC_Lon
HGC_R
LET1_A_HCI
LET1_A_PA
LET1_A_RTN
LET1_A_SA
LET1_B_HCI
LET1_B_PA
LET1_B_RTN
LET1_B_SA
Quality_Flag

5.6 PSP_ISOIS-EPIHI_L2-LET1-RATES300

HCI_Lat
HCI_Lon
HCI_R
HGC_Lat
HGC_Lon
HGC_R
LET1_A_HCI
LET1_A_PA
LET1_A_R1_SECT_HCI
LET1_A_R1_SECT_PA
LET1_A_R1_SECT_RTN
LET1_A_R1_SECT_SA
LET1_A_R26_SECT_HCI
LET1_A_R26_SECT_PA
LET1_A_R26_SECT_RTN
LET1_A_R26_SECT_SA
LET1_A_RTN
LET1_A_SA
LET1_B_HCI
LET1_B_PA
LET1_B_R1_SECT_HCI
LET1_B_R1_SECT_PA
LET1_B_R1_SECT_RTN
LET1_B_R1_SECT_SA
LET1_B_R26_SECT_HCI
LET1_B_R26_SECT_PA
LET1_B_R26_SECT_RTN
LET1_B_R26_SECT_SA
LET1_B_RTN
LET1_B_SA
Quality_Flag
R1A_CNO_SECT_Rate
R1A_FeGroup_SECT_Rate
R1A_NetoSi_SECT_Rate
R1B_CNO_SECT_Rate
R1B_FeGroup_SECT_Rate
R1B_NetoSi_SECT_Rate
R26A_CNO_SECT_Rate
R26A_FeGroup_SECT_Rate
R26A_NetoSi_SECT_Rate
R26B_CNO_SECT_Rate
R26B_FeGroup_SECT_Rate
R26B_NetoSi_SECT_Rate

5.7 PSP_ISOIS-EPIHI_L2-LET1-RATES3600

A_Al
A_Al_Rate
A_Ar
A_Ar_Rate
A_C
A_C_Rate
A_Ca
A_Ca_Rate
A_Cr
A_Cr_Rate
A_Electrons
A_Electrons_Rate
A_Fe
A_Fe_Rate
A_H
A_H_Flux
A_H_Rate
A_He
A_He_Flux
A_He_Rate
A_Mg
A_Mg_Rate
A_N
A_N_Rate
A_Na
A_Na_Rate
A_Ne
A_Ne_Rate
A_Ni
A_Ni_Rate
A_O
A_O_Rate
A_S
A_S_Rate
A_Si
A_Si_Rate
B_Al
B_Al_Rate
B_Ar
B_Ar_Rate
B_C

B_C_Rate
B_Ca
B_Ca_Rate
B_Cr
B_Cr_Rate
B_Electrons
B_Electrons_Rate
B_Fe
B_Fe_Rate
B_H
B_H_Flux
B_H_Rate
B_He
B_He_Flux
B_He_Rate
B_Mg
B_Mg_Rate
B_N
B_N_Rate
B_Na
B_Na_Rate
B_Ne
B_Ne_Rate
B_Ni
B_Ni_Rate
B_O
B_O_Rate
B_S
B_S_Rate
B_Si
B_Si_Rate
HCI_Lat
HCI_Lon
HCI_R
HGC_Lat
HGC_Lon
HGC_R
LET1_A_HCI
LET1_A_PA
LET1_A_R1_SECT_HCI
LET1_A_R1_SECT_PA
LET1_A_R1_SECT_RTN
LET1_A_R1_SECT_SA
LET1_A_R26_SECT_HCI
LET1_A_R26_SECT_PA

LET1_A_R26_SECT_RTN
LET1_A_R26_SECT_SA
LET1_A_RTN
LET1_A_SA
LET1_B_HCI
LET1_B_PA
LET1_B_R1_SECT_HCI
LET1_B_R1_SECT_PA
LET1_B_R1_SECT_RTN
LET1_B_R1_SECT_SA
LET1_B_R26_SECT_HCI
LET1_B_R26_SECT_PA
LET1_B_R26_SECT_RTN
LET1_B_R26_SECT_SA
LET1_B_RTN
LET1_B_SA
Quality_Flag
R1A_CNO_SECT_Rate
R1A_FeGroup_SECT_Rate
R1A_H_SECT_Flux
R1A_H_SECT_Rate
R1A_He_BIN
R1A_He_SECT_Flux
R1A_He_SECT_Rate
R1A_Ne_BIN
R1A_NetoSi_SECT_Rate
R1B_CNO_SECT_Rate
R1B_FeGroup_SECT_Rate
R1B_H_SECT_Flux
R1B_H_SECT_Rate
R1B_He_BIN
R1B_He_SECT_Flux
R1B_He_SECT_Rate
R1B_Ne_BIN
R1B_NetoSi_SECT_Rate
R26A_CNO_SECT_Rate
R26A_FeGroup_SECT_Rate
R26A_H_SECT_Flux
R26A_H_SECT_Rate
R26A_He_SECT_Flux
R26A_He_SECT_Rate
R26A_NetoSi_SECT_Rate
R26B_CNO_SECT_Rate
R26B_FeGroup_SECT_Rate
R26B_H_SECT_Flux

R26B_H_SECT_Rate
R26B_He_SECT_Flux
R26B_He_SECT_Rate
R26B_NetoSi_SECT_Rate
R2A_He_BIN
R2A_Ne_BIN
R2B_He_BIN
R2B_Ne_BIN
R3A_He_BIN
R3A_Ne_BIN
R3B_He_BIN
R3B_Ne_BIN
R45A_He_BIN
R45A_Ne_BIN
R45B_He_BIN
R45B_Ne_BIN
R6A_He_BIN
R6A_Ne_BIN
R6B_He_BIN
R6B_Ne_BIN

5.8 PSP_ISOIS-EPIHI_L2-LET1-RATES60

A_Al
A_Al_Rate
A_Ar
A_Ar_Rate
A_C
A_C_Rate
A_Ca
A_Ca_Rate
A_Cr
A_Cr_Rate
A_Electrons
A_Electrons_Rate
A_Fe
A_Fe_Rate
A_H
A_H_Flux
A_H_Rate
A_He
A_He_Flux
A_He_Rate
A_Mg

B_O
B_O_Rate
B_S
B_S_Rate
B_Si
B_Si_Rate
HCI_Lat
HCI_Lon
HCI_R
HGC_Lat
HGC_Lon
HGC_R
LET1_A_HCI
LET1_A_PA
LET1_A_R1_SECT_HCI
LET1_A_R1_SECT_PA
LET1_A_R1_SECT_RTN
LET1_A_R1_SECT_SA
LET1_A_R26_SECT_HCI
LET1_A_R26_SECT_PA
LET1_A_R26_SECT_RTN
LET1_A_R26_SECT_SA
LET1_A_RTN
LET1_A_SA
LET1_B_HCI
LET1_B_PA
LET1_B_R1_SECT_HCI
LET1_B_R1_SECT_PA
LET1_B_R1_SECT_RTN
LET1_B_R1_SECT_SA
LET1_B_R26_SECT_HCI
LET1_B_R26_SECT_PA
LET1_B_R26_SECT_RTN
LET1_B_R26_SECT_SA
LET1_B_RTN
LET1_B_SA
Quality_Flag
R1A_H_SECT_Flux
R1A_H_SECT_Rate
R1A_He_SECT_Flux
R1A_He_SECT_Rate
R1B_H_SECT_Flux
R1B_H_SECT_Rate
R1B_He_SECT_Flux
R1B_He_SECT_Rate

R26A_H_SECT_Flux
R26A_H_SECT_Rate
R26A_He_SECT_Flux
R26A_He_SECT_Rate
R26B_H_SECT_Flux
R26B_H_SECT_Rate
R26B_He_SECT_Flux
R26B_He_SECT_Rate

5.9 PSP_ISOIS-EPIHI_L2-LET2-RATES10

C_Electrons
C_Electrons_Rate
C_H
C_H_Flux
C_H_Rate
C_He
C_He_Flux
C_He_Rate
HCI_Lat
HCI_Lon
HCI_R
HGC_Lat
HGC_Lon
HGC_R
LET2_C_HCI
LET2_C_PA
LET2_C_RTN
LET2_C_SA
Quality_Flag

5.10 PSP_ISOIS-EPIHI_L2-LET2-RATES300

HCI_Lat
HCI_Lon
HCI_R
HGC_Lat
HGC_Lon
HGC_R
LET2_C_HCI
LET2_C_PA
LET2_C_R1_SECT_HCI
LET2_C_R1_SECT_PA

LET2_C_R1_SECT_RTN
LET2_C_R1_SECT_SA
LET2_C_R25_SECT_HCI
LET2_C_R25_SECT_PA
LET2_C_R25_SECT_RTN
LET2_C_R25_SECT_SA
LET2_C_RTN
LET2_C_SA
Quality_Flag
R1C_CNO_SECT_Rate
R1C_FeGroup_SECT_Rate
R1C_NetoSi_SECT_Rate
R25C_CNO_SECT_Rate
R25C_FeGroup_SECT_Rate
R25C_NetoSi_SECT_Rate

5.11 PSP_ISOIS-EPIHI_L2-LET2-RATES3600

C_Al
C_Al_Rate
C_Ar
C_Ar_Rate
C_C
C_C_Rate
C_Ca
C_Ca_Rate
C_Cr
C_Cr_Rate
C_Electrons
C_Electrons_Rate
C_Fe
C_Fe_Rate
C_H
C_H_Flux
C_H_Rate
C_He
C_He_Flux
C_He_Rate
C_Mg
C_Mg_Rate
C_N
C_N_Rate
C_Na
C_Na_Rate

C_Ne
C_Ne_Rate
C_Ni
C_Ni_Rate
C_O
C_O_Rate
C_S
C_S_Rate
C_Si
C_Si_Rate
HCI_Lat
HCI_Lon
HCI_R
HGC_Lat
HGC_Lon
HGC_R
LET2_C_HCI
LET2_C_PA
LET2_C_R1_SECT_HCI
LET2_C_R1_SECT_PA
LET2_C_R1_SECT_RTN
LET2_C_R1_SECT_SA
LET2_C_R25_SECT_HCI
LET2_C_R25_SECT_PA
LET2_C_R25_SECT_RTN
LET2_C_R25_SECT_SA
LET2_C_RTN
LET2_C_SA
Quality_Flag
R1C_CNO_SECT_Rate
R1C_FeGroup_SECT_Rate
R1C_H_SECT_Flux
R1C_H_SECT_Rate
R1C_He_BIN
R1C_He_SECT_Flux
R1C_He_SECT_Rate
R1C_Ne_BIN
R1C_NetoSi_SECT_Rate
R25C_CNO_SECT_Rate
R25C_FeGroup_SECT_Rate
R25C_H_SECT_Flux
R25C_H_SECT_Rate
R25C_He_SECT_Flux
R25C_He_SECT_Rate
R25C_NetoSi_SECT_Rate

R2C_He_BIN
R2C_Ne_BIN
R3C_He_BIN
R3C_Ne_BIN
R45C_He_BIN
R45C_Ne_BIN

5.12 PSP_ISOIS-EPIHI_L2-LET2-RATES60

C_Al
C_Al_Rate
C_Ar
C_Ar_Rate
C_C
C_C_Rate
C_Ca
C_Ca_Rate
C_Cr
C_Cr_Rate
C_Electrons
C_Electrons_Rate
C_Fe
C_Fe_Rate
C_H
C_H_Flux
C_H_Rate
C_He
C_He_Flux
C_He_Rate
C_Mg
C_Mg_Rate
C_N
C_N_Rate
C_Na
C_Na_Rate
C_Ne
C_Ne_Rate
C_Ni
C_Ni_Rate
C_O
C_O_Rate
C_S
C_S_Rate
C_Si

C_Si_Rate
HCI_Lat
HCI_Lon
HCI_R
HGC_Lat
HGC_Lon
HGC_R
LET2_C_HCI
LET2_C_PA
LET2_C_R1_SECT_HCI
LET2_C_R1_SECT_PA
LET2_C_R1_SECT_RTN
LET2_C_R1_SECT_SA
LET2_C_R25_SECT_HCI
LET2_C_R25_SECT_PA
LET2_C_R25_SECT_RTN
LET2_C_R25_SECT_SA
LET2_C_RTN
LET2_C_SA
Quality_Flag
R1C_H_SECT_Flux
R1C_H_SECT_Rate
R1C_He_SECT_Flux
R1C_He_SECT_Rate
R25C_H_SECT_Flux
R25C_H_SECT_Rate
R25C_He_SECT_Flux
R25C_He_SECT_Rate

5.13 PSP_ISOIS-EPIHI_L2-SECOND-RATES

HCI_Lat
HCI_Lon
HCI_R
HET_A_Electrons
HET_A_Electrons_Rate
HET_A_H
HET_A_HCI
HET_A_H_Rate
HET_A_PA
HET_A_RTN
HET_A_SA
HET_B_Electrons
HET_B_Electrons_Rate

HET_B_H
HET_B_HCI
HET_B_H_Rate
HET_B_PA
HET_B_RTN
HET_B_SA
HGC_Lat
HGC_Lon
HGC_R
LET1_A_Electrons
LET1_A_Electrons_Rate
LET1_A_H
LET1_A_HCI
LET1_A_H_Rate
LET1_A_PA
LET1_A_RTN
LET1_A_SA
LET1_B_Electrons
LET1_B_Electrons_Rate
LET1_B_H
LET1_B_HCI
LET1_B_H_Rate
LET1_B_PA
LET1_B_RTN
LET1_B_SA
LET2_C_Electrons
LET2_C_Electrons_Rate
LET2_C_H
LET2_C_HCI
LET2_C_H_Rate
LET2_C_PA
LET2_C_RTN
LET2_C_SA
Quality_Flag

5.14 PSP_ISOIS-EPILO_L2-IC

C_CountRate_ChanD
C_Counts_ChanD
Fe_CountRate_ChanC
Fe_Counts_ChanC
HCI_ChanC
HCI_ChanD
HCI_ChanP

HCI_ChanR
HCI_ChanT
HCI_Lat_ChanC
HCI_Lat_ChanD
HCI_Lat_ChanP
HCI_Lat_ChanR
HCI_Lat_ChanT
HCI_Lon_ChanC
HCI_Lon_ChanD
HCI_Lon_ChanP
HCI_Lon_ChanR
HCI_Lon_ChanT
HCI_R_ChanC
HCI_R_ChanD
HCI_R_ChanP
HCI_R_ChanR
HCI_R_ChanT
HGC_Lat_ChanC
HGC_Lat_ChanD
HGC_Lat_ChanP
HGC_Lat_ChanR
HGC_Lat_ChanT
HGC_Lon_ChanC
HGC_Lon_ChanD
HGC_Lon_ChanP
HGC_Lon_ChanR
HGC_Lon_ChanT
HGC_R_ChanC
HGC_R_ChanD
HGC_R_ChanP
HGC_R_ChanR
HGC_R_ChanT
H_CountRate_ChanP
H_CountRate_ChanR
H_CountRate_ChanT
H_Counts_ChanP
H_Counts_ChanR
H_Counts_ChanT
H_Flux_ChanP
H_Flux_ChanR
H_Flux_ChanT
He3_CountRate_ChanC
He3_Counts_ChanC
He4_CountRate_ChanC
He4_Counts_ChanC

He4_Flux_ChanC
Look_Direction_80_DELTAMINUS
Look_Direction_80_DELTAPLUS
Mg_CountRate_ChanD
Mg_Counts_ChanD
N_CountRate_ChanD
N_Counts_ChanD
Ne_CountRate_ChanD
Ne_Counts_ChanD
O_CountRate_ChanC
O_Counts_ChanC
PA_ChanC
PA_ChanD
PA_ChanP
PA_ChanR
PA_ChanT
Quality_Flag_ChanC
Quality_Flag_ChanD
Quality_Flag_ChanP
Quality_Flag_ChanR
Quality_Flag_ChanT
RTN_ChanC
RTN_ChanD
RTN_ChanP
RTN_ChanR
RTN_ChanT
SA_ChanC
SA_ChanD
SA_ChanP
SA_ChanR
SA_ChanT
Si_CountRate_ChanD
Si_Counts_ChanD

5.15 PSP_ISOIS-EPILO_L2-PE

Electron_CountRate_ChanE
Electron_CountRate_ChanF
Electron_CountRate_ChanG
Electron_Counts_ChanE
Electron_Counts_ChanF
Electron_Counts_ChanG
HCI_ChanE
HCI_ChanF

HCI_ChanG
HCI_Lat_ChanE
HCI_Lat_ChanF
HCI_Lat_ChanG
HCI_Lon_ChanE
HCI_Lon_ChanF
HCI_Lon_ChanG
HCI_R_ChanE
HCI_R_ChanF
HCI_R_ChanG
HGC_Lat_ChanE
HGC_Lat_ChanF
HGC_Lat_ChanG
HGC_Lon_ChanE
HGC_Lon_ChanF
HGC_Lon_ChanG
HGC_R_ChanE
HGC_R_ChanF
HGC_R_ChanG
H_CountRate_ChanE
H_CountRate_ChanF
H_CountRate_ChanG
H_Counts_ChanE
H_Counts_ChanF
H_Counts_ChanG
Look_Direction_08_DELTAMINUS
Look_Direction_08_DELTAPLUS
Look_Direction_80_DELTAMINUS
Look_Direction_80_DELTAPLUS
PA_ChanE
PA_ChanF
PA_ChanG
Quality_Flag_ChanE
Quality_Flag_ChanF
Quality_Flag_ChanG
RTN_ChanE
RTN_ChanF
RTN_ChanG
SA_ChanE
SA_ChanF
SA_ChanG

5.16 PSP_ISOIS_L2-EPHEM

Clock_Angle
HCI_Lat
HCI_Lon
HCI_R
HGC_Lat
HGC_Lon
HGC_R
Ram_Pointing
Roll_Angle
Spiral_HETA
Spiral_LET1A
Spiral_LET2C
Spiral_Lo
Sun_Angle
Umbra_Pointing

5.17 PSP_ISOIS_L2-SUMMARY

A_H_Rate_TS
A_Heavy_Rate_TS
Electron_CountRate_ChanE
HET_A_Electrons_Rate_TS
HET_A_H_Rate_TS
H_CountRate_ChanP_SP

6 CDF CONTENTS

6.1 PSP_ISOIS-EPILO_L2-IC

ISOIS-EPILO>Integrated Science Investigation of the Sun, Energetic Particle Instrument Lo
L2-ic>Level 2 ic
EPI-Lo, Ion Composition mode.
Instrument paper: Integrated Science Investigation of the Sun (ISIS): Design of the Energetic Particle Investigation. McComas, D. J. et al (2016). Space Sci. Rev., doi:10.1007/s11214-014-0059-1
1 minute to 1 hour
Cite McComas et al (2016), doi:10.1007/s11214-014-0059-1

6.1.1 PRIMARY VARIABLES

6.1.1.1 H_Flux_ChanP H flux channel P (HiResProtons) ($cm^{-2}sr^{-1}sec^{-1}keV^{-1}$)
Size: 80 × 48 time-varying
`particle_flux>differential_directional_number`
Ion Composition mode.
Look_Direction_80 0 – 79 (80 bins)
H_ChanP_Energy 70 – 9464 keV (39 bins)

6.1.1.2 H_Flux_ChanR H flux channel R (HiTimeResProtons) ($cm^{-2}sr^{-1}sec^{-1}keV^{-1}$)
Size: 80 × 48 time-varying
`particle_flux>differential_directional_number`
Ion Composition mode.
Look_Direction_80 0 – 79 (80 bins)
H_ChanR_Energy 80 – 7441 keV (14 bins)

6.1.1.3 H_Flux_ChanT H flux channel T (IonTOF) ($cm^{-2}sr^{-1}sec^{-1}(keV/nuc)^{-1}$)
Size: 80 × 47 time-varying
`particle_flux>differential_directional_number`
Ion Composition mode. May contain significant photon counts, particularly directions L31, L34, L35. See Hill, M.E. et al., 2020, ApJS, doi:10.3847/1538-4365/ab643d .
Look_Direction_80 0 – 79 (80 bins)
H_ChanT_Energy 20 – 34454 keV/nuc (31 bins)

6.1.1.4 He4_Flux_ChanC He4 flux channel C (Ions1) ($cm^{-2}sr^{-1}sec^{-1}keV^{-1}$)
Size: 80 × 48 time-varying
`particle_flux>differential_directional_number`

Ion Composition mode.
Look_Direction_80 0 – 79 (80 bins)
He4_ChanC_Energy 85 – 20909 keV (44 bins)

6.1.2 OTHER DATA

6.1.2.1 C_CountRate_ChanD C count rate channel D (Ions2) (counts/sec)
Size: 80 × 48 time-varying
`particle_flux>differential_directional_number_rate`
Ion Composition mode. Corrected for deadtime.
Look_Direction_80 0 – 79 (80 bins)
C_ChanD_Energy 182 – 19902 keV (22 bins)

6.1.2.2 C_Counts_ChanD C counts channel D (Ions2) (counts)
Size: 80 × 48 time-varying
`particle_flux>differential_directional_number_rate`
Ion Composition mode. Raw counts per integration.
Look_Direction_80 0 – 79 (80 bins)
C_ChanD_Energy 182 – 19902 keV (22 bins)

6.1.2.3 Fe_CountRate_ChanC Fe count rate channel C (Ions1) (counts/sec)
Size: 80 × 48 time-varying
`particle_flux>differential_directional_number_rate`
Ion Composition mode. Corrected for deadtime.
Look_Direction_80 0 – 79 (80 bins)
Fe_ChanC_Energy 444 – 23773 keV (42 bins)

6.1.2.4 Fe_Counts_ChanC Fe counts channel C (Ions1) (counts)
Size: 80 × 48 time-varying
`particle_flux>differential_directional_number_rate`
Ion Composition mode. Raw counts per integration.
Look_Direction_80 0 – 79 (80 bins)
Fe_ChanC_Energy 444 – 23773 keV (42 bins)

6.1.2.5 HCI_ChanC HCI flow direction ChanC
Size: 80 × 3 time-varying
`position>direction`
Unit vector, after Fraenz and Harper, PSS, 2002. ChanC timebase.

Look_Direction_80 0 – 79 (80 bins)

6.1.2.6 HCI_ChanD HCI flow direction ChanD
Size: 80 × 3 time-varying
`position>direction`
Unit vector, after Fraenz and Harper, PSS, 2002. ChanD timebase.
Look_Direction_80 0 – 79 (80 bins)

6.1.2.7 HCI_ChanP HCI flow direction ChanP
Size: 80 × 3 time-varying
`position>direction`
Unit vector, after Fraenz and Harper, PSS, 2002. ChanP timebase.
Look_Direction_80 0 – 79 (80 bins)

6.1.2.8 HCI_ChanR HCI flow direction ChanR
Size: 80 × 3 time-varying
`position>direction`
Unit vector, after Fraenz and Harper, PSS, 2002. ChanR timebase.
Look_Direction_80 0 – 79 (80 bins)

6.1.2.9 HCI_ChanT HCI flow direction ChanT
Size: 80 × 3 time-varying
`position>direction`
Unit vector, after Fraenz and Harper, PSS, 2002. ChanT timebase.
Look_Direction_80 0 – 79 (80 bins)

6.1.2.10 HCI_Lat_ChanC HCI latitude ChanC (degrees)
time-varying
`position>latitude`
At timestamp. After Fraenz and Harper, PSS, 2002. ChanC timebase.

6.1.2.11 HCI_Lat_ChanD HCI latitude ChanD (degrees)
time-varying
`position>latitude`
At timestamp. After Fraenz and Harper, PSS, 2002. ChanD timebase.

6.1.2.12 HCI_Lat_ChanP HCI latitude ChanP (degrees)
time-varying
`position>latitude`
At timestamp. After Fraenz and Harper, PSS, 2002. ChanP timebase.

6.1.2.13 HCI_Lat_ChanR HCI latitude ChanR (degrees)
time-varying
`position>latitude`
At timestamp. After Fraenz and Harper, PSS, 2002. ChanR timebase.

6.1.2.14 HCI_Lat_ChanT HCI latitude ChanT (degrees)
time-varying
`position>latitude`
At timestamp. After Fraenz and Harper, PSS, 2002. ChanT timebase.

6.1.2.15 HCI_Lon_ChanC HCI longitude ChanC (degrees)
time-varying
`position>longitude`
At timestamp. After Fraenz and Harper, PSS, 2002. ChanC timebase.

6.1.2.16 HCI_Lon_ChanD HCI longitude ChanD (degrees)
time-varying
`position>longitude`
At timestamp. After Fraenz and Harper, PSS, 2002. ChanD timebase.

6.1.2.17 HCI_Lon_ChanP HCI longitude ChanP (degrees)
time-varying
`position>longitude`
At timestamp. After Fraenz and Harper, PSS, 2002. ChanP timebase.

6.1.2.18 HCI_Lon_ChanR HCI longitude ChanR (degrees)
time-varying
`position>longitude`
At timestamp. After Fraenz and Harper, PSS, 2002. ChanR timebase.

6.1.2.19 HCI_Lon_ChanT HCI longitude ChanT (degrees)
time-varying
`position>longitude`
At timestamp. After Fraenz and Harper, PSS, 2002. ChanT timebase.

6.1.2.20 HCI_R_ChanC Heliocentric distance ChanC (AU)
time-varying
`position>radial`
At timestamp. After Fraenz and Harper, PSS, 2002. ChanC timebase.

6.1.2.21 HCI_R_ChanD Heliocentric distance ChanD (AU)
time-varying
`position>radial`
At timestamp. After Fraenz and Harper, PSS, 2002. ChanD timebase.

6.1.2.22 HCI_R_ChanP Heliocentric distance ChanP (AU)
time-varying
`position>radial`
At timestamp. After Fraenz and Harper, PSS, 2002. ChanP timebase.

6.1.2.23 HCI_R_ChanR Heliocentric distance ChanR (AU)
time-varying
`position>radial`
At timestamp. After Fraenz and Harper, PSS, 2002. ChanR timebase.

6.1.2.24 HCI_R_ChanT Heliocentric distance ChanT (AU)
time-varying
`position>radial`
At timestamp. After Fraenz and Harper, PSS, 2002. ChanT timebase.

6.1.2.25 HGC_Lat_ChanC HGC latitude ChanC (degrees)
time-varying
`position>latitude`
At timestamp. After Fraenz and Harper, PSS, 2002. ChanC timebase.

6.1.2.26 HGC_Lat_ChanD HGC latitude ChanD (degrees)
time-varying
`position>latitude`
At timestamp. After Fraenz and Harper, PSS, 2002. ChanD timebase.

6.1.2.27 HGC_Lat_ChanP HGC latitude ChanP (degrees)
time-varying
`position>latitude`
At timestamp. After Fraenz and Harper, PSS, 2002. ChanP timebase.

6.1.2.28 HGC_Lat_ChanR HGC latitude ChanR (degrees)
time-varying
`position>latitude`
At timestamp. After Fraenz and Harper, PSS, 2002. ChanR timebase.

6.1.2.29 HGC_Lat_ChanT HGC latitude ChanT (degrees)
time-varying
`position>latitude`
At timestamp. After Fraenz and Harper, PSS, 2002. ChanT timebase.

6.1.2.30 HGC_Lon_ChanC HGC longitude ChanC (degrees)
time-varying
`position>longitude`
At timestamp. After Fraenz and Harper, PSS, 2002. ChanC timebase.

6.1.2.31 HGC_Lon_ChanD HGC longitude ChanD (degrees)
time-varying
`position>longitude`
At timestamp. After Fraenz and Harper, PSS, 2002. ChanD timebase.

6.1.2.32 HGC_Lon_ChanP HGC longitude ChanP (degrees)
time-varying
`position>longitude`
At timestamp. After Fraenz and Harper, PSS, 2002. ChanP timebase.

6.1.2.33 HGC_Lon_ChanR HGC longitude ChanR (degrees)
time-varying
`position>longitude`
At timestamp. After Fraenz and Harper, PSS, 2002. ChanR timebase.

6.1.2.34 HGC_Lon_ChanT HGC longitude ChanT (degrees)
time-varying
`position>longitude`
At timestamp. After Fraenz and Harper, PSS, 2002. ChanT timebase.

6.1.2.35 HGC_R_ChanC Heliocentric distance ChanC (AU)
time-varying
`position>radial`
At timestamp. After Fraenz and Harper, PSS, 2002. ChanC timebase.

6.1.2.36 HGC_R_ChanD Heliocentric distance ChanD (AU)
time-varying
`position>radial`
At timestamp. After Fraenz and Harper, PSS, 2002. ChanD timebase.

6.1.2.37 HGC_R_ChanP Heliocentric distance ChanP (AU)
time-varying
`position>radial`
At timestamp. After Fraenz and Harper, PSS, 2002. ChanP timebase.

6.1.2.38 HGC_R_ChanR Heliocentric distance ChanR (AU)
time-varying
`position>radial`
At timestamp. After Fraenz and Harper, PSS, 2002. ChanR timebase.

6.1.2.39 HGC_R_ChanT Heliocentric distance ChanT (AU)
time-varying
`position>radial`
At timestamp. After Fraenz and Harper, PSS, 2002. ChanT timebase.

6.1.2.40 H_CountRate_ChanP H count rate channel P (HiResProtons) (counts/sec)
Size: 80 × 48 time-varying
`particle_flux>differential_directional_number_rate`
Ion Composition mode. Corrected for deadtime.
Look_Direction_80 0 – 79 (80 bins)
H_ChanP_Energy 70 – 9464 keV (39 bins)

6.1.2.41 H_CountRate_ChanR H count rate channel R (HiTimeResProtons) (counts/sec)
Size: 80 × 48 time-varying
`particle_flux>differential_directional_number_rate`
Ion Composition mode. Corrected for deadtime.
Look_Direction_80 0 – 79 (80 bins)
H_ChanR_Energy 80 – 7441 keV (14 bins)

6.1.2.42 H_CountRate_ChanT H count rate channel T (IonTOF) (counts/sec)
Size: 80 × 47 time-varying
`particle_flux>differential_directional_number_rate`
Ion Composition mode. Corrected for deadtime. May contain significant photon counts, particularly directions L31, L34, L35. See Hill, M.E. et al., 2020, ApJS, doi:10.3847/1538-4365/ab643d .
Look_Direction_80 0 – 79 (80 bins)
H_ChanT_Energy 20 – 34454 keV/nuc (31 bins)

6.1.2.43 H_Counts_ChanP H counts channel P (HiResProtons) (counts)
Size: 80 × 48 time-varying
`particle_flux>differential_directional_number_rate`
Ion Composition mode. Raw counts per integration.
Look_Direction_80 0 – 79 (80 bins)
H_ChanP_Energy 70 – 9464 keV (39 bins)

6.1.2.44 H_Counts_ChanR H counts channel R (HiTimeResProtons) (counts)
Size: 80 × 48 time-varying
`particle_flux>differential_directional_number_rate`
Ion Composition mode. Raw counts per integration.
Look_Direction_80 0 – 79 (80 bins)
H_ChanR_Energy 80 – 7441 keV (14 bins)

6.1.2.45 H_Counts_ChanT H counts channel T (IonTOF) (counts)
Size: 80 × 47 time-varying
`particle_flux>differential_directional_number_rate`
Ion Composition mode. Raw counts per integration. May contain significant photon counts, particularly directions L31, L34, L35. See Hill, M.E. et al., 2020, ApJS, doi:10.3847/1538-4365/ab643d .
Look_Direction_80 0 – 79 (80 bins)
H_ChanT_Energy 20 – 34454 keV/nuc (31 bins)

6.1.2.46 He3_CountRate_ChanC He3 count rate channel C (Ions1) (counts/sec)
Size: 80 × 48 time-varying
`particle_flux>differential_directional_number_rate`
Ion Composition mode. Corrected for deadtime.
Look_Direction_80 0 – 79 (80 bins)
He3_ChanC_Energy 98 – 20905 keV (44 bins)

6.1.2.47 He3_Counts_ChanC He3 counts channel C (Ions1) (counts)
Size: 80 × 48 time-varying
`particle_flux>differential_directional_number_rate`
Ion Composition mode. Raw counts per integration.
Look_Direction_80 0 – 79 (80 bins)
He3_ChanC_Energy 98 – 20905 keV (44 bins)

6.1.2.48 He4_CountRate_ChanC He4 count rate channel C (Ions1) (counts/sec)
Size: 80 × 48 time-varying
`particle_flux>differential_directional_number_rate`
Ion Composition mode. Corrected for deadtime.
Look_Direction_80 0 – 79 (80 bins)
He4_ChanC_Energy 85 – 20909 keV (44 bins)

6.1.2.49 He4_Counts_ChanC He4 counts channel C (Ions1) (counts)
Size: 80 × 48 time-varying
`particle_flux>differential_directional_number_rate`
Ion Composition mode. Raw counts per integration.
Look_Direction_80 0 – 79 (80 bins)
He4_ChanC_Energy 85 – 20909 keV (44 bins)

6.1.2.50 Mg_CountRate_ChanD Mg count rate channel D (Ions2) (counts/sec)
Size: 80 × 48 time-varying
`particle_flux>differential_directional_number_rate`
Ion Composition mode. Corrected for deadtime.
Look_Direction_80 0 – 79 (80 bins)
Mg_ChanD_Energy 231 – 20942 keV (22 bins)

6.1.2.51 Mg_Counts_ChanD Mg counts channel D (Ions2) (counts)
Size: 80 × 48 time-varying
`particle_flux>differential_directional_number_rate`
Ion Composition mode. Raw counts per integration.
Look_Direction_80 0 – 79 (80 bins)
Mg_ChanD_Energy 231 – 20942 keV (22 bins)

6.1.2.52 N_CountRate_ChanD N count rate channel D (Ions2) (counts/sec)
Size: 80 × 48 time-varying
`particle_flux>differential_directional_number_rate`
Ion Composition mode. Corrected for deadtime.
Look_Direction_80 0 – 79 (80 bins)
N_ChanD_Energy

6.1.2.53 N_Counts_ChanD N counts channel D (Ions2) (counts)
Size: 80 × 48 time-varying
`particle_flux>differential_directional_number_rate`
Ion Composition mode. Raw counts per integration.
Look_Direction_80 0 – 79 (80 bins)
N_ChanD_Energy

6.1.2.54 Ne_CountRate_ChanD Ne count rate channel D (Ions2) (counts/sec)
Size: 80 × 48 time-varying
`particle_flux>differential_directional_number_rate`
Ion Composition mode. Corrected for deadtime.
Look_Direction_80 0 – 79 (80 bins)
Ne_ChanD_Energy 652 – 17605 keV (7 bins)

6.1.2.55 Ne_Counts_ChanD Ne counts channel D (Ions2) (counts)
Size: 80 × 48 time-varying

`particle_flux>differential_directional_number_rate`
Ion Composition mode. Raw counts per integration.
Look_Direction_80 0 – 79 (80 bins)
Ne_ChanD_Energy 652 – 17605 keV (7 bins)

6.1.2.56 O_CountRate_ChanC O count rate channel C (Ions1) (counts/sec)
Size: 80 × 48 time-varying
`particle_flux>differential_directional_number_rate`
Ion Composition mode. Corrected for deadtime.
Look_Direction_80 0 – 79 (80 bins)
O_ChanC_Energy 210 – 21397 keV (43 bins)

6.1.2.57 O_Counts_ChanC O counts channel C (Ions1) (counts)
Size: 80 × 48 time-varying
`particle_flux>differential_directional_number_rate`
Ion Composition mode. Raw counts per integration.
Look_Direction_80 0 – 79 (80 bins)
O_ChanC_Energy 210 – 21397 keV (43 bins)

6.1.2.58 PA_ChanC Pitch angle ChanC (degree)
Size: 80 time-varying
`position>angle`
Look_Direction_80 0 – 79 (80 bins)

6.1.2.59 PA_ChanD Pitch angle ChanD (degree)
Size: 80 time-varying
`position>angle`
Look_Direction_80 0 – 79 (80 bins)

6.1.2.60 PA_ChanP Pitch angle ChanP (degree)
Size: 80 time-varying
`position>angle`
Look_Direction_80 0 – 79 (80 bins)

6.1.2.61 PA_ChanR Pitch angle ChanR (degree)
Size: 80 time-varying

`position>angle`
Look_Direction_80 0 – 79 (80 bins)

6.1.2.62 PA_ChanT Pitch angle ChanT (degree)
Size: 80 time-varying
`position>angle`
Look_Direction_80 0 – 79 (80 bins)

6.1.2.63 RTN_ChanC RTN flow direction ChanC
Size: 80 × 3 time-varying
`position>direction`
Unit vector, after Fraenz and Harper, PSS, 2002. ChanC timebase.
Look_Direction_80 0 – 79 (80 bins)

6.1.2.64 RTN_ChanD RTN flow direction ChanD
Size: 80 × 3 time-varying
`position>direction`
Unit vector, after Fraenz and Harper, PSS, 2002. ChanD timebase.
Look_Direction_80 0 – 79 (80 bins)

6.1.2.65 RTN_ChanP RTN flow direction ChanP
Size: 80 × 3 time-varying
`position>direction`
Unit vector, after Fraenz and Harper, PSS, 2002. ChanP timebase.
Look_Direction_80 0 – 79 (80 bins)

6.1.2.66 RTN_ChanR RTN flow direction ChanR
Size: 80 × 3 time-varying
`position>direction`
Unit vector, after Fraenz and Harper, PSS, 2002. ChanR timebase.
Look_Direction_80 0 – 79 (80 bins)

6.1.2.67 RTN_ChanT RTN flow direction ChanT
Size: 80 × 3 time-varying
`position>direction`
Unit vector, after Fraenz and Harper, PSS, 2002. ChanT timebase.

Look_Direction_80 0 – 79 (80 bins)

6.1.2.68 SA_ChanC Nominal Parker Spiral angle ChanC (degree)
Size: 80 time-varying
`position>angle`
Angle between particle direction and nominal outward Parker Spiral, based on 400km/s solar wind and corotation breakdown at 10Rs.
Look_Direction_80 0 – 79 (80 bins)

6.1.2.69 SA_ChanD Nominal Parker Spiral angle ChanD (degree)
Size: 80 time-varying
`position>angle`
Angle between particle direction and nominal outward Parker Spiral, based on 400km/s solar wind and corotation breakdown at 10Rs.
Look_Direction_80 0 – 79 (80 bins)

6.1.2.70 SA_ChanP Nominal Parker Spiral angle ChanP (degree)
Size: 80 time-varying
`position>angle`
Angle between particle direction and nominal outward Parker Spiral, based on 400km/s solar wind and corotation breakdown at 10Rs.
Look_Direction_80 0 – 79 (80 bins)

6.1.2.71 SA_ChanR Nominal Parker Spiral angle ChanR (degree)
Size: 80 time-varying
`position>angle`
Angle between particle direction and nominal outward Parker Spiral, based on 400km/s solar wind and corotation breakdown at 10Rs.
Look_Direction_80 0 – 79 (80 bins)

6.1.2.72 SA_ChanT Nominal Parker Spiral angle ChanT (degree)
Size: 80 time-varying
`position>angle`
Angle between particle direction and nominal outward Parker Spiral, based on 400km/s solar wind and corotation breakdown at 10Rs.
Look_Direction_80 0 – 79 (80 bins)

6.1.2.73 Si_CountRate_ChanD Si count rate channel D (Ions2) (counts/sec)
Size: 80 × 48 time-varying
`particle_flux>differential_directional_number_rate`
Ion Composition mode. Corrected for deadtime.
Look_Direction_80 0 – 79 (80 bins)
Si_ChanD_Energy 321 – 21454 keV (21 bins)

6.1.2.74 Si_Counts_ChanD Si counts channel D (Ions2) (counts)
Size: 80 × 48 time-varying
`particle_flux>differential_directional_number_rate`
Ion Composition mode. Raw counts per integration.
Look_Direction_80 0 – 79 (80 bins)
Si_ChanD_Energy 321 – 21454 keV (21 bins)

6.1.3 OTHER SUPPORT

6.1.3.1 Look_Direction_80_DELTAMINUS Size: 80 constant
`number`

6.1.3.2 Look_Direction_80_DELTAPLUS Size: 80 constant
`number`

6.1.3.3 Quality_Flag_ChanC Data-quality flag for channel C (Ions1)
Size: 10 time-varying
`flag>status`
Quality flag number ChanICB 0 – 9 (10 bins)

6.1.3.4 Quality_Flag_ChanD Data-quality flag for channel D (Ions2)
Size: 10 time-varying
`flag>status`
Quality flag number ChanICB 0 – 9 (10 bins)

6.1.3.5 Quality_Flag_ChanP Data-quality flag for channel P (HiResProtons)
Size: 10 time-varying
`flag>status`
Quality flag number ChanICB 0 – 9 (10 bins)

6.1.3.6 Quality_Flag_ChanR Data-quality flag for channel R (HiTimeResProtons)
Size: 10 time-varying
`flag>status`
Quality flag number ChanICB 0 – 9 (10 bins)

6.1.3.7 Quality_Flag_ChanT Data-quality flag for channel T (IonTOF)
Size: 10 time-varying
`flag>status`
Quality flag number ChanICB 0 – 9 (10 bins)

6.2 PSP_ISOIS-EPILO_L2-PE

ISOIS-EPILO>Integrated Science Investigation of the Sun, Energetic Particle Instrument Lo
L2-pe>Level 2 pe
EPI-Lo, Particle Energy mode.
Instrument paper: Integrated Science Investigation of the Sun (ISIS): Design of the Energetic Particle Investigation. McComas, D. J. et al (2016). Space Sci. Rev., doi:10.1007/s11214-014-0059-1
1 minute to 1 hour
Cite McComas et al (2016), doi:10.1007/s11214-014-0059-1

6.2.1 PRIMARY VARIABLES

6.2.2 OTHER DATA

6.2.2.1 Electron_CountRate_ChanE Electron count rate channel E (HiResElectrons) (counts/sec)
Size: 8 × 48 time-varying
`particle_flux>differential_directional_number_rate`
Particle Energy mode. Corrected for deadtime.
Look_Direction_08 0 – 7 (8 bins)
Electron_ChanE_Energy 12 – 9065 keV (32 bins)

6.2.2.2 Electron_CountRate_ChanF Electron count rate channel F (HiTimeResElectrons) (counts/sec)
Size: 8 × 48 time-varying
`particle_flux>differential_directional_number_rate`
Particle Energy mode. Corrected for deadtime.
Look_Direction_08 0 – 7 (8 bins)
Electron_ChanF_Energy 19 – 6607 keV (12 bins)

6.2.2.3 Electron_CountRate_ChanG Electron count rate channel G (HiLookResElectrons) (counts/sec)
Size: 80 × 48 time-varying
`particle_flux>differential_directional_number_rate`
Particle Energy mode. Corrected for deadtime.
Look_Direction_80 0 – 79 (80 bins)
Electron_ChanG_Energy 12 – 9065 keV (32 bins)

6.2.2.4 Electron_Counts_ChanE Electron counts channel E (HiResElectrons) (counts)
Size: 8 × 48 time-varying
`particle_flux>differential_directional_number_rate`
Particle Energy mode. Raw counts per integration.
Look_Direction_08 0 – 7 (8 bins)
Electron_ChanE_Energy 12 – 9065 keV (32 bins)

6.2.2.5 Electron_Counts_ChanF Electron counts channel F (HiTimeResElectrons) (counts)
Size: 8 × 48 time-varying
`particle_flux>differential_directional_number_rate`
Particle Energy mode. Raw counts per integration.
Look_Direction_08 0 – 7 (8 bins)
Electron_ChanF_Energy 19 – 6607 keV (12 bins)

6.2.2.6 Electron_Counts_ChanG Electron counts channel G (HiLookResElectrons) (counts)
Size: 80 × 48 time-varying
`particle_flux>differential_directional_number_rate`
Particle Energy mode. Raw counts per integration.
Look_Direction_80 0 – 79 (80 bins)
Electron_ChanG_Energy 12 – 9065 keV (32 bins)

6.2.2.7 HCI_ChanE HCI flow direction ChanE
Size: 8 × 3 time-varying
`position>direction`
Unit vector, after Fraenz and Harper, PSS, 2002. ChanE timebase.
Look_Direction_08 0 – 7 (8 bins)

6.2.2.8 HCI_ChanF HCI flow direction ChanF
Size: 8 × 3 time-varying

`position>direction`
Unit vector, after Fraenz and Harper, PSS, 2002. ChanF timebase.
Look_Direction_08 0 – 7 (8 bins)

6.2.2.9 HCI_ChanG HCI flow direction ChanG
Size: 80 × 3 time-varying
`position>direction`
Unit vector, after Fraenz and Harper, PSS, 2002. ChanG timebase.
Look_Direction_80 0 – 79 (80 bins)

6.2.2.10 HCI_Lat_ChanE HCI latitude ChanE (degrees)
time-varying
`position>latitude`
At timestamp. After Fraenz and Harper, PSS, 2002. ChanE timebase.

6.2.2.11 HCI_Lat_ChanF HCI latitude ChanF (degrees)
time-varying
`position>latitude`
At timestamp. After Fraenz and Harper, PSS, 2002. ChanF timebase.

6.2.2.12 HCI_Lat_ChanG HCI latitude ChanG (degrees)
time-varying
`position>latitude`
At timestamp. After Fraenz and Harper, PSS, 2002. ChanG timebase.

6.2.2.13 HCI_Lon_ChanE HCI longitude ChanE (degrees)
time-varying
`position>longitude`
At timestamp. After Fraenz and Harper, PSS, 2002. ChanE timebase.

6.2.2.14 HCI_Lon_ChanF HCI longitude ChanF (degrees)
time-varying
`position>longitude`
At timestamp. After Fraenz and Harper, PSS, 2002. ChanF timebase.

6.2.2.15 HCI_Lon_ChanG HCI longitude ChanG (degrees)
time-varying
`position>longitude`
At timestamp. After Fraenz and Harper, PSS, 2002. ChanG timebase.

6.2.2.16 HCI_R_ChanE Heliocentric distance ChanE (AU)
time-varying
`position>radial`
At timestamp. After Fraenz and Harper, PSS, 2002. ChanE timebase.

6.2.2.17 HCI_R_ChanF Heliocentric distance ChanF (AU)
time-varying
`position>radial`
At timestamp. After Fraenz and Harper, PSS, 2002. ChanF timebase.

6.2.2.18 HCI_R_ChanG Heliocentric distance ChanG (AU)
time-varying
`position>radial`
At timestamp. After Fraenz and Harper, PSS, 2002. ChanG timebase.

6.2.2.19 HGC_Lat_ChanE HGC latitude ChanE (degrees)
time-varying
`position>latitude`
At timestamp. After Fraenz and Harper, PSS, 2002. ChanE timebase.

6.2.2.20 HGC_Lat_ChanF HGC latitude ChanF (degrees)
time-varying
`position>latitude`
At timestamp. After Fraenz and Harper, PSS, 2002. ChanF timebase.

6.2.2.21 HGC_Lat_ChanG HGC latitude ChanG (degrees)
time-varying
`position>latitude`
At timestamp. After Fraenz and Harper, PSS, 2002. ChanG timebase.

6.2.2.22 HGC_Lon_ChanE HGC longitude ChanE (degrees)
time-varying
`position>longitude`
At timestamp. After Fraenz and Harper, PSS, 2002. ChanE timebase.

6.2.2.23 HGC_Lon_ChanF HGC longitude ChanF (degrees)
time-varying
`position>longitude`
At timestamp. After Fraenz and Harper, PSS, 2002. ChanF timebase.

6.2.2.24 HGC_Lon_ChanG HGC longitude ChanG (degrees)
time-varying
`position>longitude`
At timestamp. After Fraenz and Harper, PSS, 2002. ChanG timebase.

6.2.2.25 HGC_R_ChanE Heliocentric distance ChanE (AU)
time-varying
`position>radial`
At timestamp. After Fraenz and Harper, PSS, 2002. ChanE timebase.

6.2.2.26 HGC_R_ChanF Heliocentric distance ChanF (AU)
time-varying
`position>radial`
At timestamp. After Fraenz and Harper, PSS, 2002. ChanF timebase.

6.2.2.27 HGC_R_ChanG Heliocentric distance ChanG (AU)
time-varying
`position>radial`
At timestamp. After Fraenz and Harper, PSS, 2002. ChanG timebase.

6.2.2.28 H_CountRate_ChanE H count rate channel E (HiResElectrons) (counts/sec)
Size: 8×48 time-varying
`particle_flux>differential_directional_number_rate`
Particle Energy mode. Corrected for deadtime.
Look_Direction_08 0 – 7 (8 bins)

H_ChanE_Energy

6.2.2.29 H_CountRate_ChanF H count rate channel F (HiTimeResElectrons) (counts/sec)
Size: 8 × 48 time-varying
`particle_flux>differential_directional_number_rate`
Particle Energy mode. Corrected for deadtime.
Look_Direction_08 0 – 7 (8 bins)
H_ChanF_Energy

6.2.2.30 H_CountRate_ChanG H count rate channel G (HiLookResElectrons) (counts/sec)
Size: 80 × 48 time-varying
`particle_flux>differential_directional_number_rate`
Particle Energy mode. Corrected for deadtime.
Look_Direction_80 0 – 79 (80 bins)
H_ChanG_Energy

6.2.2.31 H_Counts_ChanE H counts channel E (HiResElectrons) (counts)
Size: 8 × 48 time-varying
`particle_flux>differential_directional_number_rate`
Particle Energy mode. Raw counts per integration.
Look_Direction_08 0 – 7 (8 bins)
H_ChanE_Energy

6.2.2.32 H_Counts_ChanF H counts channel F (HiTimeResElectrons) (counts)
Size: 8 × 48 time-varying
`particle_flux>differential_directional_number_rate`
Particle Energy mode. Raw counts per integration.
Look_Direction_08 0 – 7 (8 bins)
H_ChanF_Energy

6.2.2.33 H_Counts_ChanG H counts channel G (HiLookResElectrons) (counts)
Size: 80 × 48 time-varying
`particle_flux>differential_directional_number_rate`
Particle Energy mode. Raw counts per integration.
Look_Direction_80 0 – 79 (80 bins)
H_ChanG_Energy

6.2.2.34 PA_ChanE Pitch angle ChanE (degree)
Size: 8 time-varying
`position>angle`
Look_Direction_08 0 – 7 (8 bins)

6.2.2.35 PA_ChanF Pitch angle ChanF (degree)
Size: 8 time-varying
`position>angle`
Look_Direction_08 0 – 7 (8 bins)

6.2.2.36 PA_ChanG Pitch angle ChanG (degree)
Size: 80 time-varying
`position>angle`
Look_Direction_80 0 – 79 (80 bins)

6.2.2.37 RTN_ChanE RTN flow direction ChanE
Size: 8×3 time-varying
`position>direction`
Unit vector, after Fraenz and Harper, PSS, 2002. ChanE timebase.
Look_Direction_08 0 – 7 (8 bins)

6.2.2.38 RTN_ChanF RTN flow direction ChanF
Size: 8×3 time-varying
`position>direction`
Unit vector, after Fraenz and Harper, PSS, 2002. ChanF timebase.
Look_Direction_08 0 – 7 (8 bins)

6.2.2.39 RTN_ChanG RTN flow direction ChanG
Size: 80×3 time-varying
`position>direction`
Unit vector, after Fraenz and Harper, PSS, 2002. ChanG timebase.
Look_Direction_80 0 – 79 (80 bins)

6.2.2.40 SA_ChanE Nominal Parker Spiral angle ChanE (degree)
Size: 8 time-varying
`position>angle`

Angle between particle direction and nominal outward Parker Spiral, based on 400km/s solar wind and corotation breakdown at 10Rs.
Look_Direction_08 0 – 7 (8 bins)

6.2.2.41 SA_ChanF Nominal Parker Spiral angle ChanF (degree)
Size: 8 time-varying
`position>angle`
Angle between particle direction and nominal outward Parker Spiral, based on 400km/s solar wind and corotation breakdown at 10Rs.
Look_Direction_08 0 – 7 (8 bins)

6.2.2.42 SA_ChanG Nominal Parker Spiral angle ChanG (degree)
Size: 80 time-varying
`position>angle`
Angle between particle direction and nominal outward Parker Spiral, based on 400km/s solar wind and corotation breakdown at 10Rs.
Look_Direction_80 0 – 79 (80 bins)

6.2.3 OTHER SUPPORT

6.2.3.1 Look_Direction_08_DELTAMINUS Size: 8 constant
`number`

6.2.3.2 Look_Direction_08_DELTAPLUS Size: 8 constant
`number`

6.2.3.3 Look_Direction_80_DELTAMINUS Size: 80 constant
`number`

6.2.3.4 Look_Direction_80_DELTAPLUS Size: 80 constant
`number`

6.2.3.5 Quality_Flag_ChanE Data-quality flag for channel E (HiResElectrons)
Size: 10 time-varying
`flag>status`

Quality flag number ChanPEB 0 – 9 (10 bins)

6.2.3.6 Quality_Flag_ChanF

Data-quality flag for channel F (HiTimeResElectrons)
Size: 10 time-varying
`flag>status`
Quality flag number ChanPEB 0 – 9 (10 bins)

6.2.3.7 Quality_Flag_ChanG

Data-quality flag for channel G (HiLookResElectrons)
Size: 10 time-varying
`flag>status`
Quality flag number ChanPEB 0 – 9 (10 bins)

6.3 PSP_ISOIS-EPIHI_L2-HET-RATES10

ISOIS-EPIHI>Integrated Science Investigation of the Sun, Energetic Particle Instrument Hi
L2-HET-rates10>Level 2 HET 10-second rates
EPI-Hi 10 second rates cdf. Time tags indicate midpoint of integration.
Instrument paper: Integrated Science Investigation of the Sun (ISIS): Design of the Energetic Particle Investigation. McComas, D. J. et al (2016). Space Sci. Rev., doi:10.1007/s11214-014-0059-1
1 minute to 1 hour
Cite McComas et al (2016), doi:10.1007/s11214-014-0059-1

6.3.1 PRIMARY VARIABLES

6.3.1.1 A_H_Flux

H flux side A ($cm^{-2}sr^{-1}sec^{-1}MeV^{-1}$)
Size: 13 time-varying
`particle_flux>differential_directional_number`
Energy Bins for H 9 – 70 MeV (13 bins)

6.3.1.2 A_He_Flux

He flux side A ($cm^{-2}sr^{-1}sec^{-1}(MeV/nuc)^{-1}$)
Size: 14 time-varying
`particle_flux>differential_directional_number`
Energy Bins for He 9 – 83 MeV/nuc (14 bins)

6.3.1.3 B_H_Flux

H flux side B ($cm^{-2}sr^{-1}sec^{-1}MeV^{-1}$)
Size: 13 time-varying
`particle_flux>differential_directional_number`

Energy Bins for H 9 – 70 MeV (13 bins)

6.3.1.4 B_He_Flux He flux side B ($cm^{-2}sr^{-1}sec^{-1}(MeV/nuc)^{-1}$)
Size: 14 time-varying
`particle_flux>differential_directional_number`
Energy Bins for He 9 – 83 MeV/nuc (14 bins)

6.3.2 OTHER DATA

6.3.2.1 A_Electrons Electrons counts side A (counts)
Size: 18 time-varying
`particle_flux>differential_directional_number_rate`
Energy Bins for Electrons 1 – 10 MeV (18 bins)

6.3.2.2 A_Electrons_Rate Electrons count rate side A ($counts\,s^{-1}$)
Size: 18 time-varying
`particle_flux>differential_directional_number_rate`
Energy Bins for Electrons 1 – 10 MeV (18 bins)

6.3.2.3 A_H H counts side A (counts)
Size: 13 time-varying
`particle_flux>differential_directional_number_rate`
Energy Bins for H 9 – 70 MeV (13 bins)

6.3.2.4 A_H_Rate H count rate side A ($counts\,s^{-1}$)
Size: 13 time-varying
`particle_flux>differential_directional_number_rate`
Energy Bins for H 9 – 70 MeV (13 bins)

6.3.2.5 A_He He counts side A (counts)
Size: 14 time-varying
`particle_flux>differential_directional_number_rate`
Energy Bins for He 9 – 83 MeV/nuc (14 bins)

6.3.2.6 A_He_Rate He count rate side A ($counts\,s^{-1}$)
Size: 14 time-varying

`particle_flux>differential_directional_number_rate`
Energy Bins for He 9 – 83 MeV/nuc (14 bins)

6.3.2.7 B_Electrons Electrons counts side B (counts)
Size: 18 time-varying
`particle_flux>differential_directional_number_rate`
Energy Bins for Electrons 1 – 10 MeV (18 bins)

6.3.2.8 B_Electrons_Rate Electrons count rate side B (counts s^{-1})
Size: 18 time-varying
`particle_flux>differential_directional_number_rate`
Energy Bins for Electrons 1 – 10 MeV (18 bins)

6.3.2.9 B_H H counts side B (counts)
Size: 13 time-varying
`particle_flux>differential_directional_number_rate`
Energy Bins for H 9 – 70 MeV (13 bins)

6.3.2.10 B_H_Rate H count rate side B (counts s^{-1})
Size: 13 time-varying
`particle_flux>differential_directional_number_rate`
Energy Bins for H 9 – 70 MeV (13 bins)

6.3.2.11 B_He He counts side B (counts)
Size: 14 time-varying
`particle_flux>differential_directional_number_rate`
Energy Bins for He 9 – 83 MeV/nuc (14 bins)

6.3.2.12 B_He_Rate He count rate side B (counts s^{-1})
Size: 14 time-varying
`particle_flux>differential_directional_number_rate`
Energy Bins for He 9 – 83 MeV/nuc (14 bins)

6.3.2.13 HCI_Lat HCI latitude (degrees)
time-varying
`position>latitude`
At timestamp. After Fraenz and Harper, PSS, 2002.

6.3.2.14 HCI_Lon HCI longitude (degrees)
time-varying
`position>longitude`
At timestamp. After Fraenz and Harper, PSS, 2002.

6.3.2.15 HCI_R Heliocentric distance (AU)
time-varying
`position>radial`
At timestamp. After Fraenz and Harper, PSS, 2002.

6.3.2.16 HET_A_HCI HCI flow direction HETA
Size: 3 time-varying
`position>direction`
Unit vector, after Fraenz and Harper, PSS, 2002.

6.3.2.17 HET_A_PA Pitch angle HETA (degree)
time-varying
`position>angle`

6.3.2.18 HET_A_RTN RTN flow direction HETA
Size: 3 time-varying
`position>direction`
Unit vector, after Fraenz and Harper, PSS, 2002.

6.3.2.19 HET_A_SA Nominal Parker Spiral angle HETA (degree)
time-varying
`position>angle`
Angle between particle direction and nominal outward Parker Spiral, based on 400km/s solar wind and corotation breakdown at 10Rs.

6.3.2.20 HET_B_HCI HCI flow direction HETB
Size: 3 time-varying
`position>direction`
Unit vector, after Fraenz and Harper, PSS, 2002.

6.3.2.21 HET_B_PA Pitch angle HETB (degree)
time-varying
`position>angle`

6.3.2.22 HET_B_RTN RTN flow direction HETB
Size: 3 time-varying
`position>direction`
Unit vector, after Fraenz and Harper, PSS, 2002.

6.3.2.23 HET_B_SA Nominal Parker Spiral angle HETB (degree)
time-varying
`position>angle`
Angle between particle direction and nominal outward Parker Spiral, based on 400km/s solar wind and corotation breakdown at 10Rs.

6.3.2.24 HGC_Lat HGC latitude (degrees)
time-varying
`position>latitude`
At timestamp. After Fraenz and Harper, PSS, 2002.

6.3.2.25 HGC_Lon HGC longitude (degrees)
time-varying
`position>longitude`
At timestamp. After Fraenz and Harper, PSS, 2002.

6.3.2.26 HGC_R Heliocentric distance (AU)
time-varying
`position>radial`
At timestamp. After Fraenz and Harper, PSS, 2002.

6.3.3 OTHER SUPPORT

6.3.3.1 Quality_Flag Data-quality flag
Size: 10 time-varying
`flag>status`
Quality flag number 0 – 9 (10 bins)

6.4 PSP_ISOIS-EPIHI_L2-HET-RATES300

ISOIS-EPIHI>Integrated Science Investigation of the Sun, Energetic Particle Instrument Hi
L2-HET-rates300>Level 2 HET 5-minute rates
EPI-Hi HET 300 second rates cdf. Time tags indicate midpoint of integration.
Instrument paper: Integrated Science Investigation of the Sun (ISIS): Design of the Energetic Particle Investigation. McComas, D. J. et al (2016). Space Sci. Rev., doi:10.1007/s11214-014-0059-1
1 minute to 1 hour
Cite McComas et al (2016), doi:10.1007/s11214-014-0059-1

6.4.1 PRIMARY VARIABLES

6.4.2 OTHER DATA

6.4.2.1 A_CNO_SECT_Rate CNO sectored count rate side A (counts s^{-1})
Size: 2 × 25 time-varying
`particle_flux>differential_directional_number_rate`
Energy Bins for CNO SECT 35 – 64 MeV/nuc (2 bins)
HET_R17_SECTORS 0 – 24 (25 bins)

6.4.2.2 A_FeGroup_SECT_Rate FeGroup sectored count rate side A (counts s^{-1})
Size: 1 × 25 time-varying
`particle_flux>differential_directional_number_rate`
Energy Bins for FeGroup SECT 76 – 76 MeV/nuc (1 bins)
HET_R17_SECTORS 0 – 24 (25 bins)

6.4.2.3 A_NetoSi_SECT_Rate NetoSi sectored count rate side A (counts s^{-1})
Size: 1 × 25 time-varying
`particle_flux>differential_directional_number_rate`
Energy Bins for NetoSi SECT 54 – 54 MeV/nuc (1 bins)
HET_R17_SECTORS 0 – 24 (25 bins)

6.4.2.4 B_CNO_SECT_Rate CNO sectored count rate side B (counts s^{-1})
Size: 2 × 25 time-varying
`particle_flux>differential_directional_number_rate`
Energy Bins for CNO SECT 35 – 64 MeV/nuc (2 bins)
HET_R17_SECTORS 0 – 24 (25 bins)

6.4.2.5 B_FeGroup_SECT_Rate FeGroup sectored count rate side B (counts s^{-1})
Size: 1 × 25 time-varying
`particle_flux>differential_directional_number_rate`
Energy Bins for FeGroup SECT 76 – 76 MeV/nuc (1 bins)
HET_R17_SECTORS 0 – 24 (25 bins)

6.4.2.6 B_NetoSi_SECT_Rate NetoSi sectored count rate side B (counts s^{-1})
Size: 1 × 25 time-varying
`particle_flux>differential_directional_number_rate`
Energy Bins for NetoSi SECT 54 – 54 MeV/nuc (1 bins)
HET_R17_SECTORS 0 – 24 (25 bins)

6.4.2.7 HCI_Lat HCI latitude (degrees)
time-varying
`position>latitude`
At timestamp. After Fraenz and Harper, PSS, 2002.

6.4.2.8 HCI_Lon HCI longitude (degrees)
time-varying
`position>longitude`
At timestamp. After Fraenz and Harper, PSS, 2002.

6.4.2.9 HCI_R Heliocentric distance (AU)
time-varying
`position>radial`
At timestamp. After Fraenz and Harper, PSS, 2002.

6.4.2.10 HET_A_HCI HCI flow direction HETA
Size: 3 time-varying
`position>direction`

Unit vector, after Fraenz and Harper, PSS, 2002.

6.4.2.11 HET_A_PA Pitch angle HETA (degree)
time-varying
`position>angle`

6.4.2.12 HET_A_R17_SECT_HCI HCI flow direction HETAR17SECT
Size: 25 × 3 time-varying
`position>direction`
Unit vector, after Fraenz and Harper, PSS, 2002.
HET_R17_SECTORS 0 – 24 (25 bins)

6.4.2.13 HET_A_R17_SECT_PA Pitch angle HETAR17SECT (degree)
Size: 25 time-varying
`position>angle`
HET_R17_SECTORS 0 – 24 (25 bins)

6.4.2.14 HET_A_R17_SECT_RTN RTN flow direction HETAR17SECT
Size: 25 × 3 time-varying
`position>direction`
Unit vector, after Fraenz and Harper, PSS, 2002.
HET_R17_SECTORS 0 – 24 (25 bins)

6.4.2.15 HET_A_R17_SECT_SA Nominal Parker Spiral angle HETAR17SECT (degree)
Size: 25 time-varying
`position>angle`
Angle between particle direction and nominal outward Parker Spiral, based on 400km/s solar wind and corotation breakdown at 10Rs.
HET_R17_SECTORS 0 – 24 (25 bins)

6.4.2.16 HET_A_RTN RTN flow direction HETA
Size: 3 time-varying
`position>direction`
Unit vector, after Fraenz and Harper, PSS, 2002.

6.4.2.17 HET_A_SA Nominal Parker Spiral angle HETA (degree)
time-varying
`position>angle`
Angle between particle direction and nominal outward Parker Spiral, based on 400km/s solar wind and corotation breakdown at 10Rs.

6.4.2.18 HET_B_HCI HCI flow direction HETB
Size: 3 time-varying
`position>direction`
Unit vector, after Fraenz and Harper, PSS, 2002.

6.4.2.19 HET_B_PA Pitch angle HETB (degree)
time-varying
`position>angle`

6.4.2.20 HET_B_R17_SECT_HCI HCI flow direction HETBR17SECT
Size: 25 × 3 time-varying
`position>direction`
Unit vector, after Fraenz and Harper, PSS, 2002.
HET_R17_SECTORS 0 – 24 (25 bins)

6.4.2.21 HET_B_R17_SECT_PA Pitch angle HETBR17SECT (degree)
Size: 25 time-varying
`position>angle`
HET_R17_SECTORS 0 – 24 (25 bins)

6.4.2.22 HET_B_R17_SECT_RTN RTN flow direction HETBR17SECT
Size: 25 × 3 time-varying
`position>direction`
Unit vector, after Fraenz and Harper, PSS, 2002.
HET_R17_SECTORS 0 – 24 (25 bins)

6.4.2.23 HET_B_R17_SECT_SA Nominal Parker Spiral angle HETBR17SECT (degree)
Size: 25 time-varying
`position>angle`
Angle between particle direction and nominal outward Parker Spiral, based on 400km/s solar wind

and corotation breakdown at 10Rs.
HET_R17_SECTORS 0 – 24 (25 bins)

6.4.2.24 HET_B_RTN RTN flow direction HETB
Size: 3 time-varying
`position>direction`
Unit vector, after Fraenz and Harper, PSS, 2002.

6.4.2.25 HET_B_SA Nominal Parker Spiral angle HETB (degree)
time-varying
`position>angle`
Angle between particle direction and nominal outward Parker Spiral, based on 400km/s solar wind and corotation breakdown at 10Rs.

6.4.2.26 HGC_Lat HGC latitude (degrees)
time-varying
`position>latitude`
At timestamp. After Fraenz and Harper, PSS, 2002.

6.4.2.27 HGC_Lon HGC longitude (degrees)
time-varying
`position>longitude`
At timestamp. After Fraenz and Harper, PSS, 2002.

6.4.2.28 HGC_R Heliocentric distance (AU)
time-varying
`position>radial`
At timestamp. After Fraenz and Harper, PSS, 2002.

6.4.3 OTHER SUPPORT

6.4.3.1 Quality_Flag Data-quality flag
Size: 10 time-varying
`flag>status`
Quality flag number 0 – 9 (10 bins)

6.5 PSP_ISOIS-EPIHI_L2-HET-RATES3600

ISOIS-EPIHI>Integrated Science Investigation of the Sun, Energetic Particle Instrument Hi
L2-HET-rates3600>Level 2 HET hourly rates
EPI-Hi HET 3600 second rates cdf. Time tags indicate midpoint of integration.
Instrument paper: Integrated Science Investigation of the Sun (ISIS): Design of the Energetic Particle Investigation. McComas, D. J. et al (2016). Space Sci. Rev., doi:10.1007/s11214-014-0059-1
1 minute to 1 hour
Cite McComas et al (2016), doi:10.1007/s11214-014-0059-1

6.5.1 PRIMARY VARIABLES

6.5.1.1 A_H_Flux H flux side A ($cm^{-2}sr^{-1}sec^{-1}MeV^{-1}$)
Size: 15 time-varying
`particle_flux>differential_directional_number`
Energy Bins for H 7 – 83 MeV (15 bins)

6.5.1.2 A_H_SECT_Flux H sectored flux side A ($cm^{-2}sr^{-1}sec^{-1}MeV^{-1}$)
Size: 2×25 time-varying
`particle_flux>differential_directional_number`
Energy Bins for H SECT 17 – 32 MeV (2 bins)
HET_R17_SECTORS 0 – 24 (25 bins)

6.5.1.3 A_He_Flux He flux side A ($cm^{-2}sr^{-1}sec^{-1}(MeV/nuc)^{-1}$)
Size: 16 time-varying
`particle_flux>differential_directional_number`
Energy Bins for He 7 – 99 MeV/nuc (16 bins)

6.5.1.4 A_He_SECT_Flux He sectored flux side A ($cm^{-2}sr^{-1}sec^{-1}(MeV/nuc)^{-1}$)
Size: 2×25 time-varying
`particle_flux>differential_directional_number`
Energy Bins for He SECT 17 – 32 MeV/nuc (2 bins)
HET_R17_SECTORS 0 – 24 (25 bins)

6.5.1.5 B_H_Flux H flux side B ($cm^{-2}sr^{-1}sec^{-1}MeV^{-1}$)
Size: 15 time-varying
`particle_flux>differential_directional_number`

Energy Bins for H 7 – 83 MeV (15 bins)

6.5.1.6 B_H_SECT_Flux H sectored flux side B ($cm^{-2}sr^{-1}sec^{-1}MeV^{-1}$)
Size: 2 × 25 time-varying
`particle_flux>differential_directional_number`
Energy Bins for H SECT 17 – 32 MeV (2 bins)
HET_R17_SECTORS 0 – 24 (25 bins)

6.5.1.7 B_He_Flux He flux side B ($cm^{-2}sr^{-1}sec^{-1}(MeV/nuc)^{-1}$)
Size: 16 time-varying
`particle_flux>differential_directional_number`
Energy Bins for He 7 – 99 MeV/nuc (16 bins)

6.5.1.8 B_He_SECT_Flux He sectored flux side B ($cm^{-2}sr^{-1}sec^{-1}(MeV/nuc)^{-1}$)
Size: 2 × 25 time-varying
`particle_flux>differential_directional_number`
Energy Bins for He SECT 17 – 32 MeV/nuc (2 bins)
HET_R17_SECTORS 0 – 24 (25 bins)

6.5.2 OTHER DATA

6.5.2.1 A_Al Al counts side A (counts)
Size: 15 time-varying
`particle_flux>differential_directional_number_rate`
Energy Bins for Al 21 – 235 MeV/nuc (15 bins)

6.5.2.2 A_Al_Rate Al count rate side A ($counts\,s^{-1}$)
Size: 15 time-varying
`particle_flux>differential_directional_number_rate`
Energy Bins for Al 21 – 235 MeV/nuc (15 bins)

6.5.2.3 A_Ar Ar counts side A (counts)
Size: 15 time-varying
`particle_flux>differential_directional_number_rate`
Energy Bins for Ar 25 – 279 MeV/nuc (15 bins)

6.5.2.4 A_Ar_Rate Ar count rate side A (counts s^{-1})
Size: 15 time-varying
`particle_flux>differential_directional_number_rate`
Energy Bins for Ar 25 – 279 MeV/nuc (15 bins)

6.5.2.5 A_C C counts side A (counts)
Size: 15 time-varying
`particle_flux>differential_directional_number_rate`
Energy Bins for C 12 – 140 MeV/nuc (15 bins)

6.5.2.6 A_CNO_SECT_Rate CNO sectored count rate side A (counts s^{-1})
Size: 2×25 time-varying
`particle_flux>differential_directional_number_rate`
Energy Bins for CNO SECT 35 – 64 MeV/nuc (2 bins)
HET_R17_SECTORS 0 – 24 (25 bins)

6.5.2.7 A_C_Rate C count rate side A (counts s^{-1})
Size: 15 time-varying
`particle_flux>differential_directional_number_rate`
Energy Bins for C 12 – 140 MeV/nuc (15 bins)

6.5.2.8 A_Ca Ca counts side A (counts)
Size: 15 time-varying
`particle_flux>differential_directional_number_rate`
Energy Bins for Ca 25 – 279 MeV/nuc (15 bins)

6.5.2.9 A_Ca_Rate Ca count rate side A (counts s^{-1})
Size: 15 time-varying
`particle_flux>differential_directional_number_rate`
Energy Bins for Ca 25 – 279 MeV/nuc (15 bins)

6.5.2.10 A_Cr Cr counts side A (counts)
Size: 16 time-varying
`particle_flux>differential_directional_number_rate`
Energy Bins for Cr 25 – 332 MeV/nuc (16 bins)

6.5.2.11 A_Cr_Rate Cr count rate side A (counts s^{-1})
Size: 16 time-varying
`particle_flux>differential_directional_number_rate`
Energy Bins for Cr 25 – 332 MeV/nuc (16 bins)

6.5.2.12 A_Electrons Electrons counts side A (counts)
Size: 19 time-varying
`particle_flux>differential_directional_number_rate`
Energy Bins for Electrons 0 – 10 MeV (19 bins)

6.5.2.13 A_Electrons_Rate Electrons count rate side A (counts s^{-1})
Size: 19 time-varying
`particle_flux>differential_directional_number_rate`
Energy Bins for Electrons 0 – 10 MeV (19 bins)

6.5.2.14 A_Electrons_SECT_Rate Electrons sectored count rate side A (counts s^{-1})
Size: 2×25 time-varying
`particle_flux>differential_directional_number_rate`
Energy Bins for Electrons SECT 1 – 3 MeV (2 bins)
HET_R17_SECTORS 0 – 24 (25 bins)

6.5.2.15 A_Fe Fe counts side A (counts)
Size: 15 time-varying
`particle_flux>differential_directional_number_rate`
Energy Bins for Fe 29 – 332 MeV/nuc (15 bins)

6.5.2.16 A_FeGroup_SECT_Rate FeGroup sectored count rate side A (counts s^{-1})
Size: 1×25 time-varying
`particle_flux>differential_directional_number_rate`
Energy Bins for FeGroup SECT 76 – 76 MeV/nuc (1 bins)
HET_R17_SECTORS 0 – 24 (25 bins)

6.5.2.17 A_Fe_Rate Fe count rate side A (counts s^{-1})
Size: 15 time-varying
`particle_flux>differential_directional_number_rate`

Energy Bins for Fe 29 – 332 MeV/nuc (15 bins)

6.5.2.18 A_H H counts side A (counts)
Size: 15 time-varying
`particle_flux>differential_directional_number_rate`
Energy Bins for H 7 – 83 MeV (15 bins)

6.5.2.19 A_H_Rate H count rate side A (counts s^{-1})
Size: 15 time-varying
`particle_flux>differential_directional_number_rate`
Energy Bins for H 7 – 83 MeV (15 bins)

6.5.2.20 A_H_SECT_Rate H sectored count rate side A (counts s^{-1})
Size: 2×25 time-varying
`particle_flux>differential_directional_number_rate`
Energy Bins for H SECT 17 – 32 MeV (2 bins)
HET_R17_SECTORS 0 – 24 (25 bins)

6.5.2.21 A_He He counts side A (counts)
Size: 16 time-varying
`particle_flux>differential_directional_number_rate`
Energy Bins for He 7 – 99 MeV/nuc (16 bins)

6.5.2.22 A_He_Rate He count rate side A (counts s^{-1})
Size: 16 time-varying
`particle_flux>differential_directional_number_rate`
Energy Bins for He 7 – 99 MeV/nuc (16 bins)

6.5.2.23 A_He_SECT_Rate He sectored count rate side A (counts s^{-1})
Size: 2×25 time-varying
`particle_flux>differential_directional_number_rate`
Energy Bins for He SECT 17 – 32 MeV/nuc (2 bins)
HET_R17_SECTORS 0 – 24 (25 bins)

6.5.2.24 A_Mg Mg counts side A (counts)
Size: 15 time-varying
`particle_flux>differential_directional_number_rate`
Energy Bins for Mg 21 – 235 MeV/nuc (15 bins)

6.5.2.25 A_Mg_Rate Mg count rate side A (counts s^{-1})
Size: 15 time-varying
`particle_flux>differential_directional_number_rate`
Energy Bins for Mg 21 – 235 MeV/nuc (15 bins)

6.5.2.26 A_N N counts side A (counts)
Size: 15 time-varying
`particle_flux>differential_directional_number_rate`
Energy Bins for N 12 – 140 MeV/nuc (15 bins)

6.5.2.27 A_N_Rate N count rate side A (counts s^{-1})
Size: 15 time-varying
`particle_flux>differential_directional_number_rate`
Energy Bins for N 12 – 140 MeV/nuc (15 bins)

6.5.2.28 A_Na Na counts side A (counts)
Size: 15 time-varying
`particle_flux>differential_directional_number_rate`
Energy Bins for Na 17 – 197 MeV/nuc (15 bins)

6.5.2.29 A_Na_Rate Na count rate side A (counts s^{-1})
Size: 15 time-varying
`particle_flux>differential_directional_number_rate`
Energy Bins for Na 17 – 197 MeV/nuc (15 bins)

6.5.2.30 A_Ne Ne counts side A (counts)
Size: 15 time-varying
`particle_flux>differential_directional_number_rate`
Energy Bins for Ne 17 – 197 MeV/nuc (15 bins)

6.5.2.31 A_Ne_Rate Ne count rate side A (counts s^{-1})
Size: 15 time-varying
`particle_flux>differential_directional_number_rate`
Energy Bins for Ne 17 – 197 MeV/nuc (15 bins)

6.5.2.32 A_NetoSi_SECT_Rate NetoSi sectored count rate side A (counts s^{-1})
Size: 1 × 25 time-varying
`particle_flux>differential_directional_number_rate`
Energy Bins for NetoSi SECT 54 – 54 MeV/nuc (1 bins)
HET_R17_SECTORS 0 – 24 (25 bins)

6.5.2.33 A_Ni Ni counts side A (counts)
Size: 15 time-varying
`particle_flux>differential_directional_number_rate`
Energy Bins for Ni 29 – 332 MeV/nuc (15 bins)

6.5.2.34 A_Ni_Rate Ni count rate side A (counts s^{-1})
Size: 15 time-varying
`particle_flux>differential_directional_number_rate`
Energy Bins for Ni 29 – 332 MeV/nuc (15 bins)

6.5.2.35 A_O O counts side A (counts)
Size: 15 time-varying
`particle_flux>differential_directional_number_rate`
Energy Bins for O 15 – 166 MeV/nuc (15 bins)

6.5.2.36 A_O_Rate O count rate side A (counts s^{-1})
Size: 15 time-varying
`particle_flux>differential_directional_number_rate`
Energy Bins for O 15 – 166 MeV/nuc (15 bins)

6.5.2.37 A_S S counts side A (counts)
Size: 16 time-varying
`particle_flux>differential_directional_number_rate`
Energy Bins for S 21 – 279 MeV/nuc (16 bins)

6.5.2.38 A_S_Rate S count rate side A (counts s^{-1})
Size: 16 time-varying
`particle_flux>differential_directional_number_rate`
Energy Bins for S 21 – 279 MeV/nuc (16 bins)

6.5.2.39 A_Si Si counts side A (counts)
Size: 15 time-varying
`particle_flux>differential_directional_number_rate`
Energy Bins for Si 21 – 235 MeV/nuc (15 bins)

6.5.2.40 A_Si_Rate Si count rate side A (counts s^{-1})
Size: 15 time-varying
`particle_flux>differential_directional_number_rate`
Energy Bins for Si 21 – 235 MeV/nuc (15 bins)

6.5.2.41 B_Al Al counts side B (counts)
Size: 15 time-varying
`particle_flux>differential_directional_number_rate`
Energy Bins for Al 21 – 235 MeV/nuc (15 bins)

6.5.2.42 B_Al_Rate Al count rate side B (counts s^{-1})
Size: 15 time-varying
`particle_flux>differential_directional_number_rate`
Energy Bins for Al 21 – 235 MeV/nuc (15 bins)

6.5.2.43 B_Ar Ar counts side B (counts)
Size: 15 time-varying
`particle_flux>differential_directional_number_rate`
Energy Bins for Ar 25 – 279 MeV/nuc (15 bins)

6.5.2.44 B_Ar_Rate Ar count rate side B (counts s^{-1})
Size: 15 time-varying
`particle_flux>differential_directional_number_rate`
Energy Bins for Ar 25 – 279 MeV/nuc (15 bins)

6.5.2.45 B_C C counts side B (counts)
Size: 15 time-varying
`particle_flux>differential_directional_number_rate`
Energy Bins for C 12 – 140 MeV/nuc (15 bins)

6.5.2.46 B_CNO_SECT_Rate CNO sectored count rate side B (counts s^{-1})
Size: 2×25 time-varying
`particle_flux>differential_directional_number_rate`
Energy Bins for CNO SECT 35 – 64 MeV/nuc (2 bins)
HET_R17_SECTORS 0 – 24 (25 bins)

6.5.2.47 B_C_Rate C count rate side B (counts s^{-1})
Size: 15 time-varying
`particle_flux>differential_directional_number_rate`
Energy Bins for C 12 – 140 MeV/nuc (15 bins)

6.5.2.48 B_Ca Ca counts side B (counts)
Size: 15 time-varying
`particle_flux>differential_directional_number_rate`
Energy Bins for Ca 25 – 279 MeV/nuc (15 bins)

6.5.2.49 B_Ca_Rate Ca count rate side B (counts s^{-1})
Size: 15 time-varying
`particle_flux>differential_directional_number_rate`
Energy Bins for Ca 25 – 279 MeV/nuc (15 bins)

6.5.2.50 B_Cr Cr counts side B (counts)
Size: 16 time-varying
`particle_flux>differential_directional_number_rate`
Energy Bins for Cr 25 – 332 MeV/nuc (16 bins)

6.5.2.51 B_Cr_Rate Cr count rate side B (counts s^{-1})
Size: 16 time-varying
`particle_flux>differential_directional_number_rate`
Energy Bins for Cr 25 – 332 MeV/nuc (16 bins)

6.5.2.52 B_Electrons Electrons counts side B (counts)
Size: 19 time-varying
`particle_flux>differential_directional_number_rate`
Energy Bins for Electrons 0 – 10 MeV (19 bins)

6.5.2.53 B_Electrons_Rate Electrons count rate side B (counts s^{-1})
Size: 19 time-varying
`particle_flux>differential_directional_number_rate`
Energy Bins for Electrons 0 – 10 MeV (19 bins)

6.5.2.54 B_Electrons_SECT_Rate Electrons sectored count rate side B (counts s^{-1})
Size: 2×25 time-varying
`particle_flux>differential_directional_number_rate`
Energy Bins for Electrons SECT 1 – 3 MeV (2 bins)
HET_R17_SECTORS 0 – 24 (25 bins)

6.5.2.55 B_Fe Fe counts side B (counts)
Size: 15 time-varying
`particle_flux>differential_directional_number_rate`
Energy Bins for Fe 29 – 332 MeV/nuc (15 bins)

6.5.2.56 B_FeGroup_SECT_Rate FeGroup sectored count rate side B (counts s^{-1})
Size: 1×25 time-varying
`particle_flux>differential_directional_number_rate`
Energy Bins for FeGroup SECT 76 – 76 MeV/nuc (1 bins)
HET_R17_SECTORS 0 – 24 (25 bins)

6.5.2.57 B_Fe_Rate Fe count rate side B (counts s^{-1})
Size: 15 time-varying
`particle_flux>differential_directional_number_rate`
Energy Bins for Fe 29 – 332 MeV/nuc (15 bins)

6.5.2.58 B_H H counts side B (counts)
Size: 15 time-varying
`particle_flux>differential_directional_number_rate`

Energy Bins for H 7 – 83 MeV (15 bins)

6.5.2.59 B_H_Rate H count rate side B (counts s^{-1})
Size: 15 time-varying
`particle_flux>differential_directional_number_rate`
Energy Bins for H 7 – 83 MeV (15 bins)

6.5.2.60 B_H_SECT_Rate H sectored count rate side B (counts s^{-1})
Size: 2×25 time-varying
`particle_flux>differential_directional_number_rate`
Energy Bins for H SECT 17 – 32 MeV (2 bins)
HET_R17_SECTORS 0 – 24 (25 bins)

6.5.2.61 B_He He counts side B (counts)
Size: 16 time-varying
`particle_flux>differential_directional_number_rate`
Energy Bins for He 7 – 99 MeV/nuc (16 bins)

6.5.2.62 B_He_Rate He count rate side B (counts s^{-1})
Size: 16 time-varying
`particle_flux>differential_directional_number_rate`
Energy Bins for He 7 – 99 MeV/nuc (16 bins)

6.5.2.63 B_He_SECT_Rate He sectored count rate side B (counts s^{-1})
Size: 2×25 time-varying
`particle_flux>differential_directional_number_rate`
Energy Bins for He SECT 17 – 32 MeV/nuc (2 bins)
HET_R17_SECTORS 0 – 24 (25 bins)

6.5.2.64 B_Mg Mg counts side B (counts)
Size: 15 time-varying
`particle_flux>differential_directional_number_rate`
Energy Bins for Mg 21 – 235 MeV/nuc (15 bins)

6.5.2.65 B_Mg_Rate Mg count rate side B (counts s^{-1})
Size: 15 time-varying
`particle_flux>differential_directional_number_rate`
Energy Bins for Mg 21 – 235 MeV/nuc (15 bins)

6.5.2.66 B_N N counts side B (counts)
Size: 15 time-varying
`particle_flux>differential_directional_number_rate`
Energy Bins for N 12 – 140 MeV/nuc (15 bins)

6.5.2.67 B_N_Rate N count rate side B (counts s^{-1})
Size: 15 time-varying
`particle_flux>differential_directional_number_rate`
Energy Bins for N 12 – 140 MeV/nuc (15 bins)

6.5.2.68 B_Na Na counts side B (counts)
Size: 15 time-varying
`particle_flux>differential_directional_number_rate`
Energy Bins for Na 17 – 197 MeV/nuc (15 bins)

6.5.2.69 B_Na_Rate Na count rate side B (counts s^{-1})
Size: 15 time-varying
`particle_flux>differential_directional_number_rate`
Energy Bins for Na 17 – 197 MeV/nuc (15 bins)

6.5.2.70 B_Ne Ne counts side B (counts)
Size: 15 time-varying
`particle_flux>differential_directional_number_rate`
Energy Bins for Ne 17 – 197 MeV/nuc (15 bins)

6.5.2.71 B_Ne_Rate Ne count rate side B (counts s^{-1})
Size: 15 time-varying
`particle_flux>differential_directional_number_rate`
Energy Bins for Ne 17 – 197 MeV/nuc (15 bins)

6.5.2.72 B_NetoSi_SECT_Rate NetoSi sectored count rate side B (counts s^{-1})
Size: 1×25 time-varying
`particle_flux>differential_directional_number_rate`
Energy Bins for NetoSi SECT 54 – 54 MeV/nuc (1 bins)
HET_R17_SECTORS 0 – 24 (25 bins)

6.5.2.73 B_Ni Ni counts side B (counts)
Size: 15 time-varying
`particle_flux>differential_directional_number_rate`
Energy Bins for Ni 29 – 332 MeV/nuc (15 bins)

6.5.2.74 B_Ni_Rate Ni count rate side B (counts s^{-1})
Size: 15 time-varying
`particle_flux>differential_directional_number_rate`
Energy Bins for Ni 29 – 332 MeV/nuc (15 bins)

6.5.2.75 B_O O counts side B (counts)
Size: 15 time-varying
`particle_flux>differential_directional_number_rate`
Energy Bins for O 15 – 166 MeV/nuc (15 bins)

6.5.2.76 B_O_Rate O count rate side B (counts s^{-1})
Size: 15 time-varying
`particle_flux>differential_directional_number_rate`
Energy Bins for O 15 – 166 MeV/nuc (15 bins)

6.5.2.77 B_S S counts side B (counts)
Size: 16 time-varying
`particle_flux>differential_directional_number_rate`
Energy Bins for S 21 – 279 MeV/nuc (16 bins)

6.5.2.78 B_S_Rate S count rate side B (counts s^{-1})
Size: 16 time-varying
`particle_flux>differential_directional_number_rate`
Energy Bins for S 21 – 279 MeV/nuc (16 bins)

6.5.2.79 B_Si Si counts side B (counts)
Size: 15 time-varying
`particle_flux>differential_directional_number_rate`
Energy Bins for Si 21 – 235 MeV/nuc (15 bins)

6.5.2.80 B_Si_Rate Si count rate side B (counts s^{-1})
Size: 15 time-varying
`particle_flux>differential_directional_number_rate`
Energy Bins for Si 21 – 235 MeV/nuc (15 bins)

6.5.2.81 HCI_Lat HCI latitude (degrees)
time-varying
`position>latitude`
At timestamp. After Fraenz and Harper, PSS, 2002.

6.5.2.82 HCI_Lon HCI longitude (degrees)
time-varying
`position>longitude`
At timestamp. After Fraenz and Harper, PSS, 2002.

6.5.2.83 HCI_R Heliocentric distance (AU)
time-varying
`position>radial`
At timestamp. After Fraenz and Harper, PSS, 2002.

6.5.2.84 HET_A_HCI HCI flow direction HETA
Size: 3 time-varying
`position>direction`
Unit vector, after Fraenz and Harper, PSS, 2002.

6.5.2.85 HET_A_PA Pitch angle HETA (degree)
time-varying
`position>angle`

6.5.2.86 HET_A_R17_SECT_HCI HCI flow direction HETAR17SECT
Size: 25 × 3 time-varying
`position>direction`
Unit vector, after Fraenz and Harper, PSS, 2002.
HET_R17_SECTORS 0 – 24 (25 bins)

6.5.2.87 HET_A_R17_SECT_PA Pitch angle HETAR17SECT (degree)
Size: 25 time-varying
`position>angle`
HET_R17_SECTORS 0 – 24 (25 bins)

6.5.2.88 HET_A_R17_SECT_RTN RTN flow direction HETAR17SECT
Size: 25 × 3 time-varying
`position>direction`
Unit vector, after Fraenz and Harper, PSS, 2002.
HET_R17_SECTORS 0 – 24 (25 bins)

6.5.2.89 HET_A_R17_SECT_SA Nominal Parker Spiral angle HETAR17SECT (degree)
Size: 25 time-varying
`position>angle`
Angle between particle direction and nominal outward Parker Spiral, based on 400km/s solar wind and corotation breakdown at 10Rs.
HET_R17_SECTORS 0 – 24 (25 bins)

6.5.2.90 HET_A_RTN RTN flow direction HETA
Size: 3 time-varying
`position>direction`
Unit vector, after Fraenz and Harper, PSS, 2002.

6.5.2.91 HET_A_SA Nominal Parker Spiral angle HETA (degree)
time-varying
`position>angle`
Angle between particle direction and nominal outward Parker Spiral, based on 400km/s solar wind and corotation breakdown at 10Rs.

6.5.2.92 HET_B_HCI HCI flow direction HETB
Size: 3 time-varying
`position>direction`
Unit vector, after Fraenz and Harper, PSS, 2002.

6.5.2.93 HET_B_PA Pitch angle HETB (degree)
time-varying
`position>angle`

6.5.2.94 HET_B_R17_SECT_HCI HCI flow direction HETBR17SECT
Size: 25 × 3 time-varying
`position>direction`
Unit vector, after Fraenz and Harper, PSS, 2002.
HET_R17_SECTORS 0 – 24 (25 bins)

6.5.2.95 HET_B_R17_SECT_PA Pitch angle HETBR17SECT (degree)
Size: 25 time-varying
`position>angle`
HET_R17_SECTORS 0 – 24 (25 bins)

6.5.2.96 HET_B_R17_SECT_RTN RTN flow direction HETBR17SECT
Size: 25 × 3 time-varying
`position>direction`
Unit vector, after Fraenz and Harper, PSS, 2002.
HET_R17_SECTORS 0 – 24 (25 bins)

6.5.2.97 HET_B_R17_SECT_SA Nominal Parker Spiral angle HETBR17SECT (degree)
Size: 25 time-varying
`position>angle`
Angle between particle direction and nominal outward Parker Spiral, based on 400km/s solar wind and corotation breakdown at 10Rs.
HET_R17_SECTORS 0 – 24 (25 bins)

6.5.2.98 HET_B_RTN RTN flow direction HETB
Size: 3 time-varying
`position>direction`

Unit vector, after Fraenz and Harper, PSS, 2002.

6.5.2.99 HET_B_SA Nominal Parker Spiral angle HETB (degree)
time-varying
`position>angle`
Angle between particle direction and nominal outward Parker Spiral, based on 400km/s solar wind and corotation breakdown at 10Rs.

6.5.2.100 HGC_Lat HGC latitude (degrees)
time-varying
`position>latitude`
At timestamp. After Fraenz and Harper, PSS, 2002.

6.5.2.101 HGC_Lon HGC longitude (degrees)
time-varying
`position>longitude`
At timestamp. After Fraenz and Harper, PSS, 2002.

6.5.2.102 HGC_R Heliocentric distance (AU)
time-varying
`position>radial`
At timestamp. After Fraenz and Harper, PSS, 2002.

6.5.2.103 R1A_He_BIN R1A He Rates (counts)
Size: 5×16 time-varying
`particle_flux>differential_directional_number_rate`
Energy Bins for R1 He BIN 9 – 32 MeV/nuc (5 bins)
R1A_He_BIN_MASS_BIN 0 – 15 segment (16 bins)

6.5.2.104 R1A_Ne_BIN R1A Ne Rates (counts)
Size: 4×8 time-varying
`particle_flux>differential_directional_number_rate`
Energy Bins for R1 Ne BIN 23 – 64 MeV/nuc (4 bins)
R1A_Ne_BIN_MASS_BIN 0 – 7 segment (8 bins)

6.5.2.105 R1B_He_BIN R1B He Rates (counts)
Size: 5 × 16 time-varying
`particle_flux>differential_directional_number_rate`
Energy Bins for R1 He BIN 9 – 32 MeV/nuc (5 bins)
R1B_He_BIN_MASS_BIN 0 – 15 segment (16 bins)

6.5.2.106 R1B_Ne_BIN R1B Ne Rates (counts)
Size: 4 × 8 time-varying
`particle_flux>differential_directional_number_rate`
Energy Bins for R1 Ne BIN 23 – 64 MeV/nuc (4 bins)
R1B_Ne_BIN_MASS_BIN 0 – 7 segment (8 bins)

6.5.2.107 R2A_He_BIN R2A He Rates (counts)
Size: 4 × 16 time-varying
`particle_flux>differential_directional_number_rate`
Energy Bins for R2 He BIN 16 – 45 MeV/nuc (4 bins)
R2A_He_BIN_MASS_BIN 0 – 15 segment (16 bins)

6.5.2.108 R2A_Ne_BIN R2A Ne Rates (counts)
Size: 4 × 8 time-varying
`particle_flux>differential_directional_number_rate`
Energy Bins for R2 Ne BIN 32 – 91 MeV/nuc (4 bins)
R2A_Ne_BIN_MASS_BIN 0 – 7 segment (8 bins)

6.5.2.109 R2B_He_BIN R2B He Rates (counts)
Size: 4 × 16 time-varying
`particle_flux>differential_directional_number_rate`
Energy Bins for R2 He BIN 16 – 45 MeV/nuc (4 bins)
R2B_He_BIN_MASS_BIN 0 – 15 segment (16 bins)

6.5.2.110 R2B_Ne_BIN R2B Ne Rates (counts)
Size: 4 × 8 time-varying
`particle_flux>differential_directional_number_rate`
Energy Bins for R2 Ne BIN 32 – 91 MeV/nuc (4 bins)
R2B_Ne_BIN_MASS_BIN 0 – 7 segment (8 bins)

6.5.2.111 R3A_He_BIN R3A He Rates (counts)
Size: 4 × 16 time-varying
`particle_flux>differential_directional_number_rate`
Energy Bins for R3 He BIN 23 – 64 MeV/nuc (4 bins)
R3A_He_BIN_MASS_BIN 0 – 15 segment (16 bins)

6.5.2.112 R3A_Ne_BIN R3A Ne Rates (counts)
Size: 4 × 8 time-varying
`particle_flux>differential_directional_number_rate`
Energy Bins for R3 Ne BIN 45 – 128 MeV/nuc (4 bins)
R3A_Ne_BIN_MASS_BIN 0 – 7 segment (8 bins)

6.5.2.113 R3B_He_BIN R3B He Rates (counts)
Size: 4 × 16 time-varying
`particle_flux>differential_directional_number_rate`
Energy Bins for R3 He BIN 23 – 64 MeV/nuc (4 bins)
R3B_He_BIN_MASS_BIN 0 – 15 segment (16 bins)

6.5.2.114 R3B_Ne_BIN R3B Ne Rates (counts)
Size: 4 × 8 time-varying
`particle_flux>differential_directional_number_rate`
Energy Bins for R3 Ne BIN 45 – 128 MeV/nuc (4 bins)
R3B_Ne_BIN_MASS_BIN 0 – 7 segment (8 bins)

6.5.2.115 R4A_He_BIN R4A He Rates (counts)
Size: 3 × 16 time-varying
`particle_flux>differential_directional_number_rate`
Energy Bins for R4 He BIN 32 – 64 MeV/nuc (3 bins)
R4A_He_BIN_MASS_BIN 0 – 15 segment (16 bins)

6.5.2.116 R4A_Ne_BIN R4A Ne Rates (counts)
Size: 3 × 8 time-varying
`particle_flux>differential_directional_number_rate`
Energy Bins for R4 Ne BIN 64 – 128 MeV/nuc (3 bins)
R4A_Ne_BIN_MASS_BIN 0 – 7 segment (8 bins)

6.5.2.117 R4B_He_BIN R4B He Rates (counts)
Size: 3 × 16 time-varying
`particle_flux>differential_directional_number_rate`
Energy Bins for R4 He BIN 32 – 64 MeV/nuc (3 bins)
R4B_He_BIN_MASS_BIN 0 – 15 segment (16 bins)

6.5.2.118 R4B_Ne_BIN R4B Ne Rates (counts)
Size: 3 × 8 time-varying
`particle_flux>differential_directional_number_rate`
Energy Bins for R4 Ne BIN 64 – 128 MeV/nuc (3 bins)
R4B_Ne_BIN_MASS_BIN 0 – 7 segment (8 bins)

6.5.2.119 R5A_He_BIN R5A He Rates (counts)
Size: 3 × 16 time-varying
`particle_flux>differential_directional_number_rate`
Energy Bins for R5 He BIN 32 – 64 MeV/nuc (3 bins)
R5A_He_BIN_MASS_BIN 0 – 15 segment (16 bins)

6.5.2.120 R5A_Ne_BIN R5A Ne Rates (counts)
Size: 2 × 8 time-varying
`particle_flux>differential_directional_number_rate`
Energy Bins for R5 Ne BIN 91 – 128 MeV/nuc (2 bins)
R5A_Ne_BIN_MASS_BIN 0 – 7 segment (8 bins)

6.5.2.121 R5B_He_BIN R5B He Rates (counts)
Size: 3 × 16 time-varying
`particle_flux>differential_directional_number_rate`
Energy Bins for R5 He BIN 32 – 64 MeV/nuc (3 bins)
R5B_He_BIN_MASS_BIN 0 – 15 segment (16 bins)

6.5.2.122 R5B_Ne_BIN R5B Ne Rates (counts)
Size: 2 × 8 time-varying
`particle_flux>differential_directional_number_rate`
Energy Bins for R5 Ne BIN 91 – 128 MeV/nuc (2 bins)
R5B_Ne_BIN_MASS_BIN 0 – 7 segment (8 bins)

6.5.2.123 R6A_He_BIN R6A He Rates (counts)
Size: 3 × 16 time-varying
`particle_flux>differential_directional_number_rate`
Energy Bins for R6 He BIN 32 – 64 MeV/nuc (3 bins)
R6A_He_BIN_MASS_BIN 0 – 15 segment (16 bins)

6.5.2.124 R6A_Ne_BIN R6A Ne Rates (counts)
Size: 3 × 8 time-varying
`particle_flux>differential_directional_number_rate`
Energy Bins for R6 Ne BIN 91 – 181 MeV/nuc (3 bins)
R6A_Ne_BIN_MASS_BIN 0 – 7 segment (8 bins)

6.5.2.125 R6B_He_BIN R6B He Rates (counts)
Size: 3 × 16 time-varying
`particle_flux>differential_directional_number_rate`
Energy Bins for R6 He BIN 32 – 64 MeV/nuc (3 bins)
R6B_He_BIN_MASS_BIN 0 – 15 segment (16 bins)

6.5.2.126 R6B_Ne_BIN R6B Ne Rates (counts)
Size: 3 × 8 time-varying
`particle_flux>differential_directional_number_rate`
Energy Bins for R6 Ne BIN 91 – 181 MeV/nuc (3 bins)
R6B_Ne_BIN_MASS_BIN 0 – 7 segment (8 bins)

6.5.2.127 R7A_He_BIN R7A He Rates (counts)
Size: 2 × 16 time-varying
`particle_flux>differential_directional_number_rate`
Energy Bins for R7 He BIN 45 – 64 MeV/nuc (2 bins)
R7A_He_BIN_MASS_BIN 0 – 15 segment (16 bins)

6.5.2.128 R7A_Ne_BIN R7A Ne Rates (counts)
Size: 3 × 8 time-varying
`particle_flux>differential_directional_number_rate`
Energy Bins for R7 Ne BIN 91 – 181 MeV/nuc (3 bins)
R7A_Ne_BIN_MASS_BIN 0 – 7 segment (8 bins)

6.5.2.129 R7B_He_BIN R7B He Rates (counts)
Size: 2 × 16 time-varying
`particle_flux>differential_directional_number_rate`
Energy Bins for R7 He BIN 45 – 64 MeV/nuc (2 bins)
R7B_He_BIN_MASS_BIN 0 – 15 segment (16 bins)

6.5.2.130 R7B_Ne_BIN R7B Ne Rates (counts)
Size: 3 × 8 time-varying
`particle_flux>differential_directional_number_rate`
Energy Bins for R7 Ne BIN 91 – 181 MeV/nuc (3 bins)
R7B_Ne_BIN_MASS_BIN 0 – 7 segment (8 bins)

6.5.3 OTHER SUPPORT

6.5.3.1 Quality_Flag Data-quality flag
Size: 10 time-varying
`flag>status`
Quality flag number 0 – 9 (10 bins)

6.6 PSP_ISOIS-EPIHI_L2-HET-RATES60

ISOIS-EPIHI>Integrated Science Investigation of the Sun, Energetic Particle Instrument Hi
L2-HET-rates60>Level 2 HET 1-minute rates
EPI-Hi HET 60 second rates cdf. Time tags indicate midpoint of integration.
Instrument paper: Integrated Science Investigation of the Sun (ISIS): Design of the Energetic Particle Investigation. McComas, D. J. et al (2016). Space Sci. Rev., doi:10.1007/s11214-014-0059-1
1 minute to 1 hour
Cite McComas et al (2016), doi:10.1007/s11214-014-0059-1

6.6.1 PRIMARY VARIABLES

6.6.1.1 A_H_Flux H flux side A ($cm^{-2}sr^{-1}sec^{-1}MeV^{-1}$)
Size: 15 time-varying
`particle_flux>differential_directional_number`
Energy Bins for H 7 – 83 MeV (15 bins)

6.6.1.2 A_H_SECT_Flux H sectored flux side A ($cm^{-2}sr^{-1}sec^{-1}MeV^{-1}$)
Size: 2 × 25 time-varying
`particle_flux>differential_directional_number`

Energy Bins for H SECT 17 – 32 MeV (2 bins)
HET_R17_SECTORS 0 – 24 (25 bins)

6.6.1.3 A_He_Flux He flux side A ($cm^{-2}sr^{-1}sec^{-1}(MeV/nuc)^{-1}$)
Size: 16 time-varying
`particle_flux>differential_directional_number`
Energy Bins for He 7 – 99 MeV/nuc (16 bins)

6.6.1.4 A_He_SECT_Flux He sectored flux side A ($cm^{-2}sr^{-1}sec^{-1}(MeV/nuc)^{-1}$)
Size: 2×25 time-varying
`particle_flux>differential_directional_number`
Energy Bins for He SECT 17 – 32 MeV/nuc (2 bins)
HET_R17_SECTORS 0 – 24 (25 bins)

6.6.1.5 B_H_Flux H flux side B ($cm^{-2}sr^{-1}sec^{-1}MeV^{-1}$)
Size: 15 time-varying
`particle_flux>differential_directional_number`
Energy Bins for H 7 – 83 MeV (15 bins)

6.6.1.6 B_H_SECT_Flux H sectored flux side B ($cm^{-2}sr^{-1}sec^{-1}MeV^{-1}$)
Size: 2×25 time-varying
`particle_flux>differential_directional_number`
Energy Bins for H SECT 17 – 32 MeV (2 bins)
HET_R17_SECTORS 0 – 24 (25 bins)

6.6.1.7 B_He_Flux He flux side B ($cm^{-2}sr^{-1}sec^{-1}(MeV/nuc)^{-1}$)
Size: 16 time-varying
`particle_flux>differential_directional_number`
Energy Bins for He 7 – 99 MeV/nuc (16 bins)

6.6.1.8 B_He_SECT_Flux He sectored flux side B ($cm^{-2}sr^{-1}sec^{-1}(MeV/nuc)^{-1}$)
Size: 2×25 time-varying
`particle_flux>differential_directional_number`
Energy Bins for He SECT 17 – 32 MeV/nuc (2 bins)
HET_R17_SECTORS 0 – 24 (25 bins)

6.6.2 OTHER DATA

6.6.2.1 A_Al Al counts side A (counts)
Size: 15 time-varying
`particle_flux>differential_directional_number_rate`
Energy Bins for Al 21 – 235 MeV/nuc (15 bins)

6.6.2.2 A_Al_Rate Al count rate side A (counts s^{-1})
Size: 15 time-varying
`particle_flux>differential_directional_number_rate`
Energy Bins for Al 21 – 235 MeV/nuc (15 bins)

6.6.2.3 A_Ar Ar counts side A (counts)
Size: 15 time-varying
`particle_flux>differential_directional_number_rate`
Energy Bins for Ar 25 – 279 MeV/nuc (15 bins)

6.6.2.4 A_Ar_Rate Ar count rate side A (counts s^{-1})
Size: 15 time-varying
`particle_flux>differential_directional_number_rate`
Energy Bins for Ar 25 – 279 MeV/nuc (15 bins)

6.6.2.5 A_C C counts side A (counts)
Size: 15 time-varying
`particle_flux>differential_directional_number_rate`
Energy Bins for C 12 – 140 MeV/nuc (15 bins)

6.6.2.6 A_C_Rate C count rate side A (counts s^{-1})
Size: 15 time-varying
`particle_flux>differential_directional_number_rate`
Energy Bins for C 12 – 140 MeV/nuc (15 bins)

6.6.2.7 A_Ca Ca counts side A (counts)
Size: 15 time-varying
`particle_flux>differential_directional_number_rate`
Energy Bins for Ca 25 – 279 MeV/nuc (15 bins)

6.6.2.8 A_Ca_Rate Ca count rate side A (counts s^{-1})
Size: 15 time-varying
`particle_flux>differential_directional_number_rate`
Energy Bins for Ca 25 – 279 MeV/nuc (15 bins)

6.6.2.9 A_Cr Cr counts side A (counts)
Size: 16 time-varying
`particle_flux>differential_directional_number_rate`
Energy Bins for Cr 25 – 332 MeV/nuc (16 bins)

6.6.2.10 A_Cr_Rate Cr count rate side A (counts s^{-1})
Size: 16 time-varying
`particle_flux>differential_directional_number_rate`
Energy Bins for Cr 25 – 332 MeV/nuc (16 bins)

6.6.2.11 A_Electrons Electrons counts side A (counts)
Size: 19 time-varying
`particle_flux>differential_directional_number_rate`
Energy Bins for Electrons 0 – 10 MeV (19 bins)

6.6.2.12 A_Electrons_Rate Electrons count rate side A (counts s^{-1})
Size: 19 time-varying
`particle_flux>differential_directional_number_rate`
Energy Bins for Electrons 0 – 10 MeV (19 bins)

6.6.2.13 A_Electrons_SECT_Rate Electrons sectored count rate side A (counts s^{-1})
Size: 2×25 time-varying
`particle_flux>differential_directional_number_rate`
Energy Bins for Electrons SECT 1 – 3 MeV (2 bins)
HET_R17_SECTORS 0 – 24 (25 bins)

6.6.2.14 A_Fe Fe counts side A (counts)
Size: 15 time-varying
`particle_flux>differential_directional_number_rate`
Energy Bins for Fe 29 – 332 MeV/nuc (15 bins)

6.6.2.15 A_Fe_Rate Fe count rate side A (counts s^{-1})
Size: 15 time-varying
`particle_flux>differential_directional_number_rate`
Energy Bins for Fe 29 – 332 MeV/nuc (15 bins)

6.6.2.16 A_H H counts side A (counts)
Size: 15 time-varying
`particle_flux>differential_directional_number_rate`
Energy Bins for H 7 – 83 MeV (15 bins)

6.6.2.17 A_H_Rate H count rate side A (counts s^{-1})
Size: 15 time-varying
`particle_flux>differential_directional_number_rate`
Energy Bins for H 7 – 83 MeV (15 bins)

6.6.2.18 A_H_SECT_Rate H sectored count rate side A (counts s^{-1})
Size: 2×25 time-varying
`particle_flux>differential_directional_number_rate`
Energy Bins for H SECT 17 – 32 MeV (2 bins)
HET_R17_SECTORS 0 – 24 (25 bins)

6.6.2.19 A_He He counts side A (counts)
Size: 16 time-varying
`particle_flux>differential_directional_number_rate`
Energy Bins for He 7 – 99 MeV/nuc (16 bins)

6.6.2.20 A_He_Rate He count rate side A (counts s^{-1})
Size: 16 time-varying
`particle_flux>differential_directional_number_rate`
Energy Bins for He 7 – 99 MeV/nuc (16 bins)

6.6.2.21 A_He_SECT_Rate He sectored count rate side A (counts s^{-1})
Size: 2×25 time-varying
`particle_flux>differential_directional_number_rate`
Energy Bins for He SECT 17 – 32 MeV/nuc (2 bins)

HET_R17_SECTORS 0 – 24 (25 bins)

6.6.2.22 A_Mg Mg counts side A (counts)
Size: 15 time-varying
`particle_flux>differential_directional_number_rate`
Energy Bins for Mg 21 – 235 MeV/nuc (15 bins)

6.6.2.23 A_Mg_Rate Mg count rate side A (counts s^{-1})
Size: 15 time-varying
`particle_flux>differential_directional_number_rate`
Energy Bins for Mg 21 – 235 MeV/nuc (15 bins)

6.6.2.24 A_N N counts side A (counts)
Size: 15 time-varying
`particle_flux>differential_directional_number_rate`
Energy Bins for N 12 – 140 MeV/nuc (15 bins)

6.6.2.25 A_N_Rate N count rate side A (counts s^{-1})
Size: 15 time-varying
`particle_flux>differential_directional_number_rate`
Energy Bins for N 12 – 140 MeV/nuc (15 bins)

6.6.2.26 A_Na Na counts side A (counts)
Size: 15 time-varying
`particle_flux>differential_directional_number_rate`
Energy Bins for Na 17 – 197 MeV/nuc (15 bins)

6.6.2.27 A_Na_Rate Na count rate side A (counts s^{-1})
Size: 15 time-varying
`particle_flux>differential_directional_number_rate`
Energy Bins for Na 17 – 197 MeV/nuc (15 bins)

6.6.2.28 A_Ne Ne counts side A (counts)
Size: 15 time-varying

`particle_flux>differential_directional_number_rate`
Energy Bins for Ne 17 – 197 MeV/nuc (15 bins)

6.6.2.29 A_Ne_Rate Ne count rate side A (counts s^{-1})
Size: 15 time-varying
`particle_flux>differential_directional_number_rate`
Energy Bins for Ne 17 – 197 MeV/nuc (15 bins)

6.6.2.30 A_Ni Ni counts side A (counts)
Size: 15 time-varying
`particle_flux>differential_directional_number_rate`
Energy Bins for Ni 29 – 332 MeV/nuc (15 bins)

6.6.2.31 A_Ni_Rate Ni count rate side A (counts s^{-1})
Size: 15 time-varying
`particle_flux>differential_directional_number_rate`
Energy Bins for Ni 29 – 332 MeV/nuc (15 bins)

6.6.2.32 A_O O counts side A (counts)
Size: 15 time-varying
`particle_flux>differential_directional_number_rate`
Energy Bins for O 15 – 166 MeV/nuc (15 bins)

6.6.2.33 A_O_Rate O count rate side A (counts s^{-1})
Size: 15 time-varying
`particle_flux>differential_directional_number_rate`
Energy Bins for O 15 – 166 MeV/nuc (15 bins)

6.6.2.34 A_S S counts side A (counts)
Size: 16 time-varying
`particle_flux>differential_directional_number_rate`
Energy Bins for S 21 – 279 MeV/nuc (16 bins)

6.6.2.35 A_S_Rate S count rate side A (counts s^{-1})
Size: 16 time-varying
`particle_flux>differential_directional_number_rate`
Energy Bins for S 21 – 279 MeV/nuc (16 bins)

6.6.2.36 A_Si Si counts side A (counts)
Size: 15 time-varying
`particle_flux>differential_directional_number_rate`
Energy Bins for Si 21 – 235 MeV/nuc (15 bins)

6.6.2.37 A_Si_Rate Si count rate side A (counts s^{-1})
Size: 15 time-varying
`particle_flux>differential_directional_number_rate`
Energy Bins for Si 21 – 235 MeV/nuc (15 bins)

6.6.2.38 B_Al Al counts side B (counts)
Size: 15 time-varying
`particle_flux>differential_directional_number_rate`
Energy Bins for Al 21 – 235 MeV/nuc (15 bins)

6.6.2.39 B_Al_Rate Al count rate side B (counts s^{-1})
Size: 15 time-varying
`particle_flux>differential_directional_number_rate`
Energy Bins for Al 21 – 235 MeV/nuc (15 bins)

6.6.2.40 B_Ar Ar counts side B (counts)
Size: 15 time-varying
`particle_flux>differential_directional_number_rate`
Energy Bins for Ar 25 – 279 MeV/nuc (15 bins)

6.6.2.41 B_Ar_Rate Ar count rate side B (counts s^{-1})
Size: 15 time-varying
`particle_flux>differential_directional_number_rate`
Energy Bins for Ar 25 – 279 MeV/nuc (15 bins)

6.6.2.42 B_C C counts side B (counts)
Size: 15 time-varying
`particle_flux>differential_directional_number_rate`
Energy Bins for C 12 – 140 MeV/nuc (15 bins)

6.6.2.43 B_C_Rate C count rate side B (counts s^{-1})
Size: 15 time-varying
`particle_flux>differential_directional_number_rate`
Energy Bins for C 12 – 140 MeV/nuc (15 bins)

6.6.2.44 B_Ca Ca counts side B (counts)
Size: 15 time-varying
`particle_flux>differential_directional_number_rate`
Energy Bins for Ca 25 – 279 MeV/nuc (15 bins)

6.6.2.45 B_Ca_Rate Ca count rate side B (counts s^{-1})
Size: 15 time-varying
`particle_flux>differential_directional_number_rate`
Energy Bins for Ca 25 – 279 MeV/nuc (15 bins)

6.6.2.46 B_Cr Cr counts side B (counts)
Size: 16 time-varying
`particle_flux>differential_directional_number_rate`
Energy Bins for Cr 25 – 332 MeV/nuc (16 bins)

6.6.2.47 B_Cr_Rate Cr count rate side B (counts s^{-1})
Size: 16 time-varying
`particle_flux>differential_directional_number_rate`
Energy Bins for Cr 25 – 332 MeV/nuc (16 bins)

6.6.2.48 B_Electrons Electrons counts side B (counts)
Size: 19 time-varying
`particle_flux>differential_directional_number_rate`
Energy Bins for Electrons 0 – 10 MeV (19 bins)

6.6.2.49 B_Electrons_Rate Electrons count rate side B (counts s^{-1})
Size: 19 time-varying
`particle_flux>differential_directional_number_rate`
Energy Bins for Electrons 0 – 10 MeV (19 bins)

6.6.2.50 B_Electrons_SECT_Rate Electrons sectored count rate side B (counts s^{-1})
Size: 2 × 25 time-varying
`particle_flux>differential_directional_number_rate`
Energy Bins for Electrons SECT 1 – 3 MeV (2 bins)
HET_R17_SECTORS 0 – 24 (25 bins)

6.6.2.51 B_Fe Fe counts side B (counts)
Size: 15 time-varying
`particle_flux>differential_directional_number_rate`
Energy Bins for Fe 29 – 332 MeV/nuc (15 bins)

6.6.2.52 B_Fe_Rate Fe count rate side B (counts s^{-1})
Size: 15 time-varying
`particle_flux>differential_directional_number_rate`
Energy Bins for Fe 29 – 332 MeV/nuc (15 bins)

6.6.2.53 B_H H counts side B (counts)
Size: 15 time-varying
`particle_flux>differential_directional_number_rate`
Energy Bins for H 7 – 83 MeV (15 bins)

6.6.2.54 B_H_Rate H count rate side B (counts s^{-1})
Size: 15 time-varying
`particle_flux>differential_directional_number_rate`
Energy Bins for H 7 – 83 MeV (15 bins)

6.6.2.55 B_H_SECT_Rate H sectored count rate side B (counts s^{-1})
Size: 2 × 25 time-varying
`particle_flux>differential_directional_number_rate`
Energy Bins for H SECT 17 – 32 MeV (2 bins)

HET_R17_SECTORS 0 – 24 (25 bins)

6.6.2.56 B_He He counts side B (counts)
Size: 16 time-varying
`particle_flux>differential_directional_number_rate`
Energy Bins for He 7 – 99 MeV/nuc (16 bins)

6.6.2.57 B_He_Rate He count rate side B (counts s^{-1})
Size: 16 time-varying
`particle_flux>differential_directional_number_rate`
Energy Bins for He 7 – 99 MeV/nuc (16 bins)

6.6.2.58 B_He_SECT_Rate He sectored count rate side B (counts s^{-1})
Size: 2×25 time-varying
`particle_flux>differential_directional_number_rate`
Energy Bins for He SECT 17 – 32 MeV/nuc (2 bins)
HET_R17_SECTORS 0 – 24 (25 bins)

6.6.2.59 B_Mg Mg counts side B (counts)
Size: 15 time-varying
`particle_flux>differential_directional_number_rate`
Energy Bins for Mg 21 – 235 MeV/nuc (15 bins)

6.6.2.60 B_Mg_Rate Mg count rate side B (counts s^{-1})
Size: 15 time-varying
`particle_flux>differential_directional_number_rate`
Energy Bins for Mg 21 – 235 MeV/nuc (15 bins)

6.6.2.61 B_N N counts side B (counts)
Size: 15 time-varying
`particle_flux>differential_directional_number_rate`
Energy Bins for N 12 – 140 MeV/nuc (15 bins)

6.6.2.62 B_N_Rate N count rate side B (counts s^{-1})
Size: 15 time-varying
`particle_flux>differential_directional_number_rate`
Energy Bins for N 12 – 140 MeV/nuc (15 bins)

6.6.2.63 B_Na Na counts side B (counts)
Size: 15 time-varying
`particle_flux>differential_directional_number_rate`
Energy Bins for Na 17 – 197 MeV/nuc (15 bins)

6.6.2.64 B_Na_Rate Na count rate side B (counts s^{-1})
Size: 15 time-varying
`particle_flux>differential_directional_number_rate`
Energy Bins for Na 17 – 197 MeV/nuc (15 bins)

6.6.2.65 B_Ne Ne counts side B (counts)
Size: 15 time-varying
`particle_flux>differential_directional_number_rate`
Energy Bins for Ne 17 – 197 MeV/nuc (15 bins)

6.6.2.66 B_Ne_Rate Ne count rate side B (counts s^{-1})
Size: 15 time-varying
`particle_flux>differential_directional_number_rate`
Energy Bins for Ne 17 – 197 MeV/nuc (15 bins)

6.6.2.67 B_Ni Ni counts side B (counts)
Size: 15 time-varying
`particle_flux>differential_directional_number_rate`
Energy Bins for Ni 29 – 332 MeV/nuc (15 bins)

6.6.2.68 B_Ni_Rate Ni count rate side B (counts s^{-1})
Size: 15 time-varying
`particle_flux>differential_directional_number_rate`
Energy Bins for Ni 29 – 332 MeV/nuc (15 bins)

6.6.2.69 B_O O counts side B (counts)
Size: 15 time-varying
`particle_flux>differential_directional_number_rate`
Energy Bins for O 15 – 166 MeV/nuc (15 bins)

6.6.2.70 B_O_Rate O count rate side B (counts s^{-1})
Size: 15 time-varying
`particle_flux>differential_directional_number_rate`
Energy Bins for O 15 – 166 MeV/nuc (15 bins)

6.6.2.71 B_S S counts side B (counts)
Size: 16 time-varying
`particle_flux>differential_directional_number_rate`
Energy Bins for S 21 – 279 MeV/nuc (16 bins)

6.6.2.72 B_S_Rate S count rate side B (counts s^{-1})
Size: 16 time-varying
`particle_flux>differential_directional_number_rate`
Energy Bins for S 21 – 279 MeV/nuc (16 bins)

6.6.2.73 B_Si Si counts side B (counts)
Size: 15 time-varying
`particle_flux>differential_directional_number_rate`
Energy Bins for Si 21 – 235 MeV/nuc (15 bins)

6.6.2.74 B_Si_Rate Si count rate side B (counts s^{-1})
Size: 15 time-varying
`particle_flux>differential_directional_number_rate`
Energy Bins for Si 21 – 235 MeV/nuc (15 bins)

6.6.2.75 HCI_Lat HCI latitude (degrees)
time-varying
`position>latitude`
At timestamp. After Fraenz and Harper, PSS, 2002.

6.6.2.76 HCI_Lon HCI longitude (degrees)
time-varying
`position>longitude`
At timestamp. After Fraenz and Harper, PSS, 2002.

6.6.2.77 HCI_R Heliocentric distance (AU)
time-varying
`position>radial`
At timestamp. After Fraenz and Harper, PSS, 2002.

6.6.2.78 HET_A_HCI HCI flow direction HETA
Size: 3 time-varying
`position>direction`
Unit vector, after Fraenz and Harper, PSS, 2002.

6.6.2.79 HET_A_PA Pitch angle HETA (degree)
time-varying
`position>angle`

6.6.2.80 HET_A_R17_SECT_HCI HCI flow direction HETAR17SECT
Size: 25 × 3 time-varying
`position>direction`
Unit vector, after Fraenz and Harper, PSS, 2002.
HET_R17_SECTORS 0 – 24 (25 bins)

6.6.2.81 HET_A_R17_SECT_PA Pitch angle HETAR17SECT (degree)
Size: 25 time-varying
`position>angle`
HET_R17_SECTORS 0 – 24 (25 bins)

6.6.2.82 HET_A_R17_SECT_RTN RTN flow direction HETAR17SECT
Size: 25 × 3 time-varying
`position>direction`
Unit vector, after Fraenz and Harper, PSS, 2002.
HET_R17_SECTORS 0 – 24 (25 bins)

6.6.2.83 HET_A_R17_SECT_SA Nominal Parker Spiral angle HETAR17SECT (degree)
Size: 25 time-varying
`position>angle`
Angle between particle direction and nominal outward Parker Spiral, based on 400km/s solar wind and corotation breakdown at 10Rs.
HET_R17_SECTORS 0 – 24 (25 bins)

6.6.2.84 HET_A_RTN RTN flow direction HETA
Size: 3 time-varying
`position>direction`
Unit vector, after Fraenz and Harper, PSS, 2002.

6.6.2.85 HET_A_SA Nominal Parker Spiral angle HETA (degree)
time-varying
`position>angle`
Angle between particle direction and nominal outward Parker Spiral, based on 400km/s solar wind and corotation breakdown at 10Rs.

6.6.2.86 HET_B_HCI HCI flow direction HETB
Size: 3 time-varying
`position>direction`
Unit vector, after Fraenz and Harper, PSS, 2002.

6.6.2.87 HET_B_PA Pitch angle HETB (degree)
time-varying
`position>angle`

6.6.2.88 HET_B_R17_SECT_HCI HCI flow direction HETBR17SECT
Size: 25×3 time-varying
`position>direction`
Unit vector, after Fraenz and Harper, PSS, 2002.
HET_R17_SECTORS 0 – 24 (25 bins)

6.6.2.89 HET_B_R17_SECT_PA Pitch angle HETBR17SECT (degree)
Size: 25 time-varying
`position>angle`

HET_R17_SECTORS 0 – 24 (25 bins)

6.6.2.90 HET_B_R17_SECT_RTN RTN flow direction HETBR17SECT
Size: 25 × 3 time-varying
`position>direction`
Unit vector, after Fraenz and Harper, PSS, 2002.
HET_R17_SECTORS 0 – 24 (25 bins)

6.6.2.91 HET_B_R17_SECT_SA Nominal Parker Spiral angle HETBR17SECT (degree)
Size: 25 time-varying
`position>angle`
Angle between particle direction and nominal outward Parker Spiral, based on 400km/s solar wind and corotation breakdown at 10Rs.
HET_R17_SECTORS 0 – 24 (25 bins)

6.6.2.92 HET_B_RTN RTN flow direction HETB
Size: 3 time-varying
`position>direction`
Unit vector, after Fraenz and Harper, PSS, 2002.

6.6.2.93 HET_B_SA Nominal Parker Spiral angle HETB (degree)
time-varying
`position>angle`
Angle between particle direction and nominal outward Parker Spiral, based on 400km/s solar wind and corotation breakdown at 10Rs.

6.6.2.94 HGC_Lat HGC latitude (degrees)
time-varying
`position>latitude`
At timestamp. After Fraenz and Harper, PSS, 2002.

6.6.2.95 HGC_Lon HGC longitude (degrees)
time-varying
`position>longitude`
At timestamp. After Fraenz and Harper, PSS, 2002.

6.6.2.96 HGC_R Heliocentric distance (AU)
time-varying
`position>radial`
At timestamp. After Fraenz and Harper, PSS, 2002.

6.6.3 OTHER SUPPORT

6.6.3.1 Quality_Flag Data-quality flag
Size: 10 time-varying
`flag>status`
Quality flag number 0 – 9 (10 bins)

6.7 PSP_ISOIS-EPIHI_L2-LET1-RATES10

ISOIS-EPIHI>Integrated Science Investigation of the Sun, Energetic Particle Instrument Hi
L2-LET1-rates10>Level 2 LET1 10-second rates
EPI-Hi 10 second rates cdf. Time tags indicate midpoint of integration.
Instrument paper: Integrated Science Investigation of the Sun (ISIS): Design of the Energetic Particle Investigation. McComas, D. J. et al (2016). Space Sci. Rev., doi:10.1007/s11214-014-0059-1
1 minute to 1 hour
Cite McComas et al (2016), doi:10.1007/s11214-014-0059-1

6.7.1 PRIMARY VARIABLES

6.7.1.1 A_H_Flux H flux side A ($cm^{-2}sr^{-1}sec^{-1}MeV^{-1}$)
Size: 18 time-varying
`particle_flux>differential_directional_number`
Energy Bins for H 1 – 15 MeV (18 bins)

6.7.1.2 A_He_Flux He flux side A ($cm^{-2}sr^{-1}sec^{-1}(MeV/nuc)^{-1}$)
Size: 22 time-varying
`particle_flux>differential_directional_number`
Energy Bins for He 1 – 29 MeV/nuc (22 bins)

6.7.1.3 B_H_Flux H flux side B ($cm^{-2}sr^{-1}sec^{-1}MeV^{-1}$)
Size: 18 time-varying
`particle_flux>differential_directional_number`
Energy Bins for H 1 – 15 MeV (18 bins)

6.7.1.4 B_He_Flux He flux side B ($cm^{-2}sr^{-1}sec^{-1}(MeV/nuc)^{-1}$)
Size: 22 time-varying
`particle_flux>differential_directional_number`
Energy Bins for He 1 – 29 MeV/nuc (22 bins)

6.7.2 OTHER DATA

6.7.2.1 A_Electrons Electrons counts side A (counts)
Size: 14 time-varying
`particle_flux>differential_directional_number_rate`
Energy Bins for Electrons 1 – 5 MeV (14 bins)

6.7.2.2 A_Electrons_Rate Electrons count rate side A ($counts\,s^{-1}$)
Size: 14 time-varying
`particle_flux>differential_directional_number_rate`
Energy Bins for Electrons 1 – 5 MeV (14 bins)

6.7.2.3 A_H H counts side A (counts)
Size: 18 time-varying
`particle_flux>differential_directional_number_rate`
Energy Bins for H 1 – 15 MeV (18 bins)

6.7.2.4 A_H_Rate H count rate side A ($counts\,s^{-1}$)
Size: 18 time-varying
`particle_flux>differential_directional_number_rate`
Energy Bins for H 1 – 15 MeV (18 bins)

6.7.2.5 A_He He counts side A (counts)
Size: 22 time-varying
`particle_flux>differential_directional_number_rate`
Energy Bins for He 1 – 29 MeV/nuc (22 bins)

6.7.2.6 A_He_Rate He count rate side A ($counts\,s^{-1}$)
Size: 22 time-varying
`particle_flux>differential_directional_number_rate`
Energy Bins for He 1 – 29 MeV/nuc (22 bins)

6.7.2.7 B_Electrons Electrons counts side B (counts)
Size: 14 time-varying
`particle_flux>differential_directional_number_rate`
Energy Bins for Electrons 1 – 5 MeV (14 bins)

6.7.2.8 B_Electrons_Rate Electrons count rate side B (counts s^{-1})
Size: 14 time-varying
`particle_flux>differential_directional_number_rate`
Energy Bins for Electrons 1 – 5 MeV (14 bins)

6.7.2.9 B_H H counts side B (counts)
Size: 18 time-varying
`particle_flux>differential_directional_number_rate`
Energy Bins for H 1 – 15 MeV (18 bins)

6.7.2.10 B_H_Rate H count rate side B (counts s^{-1})
Size: 18 time-varying
`particle_flux>differential_directional_number_rate`
Energy Bins for H 1 – 15 MeV (18 bins)

6.7.2.11 B_He He counts side B (counts)
Size: 22 time-varying
`particle_flux>differential_directional_number_rate`
Energy Bins for He 1 – 29 MeV/nuc (22 bins)

6.7.2.12 B_He_Rate He count rate side B (counts s^{-1})
Size: 22 time-varying
`particle_flux>differential_directional_number_rate`
Energy Bins for He 1 – 29 MeV/nuc (22 bins)

6.7.2.13 HCI_Lat HCI latitude (degrees)
time-varying
`position>latitude`
At timestamp. After Fraenz and Harper, PSS, 2002.

6.7.2.14 HCI_Lon HCI longitude (degrees)
time-varying
`position>longitude`
At timestamp. After Fraenz and Harper, PSS, 2002.

6.7.2.15 HCI_R Heliocentric distance (AU)
time-varying
`position>radial`
At timestamp. After Fraenz and Harper, PSS, 2002.

6.7.2.16 HGC_Lat HGC latitude (degrees)
time-varying
`position>latitude`
At timestamp. After Fraenz and Harper, PSS, 2002.

6.7.2.17 HGC_Lon HGC longitude (degrees)
time-varying
`position>longitude`
At timestamp. After Fraenz and Harper, PSS, 2002.

6.7.2.18 HGC_R Heliocentric distance (AU)
time-varying
`position>radial`
At timestamp. After Fraenz and Harper, PSS, 2002.

6.7.2.19 LET1_A_HCI HCI flow direction LET1A
Size: 3 time-varying
`position>direction`
Unit vector, after Fraenz and Harper, PSS, 2002.

6.7.2.20 LET1_A_PA Pitch angle LET1A (degree)
time-varying
`position>angle`

6.7.2.21 LET1_A_RTN RTN flow direction LET1A
Size: 3 time-varying
`position>direction`
Unit vector, after Fraenz and Harper, PSS, 2002.

6.7.2.22 LET1_A_SA Nominal Parker Spiral angle LET1A (degree)
time-varying
`position>angle`
Angle between particle direction and nominal outward Parker Spiral, based on 400km/s solar wind and corotation breakdown at 10Rs.

6.7.2.23 LET1_B_HCI HCI flow direction LET1B
Size: 3 time-varying
`position>direction`
Unit vector, after Fraenz and Harper, PSS, 2002.

6.7.2.24 LET1_B_PA Pitch angle LET1B (degree)
time-varying
`position>angle`

6.7.2.25 LET1_B_RTN RTN flow direction LET1B
Size: 3 time-varying
`position>direction`
Unit vector, after Fraenz and Harper, PSS, 2002.

6.7.2.26 LET1_B_SA Nominal Parker Spiral angle LET1B (degree)
time-varying
`position>angle`
Angle between particle direction and nominal outward Parker Spiral, based on 400km/s solar wind and corotation breakdown at 10Rs.

6.7.3 OTHER SUPPORT

6.7.3.1 Quality_Flag Data-quality flag
Size: 10 time-varying
`flag>status`

Quality flag number 0 – 9 (10 bins)

6.8 PSP_ISOIS-EPIHI_L2-LET1-RATES300

ISOIS-EPIHI>Integrated Science Investigation of the Sun, Energetic Particle Instrument Hi
L2-LET1-rates300>Level 2 LET1 5-minute rates
EPI-Hi LET1 300 second rates cdf. Time tags indicate midpoint of integration.
Instrument paper: Integrated Science Investigation of the Sun (ISIS): Design of the Energetic Particle Investigation. McComas, D. J. et al (2016). Space Sci. Rev., doi:10.1007/s11214-014-0059-1
1 minute to 1 hour
Cite McComas et al (2016), doi:10.1007/s11214-014-0059-1

6.8.1 PRIMARY VARIABLES

6.8.2 OTHER DATA

6.8.2.1 HCI_Lat HCI latitude (degrees)
time-varying
`position>latitude`
At timestamp. After Fraenz and Harper, PSS, 2002.

6.8.2.2 HCI_Lon HCI longitude (degrees)
time-varying
`position>longitude`
At timestamp. After Fraenz and Harper, PSS, 2002.

6.8.2.3 HCI_R Heliocentric distance (AU)
time-varying
`position>radial`
At timestamp. After Fraenz and Harper, PSS, 2002.

6.8.2.4 HGC_Lat HGC latitude (degrees)
time-varying
`position>latitude`
At timestamp. After Fraenz and Harper, PSS, 2002.

6.8.2.5 HGC_Lon HGC longitude (degrees)
time-varying

`position>longitude`
At timestamp. After Fraenz and Harper, PSS, 2002.

6.8.2.6 HGC_R Heliocentric distance (AU)
time-varying
`position>radial`
At timestamp. After Fraenz and Harper, PSS, 2002.

6.8.2.7 LET1_A_HCI HCI flow direction LET1A
Size: 3 time-varying
`position>direction`
Unit vector, after Fraenz and Harper, PSS, 2002.

6.8.2.8 LET1_A_PA Pitch angle LET1A (degree)
time-varying
`position>angle`

6.8.2.9 LET1_A_R1_SECT_HCI HCI flow direction LET1AR1SECT
Size: 9×3 time-varying
`position>direction`
Unit vector, after Fraenz and Harper, PSS, 2002.
LET1_R1_SECTORS 0 – 8 (9 bins)

6.8.2.10 LET1_A_R1_SECT_PA Pitch angle LET1AR1SECT (degree)
Size: 9 time-varying
`position>angle`
LET1_R1_SECTORS 0 – 8 (9 bins)

6.8.2.11 LET1_A_R1_SECT_RTN RTN flow direction LET1AR1SECT
Size: 9×3 time-varying
`position>direction`
Unit vector, after Fraenz and Harper, PSS, 2002.
LET1_R1_SECTORS 0 – 8 (9 bins)

6.8.2.12 LET1_A_R1_SECT_SA Nominal Parker Spiral angle LET1AR1SECT (degree)
Size: 9 time-varying
`position>angle`
Angle between particle direction and nominal outward Parker Spiral, based on 400km/s solar wind and corotation breakdown at 10Rs.
LET1_R1_SECTORS 0 – 8 (9 bins)

6.8.2.13 LET1_A_R26_SECT_HCI HCI flow direction LET1AR26SECT
Size: 25 × 3 time-varying
`position>direction`
Unit vector, after Fraenz and Harper, PSS, 2002.
LET1_R26_SECTORS 0 – 24 (25 bins)

6.8.2.14 LET1_A_R26_SECT_PA Pitch angle LET1AR26SECT (degree)
Size: 25 time-varying
`position>angle`
LET1_R26_SECTORS 0 – 24 (25 bins)

6.8.2.15 LET1_A_R26_SECT_RTN RTN flow direction LET1AR26SECT
Size: 25 × 3 time-varying
`position>direction`
Unit vector, after Fraenz and Harper, PSS, 2002.
LET1_R26_SECTORS 0 – 24 (25 bins)

6.8.2.16 LET1_A_R26_SECT_SA Nominal Parker Spiral angle LET1AR26SECT (degree)
Size: 25 time-varying
`position>angle`
Angle between particle direction and nominal outward Parker Spiral, based on 400km/s solar wind and corotation breakdown at 10Rs.
LET1_R26_SECTORS 0 – 24 (25 bins)

6.8.2.17 LET1_A_RTN RTN flow direction LET1A
Size: 3 time-varying
`position>direction`
Unit vector, after Fraenz and Harper, PSS, 2002.

6.8.2.18 LET1_A_SA Nominal Parker Spiral angle LET1A (degree)
time-varying
`position>angle`
Angle between particle direction and nominal outward Parker Spiral, based on 400km/s solar wind and corotation breakdown at 10Rs.

6.8.2.19 LET1_B_HCI HCI flow direction LET1B
Size: 3 time-varying
`position>direction`
Unit vector, after Fraenz and Harper, PSS, 2002.

6.8.2.20 LET1_B_PA Pitch angle LET1B (degree)
time-varying
`position>angle`

6.8.2.21 LET1_B_R1_SECT_HCI HCI flow direction LET1BR1SECT
Size: 9×3 time-varying
`position>direction`
Unit vector, after Fraenz and Harper, PSS, 2002.
LET1_R1_SECTORS 0 – 8 (9 bins)

6.8.2.22 LET1_B_R1_SECT_PA Pitch angle LET1BR1SECT (degree)
Size: 9 time-varying
`position>angle`
LET1_R1_SECTORS 0 – 8 (9 bins)

6.8.2.23 LET1_B_R1_SECT_RTN RTN flow direction LET1BR1SECT
Size: 9×3 time-varying
`position>direction`
Unit vector, after Fraenz and Harper, PSS, 2002.
LET1_R1_SECTORS 0 – 8 (9 bins)

6.8.2.24 LET1_B_R1_SECT_SA Nominal Parker Spiral angle LET1BR1SECT (degree)
Size: 9 time-varying
`position>angle`
Angle between particle direction and nominal outward Parker Spiral, based on 400km/s solar wind

and corotation breakdown at 10Rs.
LET1_R1_SECTORS 0 – 8 (9 bins)

6.8.2.25 LET1_B_R26_SECT_HCI HCI flow direction LET1BR26SECT
Size: 25 × 3 time-varying
`position>direction`
Unit vector, after Fraenz and Harper, PSS, 2002.
LET1_R26_SECTORS 0 – 24 (25 bins)

6.8.2.26 LET1_B_R26_SECT_PA Pitch angle LET1BR26SECT (degree)
Size: 25 time-varying
`position>angle`
LET1_R26_SECTORS 0 – 24 (25 bins)

6.8.2.27 LET1_B_R26_SECT_RTN RTN flow direction LET1BR26SECT
Size: 25 × 3 time-varying
`position>direction`
Unit vector, after Fraenz and Harper, PSS, 2002.
LET1_R26_SECTORS 0 – 24 (25 bins)

6.8.2.28 LET1_B_R26_SECT_SA Nominal Parker Spiral angle LET1BR26SECT (degree)
Size: 25 time-varying
`position>angle`
Angle between particle direction and nominal outward Parker Spiral, based on 400km/s solar wind and corotation breakdown at 10Rs.
LET1_R26_SECTORS 0 – 24 (25 bins)

6.8.2.29 LET1_B_RTN RTN flow direction LET1B
Size: 3 time-varying
`position>direction`
Unit vector, after Fraenz and Harper, PSS, 2002.

6.8.2.30 LET1_B_SA Nominal Parker Spiral angle LET1B (degree)
time-varying
`position>angle`
Angle between particle direction and nominal outward Parker Spiral, based on 400km/s solar wind

and corotation breakdown at 10Rs.

6.8.2.31 R1A_CNO_SECT_Rate CNO sectored count rate R1A (counts s^{-1})
Size: 1×9 time-varying
`particle_flux>differential_directional_number_rate`
Energy Bins for R1 CNO SECT 3 – 3 MeV/nuc (1 bins)
LET1_R1_SECTORS 0 – 8 (9 bins)

6.8.2.32 R1A_FeGroup_SECT_Rate FeGroup sectored count rate R1A (counts s^{-1})
Size: 1×9 time-varying
`particle_flux>differential_directional_number_rate`
Energy Bins for R1 FeGroup SECT 3 – 3 MeV/nuc (1 bins)
LET1_R1_SECTORS 0 – 8 (9 bins)

6.8.2.33 R1A_NetoSi_SECT_Rate NetoSi sectored count rate R1A (counts s^{-1})
Size: 1×9 time-varying
`particle_flux>differential_directional_number_rate`
Energy Bins for R1 NetoSi SECT 3 – 3 MeV/nuc (1 bins)
LET1_R1_SECTORS 0 – 8 (9 bins)

6.8.2.34 R1B_CNO_SECT_Rate CNO sectored count rate R1B (counts s^{-1})
Size: 1×9 time-varying
`particle_flux>differential_directional_number_rate`
Energy Bins for R1 CNO SECT 3 – 3 MeV/nuc (1 bins)
LET1_R1_SECTORS 0 – 8 (9 bins)

6.8.2.35 R1B_FeGroup_SECT_Rate FeGroup sectored count rate R1B (counts s^{-1})
Size: 1×9 time-varying
`particle_flux>differential_directional_number_rate`
Energy Bins for R1 FeGroup SECT 3 – 3 MeV/nuc (1 bins)
LET1_R1_SECTORS 0 – 8 (9 bins)

6.8.2.36 R1B_NetoSi_SECT_Rate NetoSi sectored count rate R1B (counts s^{-1})
Size: 1×9 time-varying
`particle_flux>differential_directional_number_rate`
Energy Bins for R1 NetoSi SECT 3 – 3 MeV/nuc (1 bins)

LET1_R1_SECTORS 0 – 8 (9 bins)

6.8.2.37 R26A_CNO_SECT_Rate CNO sectored count rate R26A (counts s^{-1})
Size: 3 × 25 time-varying
`particle_flux>differential_directional_number_rate`
Energy Bins for R26 CNO SECT 6 – 23 MeV/nuc (3 bins)
LET1_R26_SECTORS 0 – 24 (25 bins)

6.8.2.38 R26A_FeGroup_SECT_Rate FeGroup sectored count rate R26A (counts s^{-1})
Size: 3 × 25 time-varying
`particle_flux>differential_directional_number_rate`
Energy Bins for R26 FeGroup SECT 6 – 23 MeV/nuc (3 bins)
LET1_R26_SECTORS 0 – 24 (25 bins)

6.8.2.39 R26A_NetoSi_SECT_Rate NetoSi sectored count rate R26A (counts s^{-1})
Size: 3 × 25 time-varying
`particle_flux>differential_directional_number_rate`
Energy Bins for R26 NetoSi SECT 6 – 23 MeV/nuc (3 bins)
LET1_R26_SECTORS 0 – 24 (25 bins)

6.8.2.40 R26B_CNO_SECT_Rate CNO sectored count rate R26B (counts s^{-1})
Size: 3 × 25 time-varying
`particle_flux>differential_directional_number_rate`
Energy Bins for R26 CNO SECT 6 – 23 MeV/nuc (3 bins)
LET1_R26_SECTORS 0 – 24 (25 bins)

6.8.2.41 R26B_FeGroup_SECT_Rate FeGroup sectored count rate R26B (counts s^{-1})
Size: 3 × 25 time-varying
`particle_flux>differential_directional_number_rate`
Energy Bins for R26 FeGroup SECT 6 – 23 MeV/nuc (3 bins)
LET1_R26_SECTORS 0 – 24 (25 bins)

6.8.2.42 R26B_NetoSi_SECT_Rate NetoSi sectored count rate R26B (counts s^{-1})
Size: 3 × 25 time-varying
`particle_flux>differential_directional_number_rate`
Energy Bins for R26 NetoSi SECT 6 – 23 MeV/nuc (3 bins)

LET1_R26_SECTORS 0 – 24 (25 bins)

6.8.3 OTHER SUPPORT

6.8.3.1 Quality_Flag Data-quality flag
Size: 10 time-varying
`flag>status`
Quality flag number 0 – 9 (10 bins)

6.9 PSP_ISOIS-EPIHI_L2-LET1-RATES3600

ISOIS-EPIHI>Integrated Science Investigation of the Sun, Energetic Particle Instrument Hi
L2-LET1-rates3600>Level 2 LET1 hourly rates
EPI-Hi 3600 seconds rates cdf. Time tags indicate midpoint of integration.
Instrument paper: Integrated Science Investigation of the Sun (ISIS): Design of the Energetic Particle Investigation. McComas, D. J. et al (2016). Space Sci. Rev., doi:10.1007/s11214-014-0059-1
1 minute to 1 hour
Cite McComas et al (2016), doi:10.1007/s11214-014-0059-1

6.9.1 PRIMARY VARIABLES

6.9.1.1 A_H_Flux H flux side A ($cm^{-2}sr^{-1}sec^{-1}MeV^{-1}$)
Size: 25 time-varying
`particle_flux>differential_directional_number`
Energy Bins for H 1 – 41 MeV (25 bins)

6.9.1.2 A_He_Flux He flux side A ($cm^{-2}sr^{-1}sec^{-1}(MeV/nuc)^{-1}$)
Size: 26 time-varying
`particle_flux>differential_directional_number`
Energy Bins for He 1 – 49 MeV/nuc (26 bins)

6.9.1.3 B_H_Flux H flux side B ($cm^{-2}sr^{-1}sec^{-1}MeV^{-1}$)
Size: 25 time-varying
`particle_flux>differential_directional_number`
Energy Bins for H 1 – 41 MeV (25 bins)

6.9.1.4 B_He_Flux He flux side B ($cm^{-2}sr^{-1}sec^{-1}(MeV/nuc)^{-1}$)
Size: 26 time-varying

particle_flux>differential_directional_number
Energy Bins for He 1 – 49 MeV/nuc (26 bins)

6.9.1.5 R1A_H_SECT_Flux

H sectored flux R1A ($cm^{-2}sr^{-1}sec^{-1}MeV^{-1}$)
Size: 1 × 9 time-varying
particle_flux>differential_directional_number
Energy Bins for R1 H SECT 1 – 1 MeV (1 bins)
LET1_R1_SECTORS 0 – 8 (9 bins)

6.9.1.6 R1A_He_SECT_Flux

He sectored flux R1A ($cm^{-2}sr^{-1}sec^{-1}(MeV/nuc)^{-1}$)
Size: 1 × 9 time-varying
particle_flux>differential_directional_number
Energy Bins for R1 He SECT 1 – 1 MeV/nuc (1 bins)
LET1_R1_SECTORS 0 – 8 (9 bins)

6.9.1.7 R1B_H_SECT_Flux

H sectored flux R1B ($cm^{-2}sr^{-1}sec^{-1}MeV^{-1}$)
Size: 1 × 9 time-varying
particle_flux>differential_directional_number
Energy Bins for R1 H SECT 1 – 1 MeV (1 bins)
LET1_R1_SECTORS 0 – 8 (9 bins)

6.9.1.8 R1B_He_SECT_Flux

He sectored flux R1B ($cm^{-2}sr^{-1}sec^{-1}(MeV/nuc)^{-1}$)
Size: 1 × 9 time-varying
particle_flux>differential_directional_number
Energy Bins for R1 He SECT 1 – 1 MeV/nuc (1 bins)
LET1_R1_SECTORS 0 – 8 (9 bins)

6.9.1.9 R26A_H_SECT_Flux

H sectored flux R26A ($cm^{-2}sr^{-1}sec^{-1}MeV^{-1}$)
Size: 3 × 25 time-varying
particle_flux>differential_directional_number
Energy Bins for R26 H SECT 3 – 11 MeV (3 bins)
LET1_R26_SECTORS 0 – 24 (25 bins)

6.9.1.10 R26A_He_SECT_Flux

He sectored flux R26A ($cm^{-2}sr^{-1}sec^{-1}(MeV/nuc)^{-1}$)
Size: 3 × 25 time-varying
particle_flux>differential_directional_number

Energy Bins for R26 He SECT 3 – 11 MeV/nuc (3 bins)
LET1_R26_SECTORS 0 – 24 (25 bins)

6.9.1.11 R26B_H_SECT_Flux H sectored flux R26B ($cm^{-2}sr^{-1}sec^{-1}MeV^{-1}$)
Size: 3 × 25 time-varying
`particle_flux>differential_directional_number`
Energy Bins for R26 H SECT 3 – 11 MeV (3 bins)
LET1_R26_SECTORS 0 – 24 (25 bins)

6.9.1.12 R26B_He_SECT_Flux He sectored flux R26B ($cm^{-2}sr^{-1}sec^{-1}(MeV/nuc)^{-1}$)
Size: 3 × 25 time-varying
`particle_flux>differential_directional_number`
Energy Bins for R26 He SECT 3 – 11 MeV/nuc (3 bins)
LET1_R26_SECTORS 0 – 24 (25 bins)

6.9.2 OTHER DATA

6.9.2.1 A_Al Al counts side A (counts)
Size: 28 time-varying
`particle_flux>differential_directional_number_rate`
Energy Bins for Al 1 – 117 MeV/nuc (28 bins)

6.9.2.2 A_Al_Rate Al count rate side A ($counts\,s^{-1}$)
Size: 28 time-varying
`particle_flux>differential_directional_number_rate`
Energy Bins for Al 1 – 117 MeV/nuc (28 bins)

6.9.2.3 A_Ar Ar counts side A (counts)
Size: 29 time-varying
`particle_flux>differential_directional_number_rate`
Energy Bins for Ar 1 – 140 MeV/nuc (29 bins)

6.9.2.4 A_Ar_Rate Ar count rate side A ($counts\,s^{-1}$)
Size: 29 time-varying
`particle_flux>differential_directional_number_rate`
Energy Bins for Ar 1 – 140 MeV/nuc (29 bins)

6.9.2.5 A_C C counts side A (counts)
Size: 27 time-varying
`particle_flux>differential_directional_number_rate`
Energy Bins for C 1 – 99 MeV/nuc (27 bins)

6.9.2.6 A_C_Rate C count rate side A (counts s^{-1})
Size: 27 time-varying
`particle_flux>differential_directional_number_rate`
Energy Bins for C 1 – 99 MeV/nuc (27 bins)

6.9.2.7 A_Ca Ca counts side A (counts)
Size: 30 time-varying
`particle_flux>differential_directional_number_rate`
Energy Bins for Ca 1 – 140 MeV/nuc (30 bins)

6.9.2.8 A_Ca_Rate Ca count rate side A (counts s^{-1})
Size: 30 time-varying
`particle_flux>differential_directional_number_rate`
Energy Bins for Ca 1 – 140 MeV/nuc (30 bins)

6.9.2.9 A_Cr Cr counts side A (counts)
Size: 31 time-varying
`particle_flux>differential_directional_number_rate`
Energy Bins for Cr 1 – 140 MeV/nuc (31 bins)

6.9.2.10 A_Cr_Rate Cr count rate side A (counts s^{-1})
Size: 31 time-varying
`particle_flux>differential_directional_number_rate`
Energy Bins for Cr 1 – 140 MeV/nuc (31 bins)

6.9.2.11 A_Electrons Electrons counts side A (counts)
Size: 16 time-varying
`particle_flux>differential_directional_number_rate`
Energy Bins for Electrons 0 – 6 MeV (16 bins)

6.9.2.12 A_Electrons_Rate Electrons count rate side A (counts s^{-1})
Size: 16 time-varying
`particle_flux>differential_directional_number_rate`
Energy Bins for Electrons 0 – 6 MeV (16 bins)

6.9.2.13 A_Fe Fe counts side A (counts)
Size: 32 time-varying
`particle_flux>differential_directional_number_rate`
Energy Bins for Fe 1 – 166 MeV/nuc (32 bins)

6.9.2.14 A_Fe_Rate Fe count rate side A (counts s^{-1})
Size: 32 time-varying
`particle_flux>differential_directional_number_rate`
Energy Bins for Fe 1 – 166 MeV/nuc (32 bins)

6.9.2.15 A_H H counts side A (counts)
Size: 25 time-varying
`particle_flux>differential_directional_number_rate`
Energy Bins for H 1 – 41 MeV (25 bins)

6.9.2.16 A_H_Rate H count rate side A (counts s^{-1})
Size: 25 time-varying
`particle_flux>differential_directional_number_rate`
Energy Bins for H 1 – 41 MeV (25 bins)

6.9.2.17 A_He He counts side A (counts)
Size: 26 time-varying
`particle_flux>differential_directional_number_rate`
Energy Bins for He 1 – 49 MeV/nuc (26 bins)

6.9.2.18 A_He_Rate He count rate side A (counts s^{-1})
Size: 26 time-varying
`particle_flux>differential_directional_number_rate`
Energy Bins for He 1 – 49 MeV/nuc (26 bins)

6.9.2.19 A_Mg Mg counts side A (counts)
Size: 28 time-varying
`particle_flux>differential_directional_number_rate`
Energy Bins for Mg 1 – 117 MeV/nuc (28 bins)

6.9.2.20 A_Mg_Rate Mg count rate side A (counts s^{-1})
Size: 28 time-varying
`particle_flux>differential_directional_number_rate`
Energy Bins for Mg 1 – 117 MeV/nuc (28 bins)

6.9.2.21 A_N N counts side A (counts)
Size: 27 time-varying
`particle_flux>differential_directional_number_rate`
Energy Bins for N 1 – 99 MeV/nuc (27 bins)

6.9.2.22 A_N_Rate N count rate side A (counts s^{-1})
Size: 27 time-varying
`particle_flux>differential_directional_number_rate`
Energy Bins for N 1 – 99 MeV/nuc (27 bins)

6.9.2.23 A_Na Na counts side A (counts)
Size: 28 time-varying
`particle_flux>differential_directional_number_rate`
Energy Bins for Na 1 – 117 MeV/nuc (28 bins)

6.9.2.24 A_Na_Rate Na count rate side A (counts s^{-1})
Size: 28 time-varying
`particle_flux>differential_directional_number_rate`
Energy Bins for Na 1 – 117 MeV/nuc (28 bins)

6.9.2.25 A_Ne Ne counts side A (counts)
Size: 28 time-varying
`particle_flux>differential_directional_number_rate`
Energy Bins for Ne 1 – 117 MeV/nuc (28 bins)

6.9.2.26 A_Ne_Rate Ne count rate side A (counts s^{-1})
Size: 28 time-varying
`particle_flux>differential_directional_number_rate`
Energy Bins for Ne 1 – 117 MeV/nuc (28 bins)

6.9.2.27 A_Ni Ni counts side A (counts)
Size: 33 time-varying
`particle_flux>differential_directional_number_rate`
Energy Bins for Ni 1 – 197 MeV/nuc (33 bins)

6.9.2.28 A_Ni_Rate Ni count rate side A (counts s^{-1})
Size: 33 time-varying
`particle_flux>differential_directional_number_rate`
Energy Bins for Ni 1 – 197 MeV/nuc (33 bins)

6.9.2.29 A_O O counts side A (counts)
Size: 28 time-varying
`particle_flux>differential_directional_number_rate`
Energy Bins for O 1 – 117 MeV/nuc (28 bins)

6.9.2.30 A_O_Rate O count rate side A (counts s^{-1})
Size: 28 time-varying
`particle_flux>differential_directional_number_rate`
Energy Bins for O 1 – 117 MeV/nuc (28 bins)

6.9.2.31 A_S S counts side A (counts)
Size: 29 time-varying
`particle_flux>differential_directional_number_rate`
Energy Bins for S 1 – 140 MeV/nuc (29 bins)

6.9.2.32 A_S_Rate S count rate side A (counts s^{-1})
Size: 29 time-varying
`particle_flux>differential_directional_number_rate`
Energy Bins for S 1 – 140 MeV/nuc (29 bins)

6.9.2.33 A_Si Si counts side A (counts)
Size: 29 time-varying
`particle_flux>differential_directional_number_rate`
Energy Bins for Si 1 – 140 MeV/nuc (29 bins)

6.9.2.34 A_Si_Rate Si count rate side A (counts s^{-1})
Size: 29 time-varying
`particle_flux>differential_directional_number_rate`
Energy Bins for Si 1 – 140 MeV/nuc (29 bins)

6.9.2.35 B_Al Al counts side B (counts)
Size: 28 time-varying
`particle_flux>differential_directional_number_rate`
Energy Bins for Al 1 – 117 MeV/nuc (28 bins)

6.9.2.36 B_Al_Rate Al count rate side B (counts s^{-1})
Size: 28 time-varying
`particle_flux>differential_directional_number_rate`
Energy Bins for Al 1 – 117 MeV/nuc (28 bins)

6.9.2.37 B_Ar Ar counts side B (counts)
Size: 29 time-varying
`particle_flux>differential_directional_number_rate`
Energy Bins for Ar 1 – 140 MeV/nuc (29 bins)

6.9.2.38 B_Ar_Rate Ar count rate side B (counts s^{-1})
Size: 29 time-varying
`particle_flux>differential_directional_number_rate`
Energy Bins for Ar 1 – 140 MeV/nuc (29 bins)

6.9.2.39 B_C C counts side B (counts)
Size: 27 time-varying
`particle_flux>differential_directional_number_rate`
Energy Bins for C 1 – 99 MeV/nuc (27 bins)

6.9.2.40 B_C_Rate C count rate side B (counts s^{-1})
Size: 27 time-varying
`particle_flux>differential_directional_number_rate`
Energy Bins for C 1 – 99 MeV/nuc (27 bins)

6.9.2.41 B_Ca Ca counts side B (counts)
Size: 30 time-varying
`particle_flux>differential_directional_number_rate`
Energy Bins for Ca 1 – 140 MeV/nuc (30 bins)

6.9.2.42 B_Ca_Rate Ca count rate side B (counts s^{-1})
Size: 30 time-varying
`particle_flux>differential_directional_number_rate`
Energy Bins for Ca 1 – 140 MeV/nuc (30 bins)

6.9.2.43 B_Cr Cr counts side B (counts)
Size: 31 time-varying
`particle_flux>differential_directional_number_rate`
Energy Bins for Cr 1 – 140 MeV/nuc (31 bins)

6.9.2.44 B_Cr_Rate Cr count rate side B (counts s^{-1})
Size: 31 time-varying
`particle_flux>differential_directional_number_rate`
Energy Bins for Cr 1 – 140 MeV/nuc (31 bins)

6.9.2.45 B_Electrons Electrons counts side B (counts)
Size: 16 time-varying
`particle_flux>differential_directional_number_rate`
Energy Bins for Electrons 0 – 6 MeV (16 bins)

6.9.2.46 B_Electrons_Rate Electrons count rate side B (counts s^{-1})
Size: 16 time-varying
`particle_flux>differential_directional_number_rate`
Energy Bins for Electrons 0 – 6 MeV (16 bins)

6.9.2.47 B_Fe Fe counts side B (counts)
Size: 32 time-varying
`particle_flux>differential_directional_number_rate`
Energy Bins for Fe 1 – 166 MeV/nuc (32 bins)

6.9.2.48 B_Fe_Rate Fe count rate side B (counts s^{-1})
Size: 32 time-varying
`particle_flux>differential_directional_number_rate`
Energy Bins for Fe 1 – 166 MeV/nuc (32 bins)

6.9.2.49 B_H H counts side B (counts)
Size: 25 time-varying
`particle_flux>differential_directional_number_rate`
Energy Bins for H 1 – 41 MeV (25 bins)

6.9.2.50 B_H_Rate H count rate side B (counts s^{-1})
Size: 25 time-varying
`particle_flux>differential_directional_number_rate`
Energy Bins for H 1 – 41 MeV (25 bins)

6.9.2.51 B_He He counts side B (counts)
Size: 26 time-varying
`particle_flux>differential_directional_number_rate`
Energy Bins for He 1 – 49 MeV/nuc (26 bins)

6.9.2.52 B_He_Rate He count rate side B (counts s^{-1})
Size: 26 time-varying
`particle_flux>differential_directional_number_rate`
Energy Bins for He 1 – 49 MeV/nuc (26 bins)

6.9.2.53 B_Mg Mg counts side B (counts)
Size: 28 time-varying
`particle_flux>differential_directional_number_rate`
Energy Bins for Mg 1 – 117 MeV/nuc (28 bins)

6.9.2.54 B_Mg_Rate Mg count rate side B (counts s^{-1})
Size: 28 time-varying
`particle_flux>differential_directional_number_rate`
Energy Bins for Mg 1 – 117 MeV/nuc (28 bins)

6.9.2.55 B_N N counts side B (counts)
Size: 27 time-varying
`particle_flux>differential_directional_number_rate`
Energy Bins for N 1 – 99 MeV/nuc (27 bins)

6.9.2.56 B_N_Rate N count rate side B (counts s^{-1})
Size: 27 time-varying
`particle_flux>differential_directional_number_rate`
Energy Bins for N 1 – 99 MeV/nuc (27 bins)

6.9.2.57 B_Na Na counts side B (counts)
Size: 28 time-varying
`particle_flux>differential_directional_number_rate`
Energy Bins for Na 1 – 117 MeV/nuc (28 bins)

6.9.2.58 B_Na_Rate Na count rate side B (counts s^{-1})
Size: 28 time-varying
`particle_flux>differential_directional_number_rate`
Energy Bins for Na 1 – 117 MeV/nuc (28 bins)

6.9.2.59 B_Ne Ne counts side B (counts)
Size: 28 time-varying
`particle_flux>differential_directional_number_rate`
Energy Bins for Ne 1 – 117 MeV/nuc (28 bins)

6.9.2.60 B_Ne_Rate Ne count rate side B (counts s^{-1})
Size: 28 time-varying
`particle_flux>differential_directional_number_rate`
Energy Bins for Ne 1 – 117 MeV/nuc (28 bins)

6.9.2.61 B_Ni Ni counts side B (counts)
Size: 33 time-varying
`particle_flux>differential_directional_number_rate`
Energy Bins for Ni 1 – 197 MeV/nuc (33 bins)

6.9.2.62 B_Ni_Rate Ni count rate side B (counts s^{-1})
Size: 33 time-varying
`particle_flux>differential_directional_number_rate`
Energy Bins for Ni 1 – 197 MeV/nuc (33 bins)

6.9.2.63 B_O O counts side B (counts)
Size: 28 time-varying
`particle_flux>differential_directional_number_rate`
Energy Bins for O 1 – 117 MeV/nuc (28 bins)

6.9.2.64 B_O_Rate O count rate side B (counts s^{-1})
Size: 28 time-varying
`particle_flux>differential_directional_number_rate`
Energy Bins for O 1 – 117 MeV/nuc (28 bins)

6.9.2.65 B_S S counts side B (counts)
Size: 29 time-varying
`particle_flux>differential_directional_number_rate`
Energy Bins for S 1 – 140 MeV/nuc (29 bins)

6.9.2.66 B_S_Rate S count rate side B (counts s^{-1})
Size: 29 time-varying
`particle_flux>differential_directional_number_rate`
Energy Bins for S 1 – 140 MeV/nuc (29 bins)

6.9.2.67 B_Si Si counts side B (counts)
Size: 29 time-varying
`particle_flux>differential_directional_number_rate`
Energy Bins for Si 1 – 140 MeV/nuc (29 bins)

6.9.2.68 B_Si_Rate Si count rate side B (counts s^{-1})
Size: 29 time-varying
`particle_flux>differential_directional_number_rate`
Energy Bins for Si 1 – 140 MeV/nuc (29 bins)

6.9.2.69 HCI_Lat HCI latitude (degrees)
time-varying
`position>latitude`
At timestamp. After Fraenz and Harper, PSS, 2002.

6.9.2.70 HCI_Lon HCI longitude (degrees)
time-varying
`position>longitude`
At timestamp. After Fraenz and Harper, PSS, 2002.

6.9.2.71 HCI_R Heliocentric distance (AU)
time-varying
`position>radial`
At timestamp. After Fraenz and Harper, PSS, 2002.

6.9.2.72 HGC_Lat HGC latitude (degrees)
time-varying
`position>latitude`
At timestamp. After Fraenz and Harper, PSS, 2002.

6.9.2.73 HGC_Lon HGC longitude (degrees)
time-varying
`position>longitude`
At timestamp. After Fraenz and Harper, PSS, 2002.

6.9.2.74 HGC_R Heliocentric distance (AU)
time-varying
`position>radial`
At timestamp. After Fraenz and Harper, PSS, 2002.

6.9.2.75 LET1_A_HCI HCI flow direction LET1A
Size: 3 time-varying
`position>direction`
Unit vector, after Fraenz and Harper, PSS, 2002.

6.9.2.76 LET1_A_PA Pitch angle LET1A (degree)
time-varying
`position>angle`

6.9.2.77 LET1_A_R1_SECT_HCI HCI flow direction LET1AR1SECT
Size: 9×3 time-varying
`position>direction`
Unit vector, after Fraenz and Harper, PSS, 2002.
LET1_R1_SECTORS 0 – 8 (9 bins)

6.9.2.78 LET1_A_R1_SECT_PA Pitch angle LET1AR1SECT (degree)
Size: 9 time-varying
`position>angle`
LET1_R1_SECTORS 0 – 8 (9 bins)

6.9.2.79 LET1_A_R1_SECT_RTN RTN flow direction LET1AR1SECT
Size: 9×3 time-varying
`position>direction`
Unit vector, after Fraenz and Harper, PSS, 2002.
LET1_R1_SECTORS 0 – 8 (9 bins)

6.9.2.80 LET1_A_R1_SECT_SA Nominal Parker Spiral angle LET1AR1SECT (degree)
Size: 9 time-varying
`position>angle`
Angle between particle direction and nominal outward Parker Spiral, based on 400km/s solar wind and corotation breakdown at 10Rs.
LET1_R1_SECTORS 0 – 8 (9 bins)

6.9.2.81 LET1_A_R26_SECT_HCI HCI flow direction LET1AR26SECT
Size: 25×3 time-varying
`position>direction`

Unit vector, after Fraenz and Harper, PSS, 2002.
LET1_R26_SECTORS 0 – 24 (25 bins)

6.9.2.82 LET1_A_R26_SECT_PA Pitch angle LET1AR26SECT (degree)
Size: 25 time-varying
`position>angle`
LET1_R26_SECTORS 0 – 24 (25 bins)

6.9.2.83 LET1_A_R26_SECT_RTN RTN flow direction LET1AR26SECT
Size: 25 × 3 time-varying
`position>direction`
Unit vector, after Fraenz and Harper, PSS, 2002.
LET1_R26_SECTORS 0 – 24 (25 bins)

6.9.2.84 LET1_A_R26_SECT_SA Nominal Parker Spiral angle LET1AR26SECT (degree)
Size: 25 time-varying
`position>angle`
Angle between particle direction and nominal outward Parker Spiral, based on 400km/s solar wind and corotation breakdown at 10Rs.
LET1_R26_SECTORS 0 – 24 (25 bins)

6.9.2.85 LET1_A_RTN RTN flow direction LET1A
Size: 3 time-varying
`position>direction`
Unit vector, after Fraenz and Harper, PSS, 2002.

6.9.2.86 LET1_A_SA Nominal Parker Spiral angle LET1A (degree)
time-varying
`position>angle`
Angle between particle direction and nominal outward Parker Spiral, based on 400km/s solar wind and corotation breakdown at 10Rs.

6.9.2.87 LET1_B_HCI HCI flow direction LET1B
Size: 3 time-varying
`position>direction`

Unit vector, after Fraenz and Harper, PSS, 2002.

6.9.2.88 LET1_B_PA Pitch angle LET1B (degree)
time-varying
`position>angle`

6.9.2.89 LET1_B_R1_SECT_HCI HCI flow direction LET1BR1SECT
Size: 9 × 3 time-varying
`position>direction`
Unit vector, after Fraenz and Harper, PSS, 2002.
LET1_R1_SECTORS 0 – 8 (9 bins)

6.9.2.90 LET1_B_R1_SECT_PA Pitch angle LET1BR1SECT (degree)
Size: 9 time-varying
`position>angle`
LET1_R1_SECTORS 0 – 8 (9 bins)

6.9.2.91 LET1_B_R1_SECT_RTN RTN flow direction LET1BR1SECT
Size: 9 × 3 time-varying
`position>direction`
Unit vector, after Fraenz and Harper, PSS, 2002.
LET1_R1_SECTORS 0 – 8 (9 bins)

6.9.2.92 LET1_B_R1_SECT_SA Nominal Parker Spiral angle LET1BR1SECT (degree)
Size: 9 time-varying
`position>angle`
Angle between particle direction and nominal outward Parker Spiral, based on 400km/s solar wind and corotation breakdown at 10Rs.
LET1_R1_SECTORS 0 – 8 (9 bins)

6.9.2.93 LET1_B_R26_SECT_HCI HCI flow direction LET1BR26SECT
Size: 25 × 3 time-varying
`position>direction`
Unit vector, after Fraenz and Harper, PSS, 2002.
LET1_R26_SECTORS 0 – 24 (25 bins)

6.9.2.94 LET1_B_R26_SECT_PA Pitch angle LET1BR26SECT (degree)
Size: 25 time-varying
`position>angle`
LET1_R26_SECTORS 0 – 24 (25 bins)

6.9.2.95 LET1_B_R26_SECT_RTN RTN flow direction LET1BR26SECT
Size: 25 × 3 time-varying
`position>direction`
Unit vector, after Fraenz and Harper, PSS, 2002.
LET1_R26_SECTORS 0 – 24 (25 bins)

6.9.2.96 LET1_B_R26_SECT_SA Nominal Parker Spiral angle LET1BR26SECT (degree)
Size: 25 time-varying
`position>angle`
Angle between particle direction and nominal outward Parker Spiral, based on 400km/s solar wind and corotation breakdown at 10Rs.
LET1_R26_SECTORS 0 – 24 (25 bins)

6.9.2.97 LET1_B_RTN RTN flow direction LET1B
Size: 3 time-varying
`position>direction`
Unit vector, after Fraenz and Harper, PSS, 2002.

6.9.2.98 LET1_B_SA Nominal Parker Spiral angle LET1B (degree)
time-varying
`position>angle`
Angle between particle direction and nominal outward Parker Spiral, based on 400km/s solar wind and corotation breakdown at 10Rs.

6.9.2.99 R1A_CNO_SECT_Rate CNO sectored count rate R1A (counts s^{-1})
Size: 1 × 9 time-varying
`particle_flux>differential_directional_number_rate`
Energy Bins for R1 CNO SECT 3 – 3 MeV/nuc (1 bins)
LET1_R1_SECTORS 0 – 8 (9 bins)

6.9.2.100 R1A_FeGroup_SECT_Rate FeGroup sectored count rate R1A (counts s^{-1})
Size: 1 × 9 time-varying
`particle_flux>differential_directional_number_rate`
Energy Bins for R1 FeGroup SECT 3 – 3 MeV/nuc (1 bins)
LET1_R1_SECTORS 0 – 8 (9 bins)

6.9.2.101 R1A_H_SECT_Rate H sectored count rate R1A (counts s^{-1})
Size: 1 × 9 time-varying
`particle_flux>differential_directional_number_rate`
Energy Bins for R1 H SECT 1 – 1 MeV (1 bins)
LET1_R1_SECTORS 0 – 8 (9 bins)

6.9.2.102 R1A_He_BIN R1A He Rates (counts)
Size: 5 × 16 time-varying
`particle_flux>differential_directional_number_rate`
Energy Bins for R1 He BIN 1 – 3 MeV/nuc (5 bins)
R1A_He_BIN_MASS_BIN 0 – 15 segment (16 bins)

6.9.2.103 R1A_He_SECT_Rate He sectored count rate R1A (counts s^{-1})
Size: 1 × 9 time-varying
`particle_flux>differential_directional_number_rate`
Energy Bins for R1 He SECT 1 – 1 MeV/nuc (1 bins)
LET1_R1_SECTORS 0 – 8 (9 bins)

6.9.2.104 R1A_Ne_BIN R1A Ne Rates (counts)
Size: 5 × 8 time-varying
`particle_flux>differential_directional_number_rate`
Energy Bins for R1 Ne BIN 1 – 6 MeV/nuc (5 bins)
R1A_Ne_BIN_MASS_BIN 0 – 7 segment (8 bins)

6.9.2.105 R1A_NetoSi_SECT_Rate NetoSi sectored count rate R1A (counts s^{-1})
Size: 1 × 9 time-varying
`particle_flux>differential_directional_number_rate`
Energy Bins for R1 NetoSi SECT 3 – 3 MeV/nuc (1 bins)
LET1_R1_SECTORS 0 – 8 (9 bins)

6.9.2.106 R1B_CNO_SECT_Rate CNO sectored count rate R1B (counts s^{-1})
Size: 1×9 time-varying
`particle_flux>differential_directional_number_rate`
Energy Bins for R1 CNO SECT 3 – 3 MeV/nuc (1 bins)
LET1_R1_SECTORS 0 – 8 (9 bins)

6.9.2.107 R1B_FeGroup_SECT_Rate FeGroup sectored count rate R1B (counts s^{-1})
Size: 1×9 time-varying
`particle_flux>differential_directional_number_rate`
Energy Bins for R1 FeGroup SECT 3 – 3 MeV/nuc (1 bins)
LET1_R1_SECTORS 0 – 8 (9 bins)

6.9.2.108 R1B_H_SECT_Rate H sectored count rate R1B (counts s^{-1})
Size: 1×9 time-varying
`particle_flux>differential_directional_number_rate`
Energy Bins for R1 H SECT 1 – 1 MeV (1 bins)
LET1_R1_SECTORS 0 – 8 (9 bins)

6.9.2.109 R1B_He_BIN R1B He Rates (counts)
Size: 5×16 time-varying
`particle_flux>differential_directional_number_rate`
Energy Bins for R1 He BIN 1 – 3 MeV/nuc (5 bins)
R1B_He_BIN_MASS_BIN 0 – 15 segment (16 bins)

6.9.2.110 R1B_He_SECT_Rate He sectored count rate R1B (counts s^{-1})
Size: 1×9 time-varying
`particle_flux>differential_directional_number_rate`
Energy Bins for R1 He SECT 1 – 1 MeV/nuc (1 bins)
LET1_R1_SECTORS 0 – 8 (9 bins)

6.9.2.111 R1B_Ne_BIN R1B Ne Rates (counts)
Size: 5×8 time-varying
`particle_flux>differential_directional_number_rate`
Energy Bins for R1 Ne BIN 1 – 6 MeV/nuc (5 bins)
R1B_Ne_BIN_MASS_BIN 0 – 7 segment (8 bins)

6.9.2.112 R1B_NetoSi_SECT_Rate NetoSi sectored count rate R1B (counts s^{-1})
Size: 1×9 time-varying
`particle_flux>differential_directional_number_rate`
Energy Bins for R1 NetoSi SECT 3 – 3 MeV/nuc (1 bins)
LET1_R1_SECTORS 0 – 8 (9 bins)

6.9.2.113 R26A_CNO_SECT_Rate CNO sectored count rate R26A (counts s^{-1})
Size: 3×25 time-varying
`particle_flux>differential_directional_number_rate`
Energy Bins for R26 CNO SECT 6 – 23 MeV/nuc (3 bins)
LET1_R26_SECTORS 0 – 24 (25 bins)

6.9.2.114 R26A_FeGroup_SECT_Rate FeGroup sectored count rate R26A (counts s^{-1})
Size: 3×25 time-varying
`particle_flux>differential_directional_number_rate`
Energy Bins for R26 FeGroup SECT 6 – 23 MeV/nuc (3 bins)
LET1_R26_SECTORS 0 – 24 (25 bins)

6.9.2.115 R26A_H_SECT_Rate H sectored count rate R26A (counts s^{-1})
Size: 3×25 time-varying
`particle_flux>differential_directional_number_rate`
Energy Bins for R26 H SECT 3 – 11 MeV (3 bins)
LET1_R26_SECTORS 0 – 24 (25 bins)

6.9.2.116 R26A_He_SECT_Rate He sectored count rate R26A (counts s^{-1})
Size: 3×25 time-varying
`particle_flux>differential_directional_number_rate`
Energy Bins for R26 He SECT 3 – 11 MeV/nuc (3 bins)
LET1_R26_SECTORS 0 – 24 (25 bins)

6.9.2.117 R26A_NetoSi_SECT_Rate NetoSi sectored count rate R26A (counts s^{-1})
Size: 3×25 time-varying
`particle_flux>differential_directional_number_rate`
Energy Bins for R26 NetoSi SECT 6 – 23 MeV/nuc (3 bins)
LET1_R26_SECTORS 0 – 24 (25 bins)

6.9.2.118 R26B_CNO_SECT_Rate CNO sectored count rate R26B (counts s^{-1})
Size: 3 × 25 time-varying
`particle_flux>differential_directional_number_rate`
Energy Bins for R26 CNO SECT 6 – 23 MeV/nuc (3 bins)
LET1_R26_SECTORS 0 – 24 (25 bins)

6.9.2.119 R26B_FeGroup_SECT_Rate FeGroup sectored count rate R26B (counts s^{-1})
Size: 3 × 25 time-varying
`particle_flux>differential_directional_number_rate`
Energy Bins for R26 FeGroup SECT 6 – 23 MeV/nuc (3 bins)
LET1_R26_SECTORS 0 – 24 (25 bins)

6.9.2.120 R26B_H_SECT_Rate H sectored count rate R26B (counts s^{-1})
Size: 3 × 25 time-varying
`particle_flux>differential_directional_number_rate`
Energy Bins for R26 H SECT 3 – 11 MeV (3 bins)
LET1_R26_SECTORS 0 – 24 (25 bins)

6.9.2.121 R26B_He_SECT_Rate He sectored count rate R26B (counts s^{-1})
Size: 3 × 25 time-varying
`particle_flux>differential_directional_number_rate`
Energy Bins for R26 He SECT 3 – 11 MeV/nuc (3 bins)
LET1_R26_SECTORS 0 – 24 (25 bins)

6.9.2.122 R26B_NetoSi_SECT_Rate NetoSi sectored count rate R26B (counts s^{-1})
Size: 3 × 25 time-varying
`particle_flux>differential_directional_number_rate`
Energy Bins for R26 NetoSi SECT 6 – 23 MeV/nuc (3 bins)
LET1_R26_SECTORS 0 – 24 (25 bins)

6.9.2.123 R2A_He_BIN R2A He Rates (counts)
Size: 7 × 16 time-varying
`particle_flux>differential_directional_number_rate`
Energy Bins for R2 He BIN 2 – 16 MeV/nuc (7 bins)
R2A_He_BIN_MASS_BIN 0 – 15 segment (16 bins)

6.9.2.124 R2A_Ne_BIN R2A Ne Rates (counts)
Size: 8 × 8 time-varying
`particle_flux>differential_directional_number_rate`
Energy Bins for R2 Ne BIN 3 – 32 MeV/nuc (8 bins)
R2A_Ne_BIN_MASS_BIN 0 – 7 segment (8 bins)

6.9.2.125 R2B_He_BIN R2B He Rates (counts)
Size: 7 × 16 time-varying
`particle_flux>differential_directional_number_rate`
Energy Bins for R2 He BIN 2 – 16 MeV/nuc (7 bins)
R2B_He_BIN_MASS_BIN 0 – 15 segment (16 bins)

6.9.2.126 R2B_Ne_BIN R2B Ne Rates (counts)
Size: 8 × 8 time-varying
`particle_flux>differential_directional_number_rate`
Energy Bins for R2 Ne BIN 3 – 32 MeV/nuc (8 bins)
R2B_Ne_BIN_MASS_BIN 0 – 7 segment (8 bins)

6.9.2.127 R3A_He_BIN R3A He Rates (counts)
Size: 5 × 16 time-varying
`particle_flux>differential_directional_number_rate`
Energy Bins for R3 He BIN 8 – 32 MeV/nuc (5 bins)
R3A_He_BIN_MASS_BIN 0 – 15 segment (16 bins)

6.9.2.128 R3A_Ne_BIN R3A Ne Rates (counts)
Size: 6 × 8 time-varying
`particle_flux>differential_directional_number_rate`
Energy Bins for R3 Ne BIN 16 – 91 MeV/nuc (6 bins)
R3A_Ne_BIN_MASS_BIN 0 – 7 segment (8 bins)

6.9.2.129 R3B_He_BIN R3B He Rates (counts)
Size: 5 × 16 time-varying
`particle_flux>differential_directional_number_rate`
Energy Bins for R3 He BIN 8 – 32 MeV/nuc (5 bins)
R3B_He_BIN_MASS_BIN 0 – 15 segment (16 bins)

6.9.2.130 R3B_Ne_BIN R3B Ne Rates (counts)
Size: 6 × 8 time-varying
`particle_flux>differential_directional_number_rate`
Energy Bins for R3 Ne BIN 16 – 91 MeV/nuc (6 bins)
R3B_Ne_BIN_MASS_BIN 0 – 7 segment (8 bins)

6.9.2.131 R45A_He_BIN R45A He Rates (counts)
Size: 5 × 16 time-varying
`particle_flux>differential_directional_number_rate`
Energy Bins for R45 He BIN 8 – 32 MeV/nuc (5 bins)
R45A_He_BIN_MASS_BIN 0 – 15 segment (16 bins)

6.9.2.132 R45A_Ne_BIN R45A Ne Rates (counts)
Size: 6 × 8 time-varying
`particle_flux>differential_directional_number_rate`
Energy Bins for R45 Ne BIN 16 – 91 MeV/nuc (6 bins)
R45A_Ne_BIN_MASS_BIN 0 – 7 segment (8 bins)

6.9.2.133 R45B_He_BIN R45B He Rates (counts)
Size: 5 × 16 time-varying
`particle_flux>differential_directional_number_rate`
Energy Bins for R45 He BIN 8 – 32 MeV/nuc (5 bins)
R45B_He_BIN_MASS_BIN 0 – 15 segment (16 bins)

6.9.2.134 R45B_Ne_BIN R45B Ne Rates (counts)
Size: 6 × 8 time-varying
`particle_flux>differential_directional_number_rate`
Energy Bins for R45 Ne BIN 16 – 91 MeV/nuc (6 bins)
R45B_Ne_BIN_MASS_BIN 0 – 7 segment (8 bins)

6.9.2.135 R6A_He_BIN R6A He Rates (counts)
Size: 3 × 16 time-varying
`particle_flux>differential_directional_number_rate`
Energy Bins for R6 He BIN 23 – 45 MeV/nuc (3 bins)
R6A_He_BIN_MASS_BIN 0 – 15 segment (16 bins)

6.9.2.136 R6A_Ne_BIN R6A Ne Rates (counts)
Size: 3 × 8 time-varying
`particle_flux>differential_directional_number_rate`
Energy Bins for R6 Ne BIN 45 – 91 MeV/nuc (3 bins)
R6A_Ne_BIN_MASS_BIN 0 – 7 segment (8 bins)

6.9.2.137 R6B_He_BIN R6B He Rates (counts)
Size: 3 × 16 time-varying
`particle_flux>differential_directional_number_rate`
Energy Bins for R6 He BIN 23 – 45 MeV/nuc (3 bins)
R6B_He_BIN_MASS_BIN 0 – 15 segment (16 bins)

6.9.2.138 R6B_Ne_BIN R6B Ne Rates (counts)
Size: 3 × 8 time-varying
`particle_flux>differential_directional_number_rate`
Energy Bins for R6 Ne BIN 45 – 91 MeV/nuc (3 bins)
R6B_Ne_BIN_MASS_BIN 0 – 7 segment (8 bins)

6.9.3 OTHER SUPPORT

6.9.3.1 Quality_Flag Data-quality flag
Size: 10 time-varying
`flag>status`
Quality flag number 0 – 9 (10 bins)

6.10 PSP_ISOIS-EPIHI_L2-LET1-RATES60

ISOIS-EPIHI>Integrated Science Investigation of the Sun, Energetic Particle Instrument Hi
L2-LET1-rates60>Level 2 LET1 1-minute rates
EPI-Hi LET1 60 second rates cdf. Time tags indicate midpoint of integration.
Instrument paper: Integrated Science Investigation of the Sun (ISIS): Design of the Energetic Particle Investigation. McComas, D. J. et al (2016). Space Sci. Rev., doi:10.1007/s11214-014-0059-1
1 minute to 1 hour
Cite McComas et al (2016), doi:10.1007/s11214-014-0059-1

6.10.1 PRIMARY VARIABLES

6.10.1.1 A_H_Flux H flux side A ($cm^{-2}sr^{-1}sec^{-1}MeV^{-1}$)
Size: 25 time-varying

`particle_flux>differential_directional_number`
Energy Bins for H 1 – 41 MeV (25 bins)

6.10.1.2 A_He_Flux He flux side A ($cm^{-2}sr^{-1}sec^{-1}(MeV/nuc)^{-1}$)
Size: 26 time-varying
`particle_flux>differential_directional_number`
Energy Bins for He 1 – 49 MeV/nuc (26 bins)

6.10.1.3 B_H_Flux H flux side B ($cm^{-2}sr^{-1}sec^{-1}MeV^{-1}$)
Size: 25 time-varying
`particle_flux>differential_directional_number`
Energy Bins for H 1 – 41 MeV (25 bins)

6.10.1.4 B_He_Flux He flux side B ($cm^{-2}sr^{-1}sec^{-1}(MeV/nuc)^{-1}$)
Size: 26 time-varying
`particle_flux>differential_directional_number`
Energy Bins for He 1 – 49 MeV/nuc (26 bins)

6.10.1.5 R1A_H_SECT_Flux H sectored flux R1A ($cm^{-2}sr^{-1}sec^{-1}MeV^{-1}$)
Size: 1×9 time-varying
`particle_flux>differential_directional_number`
Energy Bins for R1 H SECT 1 – 1 MeV (1 bins)
LET1_R1_SECTORS 0 – 8 (9 bins)

6.10.1.6 R1A_He_SECT_Flux He sectored flux R1A ($cm^{-2}sr^{-1}sec^{-1}(MeV/nuc)^{-1}$)
Size: 1×9 time-varying
`particle_flux>differential_directional_number`
Energy Bins for R1 He SECT 1 – 1 MeV/nuc (1 bins)
LET1_R1_SECTORS 0 – 8 (9 bins)

6.10.1.7 R1B_H_SECT_Flux H sectored flux R1B ($cm^{-2}sr^{-1}sec^{-1}MeV^{-1}$)
Size: 1×9 time-varying
`particle_flux>differential_directional_number`
Energy Bins for R1 H SECT 1 – 1 MeV (1 bins)
LET1_R1_SECTORS 0 – 8 (9 bins)

6.10.1.8 R1B_He_SECT_Flux He sectored flux R1B ($cm^{-2}sr^{-1}sec^{-1}(MeV/nuc)^{-1}$)
Size: 1×9 time-varying
`particle_flux>differential_directional_number`
Energy Bins for R1 He SECT 1 – 1 MeV/nuc (1 bins)
LET1_R1_SECTORS 0 – 8 (9 bins)

6.10.1.9 R26A_H_SECT_Flux H sectored flux R26A ($cm^{-2}sr^{-1}sec^{-1}MeV^{-1}$)
Size: 3×25 time-varying
`particle_flux>differential_directional_number`
Energy Bins for R26 H SECT 3 – 11 MeV (3 bins)
LET1_R26_SECTORS 0 – 24 (25 bins)

6.10.1.10 R26A_He_SECT_Flux He sectored flux R26A ($cm^{-2}sr^{-1}sec^{-1}(MeV/nuc)^{-1}$)
Size: 3×25 time-varying
`particle_flux>differential_directional_number`
Energy Bins for R26 He SECT 3 – 11 MeV/nuc (3 bins)
LET1_R26_SECTORS 0 – 24 (25 bins)

6.10.1.11 R26B_H_SECT_Flux H sectored flux R26B ($cm^{-2}sr^{-1}sec^{-1}MeV^{-1}$)
Size: 3×25 time-varying
`particle_flux>differential_directional_number`
Energy Bins for R26 H SECT 3 – 11 MeV (3 bins)
LET1_R26_SECTORS 0 – 24 (25 bins)

6.10.1.12 R26B_He_SECT_Flux He sectored flux R26B ($cm^{-2}sr^{-1}sec^{-1}(MeV/nuc)^{-1}$)
Size: 3×25 time-varying
`particle_flux>differential_directional_number`
Energy Bins for R26 He SECT 3 – 11 MeV/nuc (3 bins)
LET1_R26_SECTORS 0 – 24 (25 bins)

6.10.2 OTHER DATA

6.10.2.1 A_Al Al counts side A (counts)
Size: 28 time-varying
`particle_flux>differential_directional_number_rate`
Energy Bins for Al 1 – 117 MeV/nuc (28 bins)

6.10.2.2 A_Al_Rate Al count rate side A (counts s^{-1})
Size: 28 time-varying
`particle_flux>differential_directional_number_rate`
Energy Bins for Al 1 – 117 MeV/nuc (28 bins)

6.10.2.3 A_Ar Ar counts side A (counts)
Size: 29 time-varying
`particle_flux>differential_directional_number_rate`
Energy Bins for Ar 1 – 140 MeV/nuc (29 bins)

6.10.2.4 A_Ar_Rate Ar count rate side A (counts s^{-1})
Size: 29 time-varying
`particle_flux>differential_directional_number_rate`
Energy Bins for Ar 1 – 140 MeV/nuc (29 bins)

6.10.2.5 A_C C counts side A (counts)
Size: 27 time-varying
`particle_flux>differential_directional_number_rate`
Energy Bins for C 1 – 99 MeV/nuc (27 bins)

6.10.2.6 A_C_Rate C count rate side A (counts s^{-1})
Size: 27 time-varying
`particle_flux>differential_directional_number_rate`
Energy Bins for C 1 – 99 MeV/nuc (27 bins)

6.10.2.7 A_Ca Ca counts side A (counts)
Size: 30 time-varying
`particle_flux>differential_directional_number_rate`
Energy Bins for Ca 1 – 140 MeV/nuc (30 bins)

6.10.2.8 A_Ca_Rate Ca count rate side A (counts s^{-1})
Size: 30 time-varying
`particle_flux>differential_directional_number_rate`
Energy Bins for Ca 1 – 140 MeV/nuc (30 bins)

6.10.2.9 A_Cr Cr counts side A (counts)
Size: 31 time-varying
`particle_flux>differential_directional_number_rate`
Energy Bins for Cr 1 – 140 MeV/nuc (31 bins)

6.10.2.10 A_Cr_Rate Cr count rate side A (counts s^{-1})
Size: 31 time-varying
`particle_flux>differential_directional_number_rate`
Energy Bins for Cr 1 – 140 MeV/nuc (31 bins)

6.10.2.11 A_Electrons Electrons counts side A (counts)
Size: 16 time-varying
`particle_flux>differential_directional_number_rate`
Energy Bins for Electrons 0 – 6 MeV (16 bins)

6.10.2.12 A_Electrons_Rate Electrons count rate side A (counts s^{-1})
Size: 16 time-varying
`particle_flux>differential_directional_number_rate`
Energy Bins for Electrons 0 – 6 MeV (16 bins)

6.10.2.13 A_Fe Fe counts side A (counts)
Size: 32 time-varying
`particle_flux>differential_directional_number_rate`
Energy Bins for Fe 1 – 166 MeV/nuc (32 bins)

6.10.2.14 A_Fe_Rate Fe count rate side A (counts s^{-1})
Size: 32 time-varying
`particle_flux>differential_directional_number_rate`
Energy Bins for Fe 1 – 166 MeV/nuc (32 bins)

6.10.2.15 A_H H counts side A (counts)
Size: 25 time-varying
`particle_flux>differential_directional_number_rate`
Energy Bins for H 1 – 41 MeV (25 bins)

6.10.2.16 A_H_Rate H count rate side A (counts s^{-1})
Size: 25 time-varying
`particle_flux>differential_directional_number_rate`
Energy Bins for H 1 – 41 MeV (25 bins)

6.10.2.17 A_He He counts side A (counts)
Size: 26 time-varying
`particle_flux>differential_directional_number_rate`
Energy Bins for He 1 – 49 MeV/nuc (26 bins)

6.10.2.18 A_He_Rate He count rate side A (counts s^{-1})
Size: 26 time-varying
`particle_flux>differential_directional_number_rate`
Energy Bins for He 1 – 49 MeV/nuc (26 bins)

6.10.2.19 A_Mg Mg counts side A (counts)
Size: 28 time-varying
`particle_flux>differential_directional_number_rate`
Energy Bins for Mg 1 – 117 MeV/nuc (28 bins)

6.10.2.20 A_Mg_Rate Mg count rate side A (counts s^{-1})
Size: 28 time-varying
`particle_flux>differential_directional_number_rate`
Energy Bins for Mg 1 – 117 MeV/nuc (28 bins)

6.10.2.21 A_N N counts side A (counts)
Size: 27 time-varying
`particle_flux>differential_directional_number_rate`
Energy Bins for N 1 – 99 MeV/nuc (27 bins)

6.10.2.22 A_N_Rate N count rate side A (counts s^{-1})
Size: 27 time-varying
`particle_flux>differential_directional_number_rate`
Energy Bins for N 1 – 99 MeV/nuc (27 bins)

6.10.2.23 A_Na Na counts side A (counts)
Size: 28 time-varying
`particle_flux>differential_directional_number_rate`
Energy Bins for Na 1 – 117 MeV/nuc (28 bins)

6.10.2.24 A_Na_Rate Na count rate side A (counts s^{-1})
Size: 28 time-varying
`particle_flux>differential_directional_number_rate`
Energy Bins for Na 1 – 117 MeV/nuc (28 bins)

6.10.2.25 A_Ne Ne counts side A (counts)
Size: 28 time-varying
`particle_flux>differential_directional_number_rate`
Energy Bins for Ne 1 – 117 MeV/nuc (28 bins)

6.10.2.26 A_Ne_Rate Ne count rate side A (counts s^{-1})
Size: 28 time-varying
`particle_flux>differential_directional_number_rate`
Energy Bins for Ne 1 – 117 MeV/nuc (28 bins)

6.10.2.27 A_Ni Ni counts side A (counts)
Size: 33 time-varying
`particle_flux>differential_directional_number_rate`
Energy Bins for Ni 1 – 197 MeV/nuc (33 bins)

6.10.2.28 A_Ni_Rate Ni count rate side A (counts s^{-1})
Size: 33 time-varying
`particle_flux>differential_directional_number_rate`
Energy Bins for Ni 1 – 197 MeV/nuc (33 bins)

6.10.2.29 A_O O counts side A (counts)
Size: 28 time-varying
`particle_flux>differential_directional_number_rate`
Energy Bins for O 1 – 117 MeV/nuc (28 bins)

6.10.2.30 A_O_Rate O count rate side A (counts s^{-1})
Size: 28 time-varying
`particle_flux>differential_directional_number_rate`
Energy Bins for O 1 – 117 MeV/nuc (28 bins)

6.10.2.31 A_S S counts side A (counts)
Size: 29 time-varying
`particle_flux>differential_directional_number_rate`
Energy Bins for S 1 – 140 MeV/nuc (29 bins)

6.10.2.32 A_S_Rate S count rate side A (counts s^{-1})
Size: 29 time-varying
`particle_flux>differential_directional_number_rate`
Energy Bins for S 1 – 140 MeV/nuc (29 bins)

6.10.2.33 A_Si Si counts side A (counts)
Size: 29 time-varying
`particle_flux>differential_directional_number_rate`
Energy Bins for Si 1 – 140 MeV/nuc (29 bins)

6.10.2.34 A_Si_Rate Si count rate side A (counts s^{-1})
Size: 29 time-varying
`particle_flux>differential_directional_number_rate`
Energy Bins for Si 1 – 140 MeV/nuc (29 bins)

6.10.2.35 B_Al Al counts side B (counts)
Size: 28 time-varying
`particle_flux>differential_directional_number_rate`
Energy Bins for Al 1 – 117 MeV/nuc (28 bins)

6.10.2.36 B_Al_Rate Al count rate side B (counts s^{-1})
Size: 28 time-varying
`particle_flux>differential_directional_number_rate`
Energy Bins for Al 1 – 117 MeV/nuc (28 bins)

6.10.2.37 B_Ar Ar counts side B (counts)
Size: 29 time-varying
`particle_flux>differential_directional_number_rate`
Energy Bins for Ar 1 – 140 MeV/nuc (29 bins)

6.10.2.38 B_Ar_Rate Ar count rate side B (counts s^{-1})
Size: 29 time-varying
`particle_flux>differential_directional_number_rate`
Energy Bins for Ar 1 – 140 MeV/nuc (29 bins)

6.10.2.39 B_C C counts side B (counts)
Size: 27 time-varying
`particle_flux>differential_directional_number_rate`
Energy Bins for C 1 – 99 MeV/nuc (27 bins)

6.10.2.40 B_C_Rate C count rate side B (counts s^{-1})
Size: 27 time-varying
`particle_flux>differential_directional_number_rate`
Energy Bins for C 1 – 99 MeV/nuc (27 bins)

6.10.2.41 B_Ca Ca counts side B (counts)
Size: 30 time-varying
`particle_flux>differential_directional_number_rate`
Energy Bins for Ca 1 – 140 MeV/nuc (30 bins)

6.10.2.42 B_Ca_Rate Ca count rate side B (counts s^{-1})
Size: 30 time-varying
`particle_flux>differential_directional_number_rate`
Energy Bins for Ca 1 – 140 MeV/nuc (30 bins)

6.10.2.43 B_Cr Cr counts side B (counts)
Size: 31 time-varying
`particle_flux>differential_directional_number_rate`
Energy Bins for Cr 1 – 140 MeV/nuc (31 bins)

6.10.2.44 B_Cr_Rate Cr count rate side B (counts s^{-1})
Size: 31 time-varying
`particle_flux>differential_directional_number_rate`
Energy Bins for Cr 1 – 140 MeV/nuc (31 bins)

6.10.2.45 B_Electrons Electrons counts side B (counts)
Size: 16 time-varying
`particle_flux>differential_directional_number_rate`
Energy Bins for Electrons 0 – 6 MeV (16 bins)

6.10.2.46 B_Electrons_Rate Electrons count rate side B (counts s^{-1})
Size: 16 time-varying
`particle_flux>differential_directional_number_rate`
Energy Bins for Electrons 0 – 6 MeV (16 bins)

6.10.2.47 B_Fe Fe counts side B (counts)
Size: 32 time-varying
`particle_flux>differential_directional_number_rate`
Energy Bins for Fe 1 – 166 MeV/nuc (32 bins)

6.10.2.48 B_Fe_Rate Fe count rate side B (counts s^{-1})
Size: 32 time-varying
`particle_flux>differential_directional_number_rate`
Energy Bins for Fe 1 – 166 MeV/nuc (32 bins)

6.10.2.49 B_H H counts side B (counts)
Size: 25 time-varying
`particle_flux>differential_directional_number_rate`
Energy Bins for H 1 – 41 MeV (25 bins)

6.10.2.50 B_H_Rate H count rate side B (counts s^{-1})
Size: 25 time-varying
`particle_flux>differential_directional_number_rate`
Energy Bins for H 1 – 41 MeV (25 bins)

6.10.2.51 B_He He counts side B (counts)
Size: 26 time-varying
`particle_flux>differential_directional_number_rate`
Energy Bins for He 1 – 49 MeV/nuc (26 bins)

6.10.2.52 B_He_Rate He count rate side B (counts s^{-1})
Size: 26 time-varying
`particle_flux>differential_directional_number_rate`
Energy Bins for He 1 – 49 MeV/nuc (26 bins)

6.10.2.53 B_Mg Mg counts side B (counts)
Size: 28 time-varying
`particle_flux>differential_directional_number_rate`
Energy Bins for Mg 1 – 117 MeV/nuc (28 bins)

6.10.2.54 B_Mg_Rate Mg count rate side B (counts s^{-1})
Size: 28 time-varying
`particle_flux>differential_directional_number_rate`
Energy Bins for Mg 1 – 117 MeV/nuc (28 bins)

6.10.2.55 B_N N counts side B (counts)
Size: 27 time-varying
`particle_flux>differential_directional_number_rate`
Energy Bins for N 1 – 99 MeV/nuc (27 bins)

6.10.2.56 B_N_Rate N count rate side B (counts s^{-1})
Size: 27 time-varying
`particle_flux>differential_directional_number_rate`
Energy Bins for N 1 – 99 MeV/nuc (27 bins)

6.10.2.57 B_Na Na counts side B (counts)
Size: 28 time-varying
`particle_flux>differential_directional_number_rate`
Energy Bins for Na 1 – 117 MeV/nuc (28 bins)

6.10.2.58 B_Na_Rate Na count rate side B (counts s^{-1})
Size: 28 time-varying
`particle_flux>differential_directional_number_rate`
Energy Bins for Na 1 – 117 MeV/nuc (28 bins)

6.10.2.59 B_Ne Ne counts side B (counts)
Size: 28 time-varying
`particle_flux>differential_directional_number_rate`
Energy Bins for Ne 1 – 117 MeV/nuc (28 bins)

6.10.2.60 B_Ne_Rate Ne count rate side B (counts s^{-1})
Size: 28 time-varying
`particle_flux>differential_directional_number_rate`
Energy Bins for Ne 1 – 117 MeV/nuc (28 bins)

6.10.2.61 B_Ni Ni counts side B (counts)
Size: 33 time-varying
`particle_flux>differential_directional_number_rate`
Energy Bins for Ni 1 – 197 MeV/nuc (33 bins)

6.10.2.62 B_Ni_Rate Ni count rate side B (counts s^{-1})
Size: 33 time-varying
`particle_flux>differential_directional_number_rate`
Energy Bins for Ni 1 – 197 MeV/nuc (33 bins)

6.10.2.63 B_O O counts side B (counts)
Size: 28 time-varying
`particle_flux>differential_directional_number_rate`
Energy Bins for O 1 – 117 MeV/nuc (28 bins)

6.10.2.64 B_O_Rate O count rate side B (counts s^{-1})
Size: 28 time-varying
`particle_flux>differential_directional_number_rate`
Energy Bins for O 1 – 117 MeV/nuc (28 bins)

6.10.2.65 B_S S counts side B (counts)
Size: 29 time-varying
`particle_flux>differential_directional_number_rate`
Energy Bins for S 1 – 140 MeV/nuc (29 bins)

6.10.2.66 B_S_Rate S count rate side B (counts s^{-1})
Size: 29 time-varying
`particle_flux>differential_directional_number_rate`
Energy Bins for S 1 – 140 MeV/nuc (29 bins)

6.10.2.67 B_Si Si counts side B (counts)
Size: 29 time-varying
`particle_flux>differential_directional_number_rate`
Energy Bins for Si 1 – 140 MeV/nuc (29 bins)

6.10.2.68 B_Si_Rate Si count rate side B (counts s^{-1})
Size: 29 time-varying
`particle_flux>differential_directional_number_rate`
Energy Bins for Si 1 – 140 MeV/nuc (29 bins)

6.10.2.69 HCI_Lat HCI latitude (degrees)
time-varying
`position>latitude`
At timestamp. After Fraenz and Harper, PSS, 2002.

6.10.2.70 HCI_Lon HCI longitude (degrees)
time-varying
`position>longitude`
At timestamp. After Fraenz and Harper, PSS, 2002.

6.10.2.71 HCI_R Heliocentric distance (AU)
time-varying
`position>radial`
At timestamp. After Fraenz and Harper, PSS, 2002.

6.10.2.72 HGC_Lat HGC latitude (degrees)
time-varying
`position>latitude`
At timestamp. After Fraenz and Harper, PSS, 2002.

6.10.2.73 HGC_Lon HGC longitude (degrees)
time-varying
`position>longitude`
At timestamp. After Fraenz and Harper, PSS, 2002.

6.10.2.74 HGC_R Heliocentric distance (AU)
time-varying
`position>radial`
At timestamp. After Fraenz and Harper, PSS, 2002.

6.10.2.75 LET1_A_HCI HCI flow direction LET1A
Size: 3 time-varying
`position>direction`
Unit vector, after Fraenz and Harper, PSS, 2002.

6.10.2.76 LET1_A_PA Pitch angle LET1A (degree)
time-varying
`position>angle`

6.10.2.77 LET1_A_R1_SECT_HCI HCI flow direction LET1AR1SECT
Size: 9×3 time-varying
`position>direction`
Unit vector, after Fraenz and Harper, PSS, 2002.
LET1_R1_SECTORS 0 – 8 (9 bins)

6.10.2.78 LET1_A_R1_SECT_PA Pitch angle LET1AR1SECT (degree)
Size: 9 time-varying
`position>angle`
LET1_R1_SECTORS 0 – 8 (9 bins)

6.10.2.79 LET1_A_R1_SECT_RTN RTN flow direction LET1AR1SECT
Size: 9 × 3 time-varying
`position>direction`
Unit vector, after Fraenz and Harper, PSS, 2002.
LET1_R1_SECTORS 0 – 8 (9 bins)

6.10.2.80 LET1_A_R1_SECT_SA Nominal Parker Spiral angle LET1AR1SECT (degree)
Size: 9 time-varying
`position>angle`
Angle between particle direction and nominal outward Parker Spiral, based on 400km/s solar wind and corotation breakdown at 10Rs.
LET1_R1_SECTORS 0 – 8 (9 bins)

6.10.2.81 LET1_A_R26_SECT_HCI HCI flow direction LET1AR26SECT
Size: 25 × 3 time-varying
`position>direction`
Unit vector, after Fraenz and Harper, PSS, 2002.
LET1_R26_SECTORS 0 – 24 (25 bins)

6.10.2.82 LET1_A_R26_SECT_PA Pitch angle LET1AR26SECT (degree)
Size: 25 time-varying
`position>angle`
LET1_R26_SECTORS 0 – 24 (25 bins)

6.10.2.83 LET1_A_R26_SECT_RTN RTN flow direction LET1AR26SECT
Size: 25 × 3 time-varying
`position>direction`
Unit vector, after Fraenz and Harper, PSS, 2002.
LET1_R26_SECTORS 0 – 24 (25 bins)

6.10.2.84 LET1_A_R26_SECT_SA Nominal Parker Spiral angle LET1AR26SECT (degree)
Size: 25 time-varying
`position>angle`
Angle between particle direction and nominal outward Parker Spiral, based on 400km/s solar wind and corotation breakdown at 10Rs.
LET1_R26_SECTORS 0 – 24 (25 bins)

6.10.2.85 LET1_A_RTN RTN flow direction LET1A
Size: 3 time-varying
`position>direction`
Unit vector, after Fraenz and Harper, PSS, 2002.

6.10.2.86 LET1_A_SA Nominal Parker Spiral angle LET1A (degree)
time-varying
`position>angle`
Angle between particle direction and nominal outward Parker Spiral, based on 400km/s solar wind and corotation breakdown at 10Rs.

6.10.2.87 LET1_B_HCI HCI flow direction LET1B
Size: 3 time-varying
`position>direction`
Unit vector, after Fraenz and Harper, PSS, 2002.

6.10.2.88 LET1_B_PA Pitch angle LET1B (degree)
time-varying
`position>angle`

6.10.2.89 LET1_B_R1_SECT_HCI HCI flow direction LET1BR1SECT
Size: 9×3 time-varying
`position>direction`
Unit vector, after Fraenz and Harper, PSS, 2002.
LET1_R1_SECTORS 0 – 8 (9 bins)

6.10.2.90 LET1_B_R1_SECT_PA Pitch angle LET1BR1SECT (degree)
Size: 9 time-varying
`position>angle`
LET1_R1_SECTORS 0 – 8 (9 bins)

6.10.2.91 LET1_B_R1_SECT_RTN RTN flow direction LET1BR1SECT
Size: 9×3 time-varying
`position>direction`
Unit vector, after Fraenz and Harper, PSS, 2002.

LET1_R1_SECTORS 0 – 8 (9 bins)

6.10.2.92 LET1_B_R1_SECT_SA Nominal Parker Spiral angle LET1BR1SECT (degree)
Size: 9 time-varying
`position>angle`
Angle between particle direction and nominal outward Parker Spiral, based on 400km/s solar wind and corotation breakdown at 10Rs.
LET1_R1_SECTORS 0 – 8 (9 bins)

6.10.2.93 LET1_B_R26_SECT_HCI HCI flow direction LET1BR26SECT
Size: 25 × 3 time-varying
`position>direction`
Unit vector, after Fraenz and Harper, PSS, 2002.
LET1_R26_SECTORS 0 – 24 (25 bins)

6.10.2.94 LET1_B_R26_SECT_PA Pitch angle LET1BR26SECT (degree)
Size: 25 time-varying
`position>angle`
LET1_R26_SECTORS 0 – 24 (25 bins)

6.10.2.95 LET1_B_R26_SECT_RTN RTN flow direction LET1BR26SECT
Size: 25 × 3 time-varying
`position>direction`
Unit vector, after Fraenz and Harper, PSS, 2002.
LET1_R26_SECTORS 0 – 24 (25 bins)

6.10.2.96 LET1_B_R26_SECT_SA Nominal Parker Spiral angle LET1BR26SECT (degree)
Size: 25 time-varying
`position>angle`
Angle between particle direction and nominal outward Parker Spiral, based on 400km/s solar wind and corotation breakdown at 10Rs.
LET1_R26_SECTORS 0 – 24 (25 bins)

6.10.2.97 LET1_B_RTN RTN flow direction LET1B
Size: 3 time-varying
`position>direction`

Unit vector, after Fraenz and Harper, PSS, 2002.

6.10.2.98 LET1_B_SA Nominal Parker Spiral angle LET1B (degree)
time-varying
`position>angle`
Angle between particle direction and nominal outward Parker Spiral, based on 400km/s solar wind and corotation breakdown at 10Rs.

6.10.2.99 R1A_H_SECT_Rate H sectored count rate R1A (counts s^{-1})
Size: 1×9 time-varying
`particle_flux>differential_directional_number_rate`
Energy Bins for R1 H SECT 1 – 1 MeV (1 bins)
LET1_R1_SECTORS 0 – 8 (9 bins)

6.10.2.100 R1A_He_SECT_Rate He sectored count rate R1A (counts s^{-1})
Size: 1×9 time-varying
`particle_flux>differential_directional_number_rate`
Energy Bins for R1 He SECT 1 – 1 MeV/nuc (1 bins)
LET1_R1_SECTORS 0 – 8 (9 bins)

6.10.2.101 R1B_H_SECT_Rate H sectored count rate R1B (counts s^{-1})
Size: 1×9 time-varying
`particle_flux>differential_directional_number_rate`
Energy Bins for R1 H SECT 1 – 1 MeV (1 bins)
LET1_R1_SECTORS 0 – 8 (9 bins)

6.10.2.102 R1B_He_SECT_Rate He sectored count rate R1B (counts s^{-1})
Size: 1×9 time-varying
`particle_flux>differential_directional_number_rate`
Energy Bins for R1 He SECT 1 – 1 MeV/nuc (1 bins)
LET1_R1_SECTORS 0 – 8 (9 bins)

6.10.2.103 R26A_H_SECT_Rate H sectored count rate R26A (counts s^{-1})
Size: 3×25 time-varying
`particle_flux>differential_directional_number_rate`
Energy Bins for R26 H SECT 3 – 11 MeV (3 bins)

LET1_R26_SECTORS 0 – 24 (25 bins)

6.10.2.104 R26A_He_SECT_Rate He sectored count rate R26A (counts s^{-1})
Size: 3 × 25 time-varying
`particle_flux>differential_directional_number_rate`
Energy Bins for R26 He SECT 3 – 11 MeV/nuc (3 bins)
LET1_R26_SECTORS 0 – 24 (25 bins)

6.10.2.105 R26B_H_SECT_Rate H sectored count rate R26B (counts s^{-1})
Size: 3 × 25 time-varying
`particle_flux>differential_directional_number_rate`
Energy Bins for R26 H SECT 3 – 11 MeV (3 bins)
LET1_R26_SECTORS 0 – 24 (25 bins)

6.10.2.106 R26B_He_SECT_Rate He sectored count rate R26B (counts s^{-1})
Size: 3 × 25 time-varying
`particle_flux>differential_directional_number_rate`
Energy Bins for R26 He SECT 3 – 11 MeV/nuc (3 bins)
LET1_R26_SECTORS 0 – 24 (25 bins)

6.10.3 OTHER SUPPORT

6.10.3.1 Quality_Flag Data-quality flag
Size: 10 time-varying
`flag>status`
Quality flag number 0 – 9 (10 bins)

6.11 PSP_ISOIS-EPIHI_L2-LET2-RATES10

ISOIS-EPIHI>Integrated Science Investigation of the Sun, Energetic Particle Instrument Hi
L2-LET2-rates10>Level 2 LET2 10-second rates
EPI-Hi 10 second rates cdf. Time tags indicate midpoint of integration.
Instrument paper: Integrated Science Investigation of the Sun (ISIS): Design of the Energetic Particle Investigation. McComas, D. J. et al (2016). Space Sci. Rev., doi:10.1007/s11214-014-0059-1
1 minute to 1 hour
Cite McComas et al (2016), doi:10.1007/s11214-014-0059-1

6.11.1 PRIMARY VARIABLES

6.11.1.1 C_H_Flux H flux side C ($cm^{-2}sr^{-1}sec^{-1}MeV^{-1}$)
Size: 18 time-varying
`particle_flux>differential_directional_number`
Energy Bins for H 1 – 15 MeV (18 bins)

6.11.1.2 C_He_Flux He flux side C ($cm^{-2}sr^{-1}sec^{-1}(MeV/nuc)^{-1}$)
Size: 22 time-varying
`particle_flux>differential_directional_number`
Energy Bins for He 1 – 29 MeV/nuc (22 bins)

6.11.2 OTHER DATA

6.11.2.1 C_Electrons Electrons counts side C (counts)
Size: 13 time-varying
`particle_flux>differential_directional_number_rate`
Energy Bins for Electrons 1 – 4 MeV (13 bins)

6.11.2.2 C_Electrons_Rate Electrons count rate side C ($counts\,s^{-1}$)
Size: 13 time-varying
`particle_flux>differential_directional_number_rate`
Energy Bins for Electrons 1 – 4 MeV (13 bins)

6.11.2.3 C_H H counts side C (counts)
Size: 18 time-varying
`particle_flux>differential_directional_number_rate`
Energy Bins for H 1 – 15 MeV (18 bins)

6.11.2.4 C_H_Rate H count rate side C ($counts\,s^{-1}$)
Size: 18 time-varying
`particle_flux>differential_directional_number_rate`
Energy Bins for H 1 – 15 MeV (18 bins)

6.11.2.5 C_He He counts side C (counts)
Size: 22 time-varying
`particle_flux>differential_directional_number_rate`

Energy Bins for He 1 – 29 MeV/nuc (22 bins)

6.11.2.6 C_He_Rate He count rate side C (counts s^{-1})
Size: 22 time-varying
`particle_flux>differential_directional_number_rate`
Energy Bins for He 1 – 29 MeV/nuc (22 bins)

6.11.2.7 HCI_Lat HCI latitude (degrees)
time-varying
`position>latitude`
At timestamp. After Fraenz and Harper, PSS, 2002.

6.11.2.8 HCI_Lon HCI longitude (degrees)
time-varying
`position>longitude`
At timestamp. After Fraenz and Harper, PSS, 2002.

6.11.2.9 HCI_R Heliocentric distance (AU)
time-varying
`position>radial`
At timestamp. After Fraenz and Harper, PSS, 2002.

6.11.2.10 HGC_Lat HGC latitude (degrees)
time-varying
`position>latitude`
At timestamp. After Fraenz and Harper, PSS, 2002.

6.11.2.11 HGC_Lon HGC longitude (degrees)
time-varying
`position>longitude`
At timestamp. After Fraenz and Harper, PSS, 2002.

6.11.2.12 HGC_R Heliocentric distance (AU)
time-varying

`position>radial`
At timestamp. After Fraenz and Harper, PSS, 2002.

6.11.2.13 LET2_C_HCI HCI flow direction LET2C
Size: 3 time-varying
`position>direction`
Unit vector, after Fraenz and Harper, PSS, 2002.

6.11.2.14 LET2_C_PA Pitch angle LET2C (degree)
time-varying
`position>angle`

6.11.2.15 LET2_C_RTN RTN flow direction LET2C
Size: 3 time-varying
`position>direction`
Unit vector, after Fraenz and Harper, PSS, 2002.

6.11.2.16 LET2_C_SA Nominal Parker Spiral angle LET2C (degree)
time-varying
`position>angle`
Angle between particle direction and nominal outward Parker Spiral, based on 400km/s solar wind and corotation breakdown at 10Rs.

6.11.3 OTHER SUPPORT

6.11.3.1 Quality_Flag Data-quality flag
Size: 10 time-varying
`flag>status`
Quality flag number 0 – 9 (10 bins)

6.12 PSP_ISOIS-EPIHI_L2-LET2-RATES300

ISOIS-EPIHI>Integrated Science Investigation of the Sun, Energetic Particle Instrument Hi L2-LET2-rates300>Level 2 LET2 5-minute rates
EPI-Hi LET2 300 second rates cdf. Time tags indicate midpoint of integration.
Instrument paper: Integrated Science Investigation of the Sun (ISIS): Design of the Energetic Particle Investigation. McComas, D. J. et al (2016). Space Sci. Rev., doi:10.1007/s11214-014-0059-1

1 minute to 1 hour
Cite McComas et al (2016), doi:10.1007/s11214-014-0059-1

6.12.1 PRIMARY VARIABLES

6.12.2 OTHER DATA

6.12.2.1 HCI_Lat HCI latitude (degrees)
time-varying
`position>latitude`
At timestamp. After Fraenz and Harper, PSS, 2002.

6.12.2.2 HCI_Lon HCI longitude (degrees)
time-varying
`position>longitude`
At timestamp. After Fraenz and Harper, PSS, 2002.

6.12.2.3 HCI_R Heliocentric distance (AU)
time-varying
`position>radial`
At timestamp. After Fraenz and Harper, PSS, 2002.

6.12.2.4 HGC_Lat HGC latitude (degrees)
time-varying
`position>latitude`
At timestamp. After Fraenz and Harper, PSS, 2002.

6.12.2.5 HGC_Lon HGC longitude (degrees)
time-varying
`position>longitude`
At timestamp. After Fraenz and Harper, PSS, 2002.

6.12.2.6 HGC_R Heliocentric distance (AU)
time-varying
`position>radial`
At timestamp. After Fraenz and Harper, PSS, 2002.

6.12.2.7 LET2_C_HCI HCI flow direction LET2C
Size: 3 time-varying
`position>direction`
Unit vector, after Fraenz and Harper, PSS, 2002.

6.12.2.8 LET2_C_PA Pitch angle LET2C (degree)
time-varying
`position>angle`

6.12.2.9 LET2_C_R1_SECT_HCI HCI flow direction LET2CR1SECT
Size: 9×3 time-varying
`position>direction`
Unit vector, after Fraenz and Harper, PSS, 2002.
LET2_R1_SECTORS 0 – 8 (9 bins)

6.12.2.10 LET2_C_R1_SECT_PA Pitch angle LET2CR1SECT (degree)
Size: 9 time-varying
`position>angle`
LET2_R1_SECTORS 0 – 8 (9 bins)

6.12.2.11 LET2_C_R1_SECT_RTN RTN flow direction LET2CR1SECT
Size: 9×3 time-varying
`position>direction`
Unit vector, after Fraenz and Harper, PSS, 2002.
LET2_R1_SECTORS 0 – 8 (9 bins)

6.12.2.12 LET2_C_R1_SECT_SA Nominal Parker Spiral angle LET2CR1SECT (degree)
Size: 9 time-varying
`position>angle`
Angle between particle direction and nominal outward Parker Spiral, based on 400km/s solar wind and corotation breakdown at 10Rs.
LET2_R1_SECTORS 0 – 8 (9 bins)

6.12.2.13 LET2_C_R25_SECT_HCI HCI flow direction LET2CR25SECT
Size: 25×3 time-varying
`position>direction`

Unit vector, after Fraenz and Harper, PSS, 2002.
LET2_R25_SECTORS 0 – 24 (25 bins)

6.12.2.14 LET2_C_R25_SECT_PA Pitch angle LET2CR25SECT (degree)
Size: 25 time-varying
`position>angle`
LET2_R25_SECTORS 0 – 24 (25 bins)

6.12.2.15 LET2_C_R25_SECT_RTN RTN flow direction LET2CR25SECT
Size: 25 × 3 time-varying
`position>direction`
Unit vector, after Fraenz and Harper, PSS, 2002.
LET2_R25_SECTORS 0 – 24 (25 bins)

6.12.2.16 LET2_C_R25_SECT_SA Nominal Parker Spiral angle LET2CR25SECT (degree)
Size: 25 time-varying
`position>angle`
Angle between particle direction and nominal outward Parker Spiral, based on 400km/s solar wind and corotation breakdown at 10Rs.
LET2_R25_SECTORS 0 – 24 (25 bins)

6.12.2.17 LET2_C_RTN RTN flow direction LET2C
Size: 3 time-varying
`position>direction`
Unit vector, after Fraenz and Harper, PSS, 2002.

6.12.2.18 LET2_C_SA Nominal Parker Spiral angle LET2C (degree)
time-varying
`position>angle`
Angle between particle direction and nominal outward Parker Spiral, based on 400km/s solar wind and corotation breakdown at 10Rs.

6.12.2.19 R1C_CNO_SECT_Rate CNO sectored count rate R1C (counts s^{-1})
Size: 1 × 9 time-varying
`particle_flux>differential_directional_number_rate`
Energy Bins for R1 CNO SECT 3 – 3 MeV/nuc (1 bins)

LET2_R1_SECTORS 0 – 8 (9 bins)

6.12.2.20 R1C_FeGroup_SECT_Rate FeGroup sectored count rate R1C (counts s^{-1})
Size: 1 × 9 time-varying
`particle_flux>differential_directional_number_rate`
Energy Bins for R1 FeGroup SECT 3 – 3 MeV/nuc (1 bins)
LET2_R1_SECTORS 0 – 8 (9 bins)

6.12.2.21 R1C_NetoSi_SECT_Rate NetoSi sectored count rate R1C (counts s^{-1})
Size: 1 × 9 time-varying
`particle_flux>differential_directional_number_rate`
Energy Bins for R1 NetoSi SECT 3 – 3 MeV/nuc (1 bins)
LET2_R1_SECTORS 0 – 8 (9 bins)

6.12.2.22 R25C_CNO_SECT_Rate CNO sectored count rate R25C (counts s^{-1})
Size: 3 × 25 time-varying
`particle_flux>differential_directional_number_rate`
Energy Bins for R25 CNO SECT 6 – 23 MeV/nuc (3 bins)
LET2_R25_SECTORS 0 – 24 (25 bins)

6.12.2.23 R25C_FeGroup_SECT_Rate FeGroup sectored count rate R25C (counts s^{-1})
Size: 3 × 25 time-varying
`particle_flux>differential_directional_number_rate`
Energy Bins for R25 FeGroup SECT 6 – 23 MeV/nuc (3 bins)
LET2_R25_SECTORS 0 – 24 (25 bins)

6.12.2.24 R25C_NetoSi_SECT_Rate NetoSi sectored count rate R25C (counts s^{-1})
Size: 3 × 25 time-varying
`particle_flux>differential_directional_number_rate`
Energy Bins for R25 NetoSi SECT 6 – 23 MeV/nuc (3 bins)
LET2_R25_SECTORS 0 – 24 (25 bins)

6.12.3 OTHER SUPPORT

6.12.3.1 Quality_Flag Data-quality flag
Size: 10 time-varying
`flag>status`

Quality flag number 0 – 9 (10 bins)

6.13 PSP_ISOIS-EPIHI_L2-LET2-RATES3600

ISOIS-EPIHI>Integrated Science Investigation of the Sun, Energetic Particle Instrument Hi
L2-LET2-rates3600>Level 2 LET2 hourly rates
EPI-Hi LET2 3600 second rates cdf. Time tags indicate midpoint of integration.
Instrument paper: Integrated Science Investigation of the Sun (ISIS): Design of the Energetic Particle Investigation. McComas, D. J. et al (2016). Space Sci. Rev., doi:10.1007/s11214-014-0059-1
1 minute to 1 hour
Cite McComas et al (2016), doi:10.1007/s11214-014-0059-1

6.13.1 PRIMARY VARIABLES

6.13.1.1 C_H_Flux H flux side C ($cm^{-2}sr^{-1}sec^{-1}MeV^{-1}$)
Size: 24 time-varying
`particle_flux>differential_directional_number`
Energy Bins for H 1 – 35 MeV (24 bins)

6.13.1.2 C_He_Flux He flux side C ($cm^{-2}sr^{-1}sec^{-1}(MeV/nuc)^{-1}$)
Size: 25 time-varying
`particle_flux>differential_directional_number`
Energy Bins for He 1 – 41 MeV/nuc (25 bins)

6.13.1.3 R1C_H_SECT_Flux H sectored flux R1C ($cm^{-2}sr^{-1}sec^{-1}MeV^{-1}$)
Size: 1×9 time-varying
`particle_flux>differential_directional_number`
Energy Bins for R1 H SECT 1 – 1 MeV (1 bins)
LET2_R1_SECTORS 0 – 8 (9 bins)

6.13.1.4 R1C_He_SECT_Flux He sectored flux R1C ($cm^{-2}sr^{-1}sec^{-1}(MeV/nuc)^{-1}$)
Size: 1×9 time-varying
`particle_flux>differential_directional_number`
Energy Bins for R1 He SECT 1 – 1 MeV/nuc (1 bins)
LET2_R1_SECTORS 0 – 8 (9 bins)

6.13.1.5 R25C_H_SECT_Flux H sectored flux R25C ($cm^{-2}sr^{-1}sec^{-1}MeV^{-1}$)
Size: 3 × 25 time-varying
`particle_flux>differential_directional_number`
Energy Bins for R25 H SECT 3 – 11 MeV (3 bins)
LET2_R25_SECTORS 0 – 24 (25 bins)

6.13.1.6 R25C_He_SECT_Flux He sectored flux R25C ($cm^{-2}sr^{-1}sec^{-1}(MeV/nuc)^{-1}$)
Size: 3 × 25 time-varying
`particle_flux>differential_directional_number`
Energy Bins for R25 He SECT 3 – 11 MeV/nuc (3 bins)
LET2_R25_SECTORS 0 – 24 (25 bins)

6.13.2 OTHER DATA

6.13.2.1 C_Al Al counts side C (counts)
Size: 27 time-varying
`particle_flux>differential_directional_number_rate`
Energy Bins for Al 1 – 99 MeV/nuc (27 bins)

6.13.2.2 C_Al_Rate Al count rate side C ($counts\,s^{-1}$)
Size: 27 time-varying
`particle_flux>differential_directional_number_rate`
Energy Bins for Al 1 – 99 MeV/nuc (27 bins)

6.13.2.3 C_Ar Ar counts side C (counts)
Size: 28 time-varying
`particle_flux>differential_directional_number_rate`
Energy Bins for Ar 1 – 117 MeV/nuc (28 bins)

6.13.2.4 C_Ar_Rate Ar count rate side C ($counts\,s^{-1}$)
Size: 28 time-varying
`particle_flux>differential_directional_number_rate`
Energy Bins for Ar 1 – 117 MeV/nuc (28 bins)

6.13.2.5 C_C C counts side C (counts)
Size: 25 time-varying
`particle_flux>differential_directional_number_rate`

Energy Bins for C 1 – 70 MeV/nuc (25 bins)

6.13.2.6 C_C_Rate C count rate side C (counts s^{-1})
Size: 25 time-varying
`particle_flux>differential_directional_number_rate`
Energy Bins for C 1 – 70 MeV/nuc (25 bins)

6.13.2.7 C_Ca Ca counts side C (counts)
Size: 30 time-varying
`particle_flux>differential_directional_number_rate`
Energy Bins for Ca 1 – 140 MeV/nuc (30 bins)

6.13.2.8 C_Ca_Rate Ca count rate side C (counts s^{-1})
Size: 30 time-varying
`particle_flux>differential_directional_number_rate`
Energy Bins for Ca 1 – 140 MeV/nuc (30 bins)

6.13.2.9 C_Cr Cr counts side C (counts)
Size: 31 time-varying
`particle_flux>differential_directional_number_rate`
Energy Bins for Cr 1 – 140 MeV/nuc (31 bins)

6.13.2.10 C_Cr_Rate Cr count rate side C (counts s^{-1})
Size: 31 time-varying
`particle_flux>differential_directional_number_rate`
Energy Bins for Cr 1 – 140 MeV/nuc (31 bins)

6.13.2.11 C_Electrons Electrons counts side C (counts)
Size: 16 time-varying
`particle_flux>differential_directional_number_rate`
Energy Bins for Electrons 0 – 6 MeV (16 bins)

6.13.2.12 C_Electrons_Rate Electrons count rate side C (counts s^{-1})
Size: 16 time-varying

particle_flux>differential_directional_number_rate
Energy Bins for Electrons 0 – 6 MeV (16 bins)

6.13.2.13 C_Fe Fe counts side C (counts)
Size: 31 time-varying
particle_flux>differential_directional_number_rate
Energy Bins for Fe 1 – 140 MeV/nuc (31 bins)

6.13.2.14 C_Fe_Rate Fe count rate side C (counts s^{-1})
Size: 31 time-varying
particle_flux>differential_directional_number_rate
Energy Bins for Fe 1 – 140 MeV/nuc (31 bins)

6.13.2.15 C_H H counts side C (counts)
Size: 24 time-varying
particle_flux>differential_directional_number_rate
Energy Bins for H 1 – 35 MeV (24 bins)

6.13.2.16 C_H_Rate H count rate side C (counts s^{-1})
Size: 24 time-varying
particle_flux>differential_directional_number_rate
Energy Bins for H 1 – 35 MeV (24 bins)

6.13.2.17 C_He He counts side C (counts)
Size: 25 time-varying
particle_flux>differential_directional_number_rate
Energy Bins for He 1 – 41 MeV/nuc (25 bins)

6.13.2.18 C_He_Rate He count rate side C (counts s^{-1})
Size: 25 time-varying
particle_flux>differential_directional_number_rate
Energy Bins for He 1 – 41 MeV/nuc (25 bins)

6.13.2.19 C_Mg Mg counts side C (counts)
Size: 27 time-varying
`particle_flux>differential_directional_number_rate`
Energy Bins for Mg 1 – 99 MeV/nuc (27 bins)

6.13.2.20 C_Mg_Rate Mg count rate side C (counts s^{-1})
Size: 27 time-varying
`particle_flux>differential_directional_number_rate`
Energy Bins for Mg 1 – 99 MeV/nuc (27 bins)

6.13.2.21 C_N N counts side C (counts)
Size: 25 time-varying
`particle_flux>differential_directional_number_rate`
Energy Bins for N 1 – 70 MeV/nuc (25 bins)

6.13.2.22 C_N_Rate N count rate side C (counts s^{-1})
Size: 25 time-varying
`particle_flux>differential_directional_number_rate`
Energy Bins for N 1 – 70 MeV/nuc (25 bins)

6.13.2.23 C_Na Na counts side C (counts)
Size: 27 time-varying
`particle_flux>differential_directional_number_rate`
Energy Bins for Na 1 – 99 MeV/nuc (27 bins)

6.13.2.24 C_Na_Rate Na count rate side C (counts s^{-1})
Size: 27 time-varying
`particle_flux>differential_directional_number_rate`
Energy Bins for Na 1 – 99 MeV/nuc (27 bins)

6.13.2.25 C_Ne Ne counts side C (counts)
Size: 27 time-varying
`particle_flux>differential_directional_number_rate`
Energy Bins for Ne 1 – 99 MeV/nuc (27 bins)

6.13.2.26 C_Ne_Rate Ne count rate side C (counts s^{-1})
Size: 27 time-varying
`particle_flux>differential_directional_number_rate`
Energy Bins for Ne 1 – 99 MeV/nuc (27 bins)

6.13.2.27 C_Ni Ni counts side C (counts)
Size: 32 time-varying
`particle_flux>differential_directional_number_rate`
Energy Bins for Ni 1 – 166 MeV/nuc (32 bins)

6.13.2.28 C_Ni_Rate Ni count rate side C (counts s^{-1})
Size: 32 time-varying
`particle_flux>differential_directional_number_rate`
Energy Bins for Ni 1 – 166 MeV/nuc (32 bins)

6.13.2.29 C_O O counts side C (counts)
Size: 26 time-varying
`particle_flux>differential_directional_number_rate`
Energy Bins for O 1 – 83 MeV/nuc (26 bins)

6.13.2.30 C_O_Rate O count rate side C (counts s^{-1})
Size: 26 time-varying
`particle_flux>differential_directional_number_rate`
Energy Bins for O 1 – 83 MeV/nuc (26 bins)

6.13.2.31 C_S S counts side C (counts)
Size: 28 time-varying
`particle_flux>differential_directional_number_rate`
Energy Bins for S 1 – 117 MeV/nuc (28 bins)

6.13.2.32 C_S_Rate S count rate side C (counts s^{-1})
Size: 28 time-varying
`particle_flux>differential_directional_number_rate`
Energy Bins for S 1 – 117 MeV/nuc (28 bins)

6.13.2.33 C_Si Si counts side C (counts)
Size: 28 time-varying
`particle_flux>differential_directional_number_rate`
Energy Bins for Si 1 – 117 MeV/nuc (28 bins)

6.13.2.34 C_Si_Rate Si count rate side C (counts s^{-1})
Size: 28 time-varying
`particle_flux>differential_directional_number_rate`
Energy Bins for Si 1 – 117 MeV/nuc (28 bins)

6.13.2.35 HCI_Lat HCI latitude (degrees)
time-varying
`position>latitude`
At timestamp. After Fraenz and Harper, PSS, 2002.

6.13.2.36 HCI_Lon HCI longitude (degrees)
time-varying
`position>longitude`
At timestamp. After Fraenz and Harper, PSS, 2002.

6.13.2.37 HCI_R Heliocentric distance (AU)
time-varying
`position>radial`
At timestamp. After Fraenz and Harper, PSS, 2002.

6.13.2.38 HGC_Lat HGC latitude (degrees)
time-varying
`position>latitude`
At timestamp. After Fraenz and Harper, PSS, 2002.

6.13.2.39 HGC_Lon HGC longitude (degrees)
time-varying
`position>longitude`
At timestamp. After Fraenz and Harper, PSS, 2002.

6.13.2.40 HGC_R Heliocentric distance (AU)
time-varying
`position>radial`
At timestamp. After Fraenz and Harper, PSS, 2002.

6.13.2.41 LET2_C_HCI HCI flow direction LET2C
Size: 3 time-varying
`position>direction`
Unit vector, after Fraenz and Harper, PSS, 2002.

6.13.2.42 LET2_C_PA Pitch angle LET2C (degree)
time-varying
`position>angle`

6.13.2.43 LET2_C_R1_SECT_HCI HCI flow direction LET2CR1SECT
Size: 9×3 time-varying
`position>direction`
Unit vector, after Fraenz and Harper, PSS, 2002.
LET2_R1_SECTORS 0 – 8 (9 bins)

6.13.2.44 LET2_C_R1_SECT_PA Pitch angle LET2CR1SECT (degree)
Size: 9 time-varying
`position>angle`
LET2_R1_SECTORS 0 – 8 (9 bins)

6.13.2.45 LET2_C_R1_SECT_RTN RTN flow direction LET2CR1SECT
Size: 9×3 time-varying
`position>direction`
Unit vector, after Fraenz and Harper, PSS, 2002.
LET2_R1_SECTORS 0 – 8 (9 bins)

6.13.2.46 LET2_C_R1_SECT_SA Nominal Parker Spiral angle LET2CR1SECT (degree)
Size: 9 time-varying
`position>angle`
Angle between particle direction and nominal outward Parker Spiral, based on 400km/s solar wind and corotation breakdown at 10Rs.

LET2_R1_SECTORS 0 – 8 (9 bins)

6.13.2.47 LET2_C_R25_SECT_HCI HCI flow direction LET2CR25SECT
Size: 25 × 3 time-varying
`position>direction`
Unit vector, after Fraenz and Harper, PSS, 2002.
LET2_R25_SECTORS 0 – 24 (25 bins)

6.13.2.48 LET2_C_R25_SECT_PA Pitch angle LET2CR25SECT (degree)
Size: 25 time-varying
`position>angle`
LET2_R25_SECTORS 0 – 24 (25 bins)

6.13.2.49 LET2_C_R25_SECT_RTN RTN flow direction LET2CR25SECT
Size: 25 × 3 time-varying
`position>direction`
Unit vector, after Fraenz and Harper, PSS, 2002.
LET2_R25_SECTORS 0 – 24 (25 bins)

6.13.2.50 LET2_C_R25_SECT_SA Nominal Parker Spiral angle LET2CR25SECT (degree)
Size: 25 time-varying
`position>angle`
Angle between particle direction and nominal outward Parker Spiral, based on 400km/s solar wind and corotation breakdown at 10Rs.
LET2_R25_SECTORS 0 – 24 (25 bins)

6.13.2.51 LET2_C_RTN RTN flow direction LET2C
Size: 3 time-varying
`position>direction`
Unit vector, after Fraenz and Harper, PSS, 2002.

6.13.2.52 LET2_C_SA Nominal Parker Spiral angle LET2C (degree)
time-varying
`position>angle`
Angle between particle direction and nominal outward Parker Spiral, based on 400km/s solar wind

and corotation breakdown at 10Rs.

6.13.2.53 R1C_CNO_SECT_Rate CNO sectored count rate R1C (counts s^{-1})
Size: 1×9 time-varying
`particle_flux>differential_directional_number_rate`
Energy Bins for R1 CNO SECT 3 – 3 MeV/nuc (1 bins)
LET2_R1_SECTORS 0 – 8 (9 bins)

6.13.2.54 R1C_FeGroup_SECT_Rate FeGroup sectored count rate R1C (counts s^{-1})
Size: 1×9 time-varying
`particle_flux>differential_directional_number_rate`
Energy Bins for R1 FeGroup SECT 3 – 3 MeV/nuc (1 bins)
LET2_R1_SECTORS 0 – 8 (9 bins)

6.13.2.55 R1C_H_SECT_Rate H sectored count rate R1C (counts s^{-1})
Size: 1×9 time-varying
`particle_flux>differential_directional_number_rate`
Energy Bins for R1 H SECT 1 – 1 MeV (1 bins)
LET2_R1_SECTORS 0 – 8 (9 bins)

6.13.2.56 R1C_He_BIN R1C He Rates (counts)
Size: 5×16 time-varying
`particle_flux>differential_directional_number_rate`
Energy Bins for R1 He BIN 1 – 3 MeV/nuc (5 bins)
R1C_He_BIN_MASS_BIN 0 – 15 segment (16 bins)

6.13.2.57 R1C_He_SECT_Rate He sectored count rate R1C (counts s^{-1})
Size: 1×9 time-varying
`particle_flux>differential_directional_number_rate`
Energy Bins for R1 He SECT 1 – 1 MeV/nuc (1 bins)
LET2_R1_SECTORS 0 – 8 (9 bins)

6.13.2.58 R1C_Ne_BIN R1C Ne Rates (counts)
Size: 5×8 time-varying
`particle_flux>differential_directional_number_rate`
Energy Bins for R1 Ne BIN 1 – 6 MeV/nuc (5 bins)

R1C_Ne_BIN_MASS_BIN 0 – 7 segment (8 bins)

6.13.2.59 R1C_NetoSi_SECT_Rate NetoSi sectored count rate R1C (counts s^{-1})
Size: 1 × 9 time-varying
`particle_flux>differential_directional_number_rate`
Energy Bins for R1 NetoSi SECT 3 – 3 MeV/nuc (1 bins)
LET2_R1_SECTORS 0 – 8 (9 bins)

6.13.2.60 R25C_CNO_SECT_Rate CNO sectored count rate R25C (counts s^{-1})
Size: 3 × 25 time-varying
`particle_flux>differential_directional_number_rate`
Energy Bins for R25 CNO SECT 6 – 23 MeV/nuc (3 bins)
LET2_R25_SECTORS 0 – 24 (25 bins)

6.13.2.61 R25C_FeGroup_SECT_Rate FeGroup sectored count rate R25C (counts s^{-1})
Size: 3 × 25 time-varying
`particle_flux>differential_directional_number_rate`
Energy Bins for R25 FeGroup SECT 6 – 23 MeV/nuc (3 bins)
LET2_R25_SECTORS 0 – 24 (25 bins)

6.13.2.62 R25C_H_SECT_Rate H sectored count rate R25C (counts s^{-1})
Size: 3 × 25 time-varying
`particle_flux>differential_directional_number_rate`
Energy Bins for R25 H SECT 3 – 11 MeV (3 bins)
LET2_R25_SECTORS 0 – 24 (25 bins)

6.13.2.63 R25C_He_SECT_Rate He sectored count rate R25C (counts s^{-1})
Size: 3 × 25 time-varying
`particle_flux>differential_directional_number_rate`
Energy Bins for R25 He SECT 3 – 11 MeV/nuc (3 bins)
LET2_R25_SECTORS 0 – 24 (25 bins)

6.13.2.64 R25C_NetoSi_SECT_Rate NetoSi sectored count rate R25C (counts s^{-1})
Size: 3 × 25 time-varying
`particle_flux>differential_directional_number_rate`
Energy Bins for R25 NetoSi SECT 6 – 23 MeV/nuc (3 bins)

LET2_R25_SECTORS 0 – 24 (25 bins)

6.13.2.65 R2C_He_BIN R2C He Rates (counts)
Size: 7 × 16 time-varying
`particle_flux>differential_directional_number_rate`
Energy Bins for R2 He BIN 2 – 16 MeV/nuc (7 bins)
R2C_He_BIN_MASS_BIN 0 – 15 segment (16 bins)

6.13.2.66 R2C_Ne_BIN R2C Ne Rates (counts)
Size: 8 × 8 time-varying
`particle_flux>differential_directional_number_rate`
Energy Bins for R2 Ne BIN 3 – 32 MeV/nuc (8 bins)
R2C_Ne_BIN_MASS_BIN 0 – 7 segment (8 bins)

6.13.2.67 R3C_He_BIN R3C He Rates (counts)
Size: 5 × 16 time-varying
`particle_flux>differential_directional_number_rate`
Energy Bins for R3 He BIN 8 – 32 MeV/nuc (5 bins)
R3C_He_BIN_MASS_BIN 0 – 15 segment (16 bins)

6.13.2.68 R3C_Ne_BIN R3C Ne Rates (counts)
Size: 6 × 8 time-varying
`particle_flux>differential_directional_number_rate`
Energy Bins for R3 Ne BIN 16 – 91 MeV/nuc (6 bins)
R3C_Ne_BIN_MASS_BIN 0 – 7 segment (8 bins)

6.13.2.69 R45C_He_BIN R45C He Rates (counts)
Size: 5 × 16 time-varying
`particle_flux>differential_directional_number_rate`
Energy Bins for R45 He BIN 8 – 32 MeV/nuc (5 bins)
R45C_He_BIN_MASS_BIN 0 – 15 segment (16 bins)

6.13.2.70 R45C_Ne_BIN R45C Ne Rates (counts)
Size: 6 × 8 time-varying
`particle_flux>differential_directional_number_rate`
Energy Bins for R45 Ne BIN 16 – 91 MeV/nuc (6 bins)

R45C_Ne_BIN_MASS_BIN 0 – 7 segment (8 bins)

6.13.3 OTHER SUPPORT

6.13.3.1 Quality_Flag Data-quality flag
Size: 10 time-varying
`flag>status`
Quality flag number 0 – 9 (10 bins)

6.14 PSP_ISOIS-EPIHI_L2-LET2-RATES60

ISOIS-EPIHI>Integrated Science Investigation of the Sun, Energetic Particle Instrument Hi
L2-LET2-rates60>Level 2 LET2 1-minute rates
EPI-Hi LET2 60 second rates cdf. Time tags indicate midpoint of integration.
Instrument paper: Integrated Science Investigation of the Sun (ISIS): Design of the Energetic Particle Investigation. McComas, D. J. et al (2016). Space Sci. Rev., doi:10.1007/s11214-014-0059-1
1 minute to 1 hour
Cite McComas et al (2016), doi:10.1007/s11214-014-0059-1

6.14.1 PRIMARY VARIABLES

6.14.1.1 C_H_Flux H flux side C ($cm^{-2}sr^{-1}sec^{-1}MeV^{-1}$)
Size: 24 time-varying
`particle_flux>differential_directional_number`
Energy Bins for H 1 – 35 MeV (24 bins)

6.14.1.2 C_He_Flux He flux side C ($cm^{-2}sr^{-1}sec^{-1}(MeV/nuc)^{-1}$)
Size: 25 time-varying
`particle_flux>differential_directional_number`
Energy Bins for He 1 – 41 MeV/nuc (25 bins)

6.14.1.3 R1C_H_SECT_Flux H sectored flux R1C ($cm^{-2}sr^{-1}sec^{-1}MeV^{-1}$)
Size: 1×9 time-varying
`particle_flux>differential_directional_number`
Energy Bins for R1 H SECT 1 – 1 MeV (1 bins)
LET2_R1_SECTORS 0 – 8 (9 bins)

6.14.1.4 R1C_He_SECT_Flux He sectored flux R1C ($cm^{-2}sr^{-1}sec^{-1}(MeV/nuc)^{-1}$)
Size: 1×9 time-varying
`particle_flux>differential_directional_number`
Energy Bins for R1 He SECT 1 – 1 MeV/nuc (1 bins)
LET2_R1_SECTORS 0 – 8 (9 bins)

6.14.1.5 R25C_H_SECT_Flux H sectored flux R25C ($cm^{-2}sr^{-1}sec^{-1}MeV^{-1}$)
Size: 3×25 time-varying
`particle_flux>differential_directional_number`
Energy Bins for R25 H SECT 3 – 11 MeV (3 bins)
LET2_R25_SECTORS 0 – 24 (25 bins)

6.14.1.6 R25C_He_SECT_Flux He sectored flux R25C ($cm^{-2}sr^{-1}sec^{-1}(MeV/nuc)^{-1}$)
Size: 3×25 time-varying
`particle_flux>differential_directional_number`
Energy Bins for R25 He SECT 3 – 11 MeV/nuc (3 bins)
LET2_R25_SECTORS 0 – 24 (25 bins)

6.14.2 OTHER DATA

6.14.2.1 C_Al Al counts side C (counts)
Size: 27 time-varying
`particle_flux>differential_directional_number_rate`
Energy Bins for Al 1 – 99 MeV/nuc (27 bins)

6.14.2.2 C_Al_Rate Al count rate side C (counts s^{-1})
Size: 27 time-varying
`particle_flux>differential_directional_number_rate`
Energy Bins for Al 1 – 99 MeV/nuc (27 bins)

6.14.2.3 C_Ar Ar counts side C (counts)
Size: 28 time-varying
`particle_flux>differential_directional_number_rate`
Energy Bins for Ar 1 – 117 MeV/nuc (28 bins)

6.14.2.4 C_Ar_Rate Ar count rate side C (counts s^{-1})
Size: 28 time-varying

particle_flux>differential_directional_number_rate
Energy Bins for Ar 1 – 117 MeV/nuc (28 bins)

6.14.2.5 C_C C counts side C (counts)
Size: 25 time-varying
particle_flux>differential_directional_number_rate
Energy Bins for C 1 – 70 MeV/nuc (25 bins)

6.14.2.6 C_C_Rate C count rate side C (counts s^{-1})
Size: 25 time-varying
particle_flux>differential_directional_number_rate
Energy Bins for C 1 – 70 MeV/nuc (25 bins)

6.14.2.7 C_Ca Ca counts side C (counts)
Size: 30 time-varying
particle_flux>differential_directional_number_rate
Energy Bins for Ca 1 – 140 MeV/nuc (30 bins)

6.14.2.8 C_Ca_Rate Ca count rate side C (counts s^{-1})
Size: 30 time-varying
particle_flux>differential_directional_number_rate
Energy Bins for Ca 1 – 140 MeV/nuc (30 bins)

6.14.2.9 C_Cr Cr counts side C (counts)
Size: 31 time-varying
particle_flux>differential_directional_number_rate
Energy Bins for Cr 1 – 140 MeV/nuc (31 bins)

6.14.2.10 C_Cr_Rate Cr count rate side C (counts s^{-1})
Size: 31 time-varying
particle_flux>differential_directional_number_rate
Energy Bins for Cr 1 – 140 MeV/nuc (31 bins)

6.14.2.11 C_Electrons Electrons counts side C (counts)
Size: 16 time-varying
`particle_flux>differential_directional_number_rate`
Energy Bins for Electrons 0 – 6 MeV (16 bins)

6.14.2.12 C_Electrons_Rate Electrons count rate side C (counts s^{-1})
Size: 16 time-varying
`particle_flux>differential_directional_number_rate`
Energy Bins for Electrons 0 – 6 MeV (16 bins)

6.14.2.13 C_Fe Fe counts side C (counts)
Size: 31 time-varying
`particle_flux>differential_directional_number_rate`
Energy Bins for Fe 1 – 140 MeV/nuc (31 bins)

6.14.2.14 C_Fe_Rate Fe count rate side C (counts s^{-1})
Size: 31 time-varying
`particle_flux>differential_directional_number_rate`
Energy Bins for Fe 1 – 140 MeV/nuc (31 bins)

6.14.2.15 C_H H counts side C (counts)
Size: 24 time-varying
`particle_flux>differential_directional_number_rate`
Energy Bins for H 1 – 35 MeV (24 bins)

6.14.2.16 C_H_Rate H count rate side C (counts s^{-1})
Size: 24 time-varying
`particle_flux>differential_directional_number_rate`
Energy Bins for H 1 – 35 MeV (24 bins)

6.14.2.17 C_He He counts side C (counts)
Size: 25 time-varying
`particle_flux>differential_directional_number_rate`
Energy Bins for He 1 – 41 MeV/nuc (25 bins)

6.14.2.18 C_He_Rate He count rate side C (counts s^{-1})
Size: 25 time-varying
`particle_flux>differential_directional_number_rate`
Energy Bins for He 1 – 41 MeV/nuc (25 bins)

6.14.2.19 C_Mg Mg counts side C (counts)
Size: 27 time-varying
`particle_flux>differential_directional_number_rate`
Energy Bins for Mg 1 – 99 MeV/nuc (27 bins)

6.14.2.20 C_Mg_Rate Mg count rate side C (counts s^{-1})
Size: 27 time-varying
`particle_flux>differential_directional_number_rate`
Energy Bins for Mg 1 – 99 MeV/nuc (27 bins)

6.14.2.21 C_N N counts side C (counts)
Size: 25 time-varying
`particle_flux>differential_directional_number_rate`
Energy Bins for N 1 – 70 MeV/nuc (25 bins)

6.14.2.22 C_N_Rate N count rate side C (counts s^{-1})
Size: 25 time-varying
`particle_flux>differential_directional_number_rate`
Energy Bins for N 1 – 70 MeV/nuc (25 bins)

6.14.2.23 C_Na Na counts side C (counts)
Size: 27 time-varying
`particle_flux>differential_directional_number_rate`
Energy Bins for Na 1 – 99 MeV/nuc (27 bins)

6.14.2.24 C_Na_Rate Na count rate side C (counts s^{-1})
Size: 27 time-varying
`particle_flux>differential_directional_number_rate`
Energy Bins for Na 1 – 99 MeV/nuc (27 bins)

6.14.2.25 C_Ne Ne counts side C (counts)
Size: 27 time-varying
`particle_flux>differential_directional_number_rate`
Energy Bins for Ne 1 – 99 MeV/nuc (27 bins)

6.14.2.26 C_Ne_Rate Ne count rate side C (counts s^{-1})
Size: 27 time-varying
`particle_flux>differential_directional_number_rate`
Energy Bins for Ne 1 – 99 MeV/nuc (27 bins)

6.14.2.27 C_Ni Ni counts side C (counts)
Size: 32 time-varying
`particle_flux>differential_directional_number_rate`
Energy Bins for Ni 1 – 166 MeV/nuc (32 bins)

6.14.2.28 C_Ni_Rate Ni count rate side C (counts s^{-1})
Size: 32 time-varying
`particle_flux>differential_directional_number_rate`
Energy Bins for Ni 1 – 166 MeV/nuc (32 bins)

6.14.2.29 C_O O counts side C (counts)
Size: 26 time-varying
`particle_flux>differential_directional_number_rate`
Energy Bins for O 1 – 83 MeV/nuc (26 bins)

6.14.2.30 C_O_Rate O count rate side C (counts s^{-1})
Size: 26 time-varying
`particle_flux>differential_directional_number_rate`
Energy Bins for O 1 – 83 MeV/nuc (26 bins)

6.14.2.31 C_S S counts side C (counts)
Size: 28 time-varying
`particle_flux>differential_directional_number_rate`
Energy Bins for S 1 – 117 MeV/nuc (28 bins)

6.14.2.32 C_S_Rate S count rate side C (counts s^{-1})
Size: 28 time-varying
`particle_flux>differential_directional_number_rate`
Energy Bins for S 1 – 117 MeV/nuc (28 bins)

6.14.2.33 C_Si Si counts side C (counts)
Size: 28 time-varying
`particle_flux>differential_directional_number_rate`
Energy Bins for Si 1 – 117 MeV/nuc (28 bins)

6.14.2.34 C_Si_Rate Si count rate side C (counts s^{-1})
Size: 28 time-varying
`particle_flux>differential_directional_number_rate`
Energy Bins for Si 1 – 117 MeV/nuc (28 bins)

6.14.2.35 HCI_Lat HCI latitude (degrees)
time-varying
`position>latitude`
At timestamp. After Fraenz and Harper, PSS, 2002.

6.14.2.36 HCI_Lon HCI longitude (degrees)
time-varying
`position>longitude`
At timestamp. After Fraenz and Harper, PSS, 2002.

6.14.2.37 HCI_R Heliocentric distance (AU)
time-varying
`position>radial`
At timestamp. After Fraenz and Harper, PSS, 2002.

6.14.2.38 HGC_Lat HGC latitude (degrees)
time-varying
`position>latitude`
At timestamp. After Fraenz and Harper, PSS, 2002.

6.14.2.39 HGC_Lon HGC longitude (degrees)
time-varying
`position>longitude`
At timestamp. After Fraenz and Harper, PSS, 2002.

6.14.2.40 HGC_R Heliocentric distance (AU)
time-varying
`position>radial`
At timestamp. After Fraenz and Harper, PSS, 2002.

6.14.2.41 LET2_C_HCI HCI flow direction LET2C
Size: 3 time-varying
`position>direction`
Unit vector, after Fraenz and Harper, PSS, 2002.

6.14.2.42 LET2_C_PA Pitch angle LET2C (degree)
time-varying
`position>angle`

6.14.2.43 LET2_C_R1_SECT_HCI HCI flow direction LET2CR1SECT
Size: 9×3 time-varying
`position>direction`
Unit vector, after Fraenz and Harper, PSS, 2002.
LET2_R1_SECTORS 0 – 8 (9 bins)

6.14.2.44 LET2_C_R1_SECT_PA Pitch angle LET2CR1SECT (degree)
Size: 9 time-varying
`position>angle`
LET2_R1_SECTORS 0 – 8 (9 bins)

6.14.2.45 LET2_C_R1_SECT_RTN RTN flow direction LET2CR1SECT
Size: 9×3 time-varying
`position>direction`
Unit vector, after Fraenz and Harper, PSS, 2002.
LET2_R1_SECTORS 0 – 8 (9 bins)

6.14.2.46 LET2_C_R1_SECT_SA Nominal Parker Spiral angle LET2CR1SECT (degree)
Size: 9 time-varying
`position>angle`
Angle between particle direction and nominal outward Parker Spiral, based on 400km/s solar wind and corotation breakdown at 10Rs.
LET2_R1_SECTORS 0 – 8 (9 bins)

6.14.2.47 LET2_C_R25_SECT_HCI HCI flow direction LET2CR25SECT
Size: 25 × 3 time-varying
`position>direction`
Unit vector, after Fraenz and Harper, PSS, 2002.
LET2_R25_SECTORS 0 – 24 (25 bins)

6.14.2.48 LET2_C_R25_SECT_PA Pitch angle LET2CR25SECT (degree)
Size: 25 time-varying
`position>angle`
LET2_R25_SECTORS 0 – 24 (25 bins)

6.14.2.49 LET2_C_R25_SECT_RTN RTN flow direction LET2CR25SECT
Size: 25 × 3 time-varying
`position>direction`
Unit vector, after Fraenz and Harper, PSS, 2002.
LET2_R25_SECTORS 0 – 24 (25 bins)

6.14.2.50 LET2_C_R25_SECT_SA Nominal Parker Spiral angle LET2CR25SECT (degree)
Size: 25 time-varying
`position>angle`
Angle between particle direction and nominal outward Parker Spiral, based on 400km/s solar wind and corotation breakdown at 10Rs.
LET2_R25_SECTORS 0 – 24 (25 bins)

6.14.2.51 LET2_C_RTN RTN flow direction LET2C
Size: 3 time-varying
`position>direction`
Unit vector, after Fraenz and Harper, PSS, 2002.

6.14.2.52 LET2_C_SA Nominal Parker Spiral angle LET2C (degree)
time-varying
`position>angle`
Angle between particle direction and nominal outward Parker Spiral, based on 400km/s solar wind and corotation breakdown at 10Rs.

6.14.2.53 R1C_H_SECT_Rate H sectored count rate R1C (counts s^{-1})
Size: 1×9 time-varying
`particle_flux>differential_directional_number_rate`
Energy Bins for R1 H SECT 1 – 1 MeV (1 bins)
LET2_R1_SECTORS 0 – 8 (9 bins)

6.14.2.54 R1C_He_SECT_Rate He sectored count rate R1C (counts s^{-1})
Size: 1×9 time-varying
`particle_flux>differential_directional_number_rate`
Energy Bins for R1 He SECT 1 – 1 MeV/nuc (1 bins)
LET2_R1_SECTORS 0 – 8 (9 bins)

6.14.2.55 R25C_H_SECT_Rate H sectored count rate R25C (counts s^{-1})
Size: 3×25 time-varying
`particle_flux>differential_directional_number_rate`
Energy Bins for R25 H SECT 3 – 11 MeV (3 bins)
LET2_R25_SECTORS 0 – 24 (25 bins)

6.14.2.56 R25C_He_SECT_Rate He sectored count rate R25C (counts s^{-1})
Size: 3×25 time-varying
`particle_flux>differential_directional_number_rate`
Energy Bins for R25 He SECT 3 – 11 MeV/nuc (3 bins)
LET2_R25_SECTORS 0 – 24 (25 bins)

6.14.3 OTHER SUPPORT

6.14.3.1 Quality_Flag Data-quality flag
Size: 10 time-varying
`flag>status`
Quality flag number 0 – 9 (10 bins)

6.15 PSP_ISOIS-EPIHI_L2-SECOND-RATES

ISOIS-EPIHI>Integrated Science Investigation of the Sun, Energetic Particle Instrument Hi L2-second-rates>Level 2 one-second rates
EPI-Hi second rates cdf. Time tags indicate time of collection.
Instrument paper: Integrated Science Investigation of the Sun (ISIS): Design of the Energetic Particle Investigation. McComas, D. J. et al (2016). Space Sci. Rev., doi:10.1007/s11214-014-0059-1
1 minute to 1 hour
Cite McComas et al (2016), doi:10.1007/s11214-014-0059-1

6.15.1 PRIMARY VARIABLES

6.15.2 OTHER DATA

6.15.2.1 HCI_Lat HCI latitude (degrees)
time-varying
`position>latitude`
At timestamp. After Fraenz and Harper, PSS, 2002.

6.15.2.2 HCI_Lon HCI longitude (degrees)
time-varying
`position>longitude`
At timestamp. After Fraenz and Harper, PSS, 2002.

6.15.2.3 HCI_R Heliocentric distance (AU)
time-varying
`position>radial`
At timestamp. After Fraenz and Harper, PSS, 2002.

6.15.2.4 HET_A_Electrons HET A-side electron rates (counts)
Size: 3 time-varying
`particle_flux>differential_directional_number_rate`
Energy Bins for HET Electrons 1 – 3 MeV (3 bins)

6.15.2.5 HET_A_Electrons_Rate Electrons rate HET A (counts s^{-1})
Size: 3 time-varying
`particle_flux>differential_directional_number_rate`
Energy Bins for HET Electrons 1 – 3 MeV (3 bins)

6.15.2.6 HET_A_H HET A-side hydrogen rates (counts)
Size: 2 time-varying
`particle_flux>differential_directional_number_rate`
Energy Bins for HET H 12 – 23 MeV (2 bins)

6.15.2.7 HET_A_HCI HCI flow direction HETA
Size: 3 time-varying
`position>direction`
Unit vector, after Fraenz and Harper, PSS, 2002.

6.15.2.8 HET_A_H_Rate H rate HET A (counts s^{-1})
Size: 2 time-varying
`particle_flux>differential_directional_number_rate`
Energy Bins for HET H 12 – 23 MeV (2 bins)

6.15.2.9 HET_A_PA Pitch angle HETA (degree)
time-varying
`position>angle`

6.15.2.10 HET_A_RTN RTN flow direction HETA
Size: 3 time-varying
`position>direction`
Unit vector, after Fraenz and Harper, PSS, 2002.

6.15.2.11 HET_A_SA Nominal Parker Spiral angle HETA (degree)
time-varying
`position>angle`
Angle between particle direction and nominal outward Parker Spiral, based on 400km/s solar wind and corotation breakdown at 10Rs.

6.15.2.12 HET_B_Electrons HET B-side electron rates (counts)
Size: 3 time-varying
`particle_flux>differential_directional_number_rate`
Energy Bins for HET Electrons 1 – 3 MeV (3 bins)

6.15.2.13 HET_B_Electrons_Rate Electrons rate HET B (counts s^{-1})
Size: 3 time-varying
`particle_flux>differential_directional_number_rate`
Energy Bins for HET Electrons 1 – 3 MeV (3 bins)

6.15.2.14 HET_B_H HET B-side hydrogen rates (counts)
Size: 2 time-varying
`particle_flux>differential_directional_number_rate`
Energy Bins for HET H 12 – 23 MeV (2 bins)

6.15.2.15 HET_B_HCI HCI flow direction HETB
Size: 3 time-varying
`position>direction`
Unit vector, after Fraenz and Harper, PSS, 2002.

6.15.2.16 HET_B_H_Rate H rate HET B (counts s^{-1})
Size: 2 time-varying
`particle_flux>differential_directional_number_rate`
Energy Bins for HET H 12 – 23 MeV (2 bins)

6.15.2.17 HET_B_PA Pitch angle HETB (degree)
time-varying
`position>angle`

6.15.2.18 HET_B_RTN RTN flow direction HETB
Size: 3 time-varying
`position>direction`
Unit vector, after Fraenz and Harper, PSS, 2002.

6.15.2.19 HET_B_SA Nominal Parker Spiral angle HETB (degree)
time-varying
`position>angle`
Angle between particle direction and nominal outward Parker Spiral, based on 400km/s solar wind and corotation breakdown at 10Rs.

6.15.2.20 HGC_Lat HGC latitude (degrees)
time-varying
`position>latitude`
At timestamp. After Fraenz and Harper, PSS, 2002.

6.15.2.21 HGC_Lon HGC longitude (degrees)
time-varying
`position>longitude`
At timestamp. After Fraenz and Harper, PSS, 2002.

6.15.2.22 HGC_R Heliocentric distance (AU)
time-varying
`position>radial`
At timestamp. After Fraenz and Harper, PSS, 2002.

6.15.2.23 LET1_A_Electrons LET1 A-side electron rates (counts)
Size: 2 time-varying
`particle_flux>differential_directional_number_rate`
Energy Bins for LET Electrons 1 – 1 MeV (2 bins)

6.15.2.24 LET1_A_Electrons_Rate Electrons rate LET1 A (counts s^{-1})
Size: 2 time-varying
`particle_flux>differential_directional_number_rate`
Energy Bins for LET Electrons 1 – 1 MeV (2 bins)

6.15.2.25 LET1_A_H LET1 A-side hydrogen rates (counts)
Size: 3 time-varying
`particle_flux>differential_directional_number_rate`
Energy Bins for LET H 2 – 10 MeV (3 bins)

6.15.2.26 LET1_A_HCI HCI flow direction LET1A
Size: 3 time-varying
`position>direction`
Unit vector, after Fraenz and Harper, PSS, 2002.

6.15.2.27 LET1_A_H_Rate H rate LET1 A (counts s^{-1})
Size: 3 time-varying
`particle_flux>differential_directional_number_rate`
Energy Bins for LET H 2 – 10 MeV (3 bins)

6.15.2.28 LET1_A_PA Pitch angle LET1A (degree)
time-varying
`position>angle`

6.15.2.29 LET1_A_RTN RTN flow direction LET1A
Size: 3 time-varying
`position>direction`
Unit vector, after Fraenz and Harper, PSS, 2002.

6.15.2.30 LET1_A_SA Nominal Parker Spiral angle LET1A (degree)
time-varying
`position>angle`
Angle between particle direction and nominal outward Parker Spiral, based on 400km/s solar wind and corotation breakdown at 10Rs.

6.15.2.31 LET1_B_Electrons LET1 B-side electron rates (counts)
Size: 2 time-varying
`particle_flux>differential_directional_number_rate`
Energy Bins for LET Electrons 1 – 1 MeV (2 bins)

6.15.2.32 LET1_B_Electrons_Rate Electrons rate LET1 B (counts s^{-1})
Size: 2 time-varying
`particle_flux>differential_directional_number_rate`
Energy Bins for LET Electrons 1 – 1 MeV (2 bins)

6.15.2.33 LET1_B_H LET1 B-side hydrogen rates (counts)
Size: 3 time-varying
`particle_flux>differential_directional_number_rate`
Energy Bins for LET H 2 – 10 MeV (3 bins)

6.15.2.34 LET1_B_HCI HCI flow direction LET1B
Size: 3 time-varying
`position>direction`
Unit vector, after Fraenz and Harper, PSS, 2002.

6.15.2.35 LET1_B_H_Rate H rate LET1 B (counts s^{-1})
Size: 3 time-varying
`particle_flux>differential_directional_number_rate`
Energy Bins for LET H 2 – 10 MeV (3 bins)

6.15.2.36 LET1_B_PA Pitch angle LET1B (degree)
time-varying
`position>angle`

6.15.2.37 LET1_B_RTN RTN flow direction LET1B
Size: 3 time-varying
`position>direction`
Unit vector, after Fraenz and Harper, PSS, 2002.

6.15.2.38 LET1_B_SA Nominal Parker Spiral angle LET1B (degree)
time-varying
`position>angle`
Angle between particle direction and nominal outward Parker Spiral, based on 400km/s solar wind and corotation breakdown at 10Rs.

6.15.2.39 LET2_C_Electrons LET2 C-side electron rates (counts)
Size: 2 time-varying
`particle_flux>differential_directional_number_rate`
Energy Bins for LET Electrons 1 – 1 MeV (2 bins)

6.15.2.40 LET2_C_Electrons_Rate Electrons rate LET2 C (counts s^{-1})
Size: 2 time-varying
`particle_flux>differential_directional_number_rate`
Energy Bins for LET Electrons 1 – 1 MeV (2 bins)

6.15.2.41 LET2_C_H LET2 C-side hydrogen rates (counts)
Size: 3 time-varying
`particle_flux>differential_directional_number_rate`
Energy Bins for LET H 2 – 10 MeV (3 bins)

6.15.2.42 LET2_C_HCI HCI flow direction LET2C
Size: 3 time-varying
`position>direction`
Unit vector, after Fraenz and Harper, PSS, 2002.

6.15.2.43 LET2_C_H_Rate H rate LET2 C (counts s^{-1})
Size: 3 time-varying
`particle_flux>differential_directional_number_rate`
Energy Bins for LET H 2 – 10 MeV (3 bins)

6.15.2.44 LET2_C_PA Pitch angle LET2C (degree)
time-varying
`position>angle`

6.15.2.45 LET2_C_RTN RTN flow direction LET2C
Size: 3 time-varying
`position>direction`
Unit vector, after Fraenz and Harper, PSS, 2002.

6.15.2.46 LET2_C_SA Nominal Parker Spiral angle LET2C (degree)
time-varying
`position>angle`
Angle between particle direction and nominal outward Parker Spiral, based on 400km/s solar wind and corotation breakdown at 10Rs.

6.15.3 OTHER SUPPORT

6.15.3.1 Quality_Flag Data-quality flag
Size: 10 time-varying
`flag>status`
Quality flag number 0 – 9 (10 bins)

6.16 PSP_ISOIS_L2-EPHEM

ISOIS>Integrated Science Investigation of the Sun
L2-ephem>Level 2 ephem
Instrument paper: Integrated Science Investigation of the Sun (ISIS): Design of the Energetic Particle Investigation. McComas, D. J. et al (2016). Space Sci. Rev., doi:10.1007/s11214-014-0059-1
1 minute to 1 hour
Cite McComas et al (2016), doi:10.1007/s11214-014-0059-1

6.16.1 PRIMARY VARIABLES

6.16.2 OTHER DATA

6.16.2.1 Clock_Angle angle of off-pointing from ecliptic north when not in encounter (degrees)
time-varying
`position>angle`
Angle (around +R axis) between SC +Z projected into the TN plane and +N axis. Nominally zero (roughly ecliptic north). Ascends CCW (right-handed) despite the name, so positive values are toward -T (opposite ram) and negative towards +T (into ram). Undefined (fill) if Sun Angle is small.

6.16.2.2 HCI_Lat HCI latitude (degrees)
time-varying
`position>latitude`
At timestamp. After Fraenz and Harper, PSS, 2002.

6.16.2.3 HCI_Lon HCI longitude (degrees)
time-varying
`position>longitude`
At timestamp. After Fraenz and Harper, PSS, 2002.

6.16.2.4 HCI_R Heliocentric distance (AU)
time-varying
`position>radial`
At timestamp. After Fraenz and Harper, PSS, 2002.

6.16.2.5 HGC_Lat HGC latitude (degrees)
time-varying

`position>latitude`
At timestamp. After Fraenz and Harper, PSS, 2002.

6.16.2.6 HGC_Lon HGC longitude (degrees)
time-varying
`position>longitude`
At timestamp. After Fraenz and Harper, PSS, 2002.

6.16.2.7 HGC_R Heliocentric distance (AU)
time-varying
`position>radial`
At timestamp. After Fraenz and Harper, PSS, 2002.

6.16.2.8 Ram_Pointing Spacecraft is ram pointing
time-varying
`flag>status`
1 if roll angle is small, and either sun angle or clock angle are small (pointing into ram).

6.16.2.9 Roll_Angle Angle between nominal ram and actual ram, 0 in encounter (degrees)
time-varying
`position>angle`
Angle between s/c +X and RTN +T. Positive if s/c +X is towards +N (roughly ecliptic north); right-handed in RTN.

6.16.2.10 Spiral_HETA HETA look angle with nominal parker spiral (degrees)
time-varying
`position>angle`
Angle between +Z HETA frame and nominal parker spiral assuming constant 400 km/s solar wind speed and a corotation boundary of 20 solar radii

6.16.2.11 Spiral_LET1A LET1A look angle with nominal parker spiral (degrees)
time-varying
`position>angle`
Angle between +Z LET1A frame and nominal parker spiral assuming constant 400 km/s solar wind speed and a corotation boundary of 20 solar radii

6.16.2.12 Spiral_LET2C LET2C look angle with nominal parker spiral (degrees)
time-varying
`position>angle`
Angle between +Z LET2C frame and nominal parker spiral assuming constant 400 km/s solar wind speed and a corotation boundary of 20 solar radii

6.16.2.13 Spiral_Lo Lo look angle with nominal parker spiral (degrees)
time-varying
`position>angle`
Angle between +Z Lo frame (look directions x9) and nominal parker spiral assuming constant 400 km/s solar wind speed and a corotation boundry of 20 solar radii

6.16.2.14 Sun_Angle Angle between TPS and Sun, 0 in encounter (degrees)
time-varying
`position>angle`
Angle between s/c +Z and RTN -R. Always positive.

6.16.2.15 Umbra_Pointing Spacecraft is umbra pointing
time-varying
`flag>status`
1 (nominal for encounter) if Sun angle = 0 else 0

6.16.3 OTHER SUPPORT

6.17 PSP_ISOIS_L2-SUMMARY

ISOIS>Integrated Science Investigation of the Sun
L2-Summary>level 2 summary
EPI-Hi HET 3600 second rates cdf. Time tags indicate midpoint of integration.
Instrument paper: Integrated Science Investigation of the Sun (ISIS): Design of the Energetic Particle Investigation. McComas, D. J. et al (2016). Space Sci. Rev., doi:10.1007/s11214-014-0059-1
EPI-Hi 3600 seconds rates cdf. Time tags indicate midpoint of integration.
EPI-Lo, Ion Composition mode.
EPI-Lo, Particle Energy mode.
1 minute to 1 hour
Cite McComas et al (2016), doi:10.1007/s11214-014-0059-1

6.17.1 PRIMARY VARIABLES

6.17.2 OTHER DATA

6.17.2.1 A_H_Rate_TS H count rate side A 2-10MeV (counts s^{-1})
time-varying
`particle_flux>differential_directional_number_rate`

6.17.2.2 A_Heavy_Rate_TS Heavy (6<=z<=28) ion count rate side A 4-40 MeV/nuc (counts s^{-1})
time-varying
`particle_flux>differential_directional_number_rate`

6.17.2.3 Electron_CountRate_ChanE Electron count rate channel E (HiResElectrons) (counts/sec)
Size: 48 time-varying
`particle_flux>differential_directional_number_rate`
Particle Energy mode. Corrected for deadtime. May contain substantial non-electron background.
Electron_ChanE_Energy 12 – 9065 keV (32 bins)

6.17.2.4 HET_A_Electrons_Rate_TS HET Electrons count rate side A 1-5MeV (counts s^{-1})
time-varying
`particle_flux>differential_directional_number_rate`

6.17.2.5 HET_A_H_Rate_TS HET H count rate side A 10-50MeV (counts s^{-1})
time-varying
`particle_flux>differential_directional_number_rate`

6.17.2.6 H_CountRate_ChanP_SP H count rate channel P (HiResProtons) (counts/sec)
Size: 48 time-varying
`particle_flux>differential_directional_number_rate`
Ion Composition mode. Corrected for deadtime.
H_ChanP_Energy 70 – 9464 keV (39 bins)

6.17.3 OTHER SUPPORT

7 ACRONYMS

For detailed information on the various coordinate systems, refer to Franz and Harper (2002).

ApID: Application Identifier
EPI-Lo: Energetic Particle Instrument - Low Energy
EPI-Hi: Energetic Particle - High Energy
FOV: Field of View
GSE: Geocentric Solar Ecliptic
GSM: Geocentric Solar Magnetospheric
HGC: Heliographic Coordinates
HAE: Heliocentric Aries Ecliptic
HCI: Heliocentric Inertial
HEE: Heliocentric Earth Ecliptic
HEEQ: Heliocentric Earth Equatorial
IC: Ion Composition
IE: Ion Energy
IS⊙IS: Integrated Science Investigations of the Sun
PC: Particle Composition
PE: Particle Energy
PSP: Parker Solar Probe
RTN: Heliocentric
TAI: International Atomic Time, defined by SI seconds
TOF: Time of Flight
TPS: Thermal Protection System
UTC: Coordinated Universal Time

REFERENCES

McComas, D., et al. (2016). Integrated science Investigation of the Sun (ISIS): Design of the Energetic Particle Investigation. *SSRv*, 204:187–256. DOI 10.1007/s11214-014-0059-1.

Hill, M., et al. (2019). in preparation.

Szalay, J., et al. (2019). in preparation.

Franz, M. and D. Harper (2002). Heliospheric Coordinate Systems. Plan.Space Sci., 50, 217–233.